Louisiana State University
LSU Digital Commons

LSU Doctoral Dissertations | Graduate School

2010

Supercritical Pyrolysis of n-Decane

Sean Bagley
Louisiana State University and Agricultural and Mechanical College, sbagle1@lsu.edu

Follow this and additional works at: https://digitalcommons.lsu.edu/gradschool_dissertations

 Part of the Chemical Engineering Commons

Recommended Citation
Bagley, Sean, "Supercritical Pyrolysis of n-Decane" (2010). *LSU Doctoral Dissertations*. 4000.
https://digitalcommons.lsu.edu/gradschool_dissertations/4000

This Dissertation is brought to you for free and open access by the Graduate School at LSU Digital Commons. It has been accepted for inclusion in LSU Doctoral Dissertations by an authorized graduate school editor of LSU Digital Commons. For more information, please contactgradetd@lsu.edu.

SUPERCRITICAL PYROLYSIS OF *N*-DECANE

A Dissertation

Submitted to the Graduate Faculty of the
Louisiana State University
Agricultural and Mechanical College
in partial fulfillment of the
requirements for the degree of
Doctor of Philosophy

in

The Department of Chemical Engineering

by

Sean Bagley
B.S., Louisiana State University, 2003
December 2010

Acknowledgements

I gratefully acknowledge the Air Force Office of Scientific Research, for providing the necessary funding for this research. I would like to thank Dr. Arthur Lafleur and Ms. Elaine Plummer of the Massachusetts Institute of Technology and Dr. John Fetzer of Chevron Research for providing reference standards and/or UV spectra of polycyclic aromatic hydrocarbons to my professor.

I would like to thank my professor, Dr. Judy Wornat, for her wisdom and patience. The members of my group, Elmer Ledesma, Jorge Oña, Shiju Thomas, Michelle Walker, Jerome Robles, Franz Ehrenhauser, and Nimesh Poddar, each of whom contributed to my project in innumerable ways. And finally I would like to thank my parents, Mary and Patrick Bagley, who always set an example of hard work and honesty.

Table of Contents

Abstract

Fuels used in future generations of high-speed jet aircraft will be required to take on increasing heat loads in their role as the primary coolant for the absorption of waste heat from the engine. As a consequence, the hydrocarbon fuels will be exposed to elevated temperatures and pressures prior to their use as fuels, conditions which are beyond the critical point of the fuel and which lead to the formation of carbonaceous solid deposits in the pre-combustion environment.

Deposition of solids causes reduced engine performance and eventual failure, so understanding the mechanisms by which thermally stressed hydrocarbons become solids is extremely important to the continued development of high-performance aircraft. Of particular importance—and the focus of this work—are those reactions leading to the formation of polycyclic aromatic hydrocarbons (PAH), which are known to be the precursors to solid deposits. To this end, experiments were performed in which the reactant *n*-decane, chosen as a representative of the aliphatic components of real-world jet fuels, was pyrolyzed in a flow reactor under supercritical conditions, with temperatures ranging from 530 to 570 °C and pressures ranging from 40 to 100 atm.

Products of the pyrolysis experiments were analyzed by high-pressure liquid chromatography (HPLC) with diode-array ultraviolet-visible detection (UV) in series with mass spectrometry (MS). A two-dimensional HPLC technique was developed specifically for this work which allowed the identification of 281 PAH products, 254 of which had never before been reported as products of *n*-decane pyrolysis. Furthermore, 77 aromatic products consisting of one to nine rings have been quantified, and yields with respect to temperature and pressure are presented.

In the supercritical *n*-decane pyrolysis environment, single-ring aromatic products are formed first by cyclization and then dehydrogenation of the alkane reactant. Addition of alkyl and alkenyl radicals to these one-ring aromatic compounds produces alkylbenzenes, the substituent groups of which subsequently undergo cyclization and dehydrogenation to produce the two-ring PAH naphthalene. Combinations of aromatic molecules along with further additions of alkyl and alkenyl radicals lead to PAH of increasingly high molecular weight; PAH of sufficiently high molecular weight form a distinct phase, carbonaceous solid deposits.

Chapter 1. Introduction

1.1 Background and Literature Review

Hydrocarbon fuels used in future generations of high-speed jet aircraft will be exposed to increasingly high temperatures in the pre-combustion environment, due to the requirement that the fuels themselves be used as the primary coolant for the removal of excess heat from engine components. Projected requirements indicate that fuels used in this capacity may reach temperatures as high as 700 °C for periods on the order of minutes [1]. High pressure (up to 150 atm) is also necessary to maintain the fuel in a high-density state (conditions that are supercritical for most pure hydrocarbons as well as jet fuels [2]) so that sufficient heat transfer, not attainable by a low-density, gas-phase fluid, occurs.

While ambient air can provide an alternative heat removal medium, it is less efficient, as the structural components necessary to exchange heat to air are bulkier and heavier than those necessary to exchange heat to a high-density, supercritical-phase fuel. Exchanging heat to air also increases an aircraft's heat signature, a serious disadvantage if a plane is intended for military use. Another benefit to utilizing the fuel is that it allows waste heat to be stored and then later made available to the engine for propulsion during combustion [3].

Hydrocarbon fuels store heat not only by simple physical heating (accounting for the elevated temperature of the fuel) but also by undergoing endothermic chemical reactions that convert the fuel to higher-energy products [4]. Ideally, upon exposure to the stress of high temperature and pressure conditions, hydrocarbon fuels would break down into the highest-energy products, attaining the best possible heat sink from the fuel. For example, complete conversion of a kerosene fuel to ethylene would result in absorption of approximately 3560 kJ per kg of fuel converted [1]. Unfortunately, pyrolysis products are influenced by a number of

factors, and typically fall short of the ideal from the point of view of heat absorption, particularly at the high pressures encountered in the pre-combustion environment [5].

Since hydrocarbon fuels are natural in origin, their composition can vary significantly among separately produced fuels of the same type, and they are typically composed of hundreds of different chemicals. Pure compounds are attractive as jet fuels, since certain compounds will decompose into highly specific products; methylcyclohexane, for example, converts to toluene and hydrogen under thermal stressing [4]. However, the high cost of pure chemicals makes them unlikely candidates for the foreseeable future. The use of catalysts to enhance the selectivity for certain products and direct the fuel to higher energy products is also an option, but is still under development [5].

In addition to the fuel breaking down into less than favorable products in its role as a heat sink, other undesirable reaction pathways lead to a small fraction of fuel molecules being converted to insoluble products in the pre-combustion environment [6]. Over time, the increasing concentration of these insolubles leads to formation of a distinct solid phase, one that is harmful to the proper function of the turbine, that can clog fuel lines and injection nozzles, and that will eventually lead to decreased engine performance and even failure [1].

Oxygen, dissolved in the fuel by exposure to ambient air, is one source of these solids; fuel molecules react with dissolved oxygen to break down hydrocarbons through an autoxidative mechanism [7-13]. As shown below, oxygen initiates the reaction by abstracting hydrogen from a hydrocarbon fuel molecule to produce an alkyl radical. Propagation of the free radicals occurs when an alkyl radical and another oxygen molecule combine to yield a peroxide radical. These peroxide radicals can then abstract hydrogen from an alkane fuel molecule to produce another alkyl radical, further propagating the radical chain. Termination occurs when two radicals combine. Over time, a small portion of the non-polar hydrocarbon fuel is oxygenated, ultimately

resulting in the formation of polar compounds, which precipitate out of the bulk fuel to form soft, gum-like deposits.

$RH + O_2 \leftrightarrow R\cdot + HO_2\cdot$	*initiation*
$R\cdot + O_2 \leftrightarrow RO_2\cdot$	*propagation*
$RO_2\cdot + RH \leftrightarrow RO_2H + R\cdot$	*propagation*
$RO_2\cdot + RO_2\cdot \leftrightarrow$ Products	*termination*
$R\cdot + R\cdot \leftrightarrow$ Products	*termination*

By removing oxygen from the fuel or by adding antioxidants, the radical decomposition mechanism shown above can be avoided. Fuels deoxygenated to less than 1 ppm dissolved oxygen are essentially free from this low-temperature decomposition and are stable up to approximately 500 °C [7-8].

However, at temperatures greater than 500 °C, even deoxygenated hydrocarbon fuels will form solid deposits [1,7,14-18]. This temperature marks the transition from autoxidative to pyrolytic reactions being responsible for formation of solids. In the pyrolytic regime, oxygen is no longer necessary to produce free radicals; unimolecular decomposition of the fuel molecules themselves produces radicals.

Polycyclic aromatic hydrocarbons (PAH), compounds consisting of two or more fused aromatic rings, are believed to be the intermediates between the fuel and the solid deposits. Fourier transform infrared analysis of the solid deposits produced under high temperature (>500 °C), oxygen-free conditions reveals that they are composed of aromatic molecules [19], and pyrolysis of the purely aromatic reactants anthracene, phenanthrene, and 1-methylnaphthalene yields hydrocarbon coke as a byproduct [20-22]. Additionally, it has been shown that the quantity and ring-number of aromatic molecules increase with time in thermally stressed

hydrocarbon jet fuels concurrently with both fuel degradation to lighter hydrocarbon products and solid deposition [23]. Therefore it is believed that fuels first form small aromatic molecules that are initially soluble in the fuel. These aromatic molecules increase in size and ring-number under pyrolysis conditions, and eventually grow to be insoluble in the fuel such that they form a secondary phase, carbonaceous solid deposits. Unlike oxygenated compounds, which precipitate out of the fuel due to their polarity, these solids produced from pyrolytic reactions have too high a molecular weight to remain in the supercritical-phase fuel.

Hydrocarbon fuels are composed of approximately 60 % or more aliphatic compounds [5] with some coal-derived liquid fuels being entirely composed of alkanes [24]. Cyclic alkanes and aromatic molecules comprise the remainder. Since virtually all hydrocarbon fuels contain significant amounts of alkanes, an understanding of the response of alkanes to supercritical pyrolysis conditions, especially as it relates to the formation of PAH, is of critical importance to continued fuel system development.

Previous work on the formation of aromatics from the high-pressure pyrolysis of the alkane *n*-tetradecane [25] as well as actual jet fuels [26] showed an increase in cyclic alkanes with residence time and, once these cyclic alkanes achieved a sufficient concentration, an increase in aromatic molecules with time as well. Such results indicate that the linear alkane fuels first cyclize then dehydrogenate to form aromatic molecules. These studies had the limitation that large PAH (those with more than four aromatic rings) were not analyzed as part of the investigation. Therefore definitive conclusions regarding the formation of large PAH (and ultimately solid deposits) could not be made.

Studies on the supercritical pyrolysis of the model compounds toluene and 1-methylnaphthalene [27-32] identified PAH consisting of up to ten and nine rings, respectively, and gave important insight into the mechanism of PAH formation from these fuels. PAH were

found to have been “built up” to high-ring-number PAH by consecutive additions of aromatic molecules. It was also shown that the aromatic bonds of both the fuels and their pyrolysis products were too strong to break in the supercritical pyrolysis environment. Therefore lower-ring-number PAH are never produced by decomposition of higher-ring-number PAH.

The supercritical phase itself is an important factor to consider in the jet fuel pre-combustion environment. Supercritical fluids exhibit a number of properties that differ significantly from either the gas or liquid phases. Many of the physical properties, such as density, viscosity, and diffusivity are intermediate between those of a gas or a liquid and are strongly dependent on pressure and temperature [33]. Large variations in physical properties may occur with small changes in temperature and pressure, therefore reaction rates can be highly variable in a supercritical fluid, varying by orders of magnitude over a small range of reaction conditions [34].

Stewart *et al.* showed in their work regarding the supercritical pyrolysis of methylcyclohexane, decalin, and tetralin [35-36] that these reactants not only underwent conversion to products at a different rate, but also had different product distribution profiles compared to products of pyrolysis in the gas phase. Specifically, the interaction of solvent and solute is much more pronounced in the supercritical phase. Unlike the gas phase, which is characterized by long intervals of linear motion occasionally interrupted by relatively infrequent collisions, in the supercritical phase a molecule is constantly interacting with its neighbors. Such an environment creates what are known as “cage” effects, and reduces the likelihood of ring-opening reactions, which yield linear products, while simultaneously enhancing the formation of five- and six-membered ring products. Cage effects are especially important in studies of jet fuel decomposition; PAH products, known to be precursors to solid deposits, are among the cyclic products whose formation is enhanced.

1.2 Purpose of the Study

This work is a complement to previous studies of the supercritical pyrolysis of the model compounds toluene and 1-methylnaphthalene. Research on these aromatic reactants was highly effective at elucidating the reaction mechanisms governing the formation of large PAH (and by extension carbonaceous solid deposits), but to date no study has investigated the formation of large PAH from the supercritical pyrolysis of an alkane fuel.

A pure reactant, *n*-decane, was chosen as a model compound to represent the aliphatic component of real jet fuels. A model compound has the advantage of reducing the number of reactions taking place by reducing the number of reactants in the reaction environment, thereby simplifying the elucidation of reaction pathways. *n*-Decane was chosen as the reactant because of its similarity to actual fuels in terms of its critical temperature (344.5 °C) and pressure (20.7 atm). By comparison, the military jet fuels JP-7 and JP-8 have critical points of 396.7 °C, 20.8 atm and 411.1 °C, 23.1 atm respectively [5].

The *n*-decane reactant was pyrolyzed in a tubular flow reactor under supercritical conditions. The pyrolysis products were analyzed by gas and liquid chromatography in an effort to further develop specialized techniques for the analysis of PAH derived from supercritical alkane pyrolysis, to identify the products of this pyrolysis, to determine temperature- and pressure-dependent product yields, and to use this data to better understand the reaction mechanisms governing PAH formation in this reaction environment.

1.3 Structure of This Thesis

Chapter 2 presents the reactor system used in the experiments with the model compound *n*-decane to simulate the high-temperature, high-pressure pre-combustion environment to which real-world jet fuels will be exposed in engines currently under development. The experiments performed and the methods used to analyze the results of these experiments are presented.

Chapter 3 lists the products identified from supercritical *n*-decane pyrolysis and provides the evidence for their identifications. Chapter 4 presents the quantitative results of the pyrolysis experiments that are described in Chapter 2; product yields are presented, product formation mechanisms are shown, and yield trends with respect to temperature and pressure are explained. Finally Chapter 5 summarizes the conclusions drawn from the results shown in the previous three chapters and recommends future work in supercritical fuel pyrolysis research.

Chapter 2. Experimental Equipment and Analysis Techniques

2.1 Introduction

This chapter first presents the reactor system used in pyrolysis experiments with the model compound *n*-decane to simulate the high-temperature, high-pressure pre-combustion environment to which real-world jet fuels will be exposed in their capacity as a heat sink in future generations of high-speed jet aircraft. Following the reactor description, the methods used to analyze the products of these experiments are presented. Because *n*-decane produces a highly complex mixture of polycyclic aromatic hydrocarbon (PAH) products when exposed to high temperature and pressure conditions, analytical techniques which had never before been applied to supercritical fuel pyrolysis studies were developed for this work. Particular attention is paid to these PAH analysis techniques in the description of the product analysis methods.

2.2 Supercritical Fuel Pyrolysis Reactor System

The supercritical *n*-decane (critical temperature, 345ºC; critical pressure, 20.8 atm) pyrolysis experiments were conducted in an isothermal, isobaric reactor designed by Davis [37] and previously used by Stewart [35-36], Ledesma *et al*. [27], McClaine *et al*. [28-30], and Somers *et al.* [31-32] for supercritical pyrolysis of other model fuels. The reactor system, illustrated in Figure 2.1, consists of three basic parts: a fuel delivery pump, a heated reaction zone, and a product collection apparatus. Each of these parts is explained in this section.

Prior to an experiment, liquid fuel is sparged with nitrogen for three hours to remove any dissolved oxygen that could introduce auto-oxidative effects to the reaction system [38]. Once the oxygen is removed, the sparged fuel is loaded into a high-pressure syringe pump for delivery of the fuel to the reactor.

The reactor is a silica-lined stainless steel tube immersed in a temperature-controlled fluidized alumina bath. The silica lining prevents wall-catalyzed deposit formation that occurs

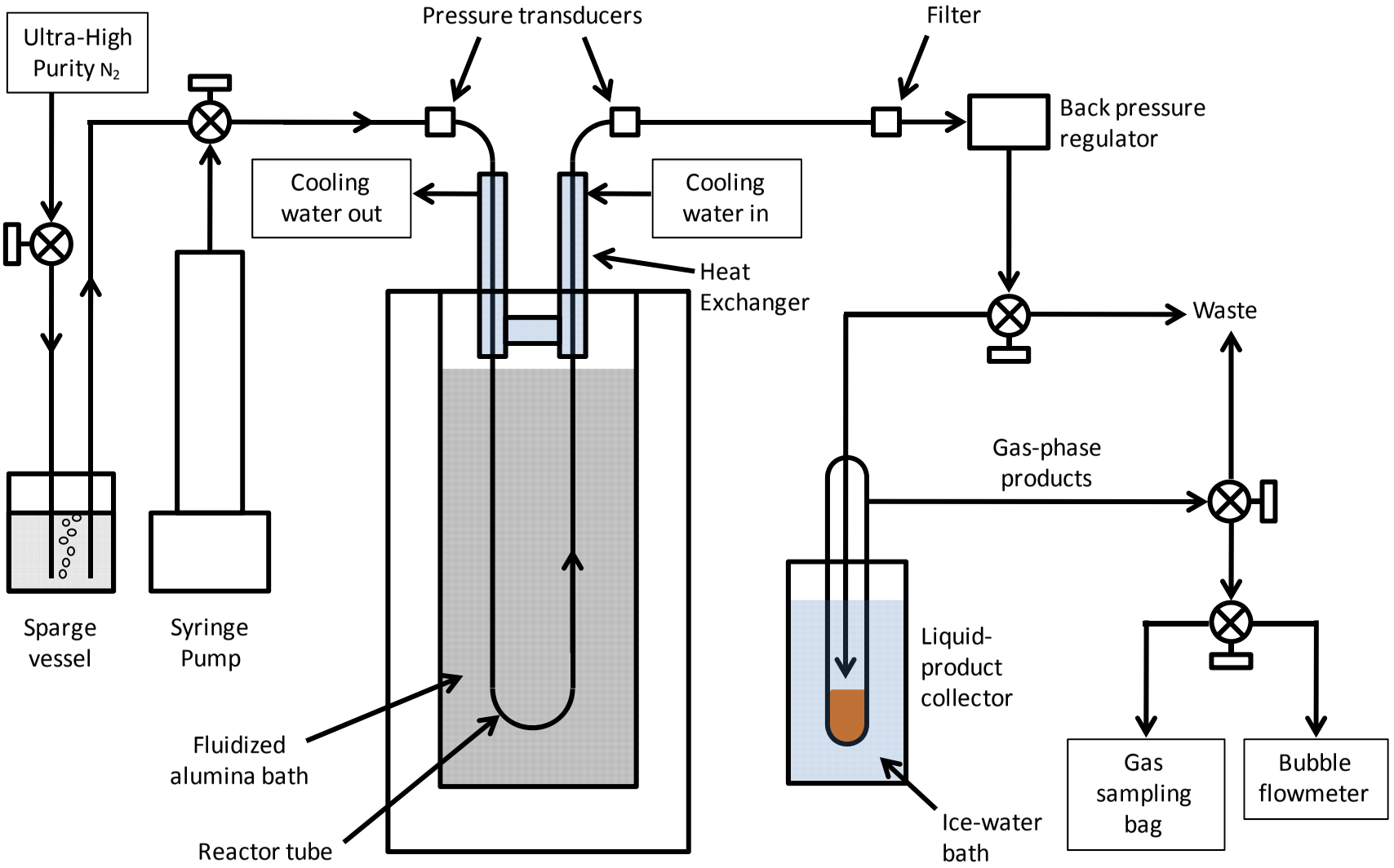

Figure 2.1 Schematic of the supercritical fuel pyrolysis reactor system

when reactants come into contact with unlined stainless steel [14,36-37]. The reactor tubing has an inner diameter of 2.16 mm and an outer diameter of 3.17 mm. The fluidized bath maintains the temperature inside the steel tubing (the reaction environment) and ensures isothermality throughout the reactor length.

As indicated in Figure 2.1, the silica-lined stainless steel tubing of the reactor extends upstream and downstream of the fluidized alumina bath and passes through a water-cooled (25 °C) shell-and-tube heat exchanger immediately before entering and after exiting the heated area. This configuration ensures a controlled thermal history for the reactants and a consistent, constant residence time in the alumina bath during each experiment. After passing through the downstream side of the heat exchanger, the quenched reaction products and unreacted *n*-decane pass through a stainless-steel filter (hole size, 10 μm) to trap any solids that may have formed inside the reactor, then pass through a dome-loaded back pressure regulator which maintains constant pressure inside the reactor. The products and unreacted fuel then proceed to the liquid- and gas-phase product collection apparatus, where they are separated by phase for later analysis. Note that the unreacted *n*-decane will be collected almost exclusively in the liquid phase; throughout this work, the liquid-phase products will be assumed to contain unreacted fuel unless specific attempts have been made to separate it from the liquid-phase products. As indicated in Figure 2.1, the gas and liquid separator of the product collection apparatus is immersed in an ice-water bath to ensure a consistent separation of phases in each run.

Experimental conditions were determined to mimic as closely as possible the conditions to which real-world jet fuels will be exposed in future-generation high-speed aircraft, conditions that could be as high as 150 atm and 700 °C for exposure times on the order of minutes [1]. A residence time of 140 sec was chosen for the *n*-decane pyrolysis experiments to approximate this exposure time and to be consistent with previous studies on model compounds in this reactor

system [27,30,32,35]. This time was set in the reactor system by the flowrate of the high pressure pump (50 mL/hr) and the length of the reactor tubing (53 cm) that is immersed in the fluidized alumina bath.

Two sets of experiments were performed, with either temperature or pressure as the independent variable. In the first set, six runs were performed at a constant pressure of 100 atm and constant temperatures of 530, 540, 550, 560, 565, and 570 °C. In the second set, six runs were performed at a constant temperature of 570 °C atm and constant pressures of 40, 60, 70, 80, 90, and 100 atm. These parameters were chosen to determine the effects of varying pressure and temperature on *n*-decane pyrolysis product yields at conditions relevant to the problem of solid formation in the pre-combustion environment. While more severe conditions are envisioned as possible, such conditions cause *n*-decane to form solids in quantities so great that they clog the reactor tubing, stopping the flow of the reactant through the reactor. (Prior to the two sets of experiments which were performed, several others were done to determine the conditions at which high quantities of PAH would be produced without producing solids in amounts too high to perform experimental runs.)

2.3 Product Analysis

As depicted in Figure 2.1, during each experiment unreacted fuel and pyrolysis products exit the back pressure regulator and enter the collection apparatus where gas and liquid products are separated. Gaseous reaction products are collected and analyzed by gas chromatography (GC) with flame-ionization detection (FID). Liquid products are removed from the collection apparatus at the conclusion of each experiment. Aliphatic, olefinic, and single-ring aromatic products are analyzed by GC/FID coupled to mass spectrometry (MS). Most of the liquid product mixture is reserved for analysis of PAH products by high-pressure liquid

chromatography (HPLC) coupled to ultraviolet-visible (UV) spectroscopy and mass spectrometry.

The next three sections describe each of the analysis methods applied to the products of supercritical *n*-decane pyrolysis. Analyses of gas- and liquid-phase products by gas chromatography are covered in Sections 2.3.1 and 2.3.2, respectively. Section 2.3.3 explains the details of a two-dimensional HPLC technique, developed specifically for this work, for separation of the PAH products and the use of UV spectroscopy and mass spectrometry to identify and quantify these PAH products.

2.3.1 Gas-Phase Product Analysis

During each experiment, gas-phase products are collected in a Teflon sampling bag, diluted in nitrogen, and injected onto an Agilent model 6980 GC/FID. Separation is achieved with a GS-GasPro fused silica capillary column (length, 30 m; inside diameter, 0.32 mm; manufactured by J&W Scientific). The carrier gas is helium at a flowrate of 5 mL/min. The injection volume is 1 mL and the split flow ratio is 5:1. The oven temperature is initially held at 35 ºC for 2 min, then ramped to 240 °C at a rate of 10 °C/min, and finally held constant for 10 min.

Products are identified primarily by matching elution times to those of reference standards. Products for which reference standards were not available are identified by their mass spectra, after injection of the gas-phase products from one experiment onto a GC/MS that employed the same separation method and column as the GC/FID.

Products are quantified by multiplying FID peak areas by response factors (RF). These response factors were determined by injecting a reference standard for each identified gas-phase product at a known concentration into the GC/FID. Several reference standards were injected at more than one concentration to confirm that products were injected onto the column at quantities

within the linear range of the FID detector and that the RF of these compounds had also been determined within this linear range. The RF of one quantified product, toluene, for which a reference standard in the gas phase was not available, was estimated by using the RF of benzene (for which a gas-phase standard was available) multiplied by a correction factor to account for the additional mass of the methyl group. This correction factor was determined by assuming that the ratio of the response of benzene and toluene was the same on the FID of the GC used for analyzing gas-phase samples and the FID of another GC used for analyzing samples in the liquid phase. Liquid-phase standards of both benzene and toluene were available.

2.3.2 Liquid-Phase Product Analysis by Gas Chromatography

After each experiment, liquid-phase products are collected, diluted in dichloromethane, and injected onto an Agilent model 6980 GC/FID in conjunction with an Agilent Model 5973 MS. Separation is achieved with a HP-5 fused silica capillary column (length, 30 m; inside diameter, 0.25 mm; film thickness, 0.1 μm; manufactured by J&W Scientific). The carrier gas is helium at a flowrate of 5 mL/min. The injection volume is 2 μL, and the split flow ratio is 5:1. The oven temperature is initially held at 40 ºC for 2 min, then ramped to 280 °C at a rate of 4 °C/min, and finally held constant for 30 min.

Products are identified either by examination of their mass spectra or comparison of their elution times to those of reference standards. Quantification is achieved by multiplying FID peak areas by response factors. The RF of aromatic products were determined by injecting into the GC/FID/MS reference standards of each identified product, at four different concentrations. The RF of aliphatic and olefinic products were estimated by using the RF of *n*-decane, injected into the GC/FID/MS at five different concentrations.

A single RF (that of *n*-decane, determined on a mass basis) was used for all *n*-alkane products because it has been shown that the FID response factors of *n*-alkanes will not differ

significantly from one another when determined on a mass basis [39]. Furthermore, during the calibration of the GC used for the analysis of gas-phase products, the RF of *n*-alkanes were found not to vary appreciably from their 1-alkene counterparts with the same number of carbons, leading to the conclusion that the RF of 1-alkenes could also be accurately estimated by using the RF of *n*-decane. (Comparisons between alkane and alkene RF were made only between those of compounds of nearly the same molecular weight because the RF of gas-phase products were determined on a molar as opposed to mass basis.)

2.3.3 Liquid-Phase Product Analysis by High Pressure Liquid Chromatography

PAH products of supercritical *n*-decane pyrolysis in the liquid phase were analyzed by high-pressure liquid chromatography (HPLC) coupled to diode-array ultraviolet-visible absorption (UV) spectroscopy and mass spectrometry (MS). UV spectroscopy and mass spectrometry are detection tools ideally suited to the identification of PAH products. Identification of PAH will be explained later in this section, but the key fact to understand at this point is that good component resolution must first be achieved by HPLC before product identification is possible.

To achieve good component resolution, a two-dimensional HPLC technique was developed in which PAH are separated based on two different aspects of their chemical structure. This scheme, outlined in Figure 2.2, is explained in detail in Section 2.3.3.1, but first the need for such a complex scheme is demonstrated by comparing the products of supercritical *n*-decane pyrolysis to those of toluene.

In previous supercritical fuel pyrolysis studies [27-32], a reversed-phase Restek Pinnacle II PAH octadecylsilica (C18) column, used in conjunction with a time-programmed sequence of the solvents acetonitrile/water, acetonitrile, and dichloromethane, gave the best component resolution of all available HPLC separation methods. Figure 2.3 presents an HPLC

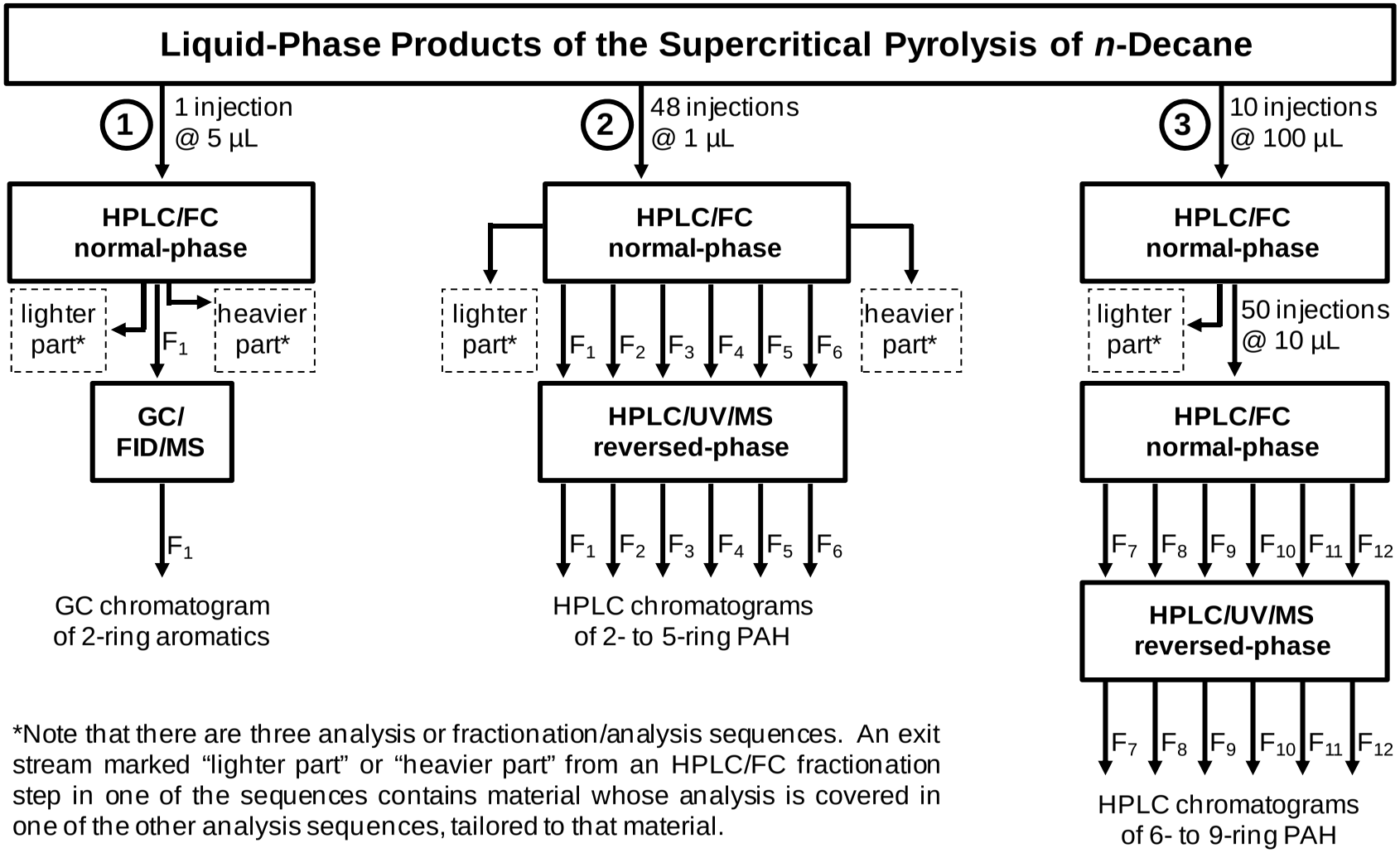

Figure 2.2. The fractionation and analysis scheme for the liquid-phase products of the supercritical pyrolysis of *n*-decane. Large circled numbers denote sequence number. “F_x” denotes “fraction number x.”

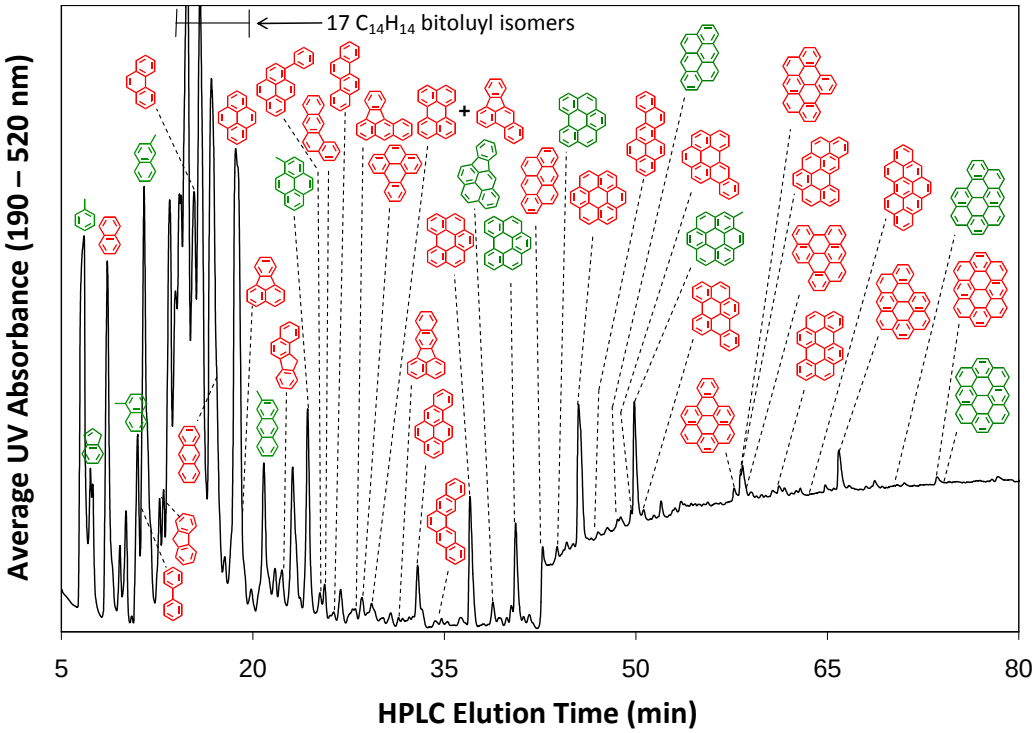

Figure 2.3 Reversed-phase HPLC chromatogram of products of supercritical toluene pyrolysis at 535 ºC, 100 atm, and 140 s residence time. The rise in the baseline at ~43 min is due to a change in the mobile phase to the UV-absorbing dichloromethane. Identified components, in order of elution, from left to right, are: toluene, indene, naphthalene, 1-methylnaphthalene, bi-phenyl, 2-methylnaphthalene, fluorene, phenanthrene, anthracene, fluoranthene, pyrene, 2-methylanthracene, benzo[*a*]fluorene, 1-methylpyrene, 1-phenylpyrene, benz[*a*]anthracene, chrysene, benzo[*a*]fluoranthene, benzo[*e*]pyrene, benzo[*b*]fluoranthene co-eluting with perylene, benzo[*k*]fluoranthene, benzo[*a*]pyrene, pentaphene, benzo[*ghi*]perylene, indeno[1,2,3-*cd*]pyrene, methylated benzo[*ghi*]perylene, anthanthrene, methylated benzo[*ghi*]perylene, coronene, naphtho[2,1-*a*]pyrene, methylated anthanthrene, dibenzo[*b*,*ghi*]perylene, 1-methylcoronene, dibenzo[*e*,*ghi*]perylene, benzo[*a*]coronene, phenanthro[5,4,3,2-*efghi*]perylene, benzo[*cd*]-naphtho[8,1,2,3-*fghi*]perylene, benzo[*ghi*]naphtho[8,1,2-*bcd*]perylene, benzo[*pqr*]naphtho-[8,1,2-*bcd*]perylene, tribenzo[*cd*,*ghi*,*lm*]perylene, naphtho[8,1,2-*abc*]coronene, methylated naphtho[8,1,2-*abc*]coronene, ovalene, and methylated ovalene. Data from McClaine and Wornat [27-30].

chromatogram of the PAH products of toluene stressed in the supercritical fuel pyrolysis reactor for 140 sec at 535 °C and 100 atm. This chromatogram was generated by first separating the products with the C18 column and time-programmed solvent sequence described above, then identifying the separated components by their UV and mass spectra. In the labeling convention followed in this chromatogram and all others presented in this work, red structures indicate unsubstituted PAH and green structures indicate PAH with a single methyl group (the position of which is labeled when known). Except for the cluster of 17 $C_{14}H_{14}$ bi-toluyls (which are better resolved by gas chromatography and thus analyzed by that means), the chromatogram of Figure 2.3 shows excellent component resolution, as is evident in the clearly defined individual component peaks. (The rise in baseline at 43 min in Figure 2.3 is not due to unresolved material but to dichloromethane, which absorbs in the UV and is introduced into the HPLC solvent program at this time.)

In contrast to the products of an aromatic fuel like toluene, *n*-decane pyrolysis products are a much more complex mixture of unsubstituted and alkylated PAH. Figure 2.4 presents an HPLC chromatogram of the products of *n*-decane pyrolyzed in the supercritical fuel reactor at 570 °C, 100 atm, and 140 sec. The convention for labeling component peaks is the same as used in Figure 2.3, with the addition of blue labels indicating (in this and all other figures in this work) alkylated PAH whose aromatic structure is known, but the number(s), identity(s), and/or location(s) of the alkyl substituent(s) are not known with certainty. This chromatogram was generated with the same sequence of solvents and a C18 column similar to the one used to separate the products of toluene pyrolysis in Figure 2.3. (There are some differences between the time programming of the solvents and the dimensions of the column used in the generation of these two chromatograms, but these differences affect the separation only slightly). Several of the compounds eluting in the first 32 min in Figure 2.4 are well resolved, and 51 of the product

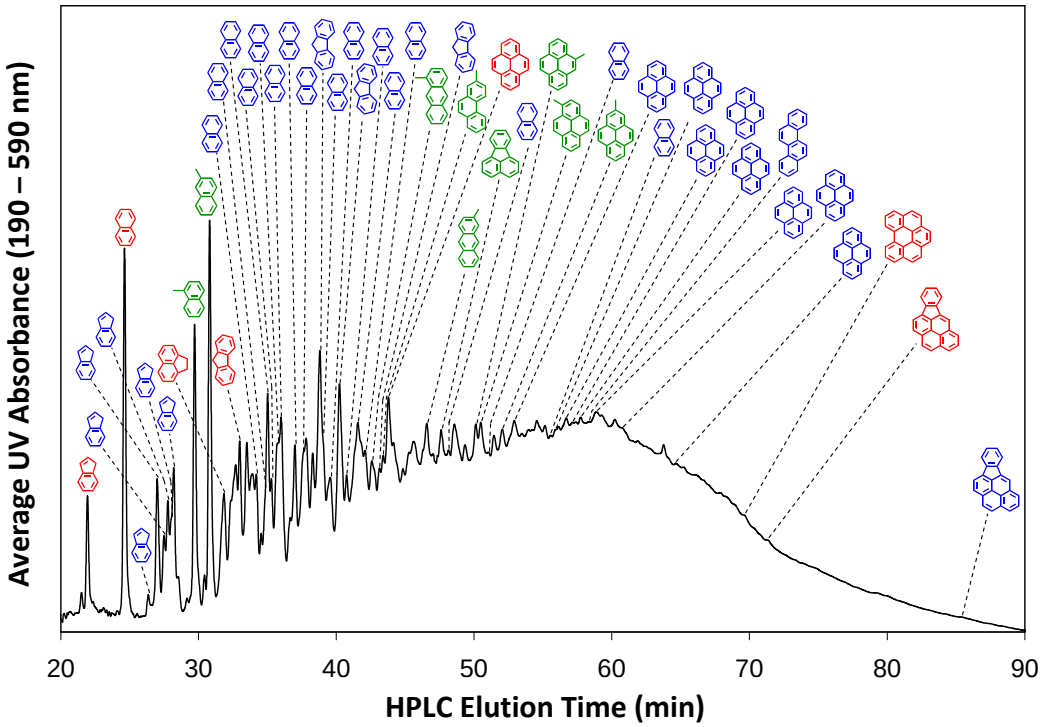

Figure 2.4 Reversed-phase HPLC chromatogram of products of supercritical n-decane pyrolysis at 570 ºC, 100 atm, and 140 s residence time. Identified components, in order of elution, from left to right, are: indene, naphthalene, six alkylated indenes, 1-methylnaphthalene, 2-methylnaphthalene, fluorene, eight alkylated naphthalenes, alkylated fluorene, three alkylated naphthalenes, 1-methylanthracene, alkylated fluorene, 2-methylphenanthrene, pyrene, methylated fluoranthene, alkylated naphthalene, 4-methylpyrene, 1-methylpyrene, alkylated naphthalene, 2-methylpyrene, alkylated pyrene, alkylated naphthalene, four alkylated pyrenes, chrysene, three alkylated pyrenes, benzo[*ghi*]perylene, indeno[1,2,3-*cd*]pyrene, and alkylated indeno[1,2,3-*cd*]pyrene.

components in Figure 2.4 are well-enough resolved to permit identification by their UV spectra—although there are varying degrees of specificity in these identifications. There are seven unsubstituted PAH whose exact identities are certain, eight methylated PAH with the methyl groups in positions which are known, and 36 other PAH for which the aromatic portion of the structure is known, but the number, identity(s), or location(s) of the alkyl substituent(s) are not. However, the rise in the baseline, starting at 32 minutes in Figure 2.4, is due to the merging of product component peaks, a result of too many products eluting from the column at the same time and indicative of poor chromatographic resolution.

To overcome the limitations of a single reversed-phase C18 column, a two-dimensional chromatographic technique was developed based on a method originally employed by Wise *et al.* [40]. The necessary component resolution of the *n*-decane pyrolysis products is achieved by first separating the product mixture in one HPLC column on the basis of the aromatic structure, then separating in a second HPLC column on the basis of both aromatic structure and alkyl substitution.

In the first dimension of separation, the liquid-phase *n*-decane pyrolysis products are separated on a normal-phase cyano stationary phase HPLC column. The lone pair of electrons on the cyano functional groups of the stationary phase interact directly with the pi-bonding electrons of the PAH analyte while at the same time interacting very little with any alkyl substituents. Therefore the normal-phase HPLC column separates unsubstituted and alkylated PAH into groups based on aromatic structure only, i.e. benzene and all alkylbenzenes elute together first, followed by naphthalene and alkylnaphthalenes, followed by three-ring PAH and their alkylated derivatives, and so on. Parent PAH of a particular molecular weight and their alkylated derivatives (daughter compounds) are collected as individual "fractions" from the normal-phase column. These fractions are then shot onto a reversed-phase C18 HPLC column for the second dimension of separation, which is sensitive to both the aromatic structure and to any alkyl substituents of the PAH that might be present. Once products are fully resolved by the C18 column, they are identified and quantified by ultraviolet-visible spectroscopy and mass spectrometry. Therefore the liquid product mixture from each experiment generates several reversed-phase HPLC chromatograms, one for each normal-phase HPLC fraction.

2.3.3.1 Product Separation and Identification

Figure 2.2 outlines the different fractionation and analysis steps developed for the analysis of PAH products from supercritical *n*-decane pyrolysis. All of the normal-phase HPLC

fractionation steps of Figure 2.2 are performed on an Agilent Model 1200 HPLC with diode-array UV absorbance detector and fraction collector (FC). For product fractionation, the HPLC/FC instrument is equipped with two normal-phase cyano columns in series (each with diameter, 4.6 mm; length, 250 mm; particle size, 5 μm) maintained at 11 °C with 1 mL/min of hexane used as the mobile phase. The different fractions are collected over different ranges of elution time on the normal-phase column—each fraction corresponding to PAH of a common ring number or isomer group, along with the alkylated derivatives of those PAH or isomer groups. Table 2.1 presents the characteristics of the main constituents of the twelve fractions obtained. For each fraction, the "primary constituents" are the unsubstituted parent PAH isomer families collected in that fraction. Alkylated derivatives of these isomer families are also collected in each fraction and actually make up the bulk of the products.

Table 2.1 Contents of the 12 Normal-Phase HPLC Fractions of an *n*-Decane Product Mixture

Fraction Number	Primary Constituents
1	2-ring, C_8H_{10}
2	3-ring, $C_{13}H_{10}$
3	3-ring, $C_{14}H_{10}$
4	4-ring, $C_{16}H_{10}$
5	4-ring, $C_{18}H_{12}$
6	5-ring, $C_{20}H_{12}$
7	6-ring, $C_{22}H_{12}$; 7-ring, $C_{24}H_{12}$
8	6-ring, $C_{24}H_{14}$
9	7-ring, $C_{26}H_{14}$ and $C_{28}H_{16}$
10	8-ring, $C_{28}H_{14}$
11	7-ring, $C_{28}H_{16}$
12	9-ring, $C_{30}H_{14}$

The analysis scheme shown in Figure 2.2 is broken into three sequences, each tailored to a particular range of product components and designated by a circled number, 1 through 3.

Sequences 2 and 3 are used to identify two- to nine-ring PAH products and quantify three- to nine-ring products. Two-ring aromatic products are quantified by Sequence 1: First 5 μL of the liquid-phase products are sent through a single normal-phase fractionation step to isolate two-ring aromatic products (Fraction 1 in Figure 2.2 and Table 2.1). This material is then injected onto the GC/FID/MS with the injection solvent hexane, and the products are quantified in the manner explained in Section 2.3.2.

Analysis of the remaining product PAH requires the other two sequences: Sequence 2 for the 2- to 5-ring PAH; Sequence 3 for the 6- to 9-ring PAH. Sequence 2 begins with a normal-phase fractionation step on the HPLC/FC, which separates the products into six fractions. To collect enough material in each of the Fractions 1-6, the fractionation actually involves 48 separate 1-μL injections of liquid-phase products, each going through a complete HPLC run before the next injection can be made. (Better resolution is obtained from smaller-diameter columns and smaller injections; hence the need for numerous injections.) After 48 rounds of the fractionation step, sufficient material is collected for the first six fractions. The fractions are then concentrated down and subjected to reversed-phase HPLC/UV/MS analysis for compositional analysis of the 2- to 5-ring PAH products, as indicated at the bottom of Sequence 2 in Figure 2.2.

The 6- to 9-ring PAH products are produced in yields that are orders of magnitude lower than those of the smaller-ring-number aromatics, so two fractionation steps are needed in order to obtain sufficient material in Fractions 7-12. As indicated in Sequence 3 of Figure 2.2, the first fractionation step (ten injections of 100 μL of material) accomplishes the removal of the lighter material and isolates the heavier PAH. This material is then condensed down, first in a Kuderna-Danish apparatus, then by blowing nitrogen to evaporate almost all of the remaining solvent. The second fractionation step—accomplished in 50 consecutive runs, each with 10 μL of material—separates the heavier PAH according to ring number and isomer group, in the 6- to 9-ring PAH

Fractions 7-12, as indicated in Table 2.1. Each of the Fractions 7-12 is then concentrated down and analyzed by reversed-phase HPLC/UV/MS, as described below, to achieve compositional analysis of the 6- to 9-ring PAH products of *n*-decane.

In order to determine the identities and quantities of the PAH products of supercritical fuel pyrolysis, each of the 12 normal-phase HPLC fractions of the liquid-phase product mixture is concentrated in a Kuderna-Danish apparatus and exchanged, under nitrogen, into 40 μL of dimethylsulfoxide, a solvent compatible with the solvents used in the reversed-phase HPLC method employed for PAH analysis. During the concentration and solvent-exchange procedure, portions of the more volatile aromatics, such as the 1- and 2-ring species, are lost to vaporization; hence these lighter aromatic products are quantified by gas chromatographic analysis as described in Section 2.3.2.

For analysis of the large aromatic products (> 3 rings) by reversed-phase HPLC, a 1- or 5-μL aliquot of the product/dimethylsulfoxide solution is injected onto an Agilent Model 1100 high-pressure liquid chromatograph, coupled to a diode-array ultraviolet-visible (UV) absorbance detector in series with a mass spectrometer (MS). Employing atmospheric-pressure photo-ionization, the MS monitors mass-to-charge ratios up to 700. The reversed-phase HPLC utilizes a Restek Pinnacle II PAH octadecylsilica column with length, 250 mm; inner diameter, 2.1 mm; and particle size, 4 μm. A time-programmed sequence of solvents, explained in detail in Section 2.3.3.2, is pumped through the column, and the PAH product components elute in order of increasing molecular size. UV absorbance spectra are taken every 0.8 sec and mass spectra are taken every 1 sec of the separated components as they exit the column.

The mass spectrum establishes the C_xH_y formula of the PAH, its molecular mass, and whether there are any substituent groups like methyl attached to the aromatic structure. The UV spectrum establishes the exact aromatic structure of the PAH, so for unsubstituted PAH, the UV

spectrum alone is sufficient to establish the exact isomer-specific identity. If a PAH has an alkyl substituent, the UV spectrum looks almost exactly like that of the parent PAH, only shifted a few nm to higher wavelength—the position(s) and length(s) of the substituent(s) dictating the details of the shift [41,42]. Therefore, for PAH, which have a multitude of sites at which substituents can be located, one must have reference standards of all possible positional isomers in order to be certain of the exact position of the alkyl substituent—a condition rarely met for large PAH or for PAH with multiple alkyl groups. Consequently, for many of the alkylated PAH products reported in Chapter 3 of this work, the exact structure of the aromatic portion of the PAH is known (from the UV spectrum), but there is uncertainty associated with the number, positions, and/or lengths of the alkyl substituents.

Figure 2.5 is an example of the identification of one PAH product from *n*-decane pyrolysis. The mass spectrum (shown in the figure inset) establishes that this product has a molecular weight of 202, corresponding to the PAH isomer family with the chemical formula $C_{16}H_{10}$. Comparison of the UV absorbance spectrum of this product (the solid line in the figure) to that of a reference standard of the PAH pyrene (dashed line), rules out all possible $C_{16}H_{10}$ isomers except pyrene, and allows this product to be unequivocally identified as pyrene.

PAH products from the supercritical fuel pyrolysis experiments are identified by matching HPLC retention times, mass spectra, and UV absorbance spectra with those of our PAH reference standards, which include both commercially available compounds as well as PAH that have been specially synthesized for our identification efforts. In some cases, in which reference standards are not available, product identities are established by matching UV spectra with those published in the literature for those compounds.

Identified PAH are quantified by multiplying the UV peak areas of products by response factors, determined from extensive calibration of the HPLC/UV instrument with reference

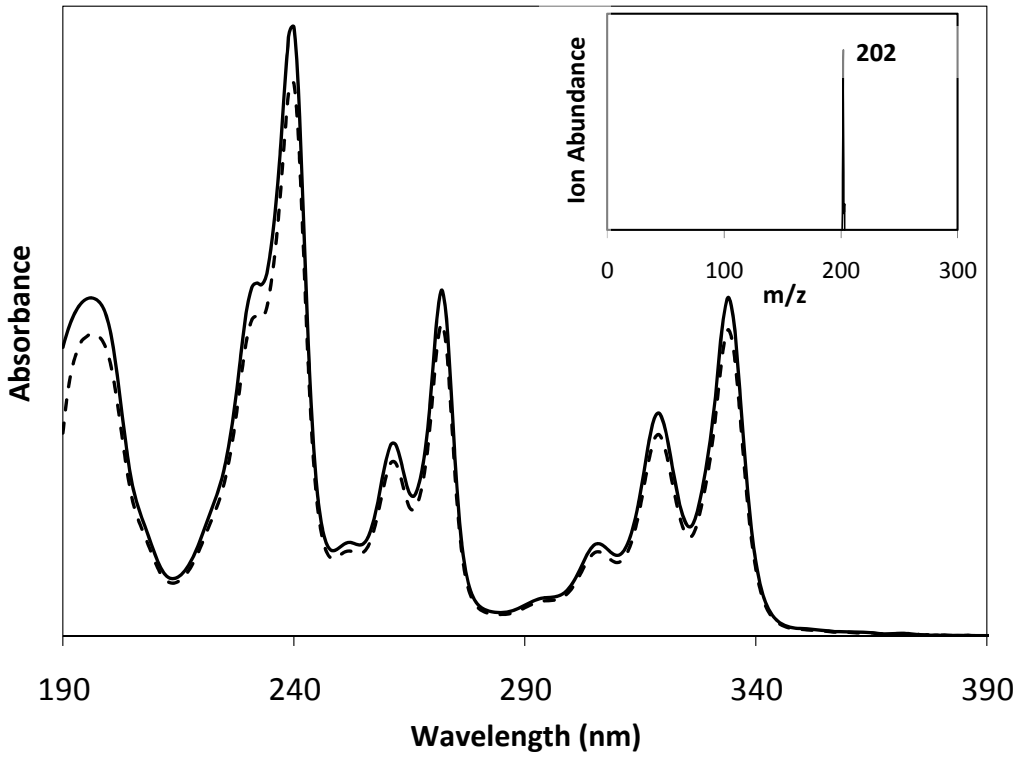

Figure 2.5 The UV spectrum of a PAH product (solid) of supercritical *n*-decane pyrolysis, overlaid with the spectrum of a reference standard of pyrene (dashed). The mass spectrum (inset) of the product determines that this product belongs to the $C_{16}H_{10}$ isomer family. The UV spectral match unequivocally identifies this product as pyrene and rules out any other isomers.

standards while taking into account nonlinearities in the response of diode-array detectors at high analyte concentrations [43]. Response factors were not available for every unsubstituted PAH, however it has been shown [44] that when UV absorbance is integrated over the entire range of wavelengths over which a PAH absorbs, the integrated UV absorbance per mass varies very little from one PAH to another. Therefore for a product that did not have an available reference standard the RF of a PAH with the nearest molecular weight for which a RF was available was used instead.

Response factors for methylated PAH are approximated by multiplying the mass-based RF of the parent compound by a correction factor equal to the molecular weight of the daughter compound divided by the molecular weight of the unsubstituted parent compound. This

approximation is possible because integrated UV response of a PAH and its methylated derivatives are the same on a molar basis [41].

Since the number of possible PAH structures grows exponentially with ring number [42], the HPLC/UV/MS technique is particularly well suited for analyzing the large PAH molecules that are precursors to fuel-line carbonaceous solids. The HPLC separates each product component; the mass spectrum narrows the field of possible component identities to a particular C_xH_y isomer group; and the fingerprint UV spectrum then permits the exact designation of the aromatic portion of the product component. The power of the HPLC/UV/MS method—in the analysis of the supercritical fuel pyrolysis products from *n*-decane—is illustrated in Chapter 3, where product identifications are described individually.

2.3.3.2 Solvent Methods for the Second Dimension of HPLC Separation

Six different HPLC solvent methods were used for the reversed-phase HPLC analysis steps of Figure 2.2. For identification of the maximum number of compounds in each of the twelve fractions, a solvent method developed previously [27-32] for PAH products of aromatic fuels was found to work very well. This method was also found to give peak resolution such that the products of Fractions 7-12 could also be quantified once they were separated by this method. In addition to this method, five more solvent methods were developed for Fractions 2 through 6 to achieve maximum separation among the unsubstituted and singly methylated PAH. These methods were used to quantify the products in these fractions. All six methods are described below.

For maximum product identification of all fractions and quantification of products found in Fractions 7-12, the fraction is shot onto a Restek Pinnacle II PAH octadecylsilica (C18) column of length, 250 mm; inner diameter, 2.1 mm; and particle size, 4 μm. The column is maintained at 30 °C with an initial solvent mixture of 60/40 water/ACN. The solvent is ramped

at a continuous rate to pure ACN over 60 min, and held for 30 min. The solvent is then ramped to pure DCM at a continuous rate for 60 min, and held for 30 min. The solvent flow rate through the column is 0.2 mL/min.

Fractions 2 through 6 in Figure 2.2 are each shot onto the C18 column with a solvent method specifically tailored to that fraction for quantification of unsubstituted and singly methylated PAH. In each method a water/acetonitrile solvent at a specific ratio is pumped isocratically through the column at 0.2 mL/min. The water/acetonitrile ratio, column temperature, and duration of each method are listed in Table 2.2. Examples of chromatograms of Fractions 2 through 6, generated by these methods, are presented in Appendix A.

Table 2.2 HPLC methods for the quantification of liquid-phase PAH products of supercritical *n*-decane pyrolysis in Fractions 2 through 6.

Fraction	ACN/H_2O ratio	Duration (min)	Temperature (°C)
2	50/50	70	40
3	65/35	30	40
4	65/35	40	40
5	60/40	50	50
6	65/35	60	50

2.3.3.3 Determination of Fraction Elution Times

Before the fractionation of a liquid-phase product mixture could be performed, it was necessary to determine when individual PAH products or PAH isomer groups eluted from the normal-phase cyano HPLC column. The divisions of the first six fractions were determined by shooting onto the column a mixture of pure, unsubstituted PAH reference standards representative of the products in the sample. Figure 2.6 presents a normal-phase HPLC chromatogram of this standard solution separated on the cyano column, with fraction demarcations labeled.

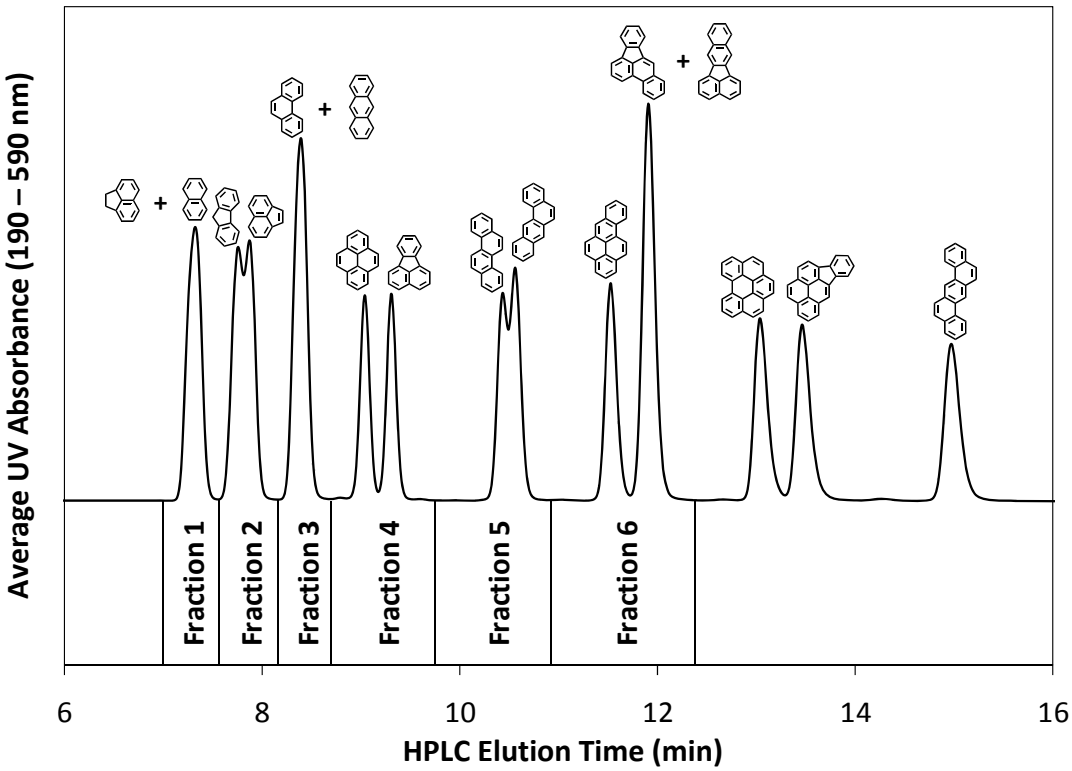

Figure 2.6 A normal-phase HPLC chromatogram of a reference standard solution of 16 PAH and demarcations of the first six fractions as determined by this chromatogram

To determine the division of the last six fractions, the cyano columns were installed in the HPLC/UV/MS, and liquid-phase products from one of the *n*-decane pyrolysis experiments were injected repeatedly onto the column. For each successive injection, a different single-ion mass was monitored with the mass spectrometer. (The high-molecular weight, later-eluting PAH products are produced in such low yields that only one ion mass could be monitored per run for a sufficiently strong signal to be detected.) Demarcation times for Fractions 7-12 were determined in the same manner as for Fractions 1-6 but with each fraction encompassing entire isomer groups rather than one or a few PAH products.

2.4 Concluding Remarks

The experimental methods used to conduct the *n*-decane supercritical pyrolysis experiments have now been presented, and the analytical techniques employed to analyze the

pyrolysis products resulting from these experiments have been described in detail. In the next chapter, application of these techniques is demonstrated by listing the *n*-decane pyrolysis products identified with these techniques and presenting the evidence for these identifications.

Chapter 3. Product Identification

3.1 Introduction

This chapter provides the evidence for identifications of the products of supercritical *n*-decane pyrolysis. Products generated during pyrolysis fall into three categories: gas-phase light hydrocarbons; liquid-phase aliphatic, olefinic, and single-ring aromatic compounds; and polycyclic aromatic hydrocarbons (PAH). The components in each of these three are separated by different chromatographic techniques, as described in the previous chapter, and are then identified by UV spectroscopy, mass spectrometry, and/or elution time data. In the following sections, the identified *n*-decane pyrolysis products are listed and then the evidence supporting their identification is given. The first two sections cover gas- and liquid-phase products analyzed by GC; these include aliphatic, olefinic, and single-ring aromatic compounds. Following those two sections is a section covering PAH products.

3.2 Gas-Phase Product Identification

Products in the gas phase are separated by gas chromatography as described in Section 2.3.1; they are identified either by matching product GC elution times to those of reference standards or by examination of their mass spectra. The gas-phase products of supercritical *n*-decane pyrolysis are shown in Table 3.1 with their chemical formulas, molecular masses, and chemical structures. C_1 to C_4 hydrocarbon gases and benzene are identified by comparison of the GC elution times of these products to those of reference standards. Toluene, *n*-pentane, and 1-pentene are identified by examination of their mass spectra.

3.3 Liquid-Phase Product Identification by Gas Chromatography

Products in the liquid phase are separated by gas chromatography as described in Section 2.3.2; they are identified either by matching product GC elution times to those of reference standards or by examination of their mass spectra. For some compounds, both mass spectral and

Table 3.1 Gas-phase products of supercritical *n*-decane pyrolysis.

Product	Chemical Formula	Molecular Mass (Da)	Structure
Methane	CH_4	16	CH_4
Ethane	C_2H_6	30	$H_3C\text{-}CH_3$
Ethylene	C_2H_4	28	$H_2C{=}CH_2$
Propane	C_3H_8	44	
Propene	C_3H_6	42	
n-Butane	C_4H_{10}	58	
1-Butene	C_4H_8	56	
1,3-Butadiene	C_4H_6	54	
n-Pentane	C_5H_{12}	72	
1-Pentene	C_5H_{10}	70	
Benzene	C_6H_6	78	
Toluene	C_7H_8	92	

GC elution time data are available and used for identification. The liquid-phase products of supercritical *n*-decane pyrolysis are shown in Table 3.2 along with their chemical formulas, molecular masses, and chemical structures. (The products benzene, toluene, *n*-pentane, and 1-pentene are present in both the gas and liquid phases; they are listed in Table 3.1.)

n-Alkanes and 1-alkenes present in the liquid phase are identified by examination of their mass spectra. Benzene, toluene, ethylbenzene, and the three xylene isomers are identified by matching GC elution times and mass spectra to those of reference standards. Several alkylbenzenes with alkyl substituents composed of three or more carbons are identified by examination their mass spectra. Isopropylbenzene, *n*-propylbenzene, and *n*-butylbenzene have distinct mass spectra and can be confidently identified by their mass fragmentation patterns alone. Four more alkylbenzenes with alkyl substituents composed of three carbons and five

Table 3.2 Liquid-phase aliphatic, olefinic, and single-ring aromatic products of supercritical *n*-decane pyrolysis. (Benzene, toluene, *n*-pentane, and 1-pentene, present in both the gas and liquid phases, are shown in Table 3.1.)

Product	Chemical Formula	Molecular Mass (Da)	Structure
n-Hexane	C_6H_{14}	86	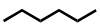
1-Hexene	C_6H_{12}	84	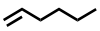
n-Heptane	C_7H_{16}	100	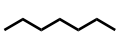
1-Heptene	C_7H_{14}	98	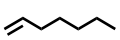
n-Octane	C_8H_{18}	114	
1-Octene	C_8H_{16}	112	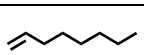
n-Nonane	C_9H_{20}	128	
1-Nonene	C_9H_{18}	126	
Ethylbenzene	C_8H_{10}	106	
o-Xylene	C_8H_{10}	106	
m-Xylene	C_8H_{10}	106	
p-Xylene	C_8H_{10}	106	
Isopropylbenzene	C_9H_{12}	120	
n-Propylbenzene	C_9H_{12}	120	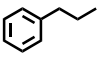
n-Butylbenzene	$C_{10}H_{14}$	134	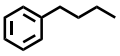

others with alkyl substituents composed of four carbons are also identified, but based on the mass spectra of these nine compounds a determination could not be made regarding the number, positions, or lengths of their various alkyl substituent groups.

3.4 Identification of PAH Products

As described in Section 2.3.3, PAH product identifications are achieved through the use of a two-dimensional high-pressure liquid chromatographic (HPLC) technique with diode-array

ultraviolet-visible (UV) spectroscopy and mass spectrometry (MS). After the first dimension of HPLC separation, in which the liquid product mixture is separated by aromatic structure into 12 fractions, a second HPLC separates the product components of each fraction individually so that a combination of UV and mass spectral evidence and elution time data can be used to identify each PAH product.

PAH product identifications are presented in the following sections, with a section devoted to each of the twelve fractions of the liquid-phase samples generated from the *n*-decane pyrolysis experiments (Fractions 10 and 12 are combined in a single section). In each section, products identified in a particular fraction are first presented, then the evidence supporting these identifications is given.

3.4.1 Identification of PAH Products in Fraction 1

The first fraction of the condensed-phase products of supercritical *n*-decane pyrolysis contains the two-ring PAH naphthalene and its alkylated derivatives. Figure 3.1 presents a reversed-phase HPLC chromatogram of this fraction of the products from the highest stressing experimental conditions (570 °C and 100 atm). The convention used for labeling chromatographic peaks is the same as used throughout this chapter: red labels represent unsubstituted PAH; green labels represent singly methylated PAH (with the location of the methyl group labeled when known); and blue labels represent alkylated PAH for which the number, position(s), and/or length(s) of the various alkyl substituent groups are not known. A blue PAH label does not necessarily indicate that a PAH does not have a single methyl group; it means that knowledge of the alkyl group(s) is not available.

As can be seen in Figure 3.1, Fraction 1 includes naphthalene and 49 alkylated derivatives of naphthalene. The aromatic structure as well as the the positions and identities of attached alkyl groups are known for the compounds naphthalene, 1-methylnaphthalane,

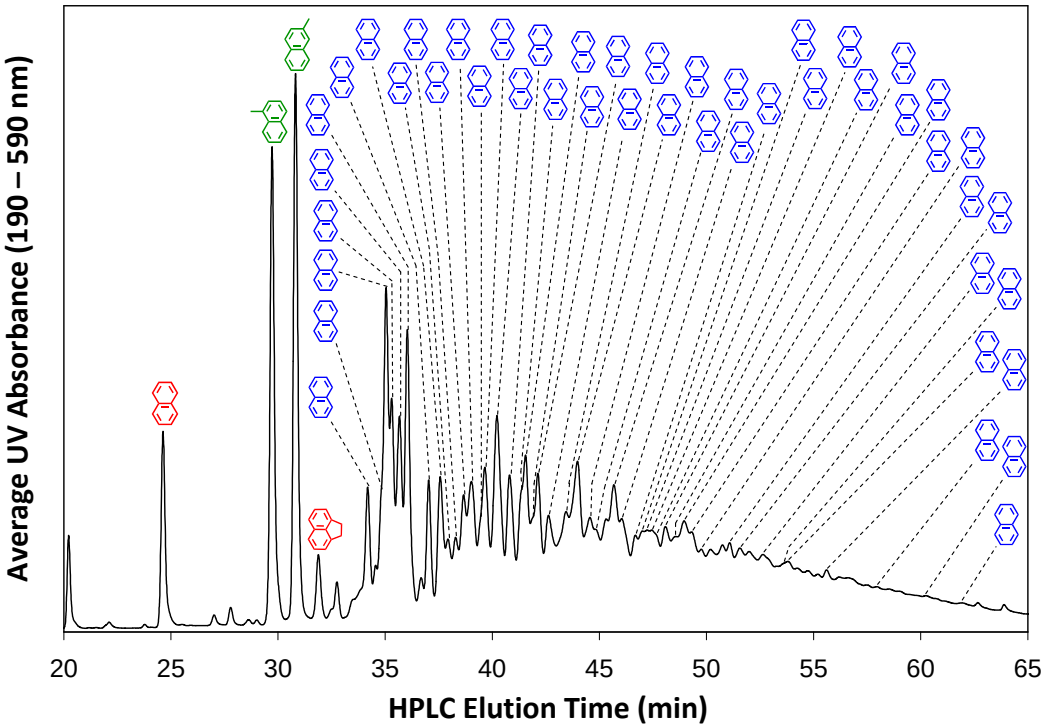

Figure 3.1 A reversed-phase HPLC chromatogram of the first fraction of the liquid-phase products of *n*-decane pyrolyzed at 570 °C and 100 atm. This fraction contains the two-ring PAH naphthalene and its alkylated derivatives. Red labels represent unsubstituted PAH; green labels represent singly methylated PAH; blue labels represent alkylated PAH that have substituents whose number, positions, and/or identities are not known with certainty.

2-methylnaphthalene, and acenaphthene. These four compounds, along with their chemical formulas, molecular masses, and structures are displayed in Table 3.3. The other 46 alkylated naphthalenes have substituents whose number, positions, and/or identities are not known with certainty.

Figures 3.2 and Figures 3.3a through 3.3c display the UV spectra of the four products of Table 3.3, overlaid with their respective reference spectra. A UV spectral match unequivocally identifies each of these compounds. While no additional information is necessary to establish the identity of these products, HPLC elution times also match those of reference standards of these four compounds. Furthermore, the mass spectra of naphthalene, 1-methylnaphthalane, and 2-methylnaphthalene (insets in Figures 3.2, 3.3a, and 3.3b) also show that the molecular weights

Table 3.3 PAH products identified in the first fraction of liquid-phase products of supercritical *n*-decane pyrolysis.

Product	Chemical Formula	Molecular Mass (Da)	Structure
Naphthalene	$C_{10}H_8$	128	
1-Methylnaphthalene	$C_{11}H_{10}$	142	
2-Methylnaphthalene	$C_{11}H_{10}$	142	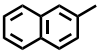
Acenaphthene	$C_{12}H_{10}$	154	

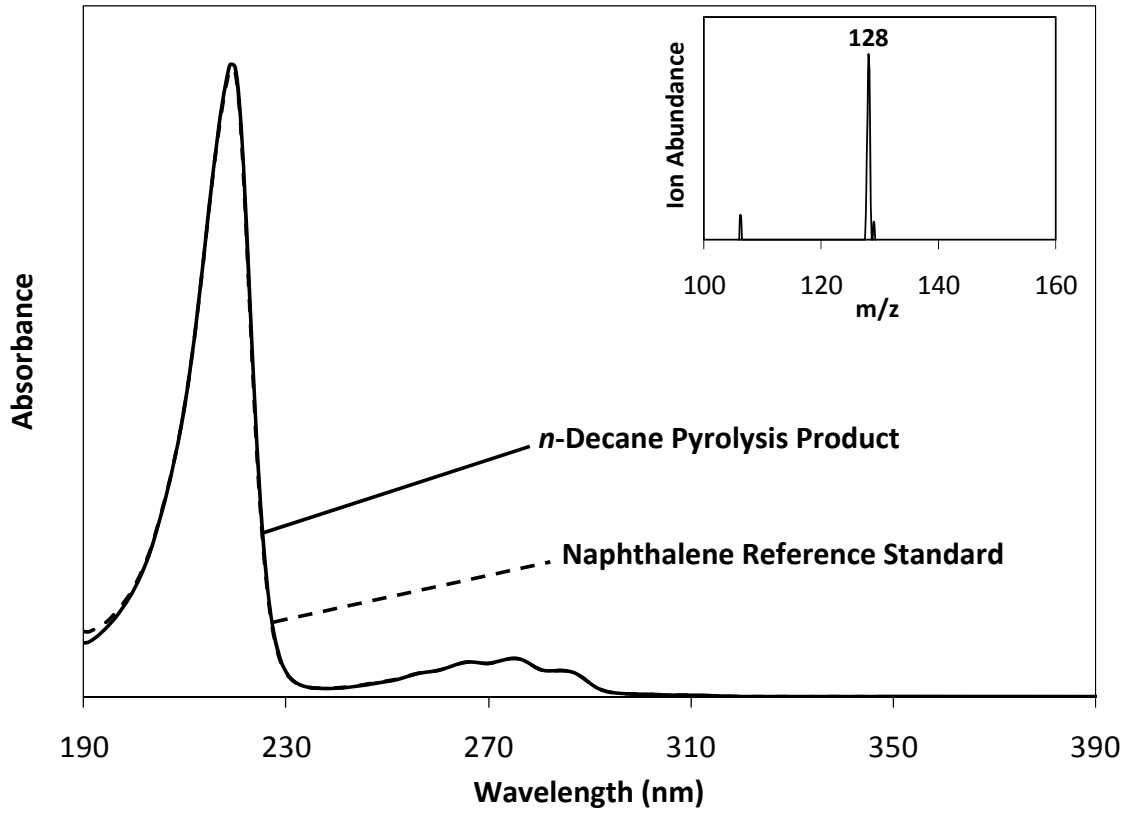

Figure 3.2 UV absorbance spectrum of the reference standard of naphthalene (dashed line) and of the *n*-decane pyrolysis product (solid line) identified as naphthalene, eluting at 25 min in the chromatogram in Figure 3.1. The mass spectrum of this product is displayed in the inset.

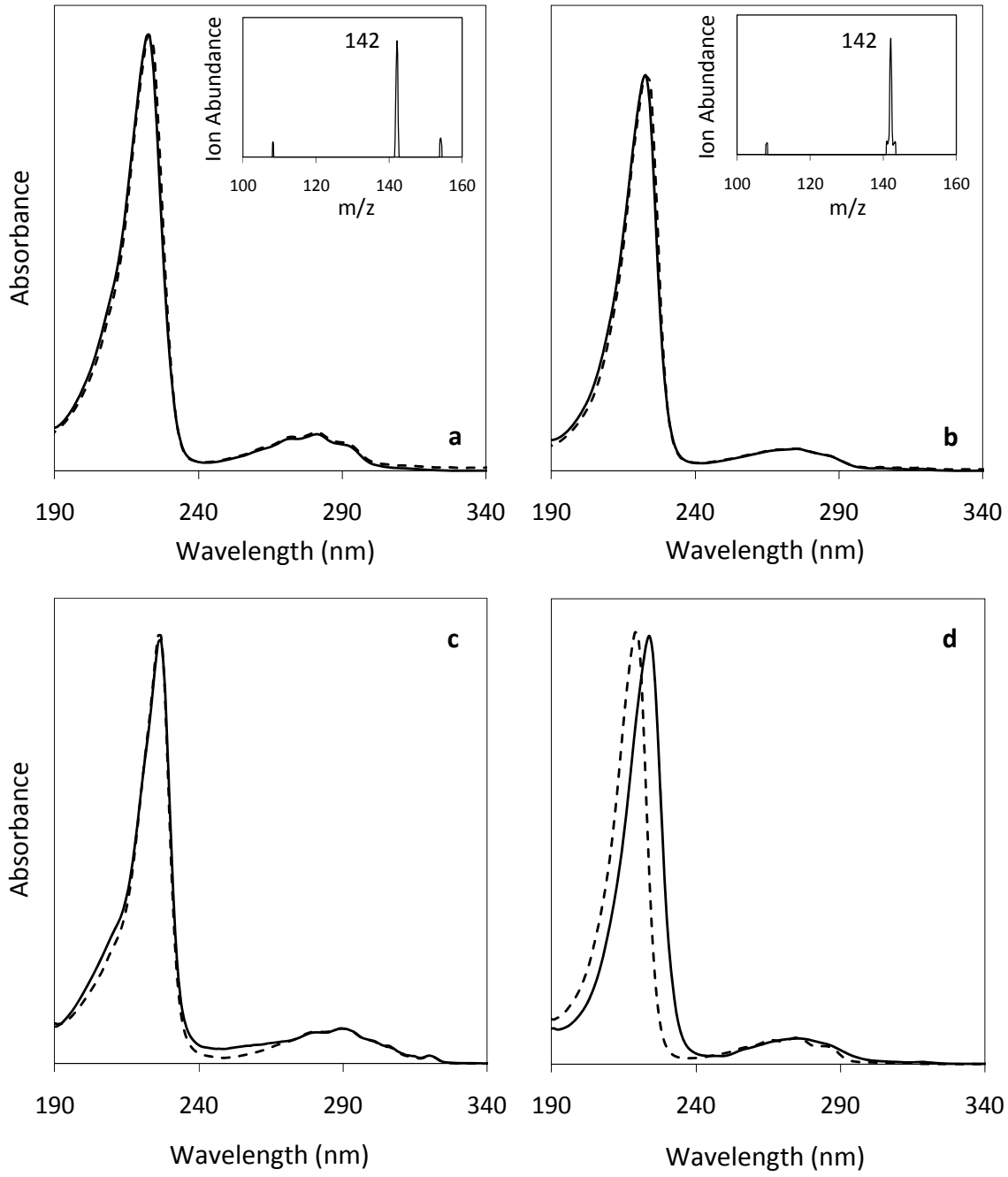

Figure 3.3 Comparison of UV spectra of *n*-decane pyrolysis products from the chromatogram in Figure 3.1 (solid lines) to the UV spectra of reference standards (dashed lines). UV spectra of the products identified as (a) 1-methylnaphthalene, eluting at 30 min, (b) 2-methylnaphthalene, eluting at 31 min, and (c) acenaphthene, eluting at 32 min in Figure 3.1, are shown overlaid with the UV spectra of their respective reference standards. The mass spectra of the two methylated naphthalenes are displayed as insets to the figures (a and b). The UV spectrum of the product identified in (d) as an alkylated naphthalene, eluting at 37 min in Figure 3.1, is shown overlaid with the UV spectrum of naphthalene.

of these three compounds are consistent with the identifications made. The mass spectrum of the *n*-decane pyrolysis product identified as acenaphthene in Figure 3.3c is not available because this product is found in too low a concentration for a strong mass signal to be detected. Mass spectra are also not available for many of the other products of *n*-decane pyrolysis because low yields of these products, coupled with the lower sensitivity of the mass spectrometer compared to the UV detector, result in low or non-existent mass signals.

The other 46 alkylnaphthalenes are identified by comparison of their UV spectra to the spectrum of a reference standard of naphthalene. Figure 3.3d shows one such comparison of the UV spectrum of naphthalene to a product eluting at 37 min in the chromatogram in Figure 3.1. While the spectrum of the product PAH is shifted to higher wavelengths (relative to that of the naphthalene reference standard) due to the effect of the alkyl substituent group, the spectrum still retains the same features as those of the spectrum of naphthalene. As explained in Section 2.3.3.1, a PAH with an alkyl substituent has a UV spectrum that looks almost exactly like that of its parent PAH, only shifted a few nm to higher wavelengths [41-42]. Therefore the UV spectral comparison in Figure 3.3d shows that the aromatic portion of the structure of the product is naphthalene and that an alkyl substituent or substituents are present. Also, while the mass spectrum is not available, this product cannot be singly methylated because the peaks corresponding to both of the singly methylated naphthalenes have already been identified and because—on the C18 column used for the separation of these products—more highly alkylated PAH always elute after less alkylated PAH with the same aromatic structure. By this reasoning, the total number of carbons in the alkyl functionalities of any one these 46 alkylnaphthalenes has to be greater than or equal to two.

One unsubstituted and 49 alkylated PAH products have been identified in the first fraction of the liquid-phase products of supercritical *n*-decane pyrolysis. Naphthalene,

1-methylnaphthalane, 2-methylnaphthalene, and acenaphthene have each been reported previously as *n*-decane pyrolysis products [45,46], but 46 of the alkylated naphthalenes identified here are being reported as products of *n*-decane pyrolysis for the first time.

3.4.2 Identification of PAH Products in Fraction 2

The second fraction of liquid-phase products of *n*-decane pyrolysis includes the three-ring PAH acenaphthylene and fluorene, along with their alkylated derivatives. Figure 3.4 presents a reversed-phase HPLC chromatogram of this fraction of the products from the highest stressing experimental conditions (570 °C and 100 atm).

Acenaphthylene and one methylated acenaphthylene, eluting at 28 and 34 minutes, respectively, in the chromatogram in Figure 3.4, are identified from their UV and mass spectra. Figure 3.5 shows the comparison of the UV spectra of both of these compounds to that of a reference standard of acenaphthylene, determining with certainty the aromatic portion of the structure of these products. Furthermore, the molecular weights of these two compounds, as determined by mass spectrometry, are 152 and 166 (with the lighter compound eluting earlier). Therefore the first eluting of the two is the unsubstituted acenaphthylene followed by the singly methylated acenaphthylene, for which the identity but not the position of the methyl group is known. The chemical formula, molecular mass, and structure of acenaphthylene are displayed in Table 3.4.

Fluorene, 1-methylfluroene, and 4-methylfluorene, eluting at 33, 39, and 38 min, respectively, in the chromatogram in Figure 3.4, are identified by matching their UV spectra to those of the reference standards of each of these compounds. Mass spectra of these product components are also consistent with these identifications. The UV spectral matches and mass spectra are shown in Figure 3.6. Due to co-elution with another product, the spectrum of the product component identified as fluorene (in Figure 3.6a) does not match the UV spectrum of the

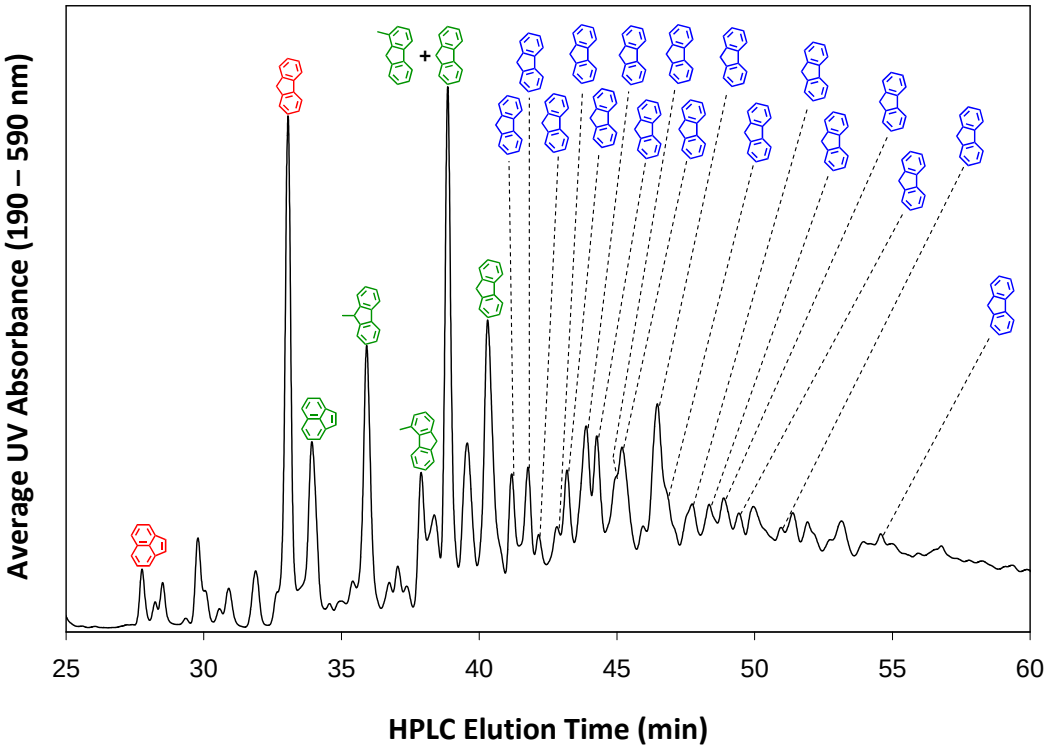

Figure 3.4 A reversed-phase HPLC chromatogram of the second fraction of the liquid-phase products of *n*-decane pyrolyzed at 570 °C and 100 atm. This fraction contains the three-ring PAH acenaphthylene, fluorene, and their alkylated derivatives. Red labels represent unsubstituted PAH; green labels represent singly methylated PAH (with the position of the methyl group labeled when known); blue labels represent alkylated PAH that have substituents whose number, positions, and/or identities are not known with certainty.

fluorene reference standard between 230 and 258 nm. However, the UV absorbance maxima of this product component do match those of the fluorene reference standard exactly at 206, 262, 289, and 299 nm, leaving no doubt as to the identity of this product. 1-Methylfluorene, identified in Figure 3.6b, co-elutes with another methylfluorene at 39 min in the chromatogram in Figure 3.4, but these two compounds have been resolved chromatographically by another HPLC method. The chromatogram in which these two are fully separated from one another is shown in Appendix A. The UV and mass spectrum of 4-methylfluorene are presented in Figure 3.6c

9-Methylfluorene, eluting at 36 min in the chromatogram in Figure 3.4, is identified by its UV and mass spectra and HPLC elution time evidence. As illustrated in Figure 3.7a, the UV

Table 3.4 PAH identified in the second fraction of liquid-phase products of *n*-decane pyrolysis.

Product	Chemical Formula	Molecular Mass (Da)	Structure
Acenaphthylene	$C_{12}H_8$	152	
Fluorene	$C_{13}H_{10}$	166	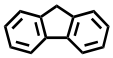
1-Methylfluorene	$C_{14}H_{12}$	180	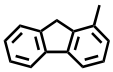
2-Methylfluorene	$C_{14}H_{12}$	180	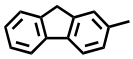
3-Methylfluorene	$C_{14}H_{12}$	180	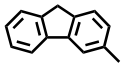
4-Methylfluorene	$C_{14}H_{12}$	180	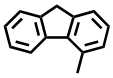
9-Methylfluorene	$C_{14}H_{12}$	180	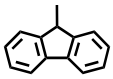

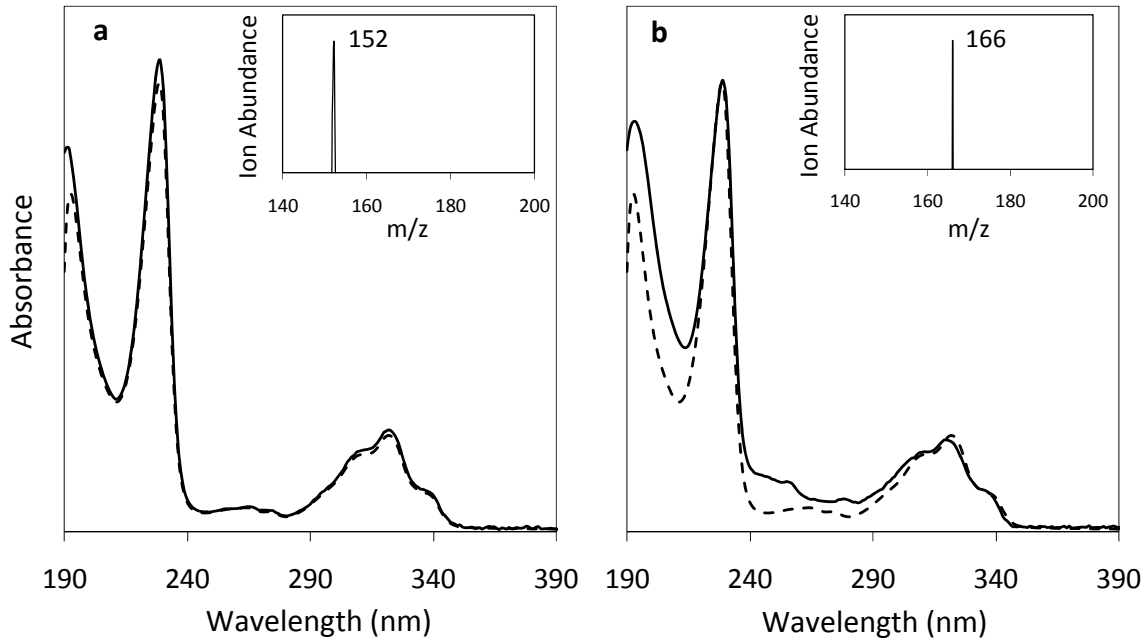

Figure 3.5 Comparisons of the UV spectra of *n*-decane pyrolysis products from the chromatogram in Figure 3.4 (solid lines) to that of a reference standard of acenaphthylene (dashed lines). Comparisons are shown for the products identified as (a) acenaphthylene, eluting at 28 min, and (b) methylacenaphthylene eluting at 34 min in Figure 3.4. The mass spectra of these products are displayed as insets to the figures.

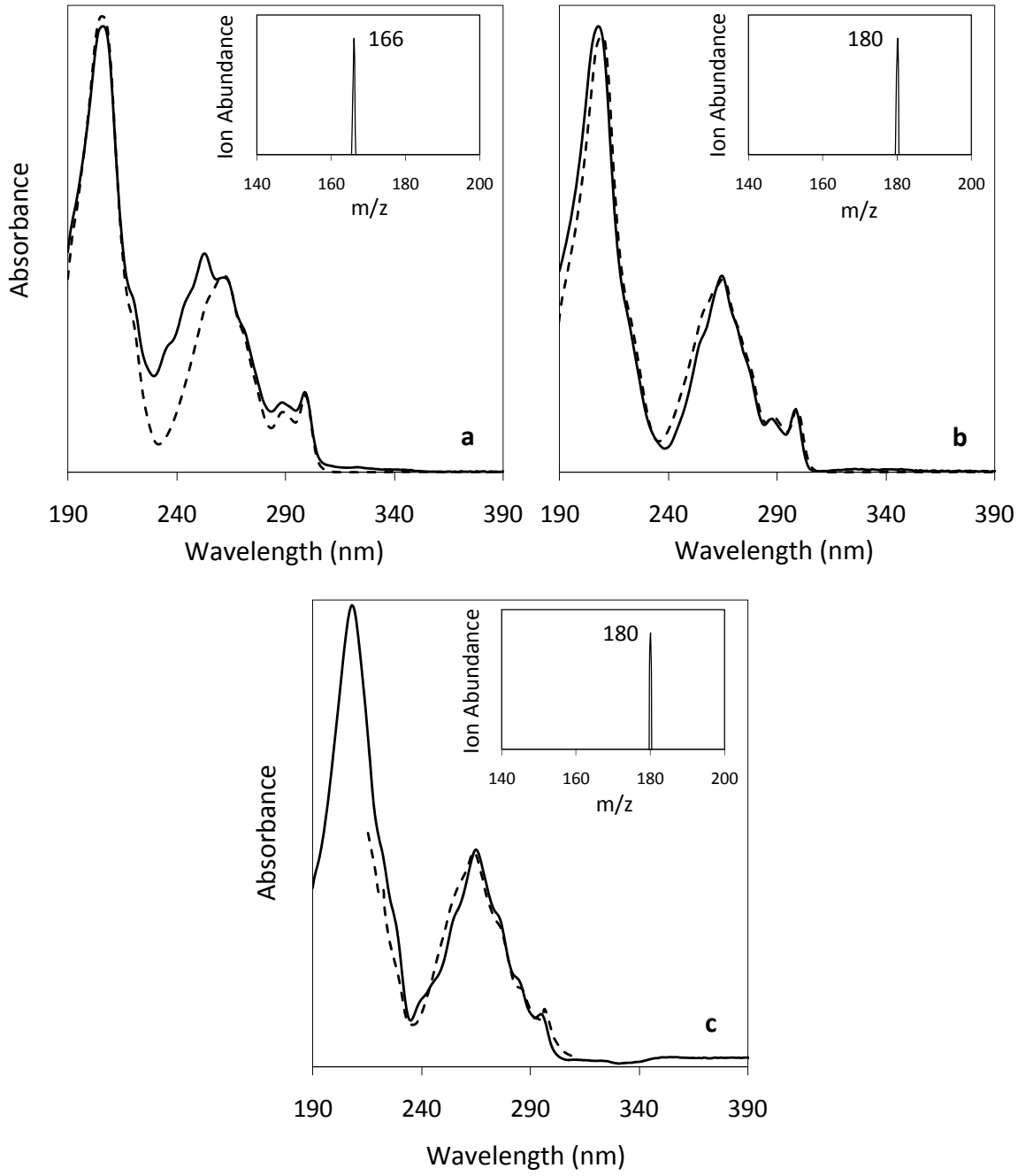

Figure 3.6 Comparisons of the UV spectra of *n*-decane pyrolysis products from the chromatogram in Figure 3.4 (solid lines) to the spectra of their corresponding reference standards (dashed lines). Matches are shown for the products identified as (a) fluorene, eluting at 33 min; (b) 1-methylfluorene, eluting at 39 min; and (c) 4-methylfluorene, eluting at 38 min in Figure 3.4. The mass spectra of these products are displayed as insets to the figures.

spectrum of this compound matches that of fluorene; therefore it must have the same aromatic structure as fluorene. Its molecular weight, determined by mass spectrometry, is 180, so it must also have a single methyl substituent. This compound also elutes from the HPLC before the other four methylfluorene isomers. The early elution time is an indication that this molecule deviates from planarity, since non-planar molecules elute before planar molecules of the same molecular weight on the column used to separate this fraction [47]. Among all the methylfluorenes, a methyl group in the 9 position causes a methylated fluorene to deviate from planarity by the greatest amount. Therefore this compound is identified as 9-methylfluorene.

The two remaining isomers of methylfluorene, eluting at 39 and 40 min, respectively, in the chromatogram in Figure 3.4, are identified in Figures 3.7b and 3.7c. The UV spectra of these two compounds match the spectrum of fluorene (indicating the aromatic structure of these compounds) and their mass spectra are consistent with that of a methylated fluorene (showing that each has one methyl substituent). It is not known which of the peaks at 39 and 40 min correspond to which isomer of methylfluorene, but because there are five isomers of methylfluorene and three are already accounted for, one of them must be 2-methylfluorene and the other 3-methylfluorene. The chemical formulas, molecular masses, and structures of fluorene and the five methylfluorenes are displayed in Table 3.4.

Seventeen more alkylated fluorenes are identified by comparison of their UV spectra to the spectrum of a reference standard of fluorene. Mass spectra of these product components are not available, but none of them can be singly methylated, since all five of the singly methylated fluorenes are accounted for. A comparison of the UV spectrum of one of these alkylfluorenes, the product eluting at 41 min in the chromatogram in Figure 3.4, to the spectrum of fluorene is shown in Figure 3.7d.

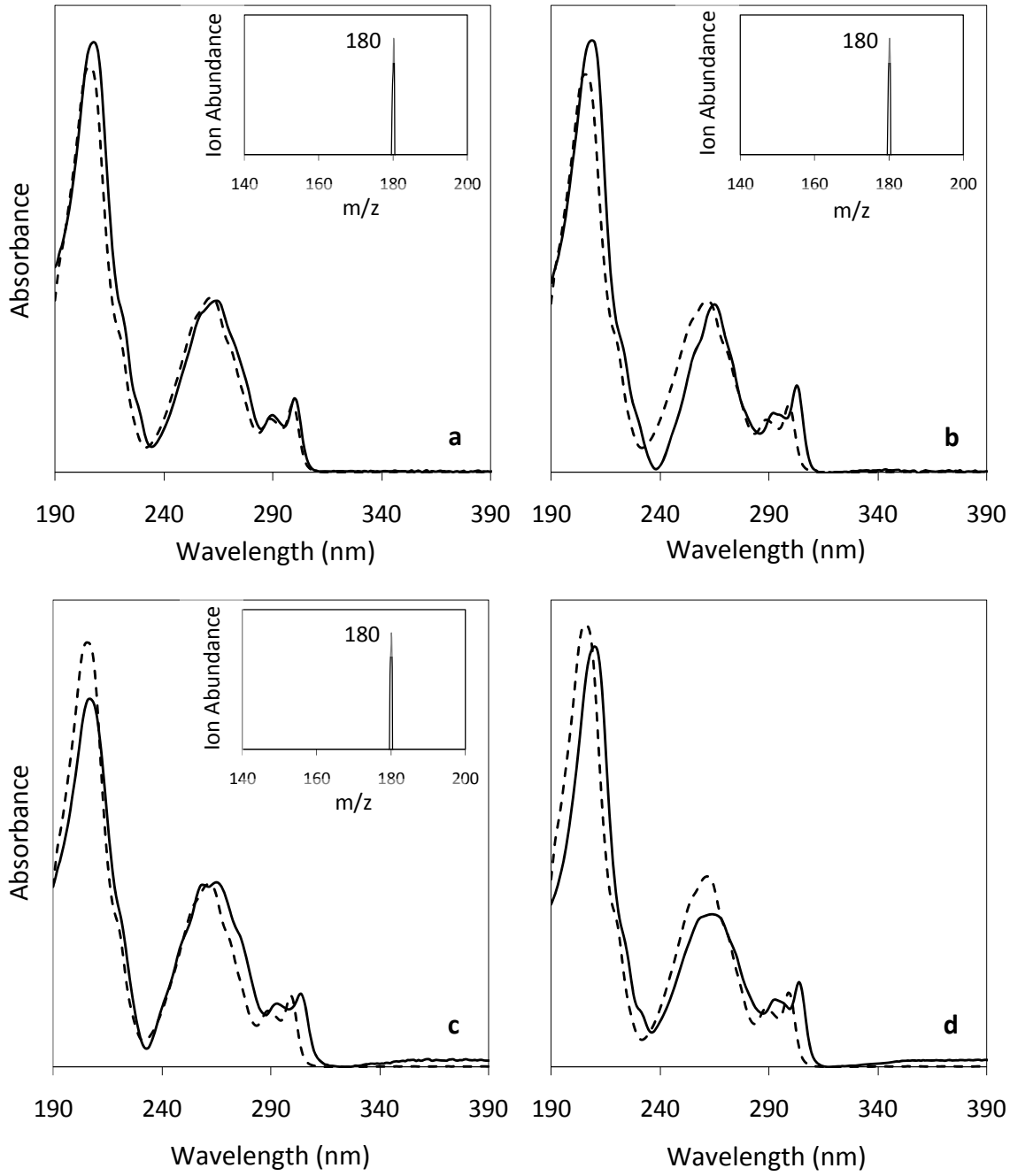

Figure 3.7 Comparisons of the UV spectra of *n*-decane pyrolysis products from the chromatogram in Figure 3.7 (solid lines) to the spectrum of a reference standard of fluorene (dashed lines). Comparisons are shown for the products identified as (a) 9-methylfluorene, eluting at 36 min; (b) a methylated fluorene eluting at 39 min; (c) a methylated fluorene eluting at 40 min; and (d) an alkylated fluorene eluting at 41 min in Figure 3.4. The mass spectra of the three methylated fluorenes are displayed as insets to the figures.

Altogether, two unsubstituted and 23 alkylated PAH products have been identified from the second fraction of the liquid-phase products of supercritical *n*-decane pyrolysis. Fluorene and acenaphthylene have been reported previously as *n*-decane pyrolysis products [45,46], but the one methylated acenaphthylene and the 22 alkylated fluorene product components are reported here as *n*-decane pyrolysis products for the first time.

3.4.3 Identification of PAH Products in Fraction 3

The third fraction of liquid-phase products of *n*-decane pyrolysis includes the three-ring PAH phenanthrene and anthracene, along with their alkylated derivatives. Figure 3.8 presents a reversed-phase HPLC chromatogram of this fraction of the products from the highest stressing experimental conditions (570 °C and 100 atm).

Phenanthrene, four of the five isomers of methylphenanthrene, and cyclopenta[*def*]phenanthrene are identified as products by matching their UV spectra to those of the reference standards for each of these compounds. Mass spectra of these product components are also consistent with these identifications. The UV spectral matches and mass spectra of these products are shown in Figures 3.9, 3.10a, and 3.10b. 2-Methylphenanthrene is identified as a product by comparison of its UV spectrum to that of phenanthrene (which shows that the aromatic portion of this compound is the same as that of phenanthrene) and examination of its mass spectrum (which shows that this compound has a molecular weight consistent with a singly methylated phenanthrene). Comparison of the UV spectrum of this compound to that of phenanthrene and its mass spectrum are shown in Figure 3.10c. Since there are five isomers of methylphenanthrene, and the other four are accounted for among the products, the product component eluting at 44 min in the chromatogram in Figure 3.8 must be 2-methylphenanthrene. The chemical formulas, molecular masses, and structures of phenanthrene, cyclopenta[*def*]phenanthrene, and the five methylphenanthrenes are displayed in Table 3.5.

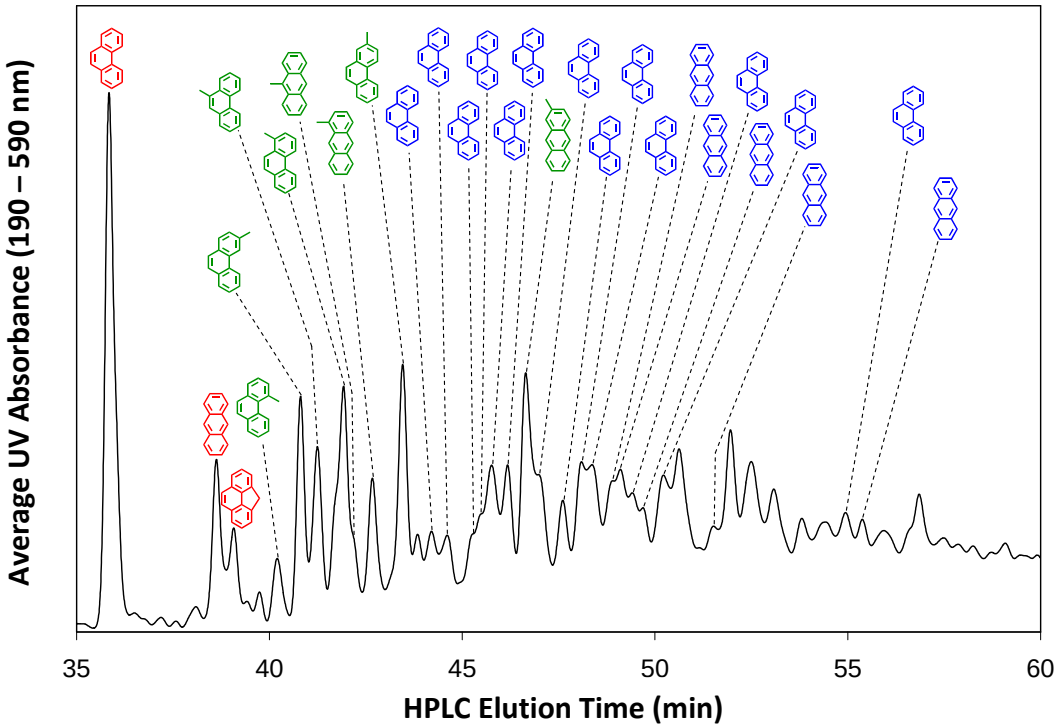

Figure 3.8 A reversed-phase HPLC chromatogram of the third fraction of the liquid-phase products of *n*-decane pyrolyzed at 570 °C and 100 atm. This fraction contains the three-ring PAH phenanthrene, anthracene, and their alkylated derivatives. Red labels represent unsubstituted PAH; green labels represent singly methylated PAH; blue labels represent alkylated PAH that have substituents whose number, positions, and/or identities are not known with certainty.

In addition to these seven products which are identified exactly, there are another 13 alkylated phenanthrenes with alkyl groups of unknown number, position, and/or length. These products are identified by comparison of their UV spectra to that of a reference standard of phenanthrene. Figure 3.10d shows a comparison of the UV spectrum of one of these alkylated phenanthrenes, the compound eluting at 50 min in the chromatogram in Figure 3.8, to the spectrum of a reference standard of phenanthrene. Since all the singly methylated phenanthrenes are accounted for, none of these alkylated phenanthrenes can be singly methylated.

Anthracene and the three isomers of methylanthracene are identified as products by matching their UV spectra to those of reference standards for each of these compounds. Mass spectra of these product components are also consistent with these identifications. The UV

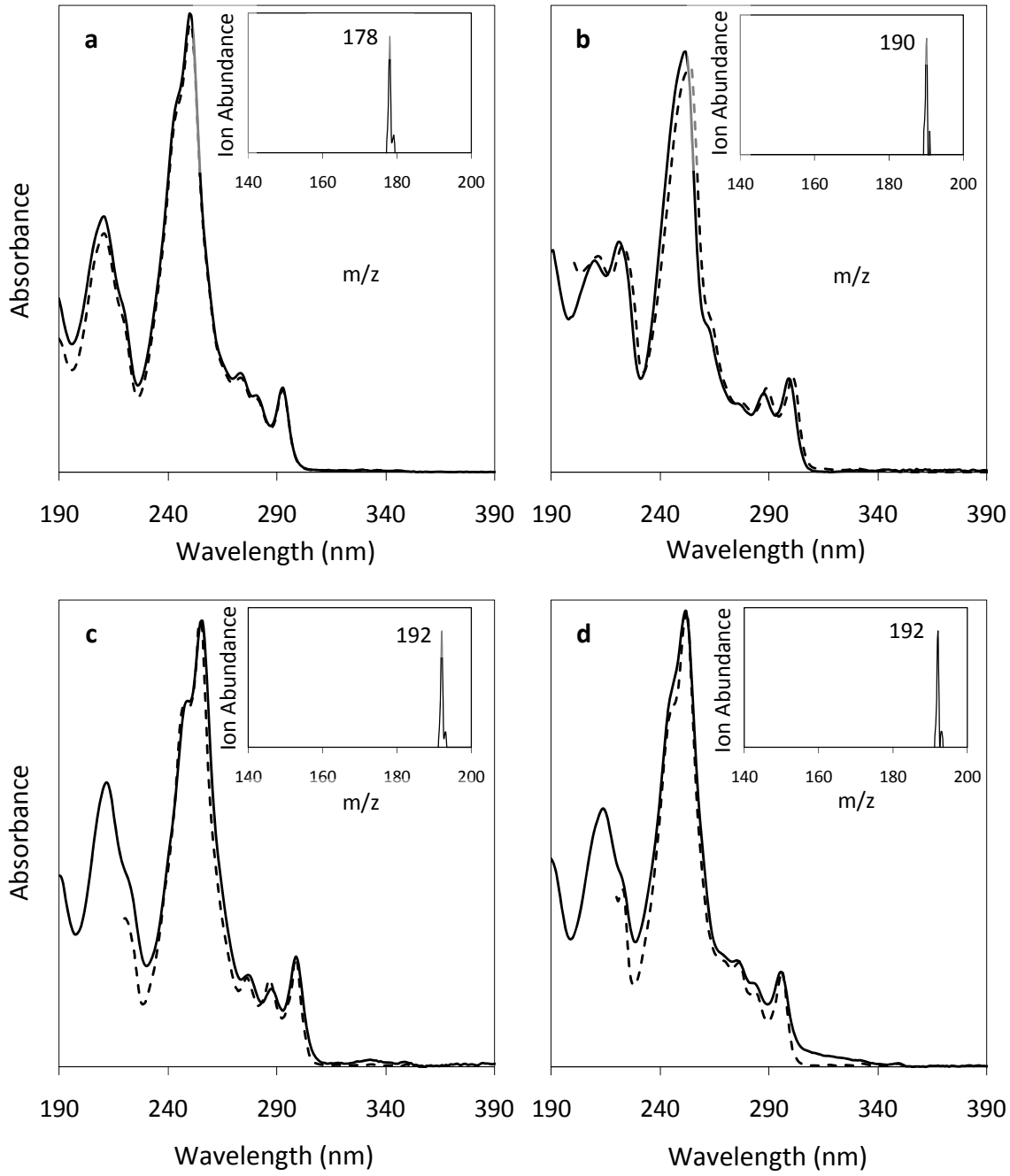

Figure 3.9 Comparisons of the UV spectra of *n*-decane pyrolysis products from the chromatogram in Figure 3.8 (solid lines) to the spectra of their corresponding reference standards (dashed lines). Matches are shown for the products identified as (a) phenanthrene, eluting at 36 min; (b) cyclopenta[*def*]phenanthrene, eluting at 39 min; (c) 1-methylphenanthrene, eluting at 42 min; and (d) 3-methylphenanthrene, eluting at 41 min in Figure 3.8. The mass spectra of these products are displayed as insets to the figures.

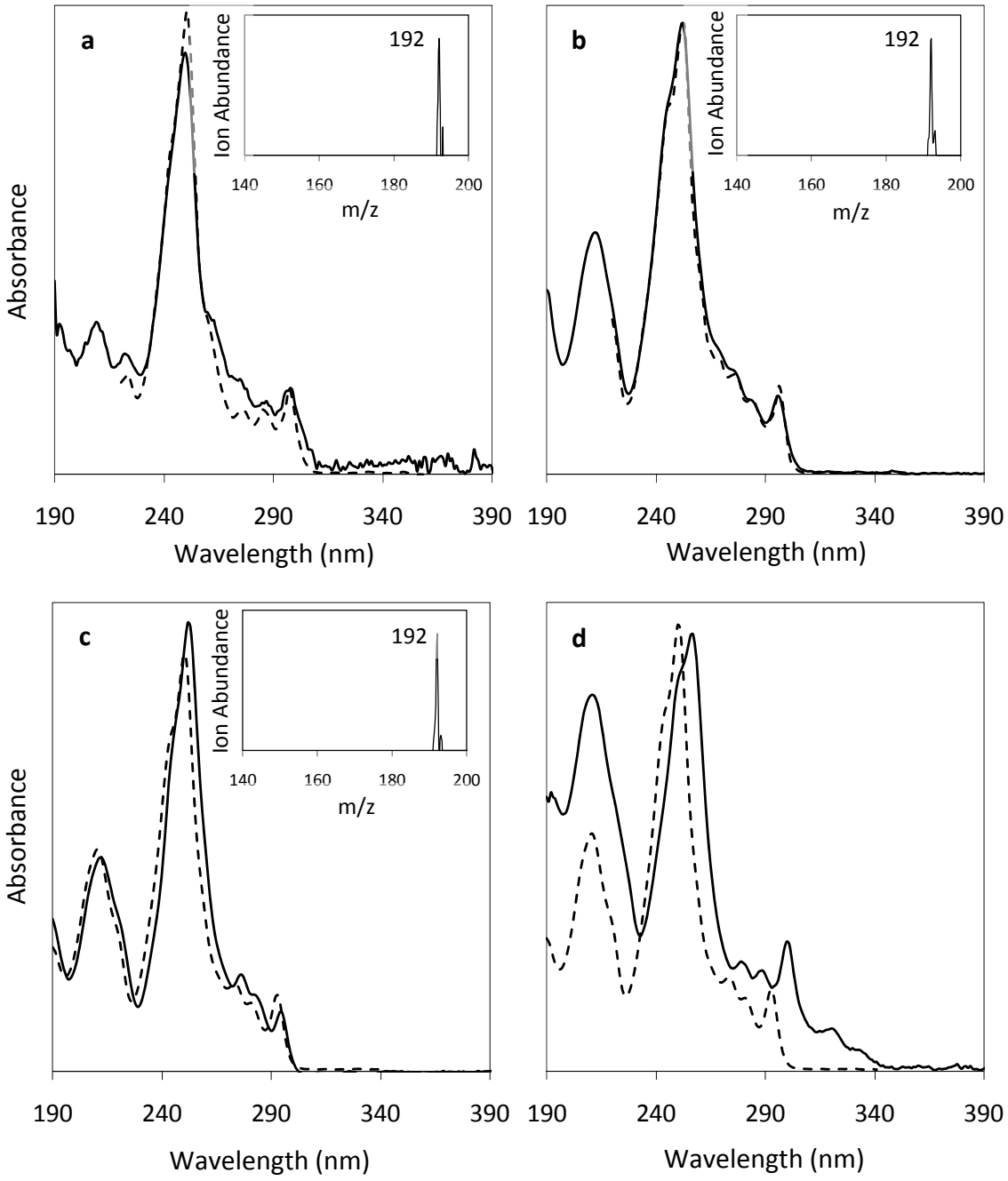

Figure 3.10 Comparison of UV spectra of *n*-decane pyrolysis products from the chromatogram in Figure 3.8 (solid lines) to the UV spectra of reference standards (dashed lines). UV spectra of the products identified as (a) 4-methylphenanthrene, eluting at 40 min, and (b) 9-methylphenanthrene, eluting at 41 min in Figure 3.8, are shown overlaid with the UV spectra of reference standards of those compounds. UV spectra of the products identified as (c) 2-methylphenanthrene, eluting at 44 min, and (d) an alkylated phenanthrene, eluting at 50 min in Figure 3.8, are shown overlaid with the UV spectrum of phenanthrene. The mass spectra of the three methylated phenanthrenes are displayed as insets to the figures.

Table 3.5 PAH identified in the third fraction of liquid-phase products of *n*-decane pyrolysis.

Product	Chemical Formula	Molecular Mass (Da)	Structure
Phenanthrene	$C_{14}H_{10}$	178	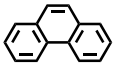
1-Methylphenanthrene	$C_{15}H_{12}$	192	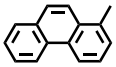
2-Methylphenanthrene	$C_{15}H_{12}$	192	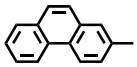
3-Methylphenanthrene	$C_{15}H_{12}$	192	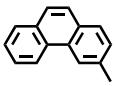
4-Methylphenanthrene	$C_{15}H_{12}$	192	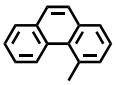
9-Methylphenanthrene	$C_{15}H_{12}$	192	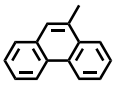
Cyclopenta[*def*]-phenanthrene	$C_{15}H_{10}$	190	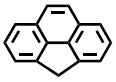
Anthracene	$C_{14}H_{10}$	178	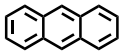
1-Methylanthracene	$C_{15}H_{12}$	192	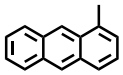
2-Methylanthracene	$C_{15}H_{12}$	192	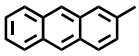
9-Methylanthracene	$C_{15}H_{12}$	192	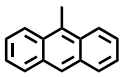

spectral matches and mass spectra of these products are shown in Figures 3.11a and 3.12. The chemical formulas, molecular masses, and structures of anthracene and the three methylated anthracenes are displayed in Table 3.5.

In addition to these four products which are identified exactly, there are another four alkylated anthracenes with alkyl groups of unknown number, position, and/or length. These products are identified by comparison of their UV spectra to that of a reference standard of

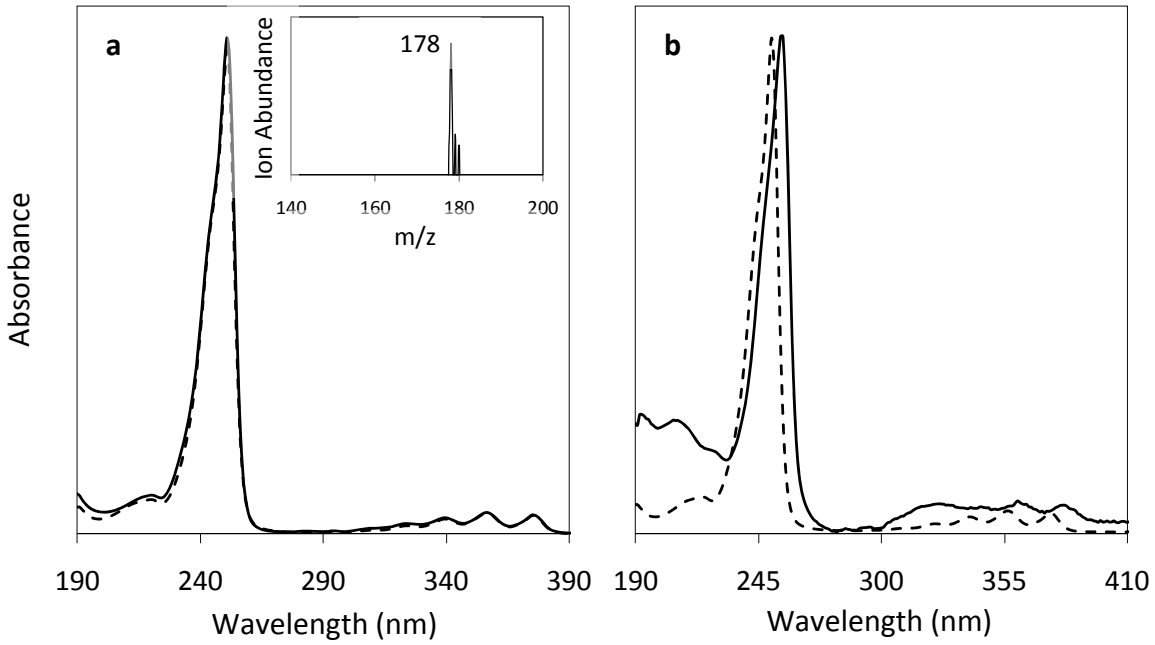

Figure 3.11 Comparisons of the UV spectra of *n*-decane pyrolysis products from the chromatogram in Figure 3.8 (solid) to that of a reference standard of anthracene (dashed). Comparisons are shown for the products identified as (a) anthracene, eluting at 38 min, and (b) an alkylated anthracene eluting at 49 min. The mass spectrum of the product anthracene is displayed as an inset to the figure.

anthracene. Figure 3.11b shows a comparison of the UV spectrum of one of these alkylated anthracenes, the compound eluting at 49 min in the chromatogram in Figure 3.8, to the spectrum of anthracene. Since all the singly methylated anthracenes are already accounted for, none of the four additional alkylated anthracenes can be singly methylated.

Altogether, two unsubstituted $C_{14}H_{10}$ PAH, phenanthrene and anthracene, as well as 30 alkylated phenanthrenes and anthracenes have been identified as supercritical *n*-decane pyrolysis products in the third fraction of liquid-phase products (with cyclopenta[*def*]phenanthrene being counted as an alkylated derivative of phenanthrene). Phenanthrene and anthracene have both been reported previously as pyrolysis products of *n*-decane [45,46], while the 30 alkylated PAH are reported here for the first time as products of *n*-decane pyrolysis.

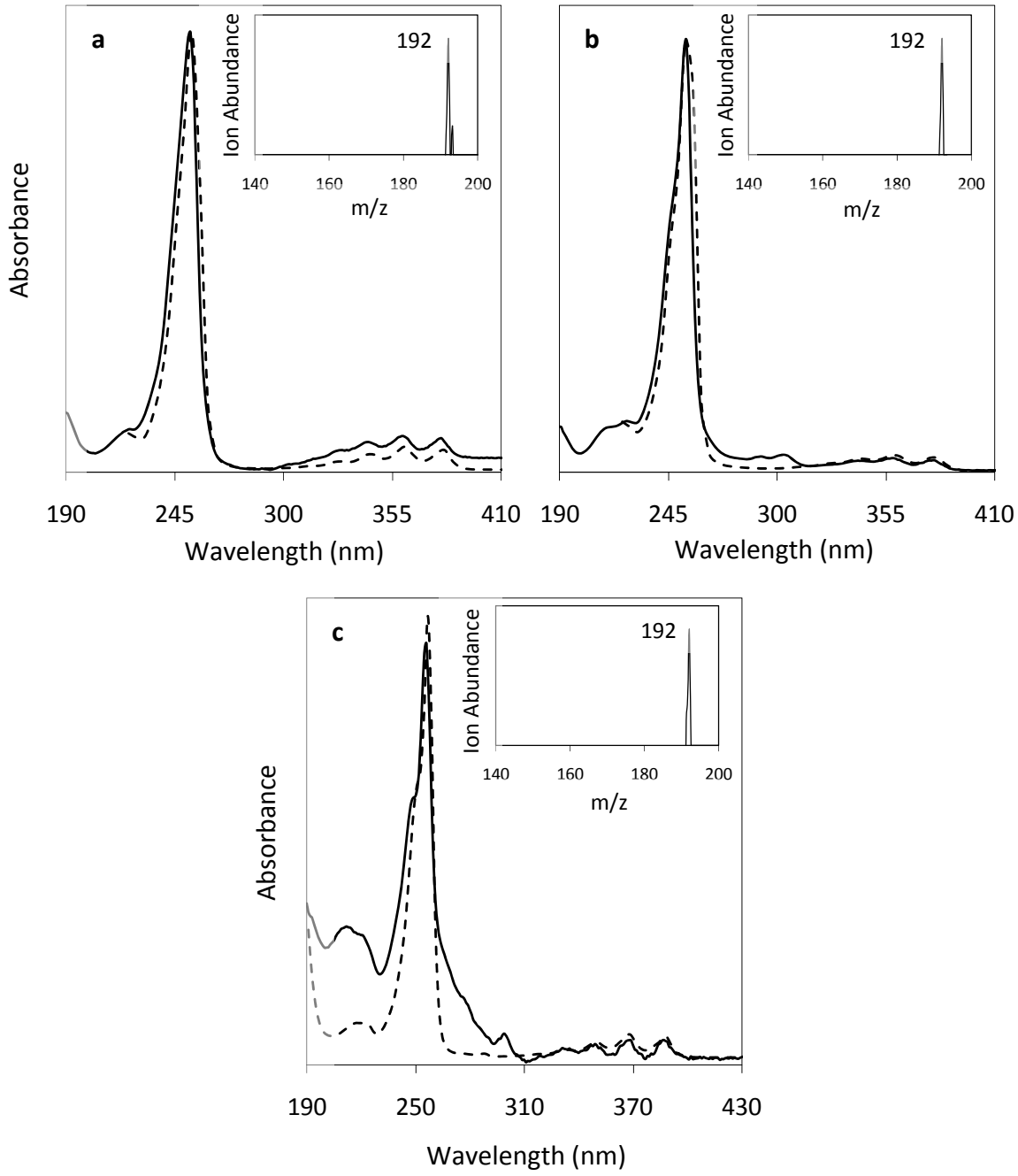

Figure 3.12 Comparisons of the UV spectra of *n*-decane pyrolysis products from the chromatogram in Figure 3.8 (solid) to the spectra of their corresponding reference standards (dashed). Matches are shown for the products identified as (a) 9-methylanthracene, eluting at 42 min; (b) 1-methylanthracene, eluting at 43 min; and (c) 2-methylanthracene, eluting at 47 min. The mass spectra of these products are displayed as insets to the figures.

3.4.4 Identification of PAH Products in Fraction 4

The fourth fraction of liquid-phase products of *n*-decane pyrolysis includes the four-ring PAH pyrene, fluoranthene, acephenanthrylene, and benzo[*b*]fluorene, along with their alkylated derivatives. Figure 3.13 presents a reversed-phase HPLC chromatogram of this fraction of the products from the highest stressing experimental conditions (570 °C and 100 atm).

Pyrene and the three isomers of methylpyrene are identified by matching their UV spectra to those of the corresponding reference standards. Mass spectra of these product components are also consistent with these identifications. The UV spectral matches and mass spectra of these products are shown in Figures 3.14a and 3.15. In addition to these four compounds which are identified exactly, there are another 22 alkylated pyrenes for which the number, position(s), and/or identity(s) of the alkyl groups are not known with certainty. These are identified by comparing their UV spectra to the spectrum of pyrene. A comparison of the UV spectrum of one of these alkylated pyrenes, the product eluting at 57 min in the chromatogram in Figure 3.13, to the spectrum of pyrene is shown in Figure 3.14b. Since all three of the singly methylated pyrenes are accounted for, none of these alkylated pyrenes can be singly methylated. The chemical formulas, molecular masses, and structures of pyrene and the three methylated pyrenes are displayed in Table 3.6.

Acephenanthrylene and benzo[*b*]fluorene are identified by matching the UV spectra of these compounds to the spectra of the corresponding reference standards. These spectral matches are shown in Figure 3.16. The chemical formulas, molecular masses, and structures of these two compounds are displayed in Table 3.6. Reference standards were not shot to determine the elution times of either of these compounds, and mass spectra of the product components were not available, but they are both nonetheless identified as PAH having no alkyl substituents. Unsubstituted PAH always elute before alkylated PAH on the C18 column used to separate this

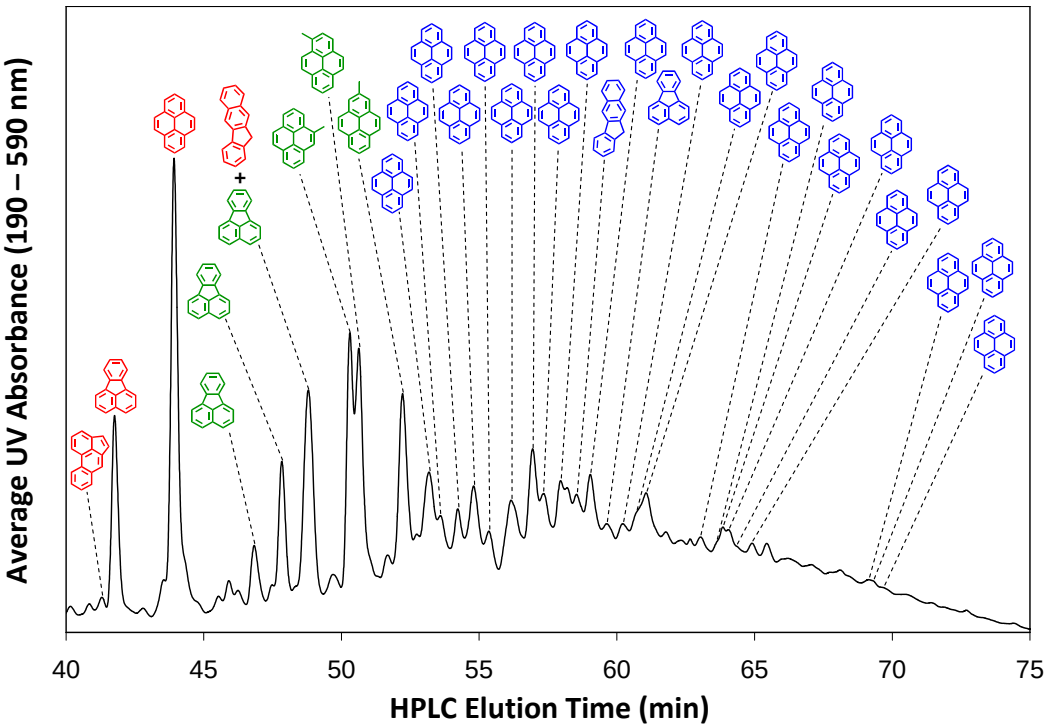

Figure 3.13 A reversed-phase HPLC chromatogram of the fourth fraction of the liquid-phase products of *n*-decane pyrolyzed at 570 °C and 100 atm. This fraction primarily contains the $C_{16}H_{10}$ PAH isomer family and its alkylated derivatives. Red labels represent unsubstituted PAH; green labels represent singly methylated PAH (with the position of the methyl group labeled when known); blue labels represent alkylated PAH that have substituents whose number, positions, and/or identities are not known with certainty.

sample, and these are the first compounds with UV spectra matching those of the corresponding unsubstituted PAH reference standards, therefore they are identified as the unsubstituted parent PAH and not as alkylated daughter compounds. By this reasoning, in a chromatogram of any fraction the earliest eluting compound whose UV spectrum matches that of an unsubstituted PAH reference standard is always assumed to be the unsubstituted parent PAH unless additional analytical data indicate otherwise. One alkylated benzo[*b*]fluorene is also identified by comparison of its UV spectrum to that of its unsubstituted parent PAH.

Fluoranthene is identified by matching its UV spectrum to that of a reference standard for this compound. The mass spectrum of this product component is also consistent with this

Table 3.6 PAH identified in the fourth fraction of liquid-phase products of *n*-decane pyrolysis.

Product	Chemical Formula	Molecular Mass (Da)	Structure
Acephenanthrylene	$C_{16}H_{10}$	202	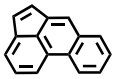
Benzo[*b*]fluorene	$C_{17}H_{12}$	216	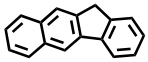
Fluoranthene	$C_{16}H_{10}$	202	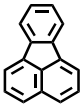
Pyrene	$C_{16}H_{10}$	202	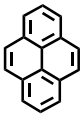
1-Methylpyrene	$C_{17}H_{12}$	216	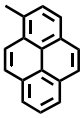
2-Methylpyrene	$C_{17}H_{12}$	216	
4-Methylpyrene	$C_{17}H_{12}$	216	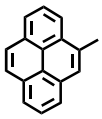

identification. Four methylfluoranthenes are identified as products by comparison of their UV spectra to that of fluoranthene (which shows that the aromatic portion of these compounds are fluoranthene) and examination of their mass spectra (which shows that these compounds each have a molecular weight consistent with a singly methylated fluoranthene). Comparisons of the UV spectra of the product identified as fluoranthene and one of the products identified as a methylated fluoranthene to the spectrum of a reference standard of fluoranthene are presented in Figure 3.17. The mass spectra of these two product components are also shown in the figure. The chromatogram in Figure 3.13 only shows three methylfluoranthenes, but four are resolved by

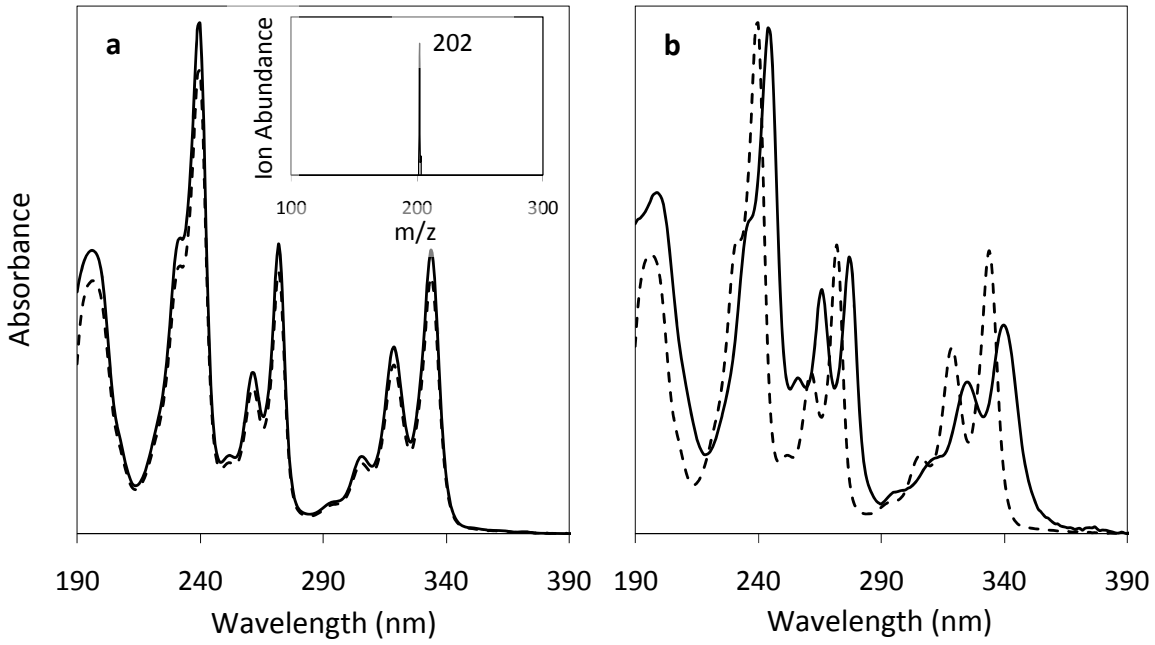

Figure 3.14 Comparisons of the UV spectra of *n*-decane pyrolysis products from the chromatogram in Figure 3.13 (solid lines) to that of a reference standard of pyrene (dashed lines). Comparisons are shown for the products identified as (a) pyrene, eluting at 44 min, and (b) an alkylated pyrene eluting at 57 min in Figure 3.13. The mass spectrum of the product pyrene is displayed as an inset to the figure.

another HPLC method; the chromatogram generated from this other method is presented in Appendix A. Since there are five isomers of methylfluoranthene but only four are resolved, one of the five isomers might not be produced by supercritical *n*-decane pyrolysis. Alternatively, all five isomers might be present, with two methylfluoranthenes co-eluting and seen as a single peak in the chromatogram in Appendix A. One more alkylated fluoranthene is identified by comparison of its UV spectrum to the spectrum of its unsubstituted parent PAH. The chemical formula, molecular mass, and structure of fluoranthene are displayed in Table 3.6.

Altogether, the four-ring PAH pyrene, fluoranthene, acephenanthrylene, and benzo[*b*]fluorene, along with 31 of their alkylated derivatives have been identified as supercritical *n*-decane pyrolysis products in the fourth fraction of the liquid-phase products. Three of these, benzo[*b*]fluorene, fluoranthene, and pyrene, have been reported as products of

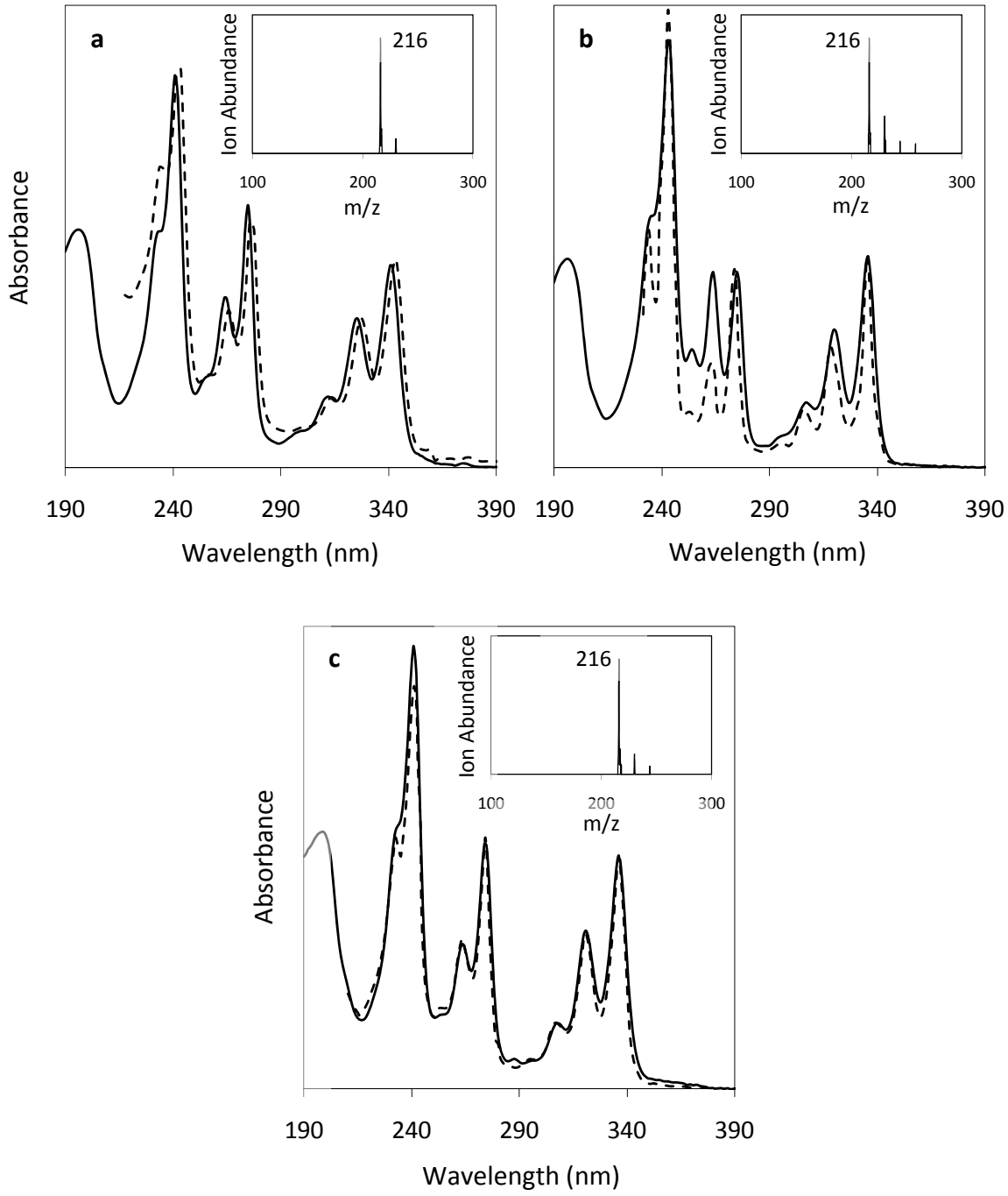

Figure 3.15 Comparisons of the UV spectra of *n*-decane pyrolysis products from the chromatogram in Figure 3.13 (solid lines) to the spectra of their corresponding reference standards (dashed lines). Matches are shown for the products identified as (a) 4-methylpyrene, eluting at 50.5 min; (b) 1-methylpyrene, eluting at 51 min; and (c) 2-methylpyrene, eluting at 52 min in Figure 3.13. The mass spectra of these products are displayed as insets to the figures.

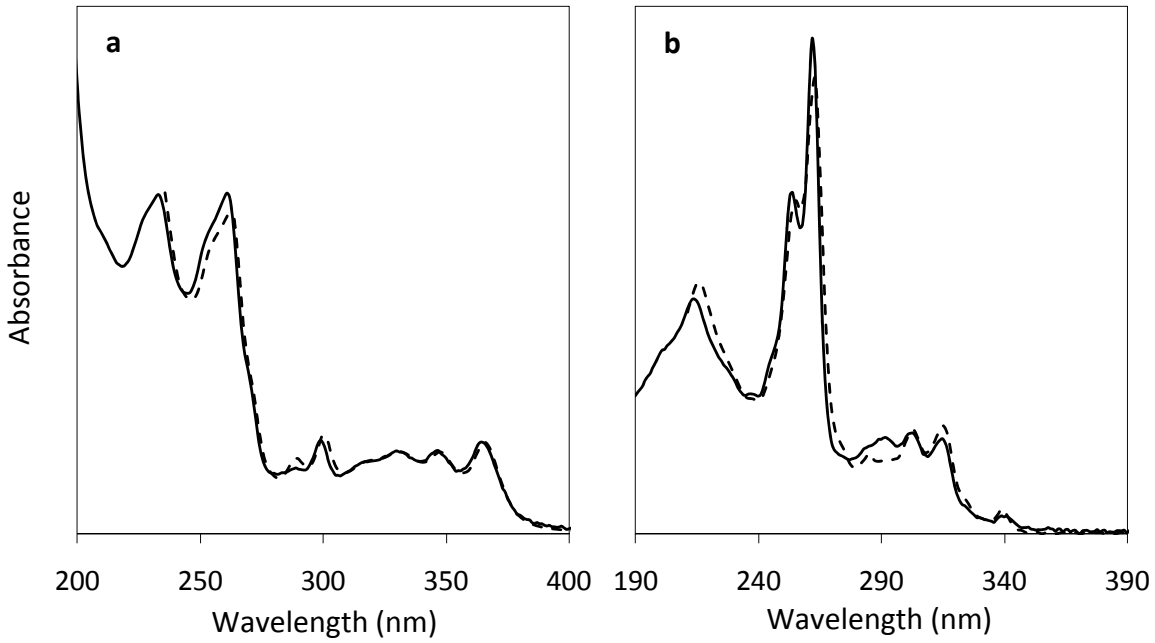

Figure 3.16 Comparisons of the UV spectra of *n*-decane pyrolysis products from the chromatogram in Figure 3.13 (solid lines) to the spectra of the corresponding reference standards (dashed lines). Matches are shown for the products identified as (a) acephenanthrylene, eluting at 41 min, and (b) benzo[*b*]fluorene, eluting at 49 min in Figure 3.13.

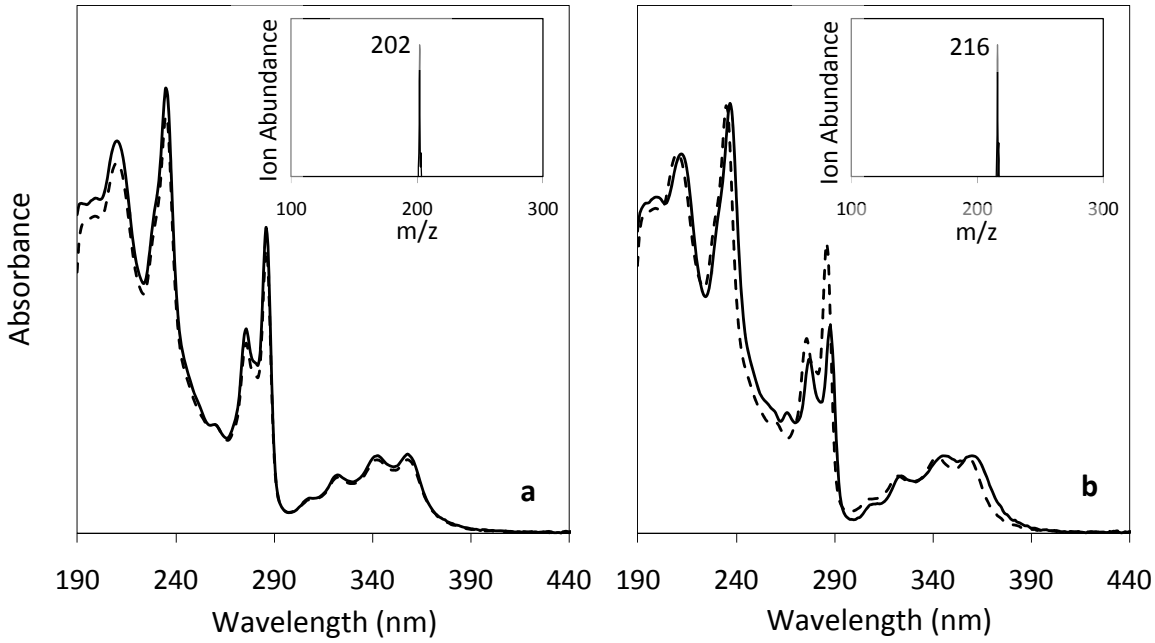

Figure 3.17 Comparisons of the UV spectra of *n*-decane pyrolysis products from the chromatogram in Figure 3.13 (solid line) to that of a reference standard of fluoranthene (dashed line). Comparisons are shown for the products identified as (a) fluoranthene, eluting at 42 min, and (b) a methylated fluoranthene eluting at 59 min in Figure 3.13. The mass spectra of these products are displayed as insets to the figure.

n-decane pyrolysis before [45,46], but acephenanthrylene and the 31 alkylated PAH are reported here as products of *n*-decane pyrolysis for the first time.

3.4.5 Identification of PAH Products in Fraction 5

The fifth fraction of liquid-phase products of *n*-decane pyrolysis includes the PAH chrysene, benz[*a*]anthracene, cyclopenta[*cd*]pyrene, and triphenylene, along with their alkylated derivatives. Figure 3.18 presents a reversed-phase HPLC chromatogram of this fraction of the products from the highest stressing experimental conditions (570 °C and 100 atm).

All four of the unsubstituted products are identified by matching their UV spectra to those of the corresponding reference standards. Chrysene and benz[*a*]anthracene also both have elution times which match those of reference standards separated with the same HPLC method used to generate the chromatogram in Figure 3.18. Comparisons of the UV spectra of these four unsubstituted PAH products to the spectra of their reference standards are shown in Figure 3.19. The chemical formulas, molecular masses, and structures of these four compounds are displayed in Table 3.7. In addition to these four products which are identified exactly, there are ten alkylated chrysenes, four alkylated benz[*a*]anthracenes, and one alkylated triphenylene for which the positions and identities of the alkyl groups are not known with certainty. Figure 3.20 shows the comparisons of the UV spectra of these products to the spectra of reference standards of the appropriate unsubstituted parent PAH.

Altogether, the PAH chrysene, benz[*a*]anthracene, triphenylene, and cyclopenta[*cd*]pyrene, along with 15 of their alkylated derivatives, have been identified as products of supercritical *n*-decane pyrolysis in the fifth fraction of liquid-phase products. Three of these, chrysene, benz[*a*]anthracene, and triphenylene, have been reported previously as *n*-decane pyrolysis products [45], but cyclopenta[*cd*]pyrene and the 15 alkylated PAH are reported here for the first time as product of *n*-decane pyrolysis.

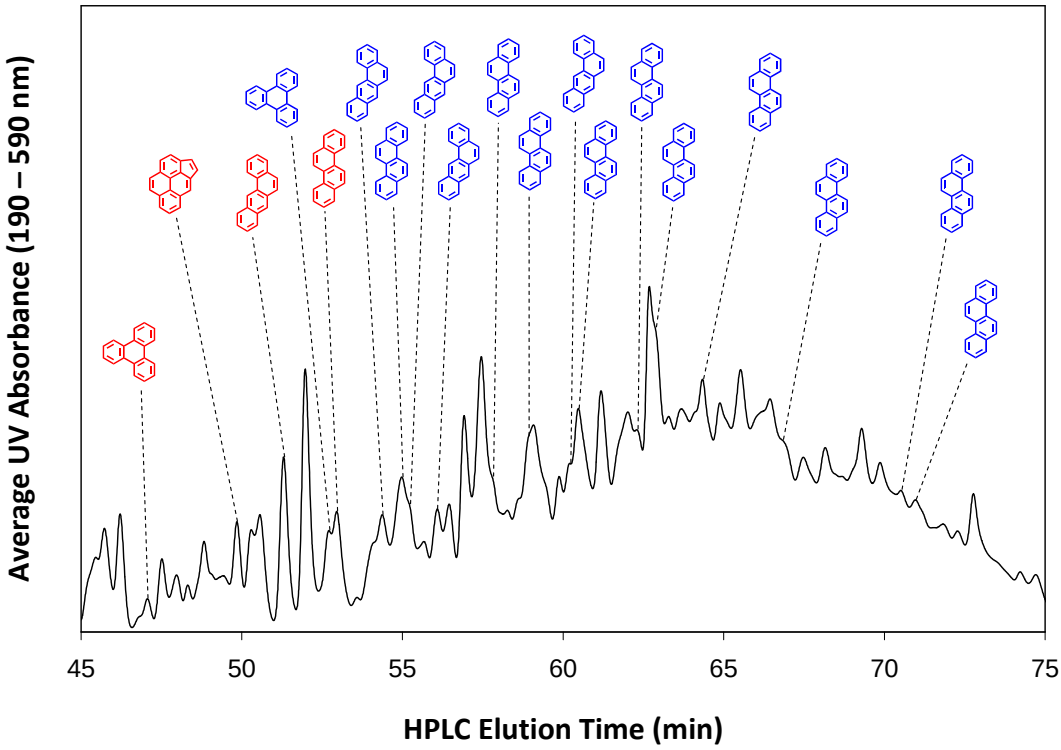

Figure 3.18 A reversed-phase HPLC chromatogram of the fifth fraction of the liquid-phase products of *n*-decane pyrolyzed at 570 °C and 100 atm. This fraction primarily contains the $C_{18}H_{12}$ PAH isomer family and its alkylated derivatives. Red labels represent unsubstituted PAH; blue labels represent alkylated PAH that have substituents whose number, positions, and/or identities are not known with certainty.

Table 3.7 PAH identified in the fifth fraction of liquid-phase products of *n*-decane pyrolysis.

Product	Chemical Formula	Molecular Mass (Da)	Structure
Cyclopenta[*cd*]pyrene	$C_{18}H_{10}$	226	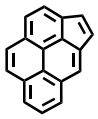
Chrysene	$C_{18}H_{12}$	228	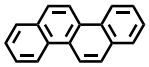
Benz[*a*]anthracene	$C_{18}H_{12}$	228	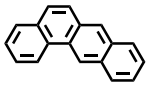
Triphenylene	$C_{18}H_{12}$	228	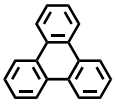

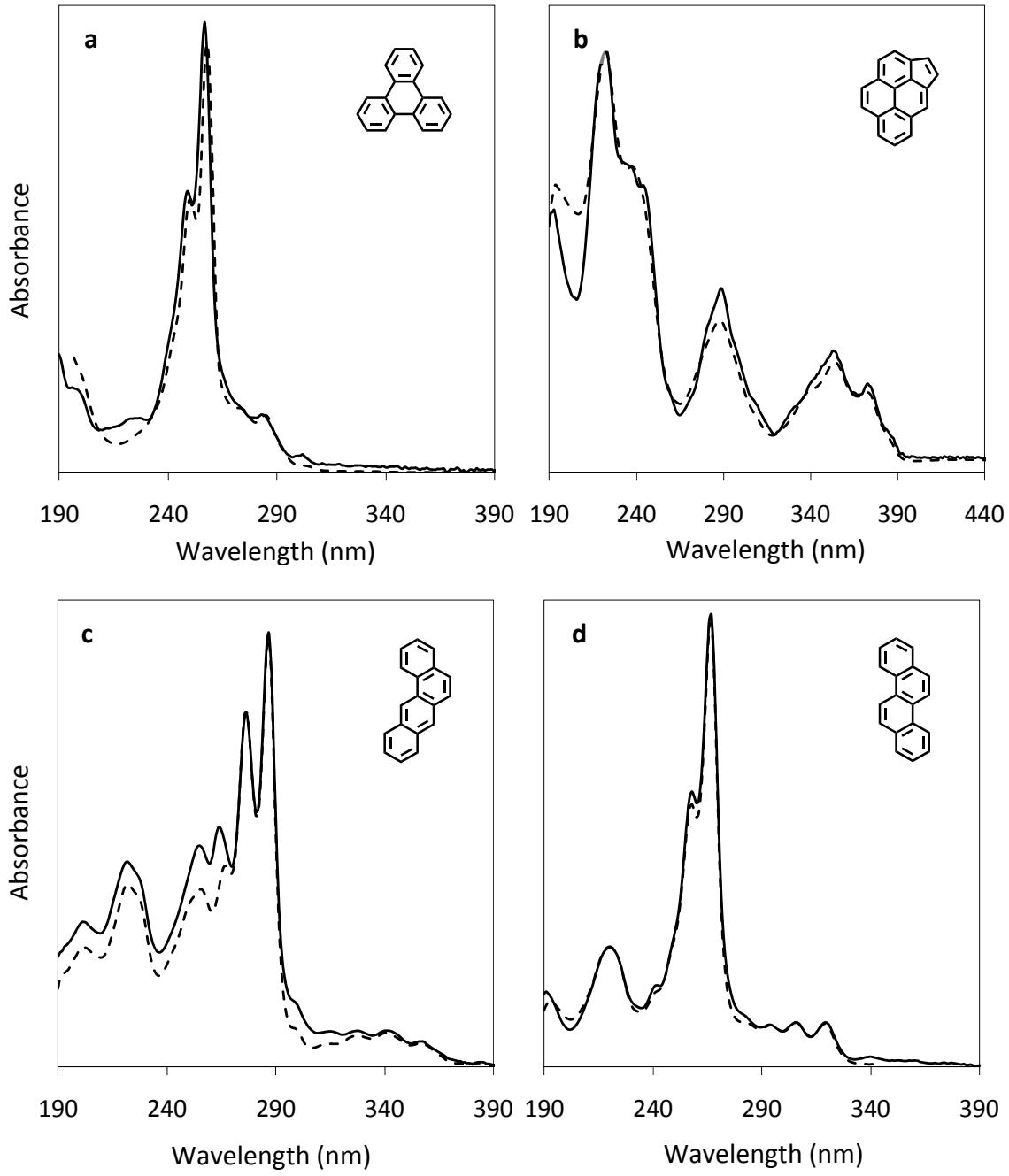

Figure 3.19 Comparisons of the UV spectra of *n*-decane pyrolysis products from the chromatogram in Figure 3.18 (solid lines) to the spectra of their corresponding reference standards (dashed lines). Matches are shown for the products identified as (a) triphenylene, eluting at 47 min; (b) cyclopenta[*cd*]pyrene, eluting at 50 min; (c), benz[*a*]anthracene eluting at 51 min; and (d) chrysene, eluting at 53 min in Figure 3.18. Structures of these products are shown next to the spectra.

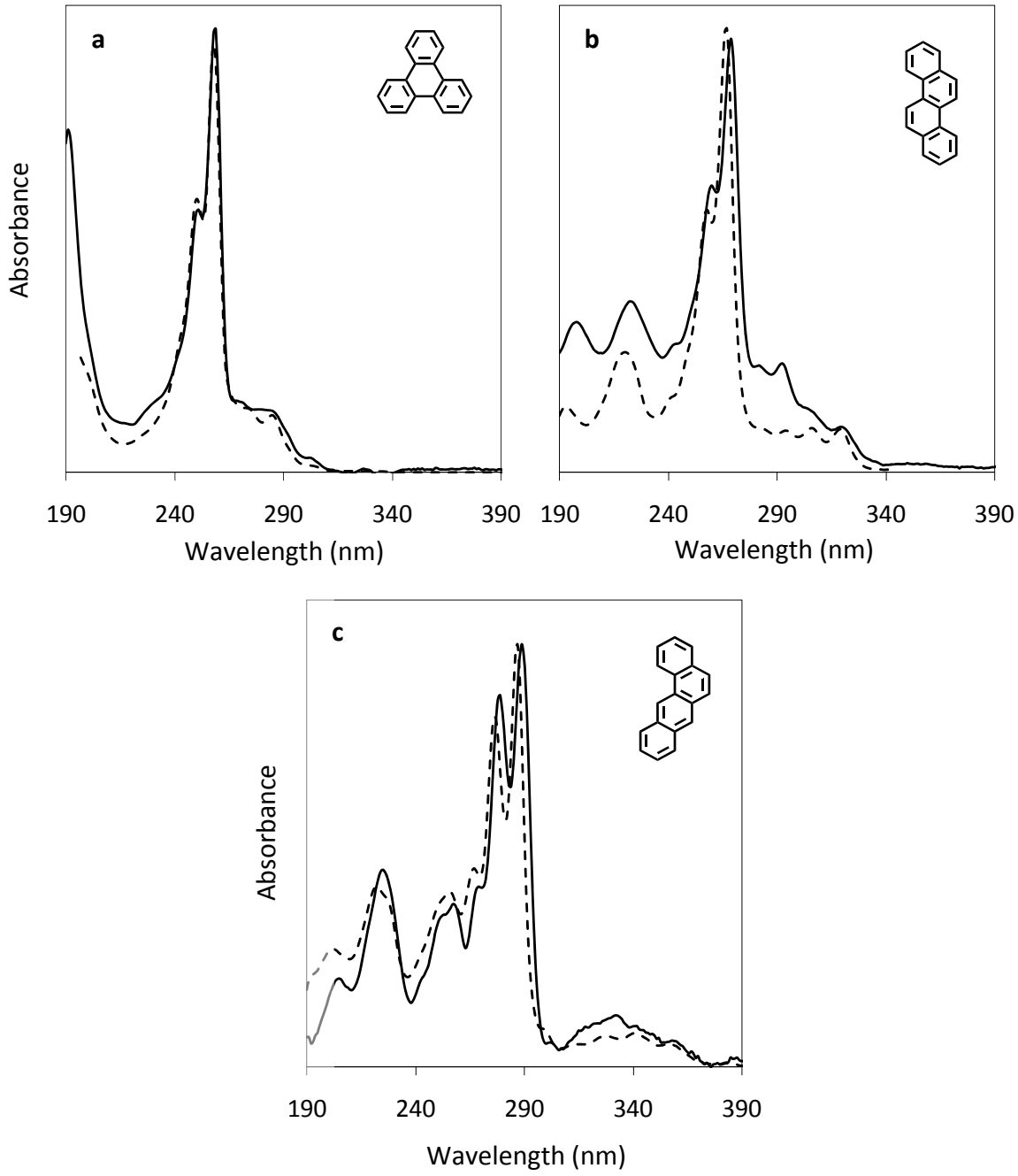

Figure 3.20 Comparisons of the UV spectra of *n*-decane pyrolysis products from the chromatogram in Figure 3.18 (solid lines) to the spectra of their corresponding reference standards (dashed lines). Comparisons are shown for (a) an alkylated triphenylene, eluting at 53 min; (b) an alkylated chrysene, eluting at 63 min; and (c) an alkylated benz[*a*]anthracene, eluting at 54 min in Figure 3.18. Structures of the parent PAH of these alkylated products are shown next to the spectra.

3.4.6 Identification of PAH Products in Fraction 6

The sixth fraction of liquid-phase products of *n*-decane pyrolysis includes the PAH benzo[*a*]pyrene, benzo[*e*]pyrene, benzo[*b*]fluoranthene, benzo[*j*]fluoranthene, benzo[*k*]fluoranthene, and perylene, along with their alkylated derivatives. Figure 3.21 presents a reversed-phase HPLC chromatogram of this fraction of the products from the highest stressing experimental conditions (570 °C and 100 atm).

The six unsubstituted five-ring PAH products are identified by matching their UV spectra to those of reference standards of each of these compounds. Benzo[*a*]pyrene, benzo[*b*]fluoranthene, and benzo[*k*]fluoranthene also have elution times which match those of reference standards separated with the same HPLC method used to generate the chromatogram in Figure 3.21. Comparisons of the UV spectra of these six five-ring PAH to the spectra of their reference standards are shown in Figures 3.22 and 3.23. The chemical formulas, molecular masses, and structures of these compounds are displayed in Table 3.8.

Shown in Figure 3.23c, co-elution with another product prevents a UV spectral match of the product identified as perylene to the spectra of a reference standard of this compound between the wavelengths 190 and 390 nm. The resemblance between the features of the UV spectra in Figures 3.22a and 3.23c indicates that the co-eluting product is benzo[*b*]fluoranthene. Perylene is identified as a product because its UV spectrum matches the UV spectrum of a perylene reference standard in the range of wavelengths that benzo[*b*]fluoranthene does not absorb (> 390 nm). Furthermore, perylene is known to have nearly the same elution time as benzo[*b*]fluoranthene on the C18 column used to separate this fraction [48].

In addition to the six unsubstituted products which are identified in Figures 3.22 and 3.23, there are 14 alkylated benzo[*a*]pyrenes, eight alkylated benzo[*e*]pyrenes, and two alkylated benzo[*j*]fluoranthenes for which the positions and/or identities of the alkyl groups are not known

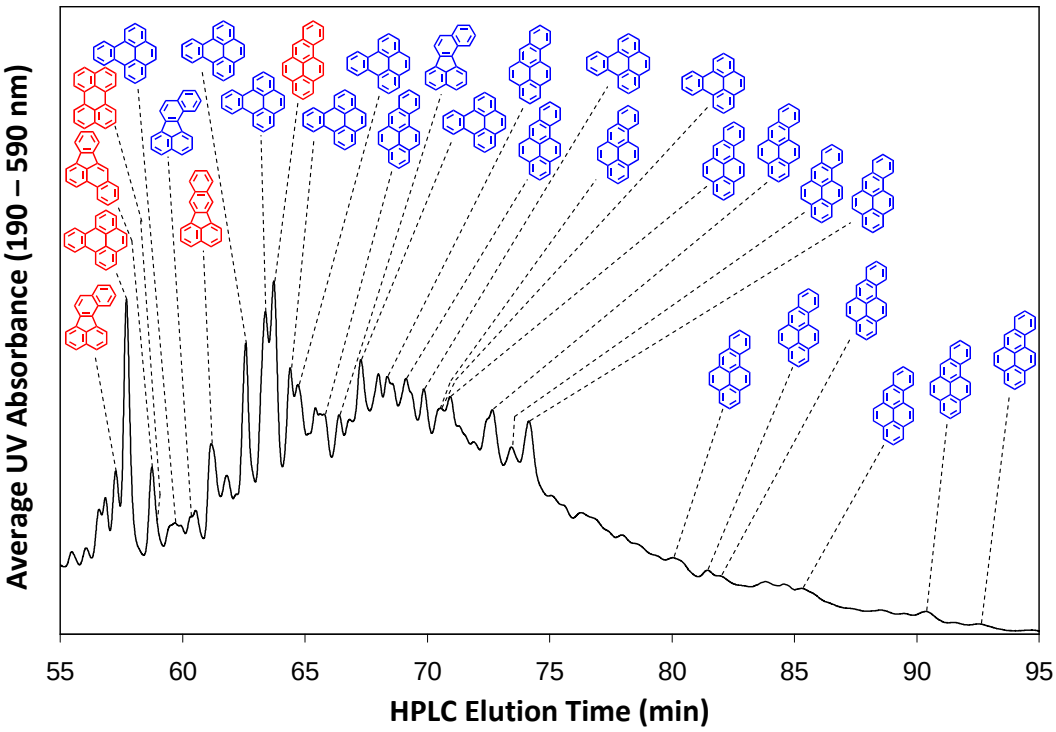

Figure 3.21 A reversed-phase HPLC chromatogram of the sixth fraction of the liquid-phase products of *n*-decane pyrolyzed at 570 °C and 100 atm. This fraction contains the $C_{20}H_{12}$ PAH isomer family and its alkylated derivatives. Red labels represent unsubstituted PAH; blue labels represent alkylated PAH for which the number, positions, and/or identities of the alkyl substituents are not known.

with certainty. These products are identified by comparison of their UV spectra to the spectra of their unsubstituted parent PAH. Comparisons of the UV spectra of one of each of these three types of alkylated PAH to the spectra of the corresponding parent PAH are shown in Figure 3.24.

Altogether, the six $C_{20}H_{12}$ PAH benzo[*a*]pyrene, benzo[*e*]pyrene, benzo[*b*]fluoranthene, benzo[*j*]fluoranthene, benzo[*k*]fluoranthene, and perylene, as well as 24 of their alkylated derivatives, have been identified as products of supercritical *n*-decane pyrolysis in the sixth fraction of liquid-phase products. The six unsubstituted PAH in this fraction have been reported before as products of *n*-decane pyrolysis [45], but the 26 alkylated derivatives are reported here for the first time.

Table 3.8 PAH identified in the sixth fraction of liquid-phase products of *n*-decane pyrolysis.

Product	Chemical Formula	Molecular Mass (Da)	Structure
Perylene	$C_{20}H_{12}$	252	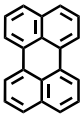
Benzo[*a*]pyrene	$C_{20}H_{12}$	252	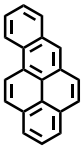
Benzo[*e*]pyrene	$C_{20}H_{12}$	252	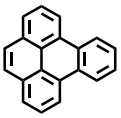
Benzo[*b*]fluoranthene	$C_{20}H_{12}$	252	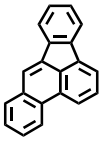
Benzo[*j*]fluoranthene	$C_{20}H_{12}$	252	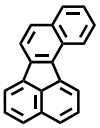
Benzo[*k*]fluoranthene	$C_{20}H_{12}$	252	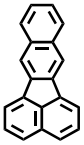

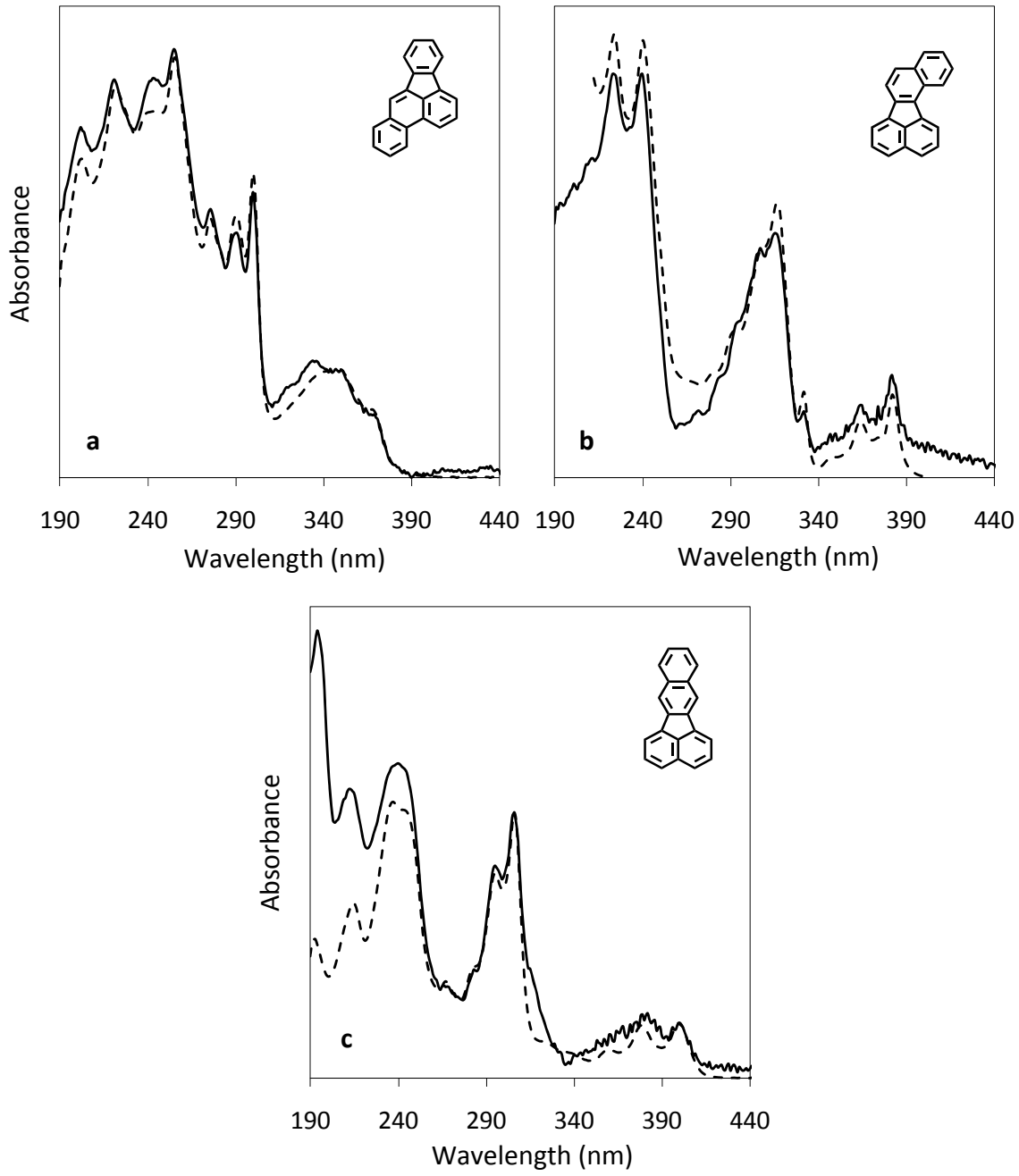

Figure 3.22 Comparisons of the UV spectra of *n*-decane pyrolysis products from the chromatogram in Figure 3.21 (solid lines) to the spectra of the corresponding reference standards (dashed lines). Matches are shown for the products identified as (a) benzo[*b*]fluoranthene, eluting at 58 min; (b) benzo[*j*]fluoranthene, eluting at 57 min; and (c) benzo[*k*]fluoranthene, eluting at 61 min in Figure 3.21. Structures of the products are shown next to the spectra.

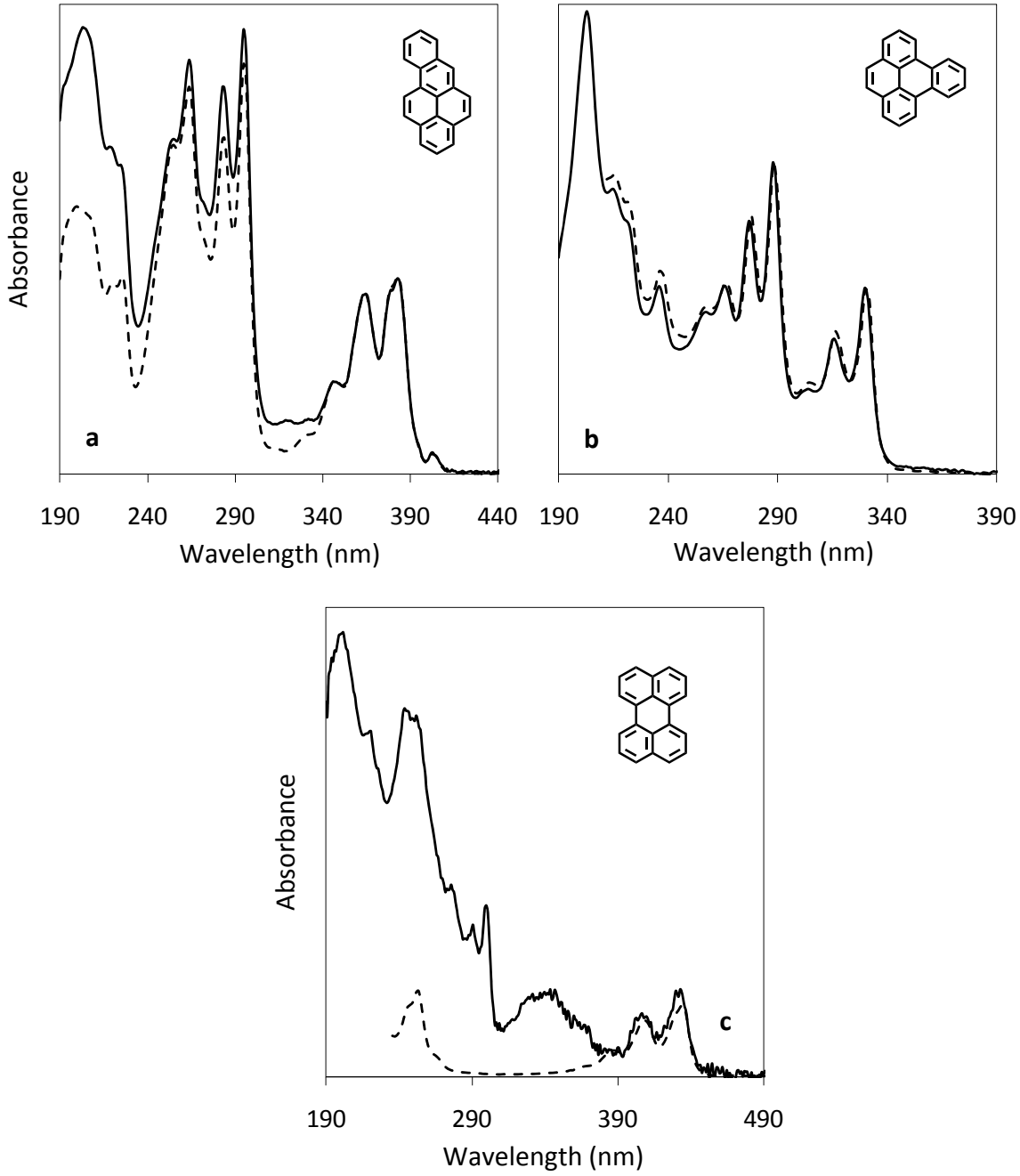

Figure 3.23 Comparisons of the UV spectra of *n*-decane pyrolysis products from the chromatogram in Figure 3.21 (solid lines) to the spectra of the corresponding reference standards (dashed lines). Matches are shown for the products identified as (a) benzo[*a*]pyrene, eluting at 64 min; (b) benzo[*e*]pyrene, eluting at 58 min; and (c) perylene, eluting at 59 min in Figure 3.21. Co-elution of benzo[*b*]fluoranthene with perylene is responsible for the UV absorbance between 190 and 390 nm in the product spectra of (c). Structures of these products are shown next to the spectra.

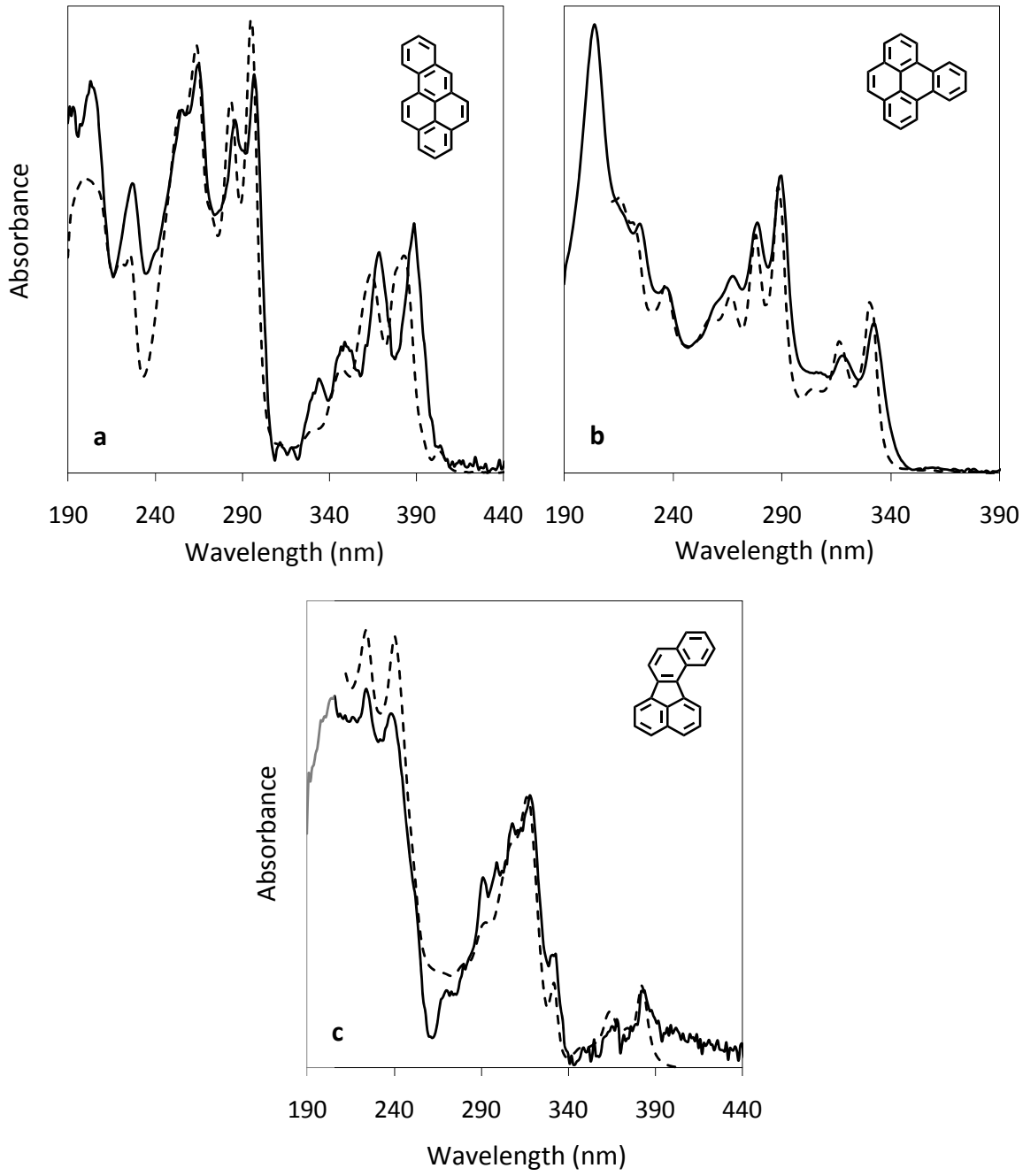

Figure 3.24 Comparisons of the UV spectra of alkylated *n*-decane pyrolysis products from the chromatogram in Figure 3.21 (solid lines) to the spectra of the corresponding unsubstituted PAH reference standards (dashed lines). Comparisons are shown for (a) an alkylated benzo[*a*]pyrene, eluting at 68 min; (b) an alkylated benzo[*e*]pyrene, eluting at 63 min; and (c) an alkylated benzo[*j*]fluoranthene, eluting at 66 min in Figure 3.21. Structures of the parent PAH of these alkylated products are shown next to the spectra.

3.4.7 Identification of PAH Products in Fraction 7

The seventh fraction of liquid-phase products of *n*-decane pyrolysis includes the six- and seven-ring PAH benzo[*ghi*]perylene, anthanthrene, indeno[1,2,3-*cd*]pyrene, and coronene, along with their alkylated derivatives. Figure 3.25 presents a reversed-phase HPLC chromatogram of this fraction of the products from the highest stressing experimental conditions (570 °C and 100 atm).

The four unsubstituted six- and seven-ring PAH products are identified by matching their UV spectra to those of the reference standards for each of these compounds. Also, benzo[*ghi*]perylene and indeno[1,2,3-*cd*]pyrene have elution times which match those of reference standards separated with the same HPLC method used to generate the chromatogram in Figure 3.25. Comparison of the UV spectra of the four PAH products to the spectra of reference standards are shown in Figure 3.26. The chemical formulas, molecular masses, and structures of these compounds are displayed in Table 3.9.

Methylcoronene, eluting at 101 min in Figure 3.25, is identified as a product by UV spectral and HPLC elution time data. Comparison of the UV spectrum of this product to that of a reference standard of coronene shows that the aromatic portion of the structure of this compound is coronene. Furthermore, its elution time relative to its unsubstituted parent PAH is known by analysis of other product samples on the C18 column used to separate this fraction [49]. Due to the symmetry of coronene, it has only one singly methylated derivative.

In addition to these five products which are identified exactly, there are 11 alkylated indeno[1,2,3-*cd*]pyrenes, six alkylated benzo[*ghi*]perylenes, four alkylated coronenes, and four alkylated anthanthrenes for which the number, positions, and/or identities of the alkyl groups are not known with certainty. These alkylated PAH are identified by comparing the UV spectra of the products to the spectra of reference standards of the appropriate unsubstituted parent PAH.

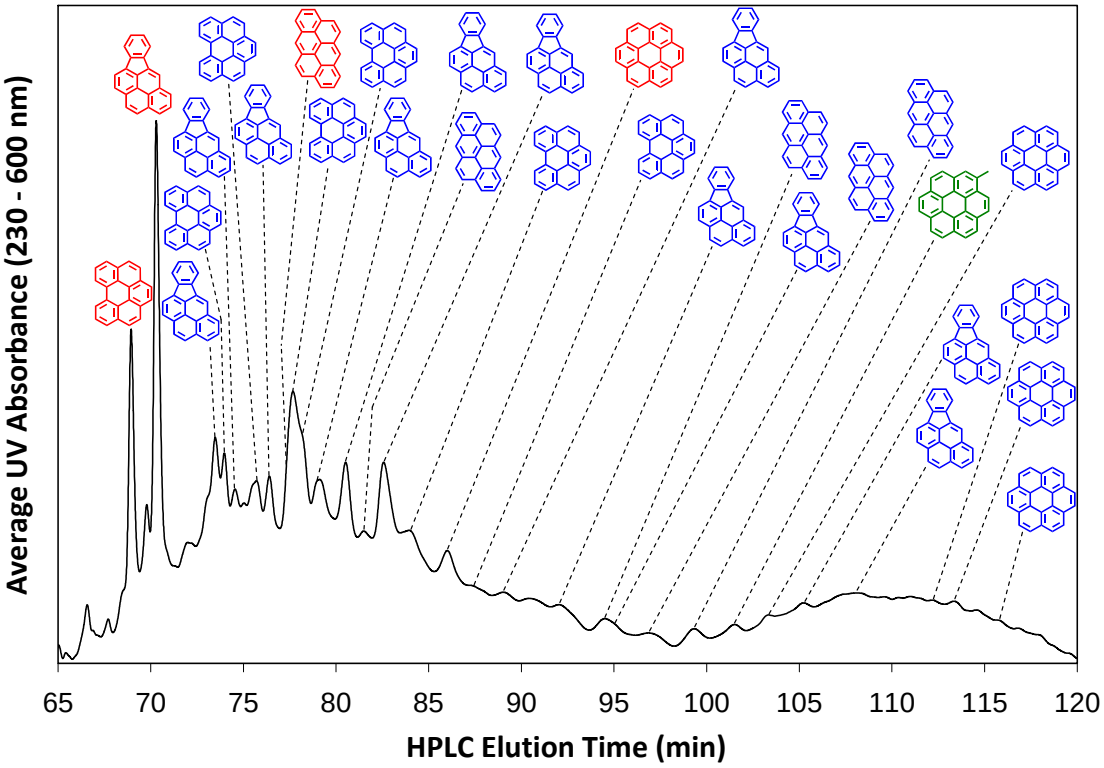

Figure 3.25 A reversed-phase HPLC chromatogram of the seventh fraction of the liquid-phase products of *n*-decane pyrolyzed at 570 °C and 100 atm. This fraction primarily contains the $C_{22}H_{12}$ PAH isomer family and its alkylated derivatives. Red labels represent unsubstituted PAH; green labels represent singly methylated PAH (the position of the methyl group labeled when known); blue labels represent alkylated PAH for which the number, positions and/or identities of the alkyl substituents are not known.

Table 3.9 PAH identified in the seventh fraction of liquid-phase products of *n*-decane pyrolysis.

Product	Chemical Formula	Molecular Mass (Da)	Structure
Benzo[*ghi*]perylene	$C_{22}H_{12}$	276	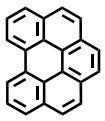
Anthanthrene	$C_{22}H_{12}$	276	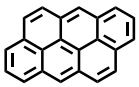
Indeno[1,2,3-*cd*]pyrene	$C_{22}H_{12}$	276	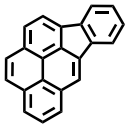
Coronene	$C_{24}H_{12}$	300	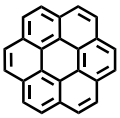

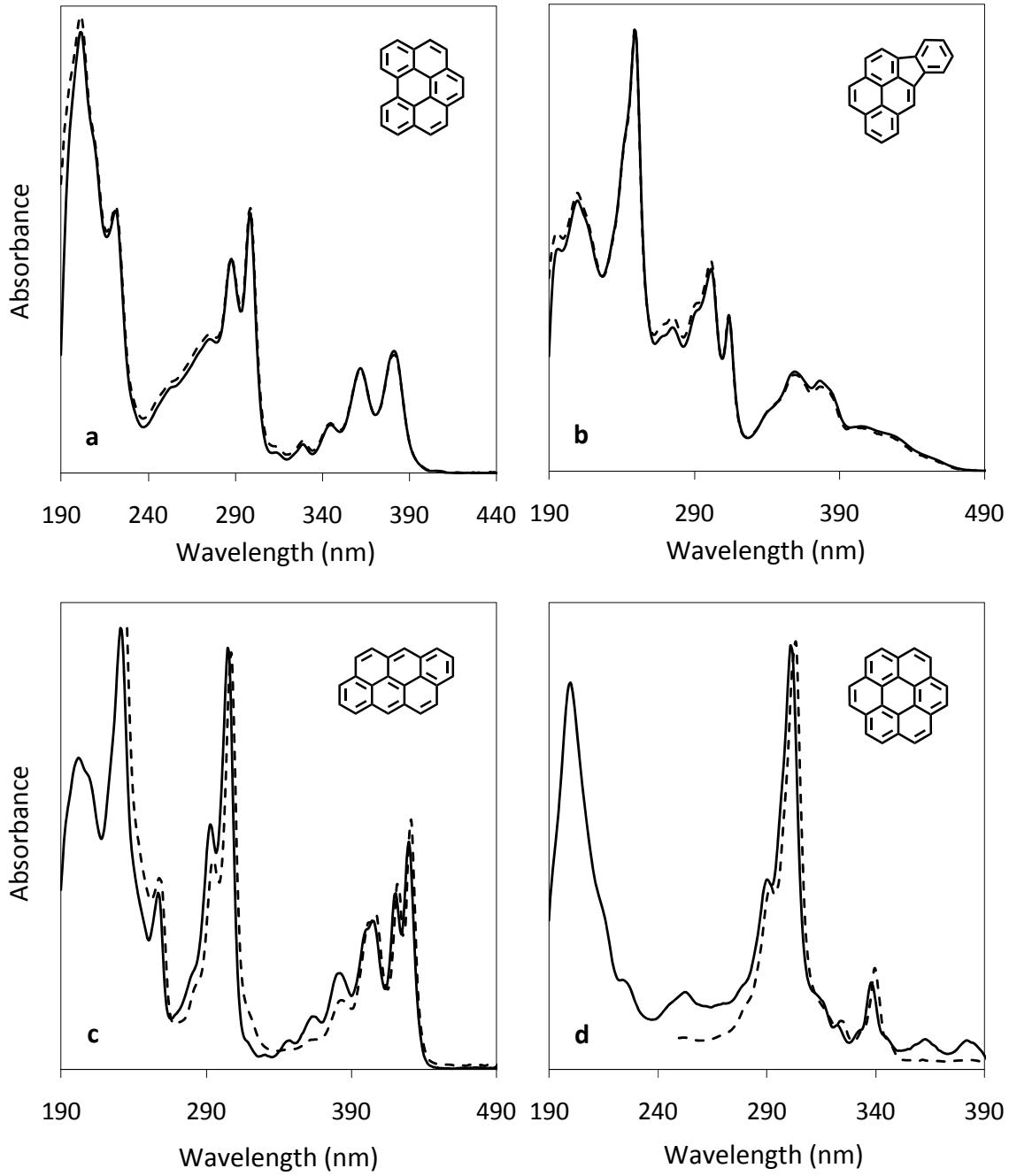

Figure 3.26 Comparisons of the UV spectra of *n*-decane pyrolysis products from the chromatogram in Figure 3.25 (solid lines) to the spectra of the corresponding reference standards (dashed lines). Matches are shown for the products identified as (a) benzo[*ghi*]perylene, eluting at 69 min; (b) indeno[1,2,3-*cd*]pyrene, eluting at 70 min; (c) anthanthrene, eluting at 77 min; and (d) coronene, eluting at 86 min in Figure 3.25. Structures of these products are shown next to the spectra.

Comparisons of the UV spectra of one of each of these four types of alkylated PAH to the spectra of the corresponding parent PAH are shown in Figure 3.27.

Altogether, benzo[*ghi*]perylene, anthanthrene, indeno[1,2,3-*cd*]pyrene, and coronene, as well as 26 alkylated derivatives of these products have been identified as products of supercritical *n*-decane pyrolysis in the seventh fraction of liquid-phase products. The four unsubstituted PAH in this fraction have been reported before as products of *n*-decane pyrolysis [45], but the 26 alkylated derivatives are reported here for the first time.

3.4.8 Identification of PAH Products in Fraction 8

The eighth fraction of liquid-phase products of *n*-decane pyrolysis includes the six-ring PAH naphtho[2,1-*a*]pyrene, naphtho[2,3-*a*]pyrene, naphtho[2,3-*e*]pyrene, dibenzo[*a,e*]pyrene, dibenzo[*a,i*]pyrene, dibenzo[*a,h*]pyrene, dibenzo[*e,l*]pyrene, naphtho[1,2-*b*]fluoranthene, naphtho[2,3-*b*]fluoranthene, naphtho[2,3-*j*]fluoranthene, dibenzo[*a,k*]fluoranthene, dibenzo[*j,l*]fluoranthene, and benzo[*b*]perylene, along with several of their alkylated derivatives. One product is found only as an alkylated derivative; the unsubstituted parent PAH of this product is naphtho[1,2-*k*]fluoranthene. Figure 3.28 presents a reversed-phase HPLC chromatogram of this fraction of the products from the highest stressing experimental conditions (570 °C and 100 atm).

The thirteen unsubstituted six-ring PAH products are identified by matching their UV spectra to those of the reference standards for each of these compounds. Comparisons of the UV spectra of these thirteen unsubstituted PAH products to the spectra of the corresponding standards are shown in Figures 3.29 through 3.33. The chemical formulas, molecular masses, and structures of these compounds are displayed in Tables 3.10 and 3.11.

The strong coincidence of the product and reference-standard UV spectra in Figures 3.29 to 3.32 leads to straightforward identifications of twelve of the unsubstituted product PAH in

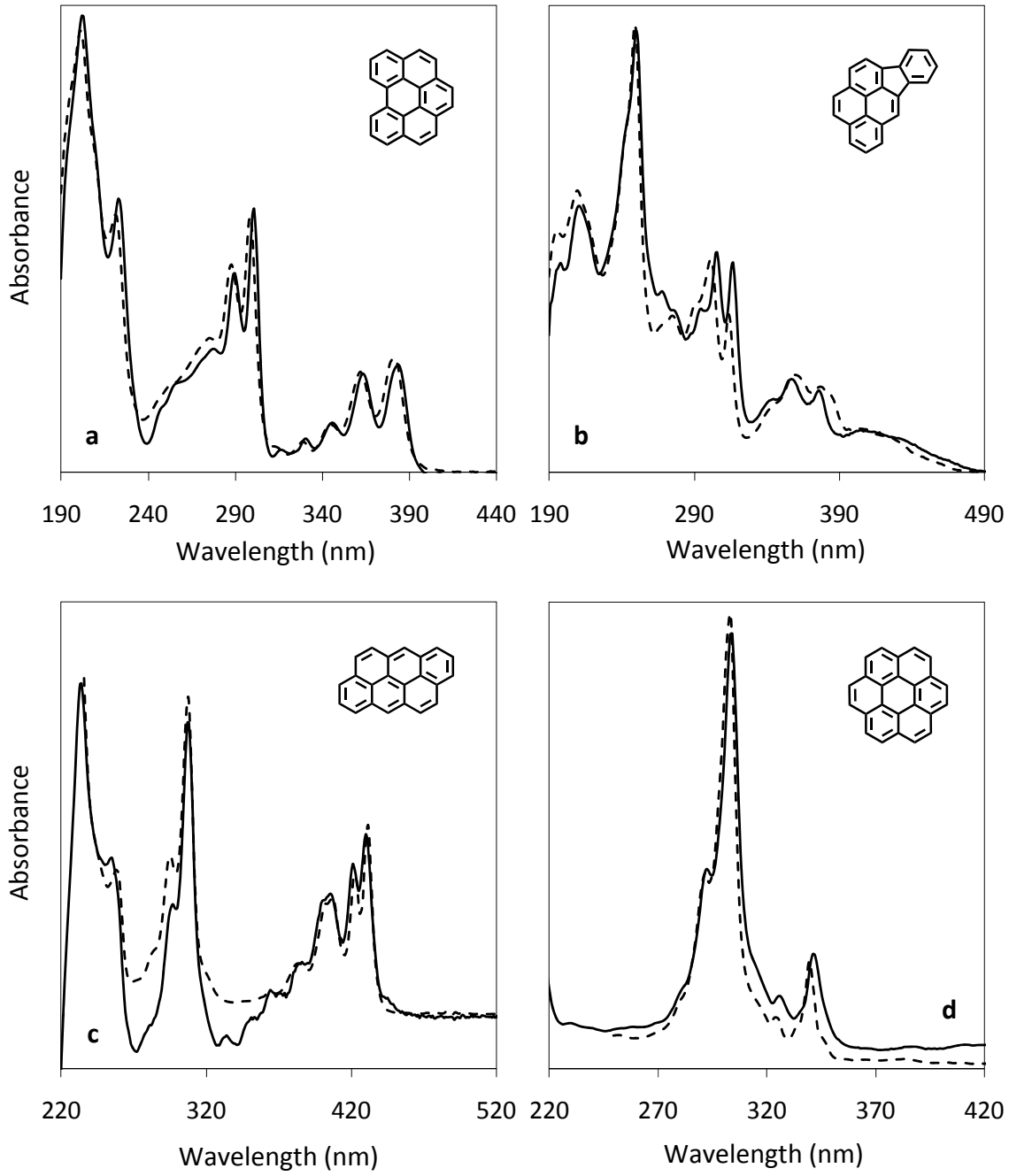

Figure 3.27 Comparisons of the UV spectra of *n*-decane pyrolysis products from the chromatogram in Figure 3.25 (solid lines) to the spectra of reference standards (dashed lines) of appropriate unsubstituted PAH. Comparisons are shown for (a) an alkylated benzo[*ghi*]perylene, eluting at 74 min; (b) an alkylated indeno[1,2,3-*cd*]pyrene, eluting at 76 min; (c) an alkylated anthanthrene, eluting at 97 min; and (d) an alkylated coronene, eluting at 103 min in Figure 3.25. Structures of the unsubstituted parent PAH of these alkylated PAH products are shown next to the spectra.

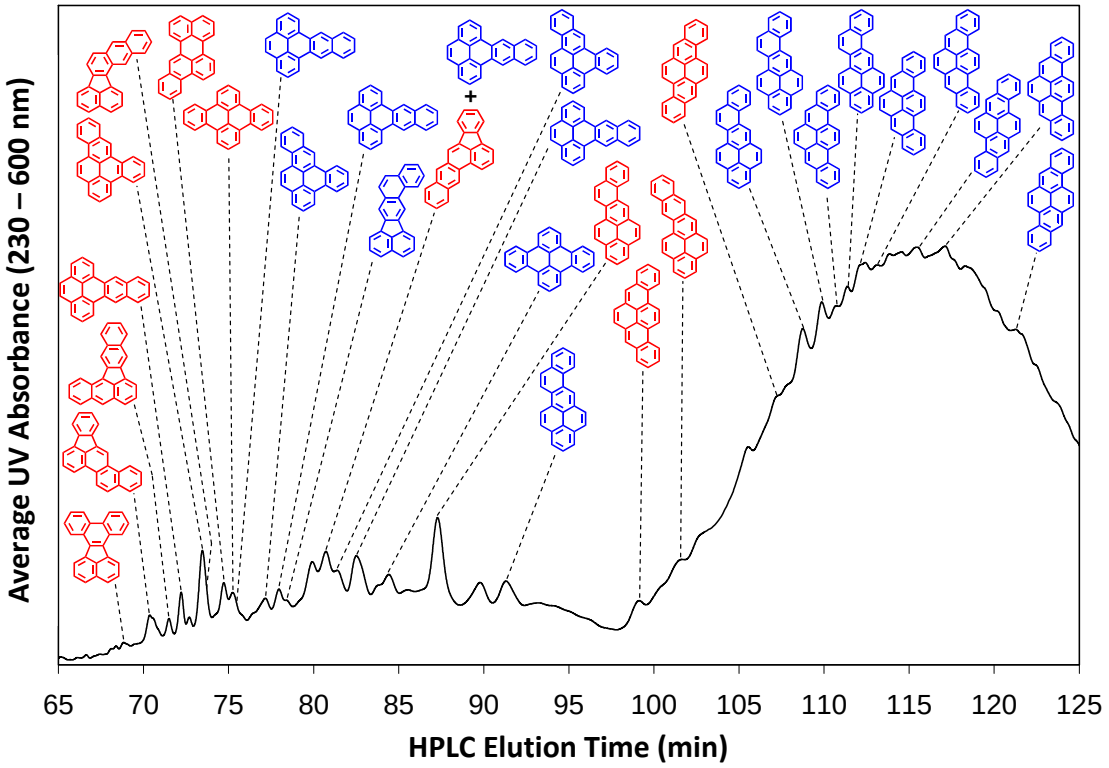

Figure 3.28 A reversed-phase HPLC chromatogram of the eighth fraction of the liquid-phase products of *n*-decane pyrolyzed at 570 °C and 100 atm. This fraction contains the $C_{24}H_{14}$ PAH isomer family and its alkylated derivatives. Red labels represent unsubstituted PAH; blue labels represent alkylated PAH for which the number, positions, and/or identities of the alkyl substituents are not known.

Figure 3.28. However, as shown in Figure 3.28, naphtho[2,3-*b*]fluoranthene co-elutes (at 81 minutes) with an alkylated derivative of naphtho[2,3-*e*]pyrene. These two products are identified by comparison of the UV spectrum of the two co-eluting products with the spectra of the appropriate reference standards. This comparison is shown in Figure 3.33. Absorbance maxima at 279, 365, 384, and 408 nm match those of the spectrum of naphtho[2,3-*b*]fluoranthene, showing that one of the co-eluting products is this compound. Absorbance maxima at 232, 247, and 272 nm match those of the spectrum of naphtho[2,3-*e*]pyrene, showing that the other co-eluting product is an alkylated derivative of this compound (since the unsubstituted parent PAH of this compound is identified at 72 minutes in the chromatogram in Figure 3.28). Both

Table 3.10 PAH identified in the eighth fraction of liquid-phase products of *n*-decane pyrolysis. Note that only an alkylated derivative of naphtho[1,2-*k*]fluoranthene is identified among the pyrolysis products, even though the unsubstituted PAH is shown here.

Product	Chemical Formula	Molecular Mass (Da)	Structure
Benzo[*b*]perylene	$C_{24}H_{14}$	302	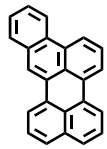
Naphtho[1,2-*b*]-fluoranthene	$C_{24}H_{14}$	302	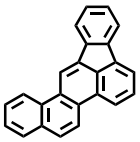
Naphtho[2,3-*b*]-fluoranthene	$C_{24}H_{14}$	302	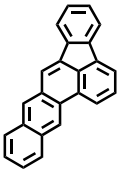
Naphtho[2,3-*j*]fluoranthene	$C_{24}H_{14}$	302	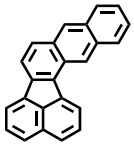
Naphtho[1,2-*k*]fluoranthene	$C_{24}H_{14}$	302	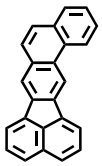
Dibenzo[*a*,*k*]fluoranthene	$C_{24}H_{14}$	302	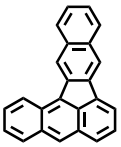
Dibenzo[*j*,*l*]fluoranthene	$C_{24}H_{14}$	302	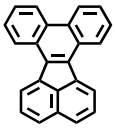

Table 3.11 PAH identified in the eighth fraction of liquid-phase products of *n*-decane pyrolysis.

Product	Chemical Formula	Molecular Mass (Da)	Structure
Naphtho[2,1-*a*]pyrene	$C_{24}H_{14}$	302	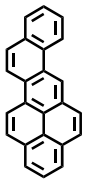
Naphtho[2,3-*a*]pyrene	$C_{24}H_{14}$	302	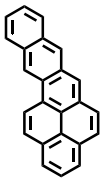
Naphtho[2,3-*e*]pyrene	$C_{24}H_{14}$	302	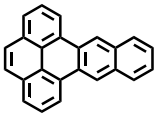
Dibenzo[*a*,*e*]pyrene	$C_{24}H_{14}$	302	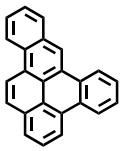
Dibenzo[*a*,*h*]pyrene	$C_{24}H_{14}$	302	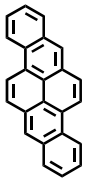
Dibenzo[*a*,*i*]pyrene	$C_{24}H_{14}$	302	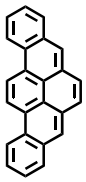
Dibenzo[*e*,*l*]pyrene	$C_{24}H_{14}$	302	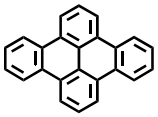

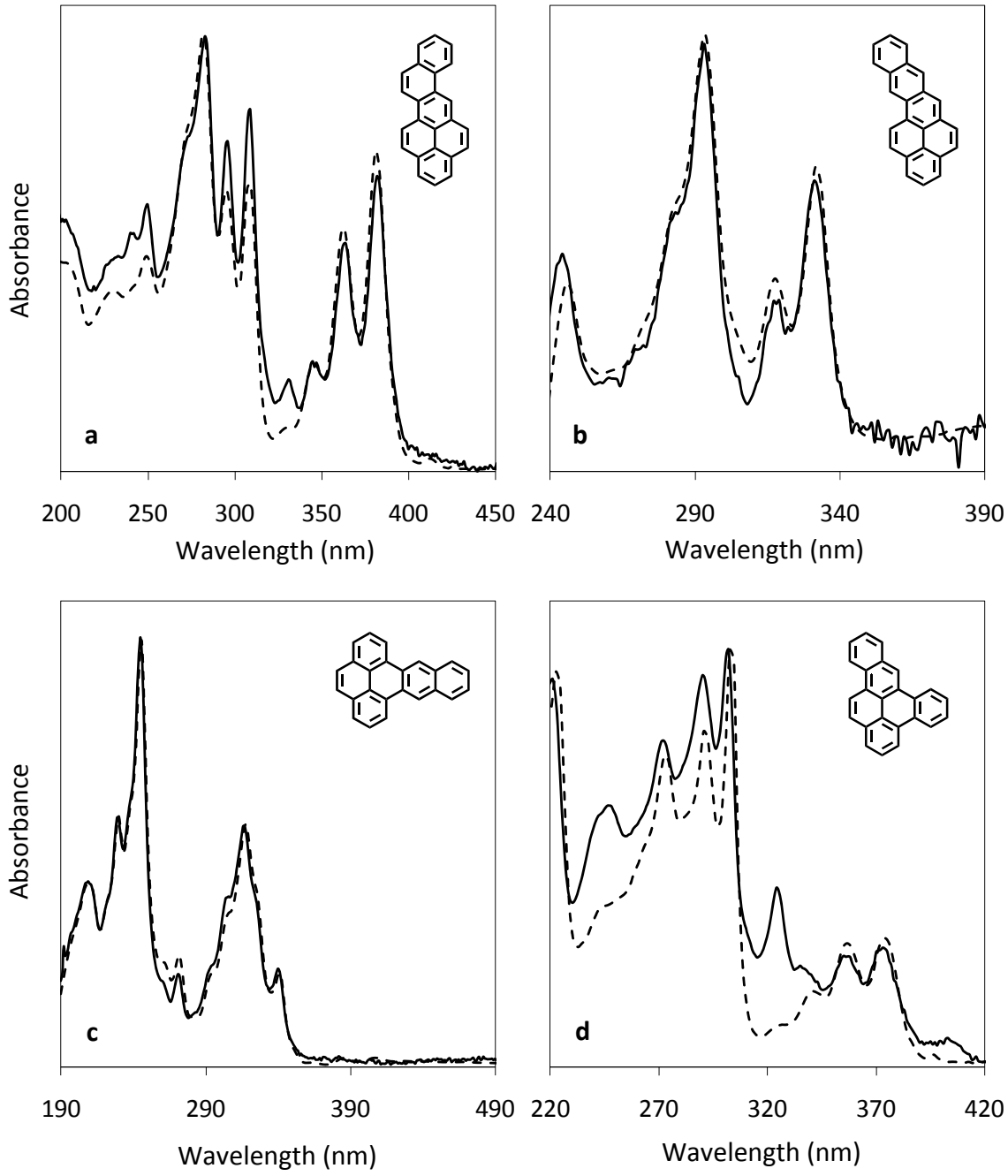

Figure 3.29 Comparisons of the UV spectra of *n*-decane pyrolysis products from the chromatogram in Figure 3.28 (solid lines) to the spectra of the corresponding reference standards (dashed lines). Matches are shown for the products identified as (a) naphtho[2,1-*a*]pyrene, eluting at 87 min; (b) naphtho[2,3-*a*]pyrene, eluting at 101 min; (c) naphtho[2,3-*e*]pyrene, eluting at 72 min; and (d) dibenzo[*a*,*e*]pyrene, eluting at 73 min in Figure 3.28. Structures of these products are shown next to the spectra.

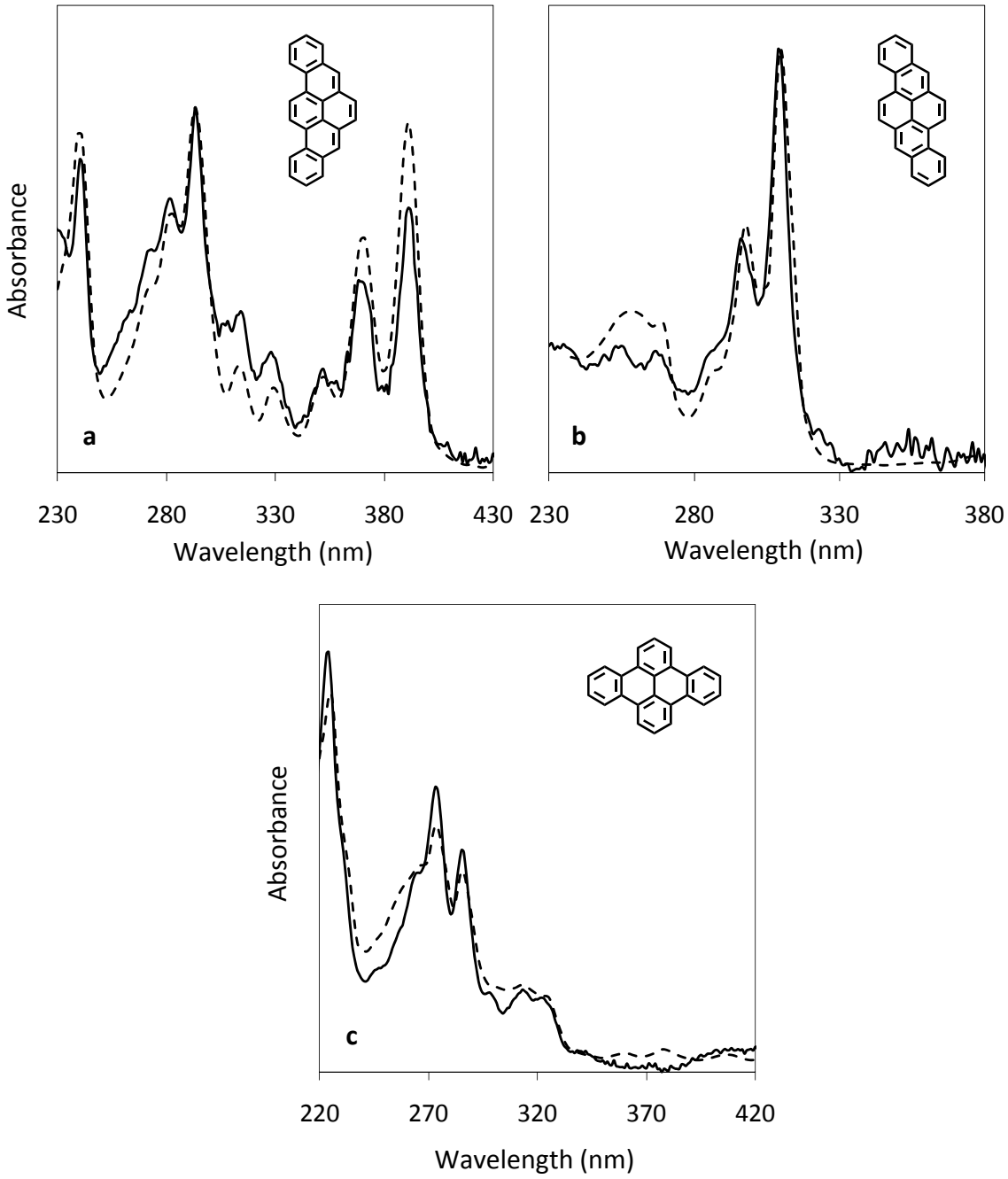

Figure 3.30 Comparisons of the UV spectra of *n*-decane pyrolysis products from the chromatogram in Figure 3.28 (solid lines) to the spectra of the corresponding reference standards (dashed lines). Matches are shown for the products identified as (a) dibenzo[*a*,*i*]pyrene, eluting at 99 min; (b) dibenzo[*a*,*h*]pyrene, eluting at 107 min; and (c) dibenzo[*e*,*l*]pyrene, eluting at 76 min in Figure 3.28. Structures of these products are shown next to the spectra.

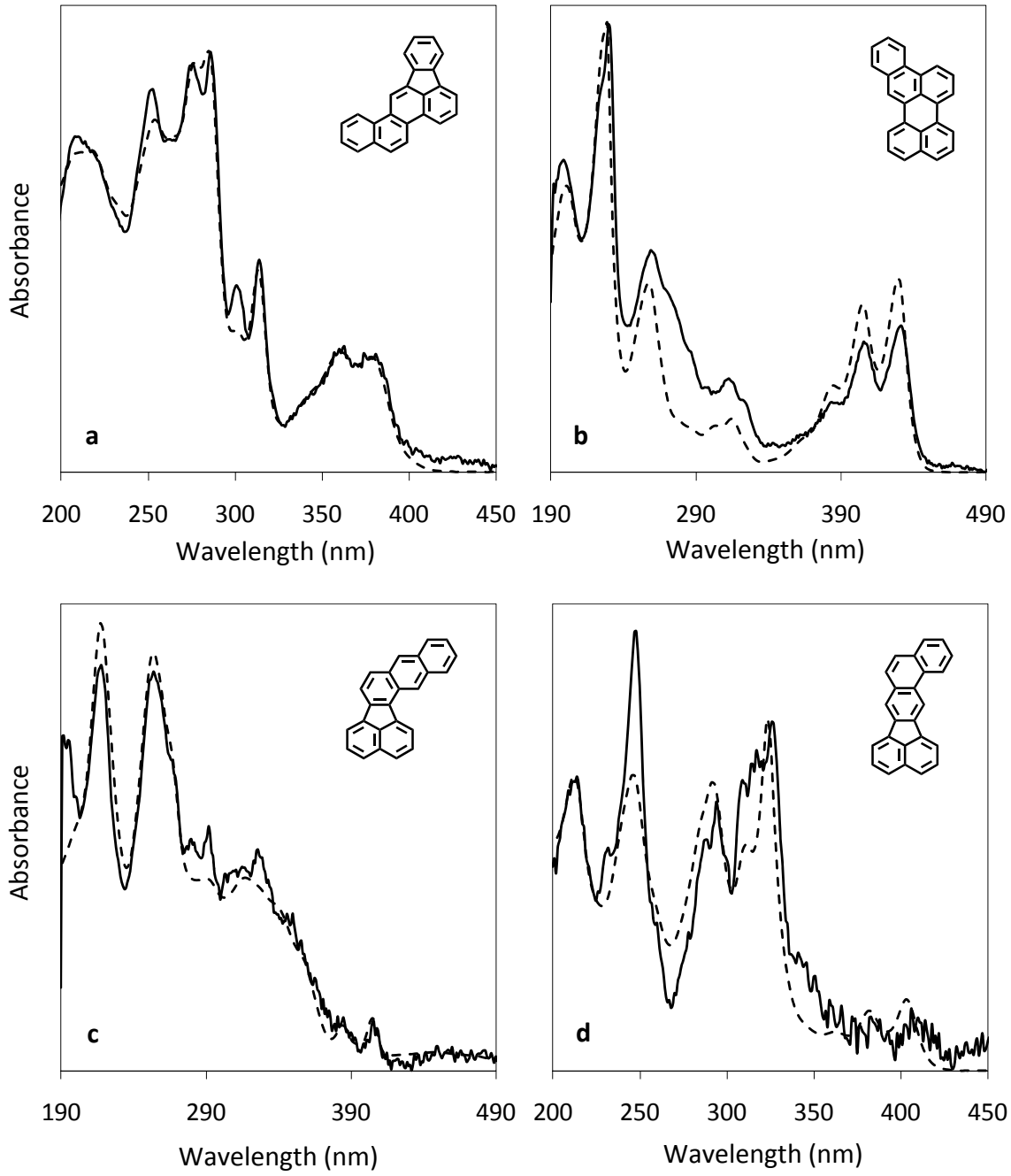

Figure 3.31 Comparisons of the UV spectra of *n*-decane pyrolysis products from the chromatogram in Figure 3.28 (solid lines) to the spectra of the corresponding reference standards (dashed lines). Comparisons are shown for the products identified as (a) naphtho[1,2-*b*]fluoranthene, eluting at 71 min; (b) benzo[*b*]perylene, eluting at 75 min; (c) naphtho[2,3-*j*]fluoranthene, eluting at 73 min; and (d) an alkylated naphtho[1,2-*k*]fluoranthene, eluting at 78 min in Figure 3.28. Structures of the products are shown next to the spectra in a, b, and c; in d the structure of the unsubstituted parent PAH of naphtho[1,2-*k*]fluoranthene is shown.

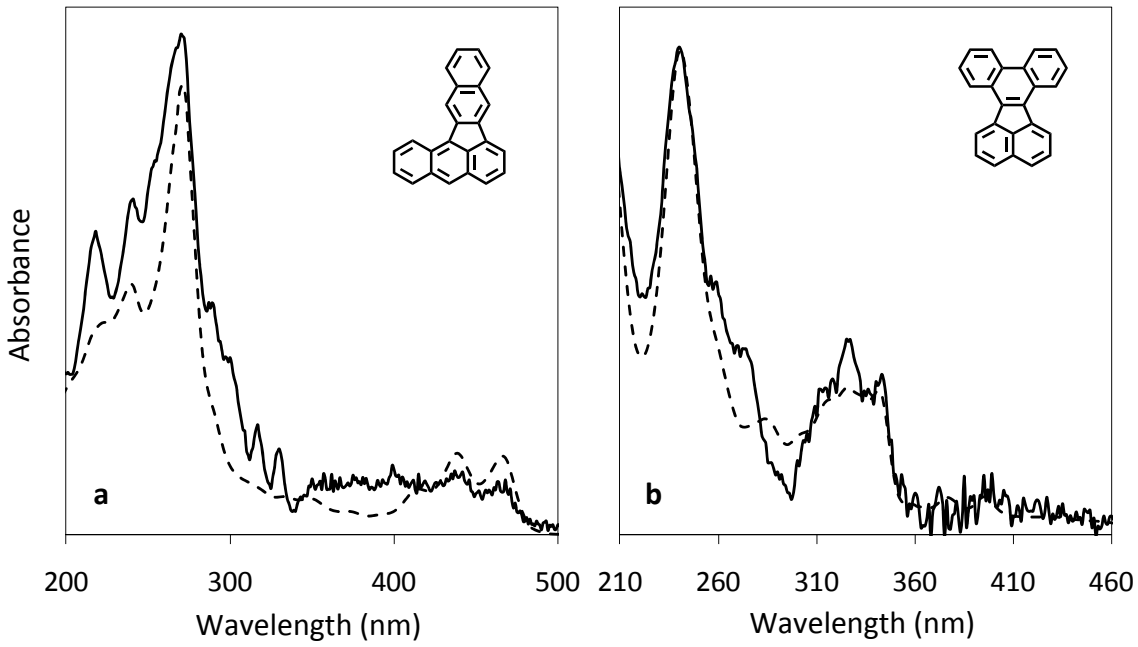

Figure 3.32 Comparisons of the UV spectra of *n*-decane pyrolysis products from the chromatogram in Figure 3.28 (solid lines) to the spectra of the corresponding reference standards (dashed lines). Matches are shown for the products identified as (a) dibenzo[*a,k*]fluoranthene, eluting at 71 min, and (b) dibenzo[*j,l*]fluoranthene, eluting at 69 min in Figure 3.28. Structures of these products are shown next to the spectra.

compounds have absorbance maxima between 315 and 318 nm, causing the UV spectrum of the co-eluting products to exhibit a maximum at 316 nm. Also, the HPLC elution time of naphtho[2,3-*b*]fluoranthene (on the C18 column used to separate this fraction), relative to those of other members of its isomer family, is known [49]—providing further confirmation of the identity of this product PAH. The chemical formula, molecular mass, and structure of naphtho[2,3-*b*]fluoranthene is displayed in Table 3.10.

The product identified as an alkylated naphtho[1,2-*k*]fluoranthene is the earliest eluting PAH with a UV spectrum matching the reference spectrum of naphtho[1,2-*k*]fluoranthene but is not identified as an unsubstituted PAH. Naphtho[1,2-*k*]fluoranthene is known to elute before benzo[*b*]perylene on the C18 column used in the separation of this fraction [49]. Since this

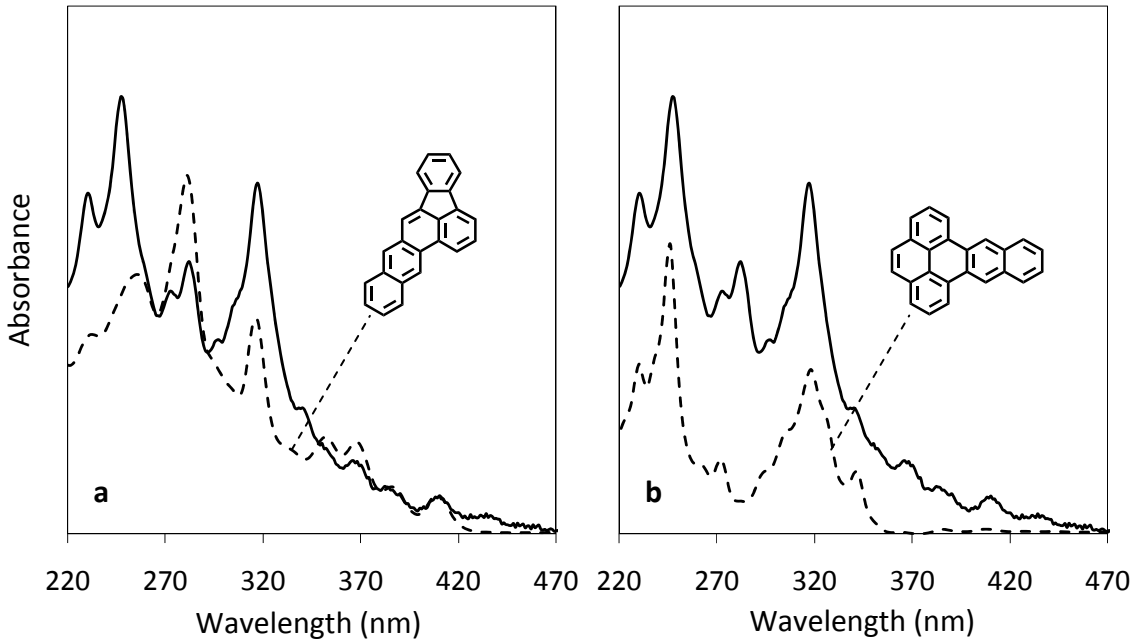

Figure 3.33 Comparisons of the UV spectrum of the two *n*-decane pyrolysis products co-eluting at 81 min in the chromatogram in Figure 3.28 (solid lines) to the spectra of reference standards (dashed lines). Reference standard spectra are (a) naphtho[2,3-*b*]fluoranthene and (b) naphtho[2,3-*e*]pyrene. Absorbance maxima at 279, 365, 384, and 408 nm match those of the spectrum of naphtho[2,3-*b*]fluoranthene, showing that one of the co-eluting products is this compound. Absorbance maxima at 232, 247, and 272 nm match those of the spectrum of naphtho[2,3-*e*]pyrene, showing that the other co-eluting product is the alkylated derivative of this compound (Figure 3.29c shows that the unsubstituted parent PAH of this compound is identified at 72 minutes in the chromatogram). Both compounds have absorbance maxima between 315 and 318 nm, causing the spectrum of the co-eluting products to exhibit a maximum at 316 nm. Product structures of the reference standards are shown next to the spectra.

compound elutes after benzo[*b*]perylene and alkylated PAH are known to elute later than their unsubstituted parent PAH on this C18 column, this product is identified as the alkylated derivative. The chemical formula, molecular mass, and structure of the unsubstituted parent PAH of this compound are displayed in Table 3.10. Comparison of the UV spectrum of the product identified as an alkylated naphtho[1,2-*k*]fluoranthene to that of its unsubstituted parent PAH is shown in Figure 3.31d.

In addition to the 13 unsubstituted and two alkylated PAH products identified in Figures 3.29 to 3.33, Fraction 8 has been found to contain four alkylated derivatives of

dibenzo[*a,i*]pyrene, four of naphtho[2,1-*a*]pyrene, three of naphtho[2,3-*e*]pyrene, two of dibenzo[*a,e*]pyrene, two of dibenzo[*a,h*]pyrene, and one of dibenzo[*e,l*]pyrene for which the number, positions, and/or identities of the alkyl groups are not known with certainty. They are identified by comparing the UV spectra of the products to the spectra of reference standards of the appropriate unsubstituted parent PAH. Comparisons of the UV spectra of one of each of these six types of alkylated PAH to the spectra of the corresponding parent PAH are shown in Figures 3.34 and 3.35.

Altogether, 13 unsubstituted PAH belonging to the $C_{24}H_{14}$ isomer family as well as 17 alkylated derivatives of these products (and one alkylated PAH whose parent PAH was not identified among the products) have been identified as products of supercritical *n*-decane pyrolysis in the eighth fraction of liquid-phase products. Of these, only three, dibenzo[*a,i*]pyrene, dibenzo[*a,h*]pyrene, and dibenzo[*a,e*]pyrene, have ever been reported before as products of *n*-decane pyrolysis or combustion [45]. The other ten unsubstituted $C_{24}H_{14}$ PAH and 18 alkylated PAH are reported here for the first time.

3.4.9 Identification of PAH Products in Fraction 9

The ninth fraction of *n*-decane pyrolysis products includes the seven-ring PAH dibenzo[*b,ghi*]perylene, dibenzo[*e,ghi*]perylene, naphtho[1,2,3,4-*ghi*]perylene, dibenzo-[*cd,lm*]perylene, and phenanthro[2,3-*a*]pyrene, along with some of their alkylated derivatives. Figure 3.36 presents a reversed-phase HPLC chromatogram of this fraction of the products from the highest stressing experimental conditions (570 °C and 100 atm).

The five unsubstituted seven-ring PAH products in this fraction are identified by matching their UV spectra to those of the reference standards for each of these compounds. Comparisons of the UV spectra of these five PAH products to the spectra of the corresponding reference standards are shown in Figures 3.37 and 3.38. Three of these products,

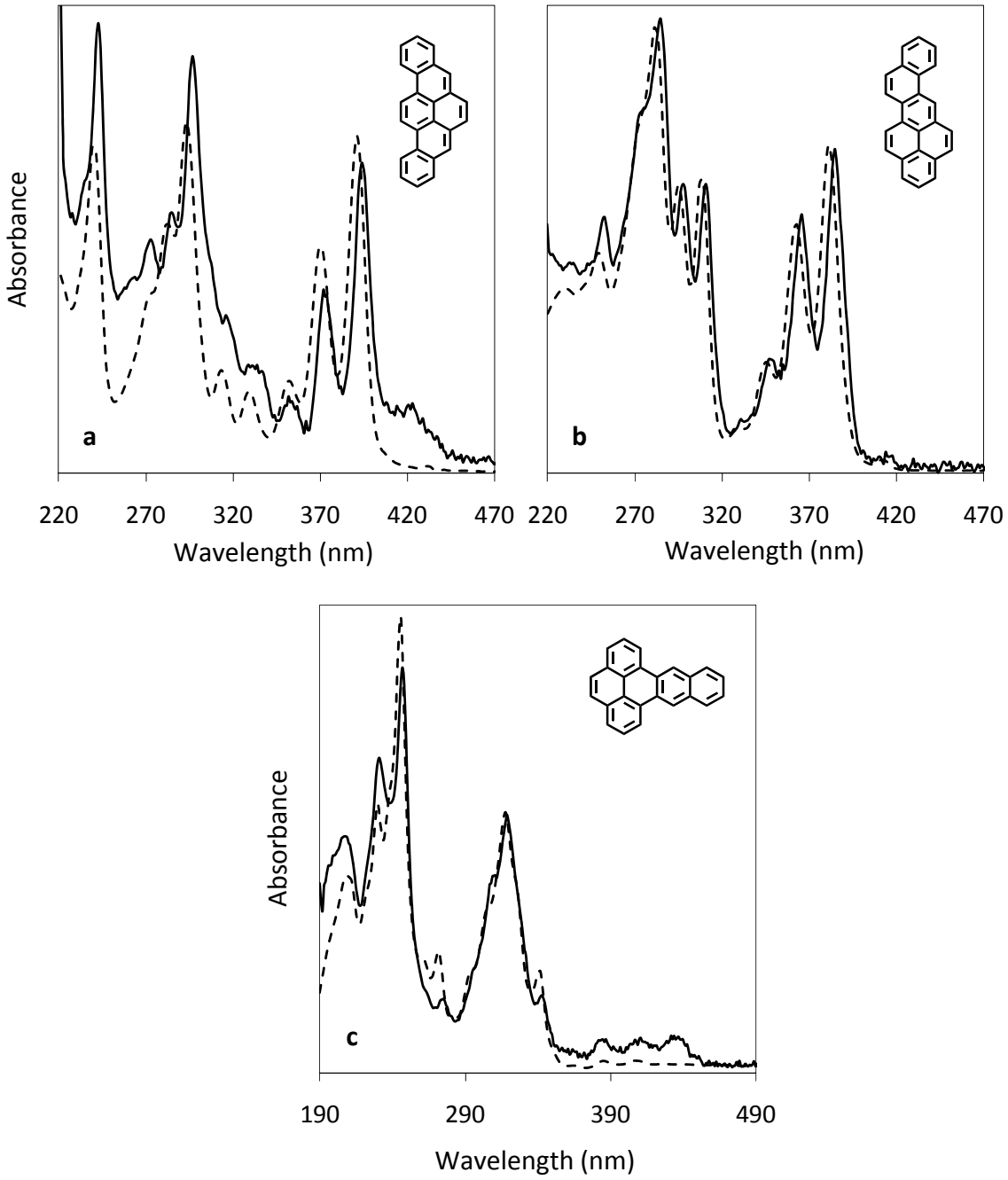

Figure 3.34 Comparisons of the UV spectra of *n*-decane pyrolysis products from the chromatogram in Figure 3.28 (solid lines) to the spectra of the corresponding reference standards (dashed lines). Comparisons are shown for the products identified as (a) an alkylated dibenzo[*a*,*i*]pyrene, eluting at 117 min; (b) an alkylated naphtho[2,1-*a*]pyrene, eluting at 110 min; and (c) an alkylated naphtho[2,3-*e*]pyrene, eluting at 78 min in Figure 3.28. Structures of the unsubstituted parent PAH of these products are shown next to the spectra.

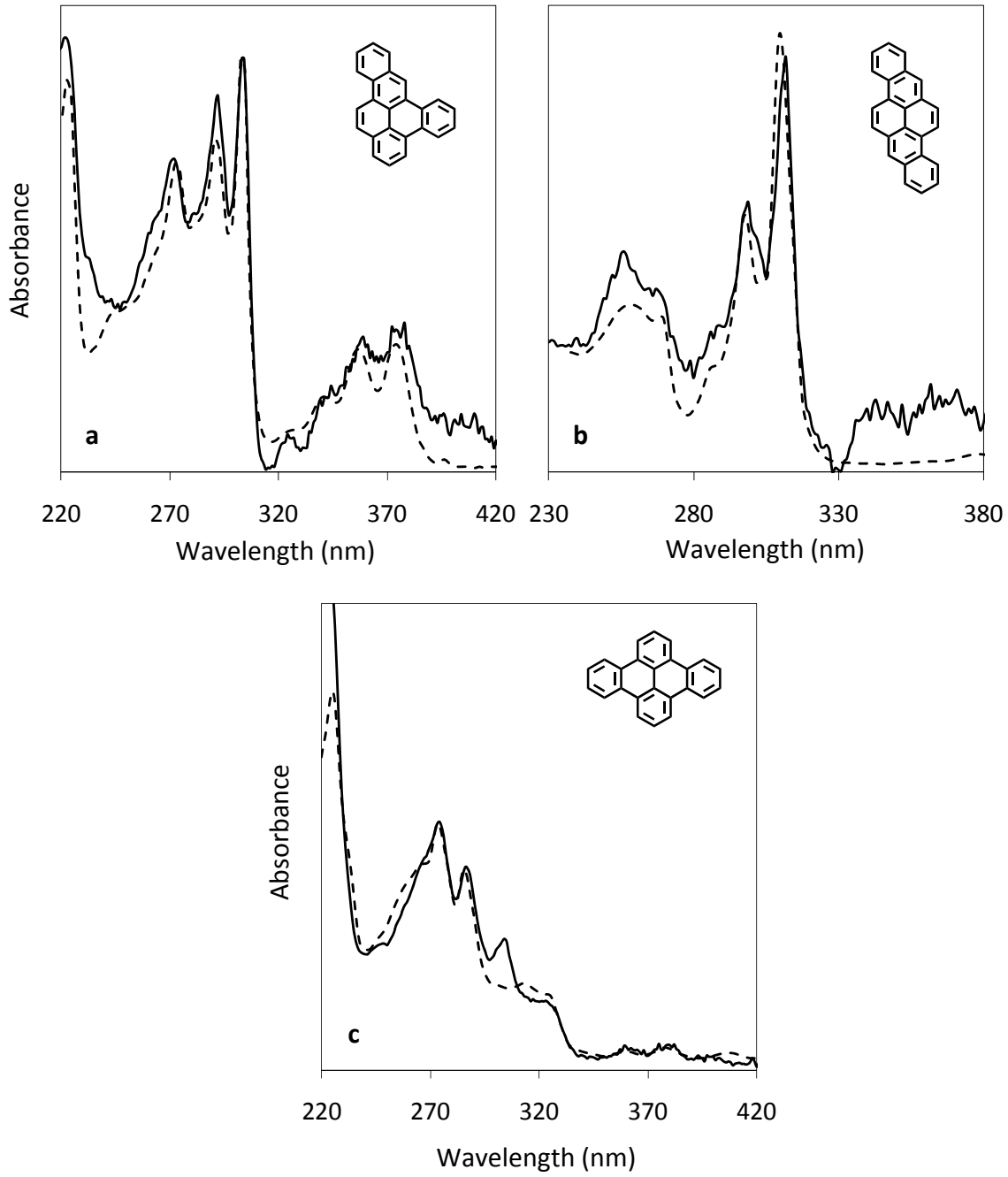

Figure 3.35 Comparisons of the UV spectra of *n*-decane pyrolysis products from the chromatogram in Figure 3.28 (solid lines) to the spectra of the corresponding reference standards (dashed lines). Comparisons are shown for the products identified as (a) an alkylated dibenzo[*a*,*e*]pyrene, eluting at 77 min; (b) an alkylated dibenzo[*a*,*h*]pyrene, eluting at 115 min; and (c) an alkylated dibenzo[*e*,*l*]pyrene, eluting at 85 min in Figure 3.28. Structures of the unsubstituted parent PAH of these products are shown next to the spectra.

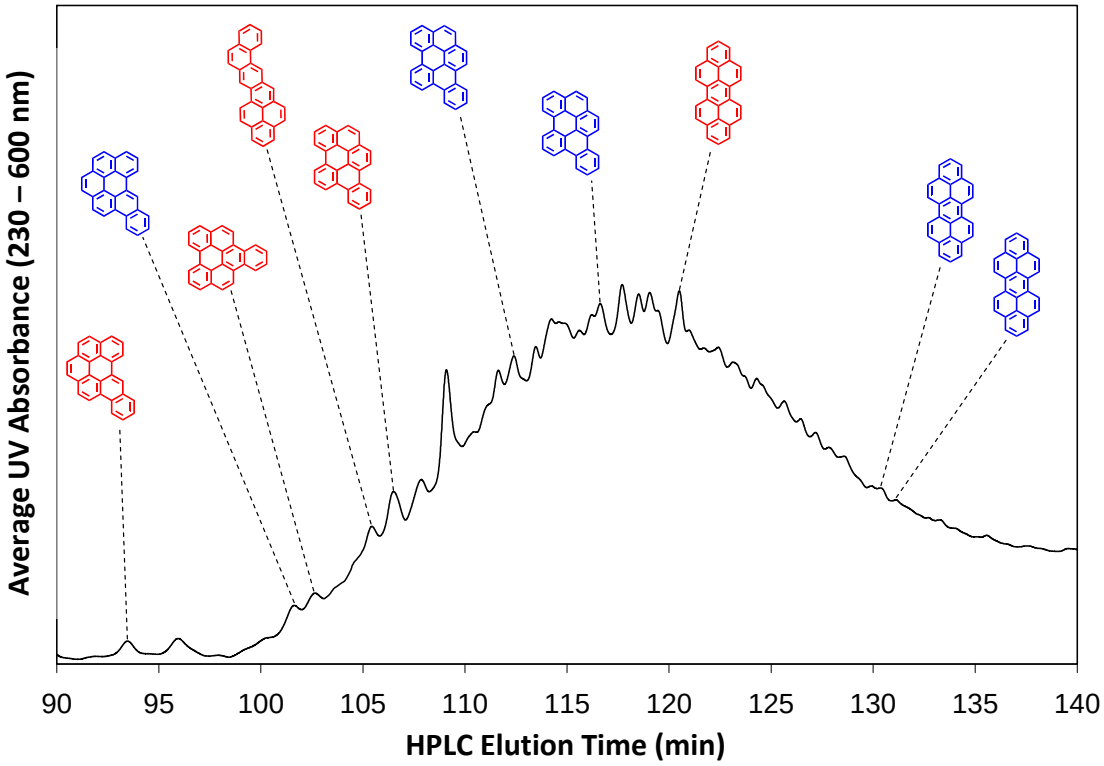

Figure 3.36 A reversed-phase HPLC chromatogram of the ninth fraction of the liquid-phase products of *n*-decane pyrolyzed at 570 °C and 100 atm. This fraction primarily contains the $C_{26}H_{14}$ PAH isomer family and its alkylated derivatives. Red labels represent unsubstituted PAH; blue labels represent alkylated PAH for which the number, positions, and/or identities of the alkyl substituents are not known.

dibenzo[*b*,*ghi*]perylene (Figure 3.37a), dibenzo[*e*,*ghi*]perylene (Figure 3.37b), and naphtho[1,2,3,4-*ghi*]perylene (Figure 3.37c), have UV spectra which are shifted to higher or lower wavelengths compared to the spectra of the corresponding reference standards. These shifts are due to the spectra of the product PAH having been obtained in solvents different from the solvents in which the corresponding reference spectra were obtained [61]. The chemical formulas, molecular masses, and structures of these compounds are displayed in Table 3.12.

The UV spectra of dibenzo[*e*,*ghi*]perylene (Figure 3.37b) and phenanthro[2,3-*a*]pyrene (Figure 3.38a) closely match those of the appropriate reference standards, leading to the straightforward identification of these two products (once the solvent effects on the UV spectrum

Table 3.12 PAH identified in the ninth fraction of liquid-phase products of *n*-decane pyrolysis.

Product	Chemical Formula	Molecular Mass (Da)	Structure
Dibenzo[*b,ghi*]perylene	$C_{26}H_{14}$	326	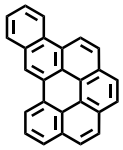
Dibenzo[*e,ghi*]perylene	$C_{26}H_{14}$	326	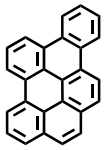
Naphtho[1,2,3,4-*ghi*]-perylene	$C_{26}H_{14}$	326	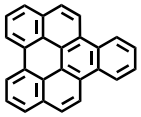
Dibenzo[*cd,lm*]perylene	$C_{26}H_{14}$	326	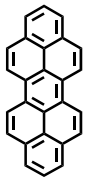
Phenanthro-[2,3-*a*]pyrene	$C_{28}H_{16}$	352	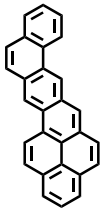

of dibenzo[*e,ghi*]perylene are taken into account). In contrast, the other three unsubstituted PAH products identified in this fraction, dibenzo[*b,ghi*]perylene (Figure 3.37a), naphtho[1,2,3,4-*ghi*]perylene (Figure 3.37c), and dibenzo[*cd,lm*]perylene (Figure 3.38b), all have UV spectra which deviate significantly from the spectra of the corresponding reference standards, due to co-elution with other, unidentified products. Each of these three PAH is identified by matching the absorbance maxima of the corresponding reference standards with absorbance maxima of the product spectra, while attributing additional absorbance maxima in the UV spectra of the product to co-eluting material.

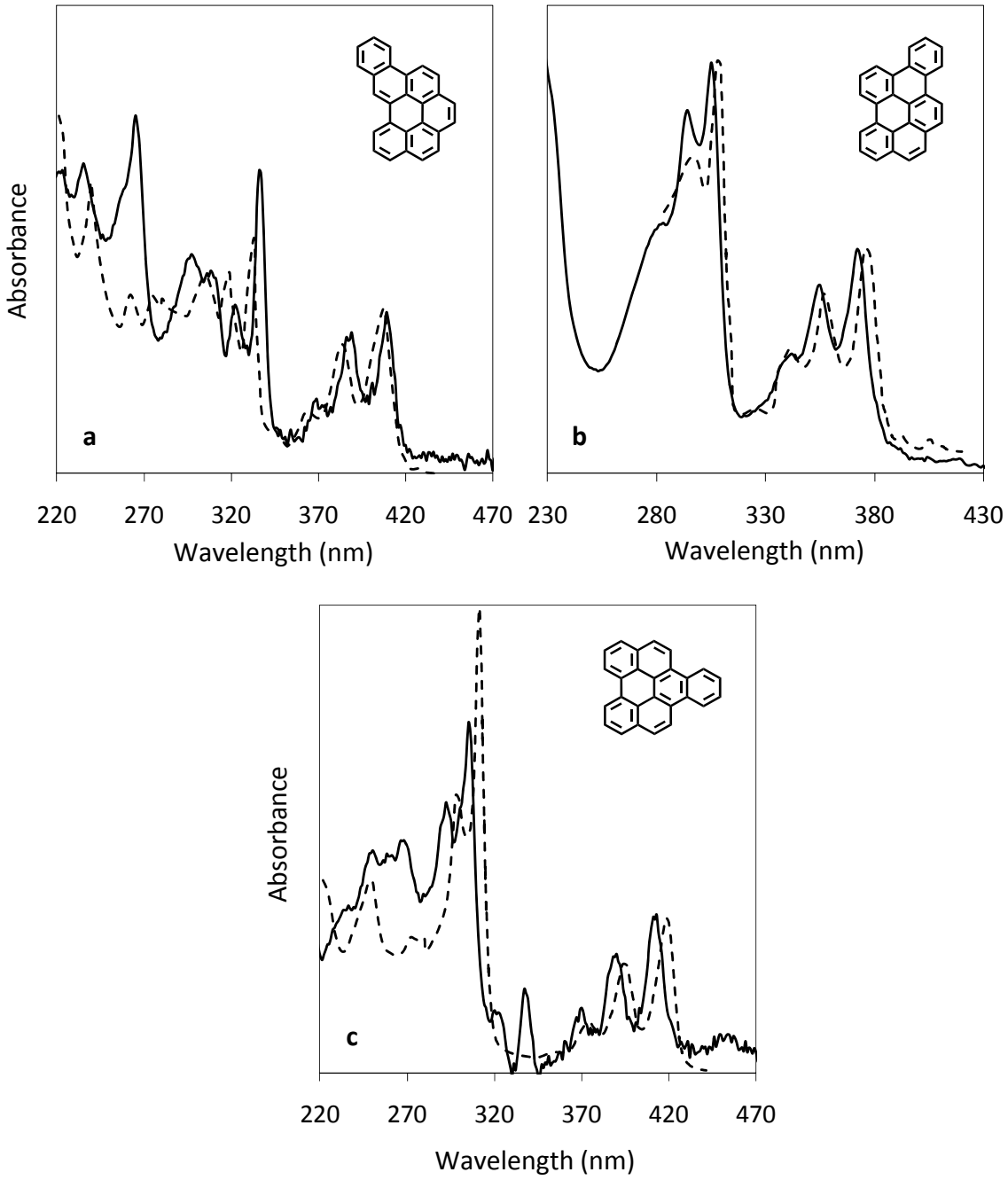

Figure 3.37 Comparisons of the UV spectra of *n*-decane pyrolysis products from the chromatogram in Figure 3.36 (solid lines) to the spectra of their corresponding reference standards (dashed lines). Matches are shown for the products identified as (a) dibenzo[*b,ghi*]perylene, eluting at 93 min; (b) dibenzo[*e,ghi*]perylene, eluting at 106 min; and (c) naphtho[1,2,3,4-*ghi*]perylene, eluting at 103 min in Figure 3.36. Structures of these products are shown next to the spectra.

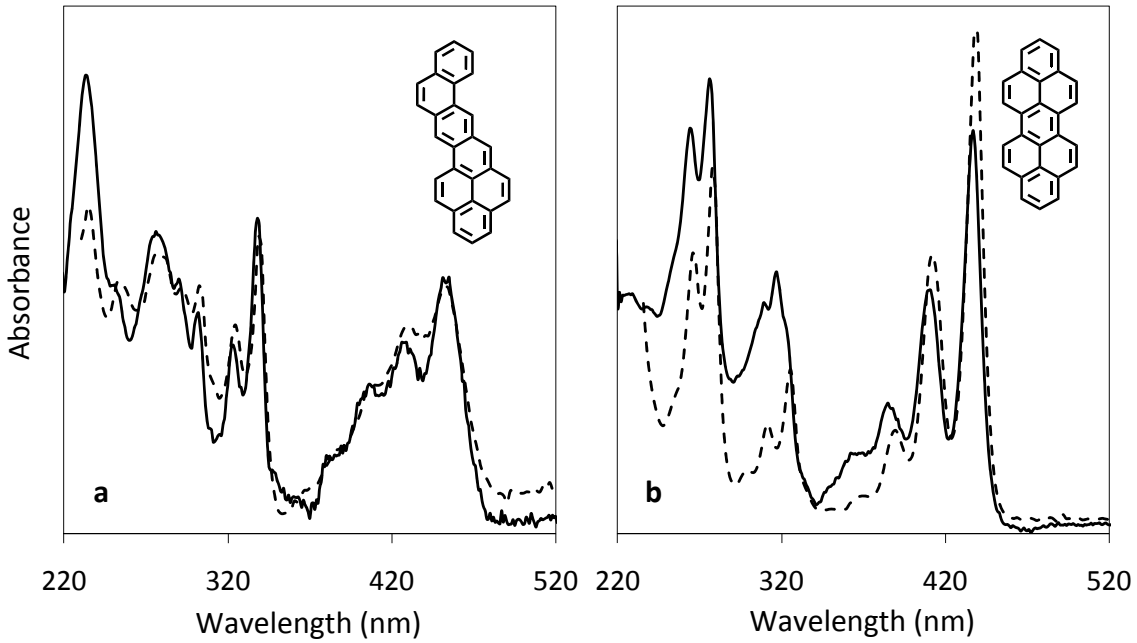

Figure 3.38 Comparisons of the UV spectra of *n*-decane pyrolysis products from the chromatogram in Figure 3.36 (solid lines) to the spectra of their corresponding reference standards (dashed lines). Matches are shown for the products identified as (a) phenanthro[2,3-*a*]pyrene, eluting at 105 min, and (b) dibenzo[*cd,lm*]perylene, eluting at 120 min in Figure 3.36. Structures of these products are shown next to the spectra.

In addition to the five unsubstituted PAH products identified in Figures 3.37 and 3.38, there are two alkylated benzo[*cd,lm*]perylenes, two alkylated dibenzo[*e,ghi*]perylenes, and one alkylated dibenzo[*b,ghi*]perylene for which the number, positions, and/or identities of the alkyl groups are not known with certainty. They are identified by comparing the UV spectra of the products to the spectra of reference standards of the corresponding unsubstituted parent PAH. Comparisons of the UV spectra of one of each of these three types of alkylated PAH to the spectra of the corresponding parent PAH are shown in Figure 3.39. While a good match is obtained between the spectrum of the alkylated dibenzo[*b,ghi*]perylene product and the spectrum of the appropriate reference standard (Figure 3.39a), there is significant deviation between the spectra of the alkylated dibenzo[*e,ghi*]perylene (Figure 3.39b) and dibenzo[*cd,lm*]perylene (Figure 3.39c) and the appropriate reference standards. This deviation is due to co-eluting

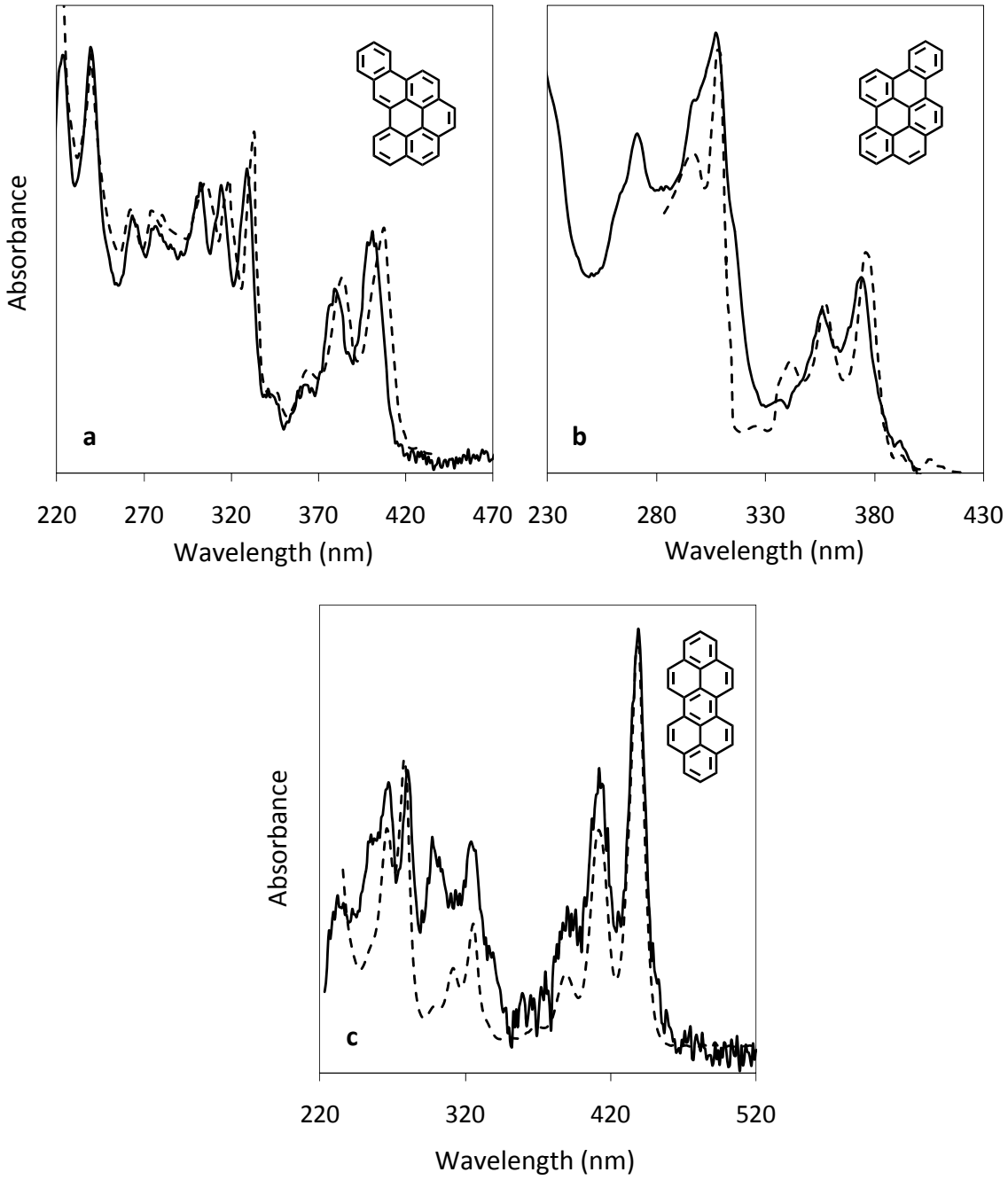

Figure 3.39 Comparisons of the UV spectra of *n*-decane pyrolysis products from the chromatogram in Figure 3.36 (solid lines) to the spectra of the corresponding unsubstituted PAH reference standards (dashed lines). Comparisons are shown for the products identified as (a) an alkylated dibenzo[*b,ghi*]perylene, eluting at 102 min; (b) an alkylated dibenzo[*e,ghi*]perylene, eluting at 113 min; and (c) an alkylated dibenzo[*cd,lm*]perylene, eluting at 121 min in Figure 3.36. Structures of the unsubstituted parent PAH of these products are shown next to the spectra.

material; these two alkylated PAH products are identified by matching the absorbance maxima of the corresponding reference standards with absorbance maxima of the product spectra, while attributing additional absorbance maxima in the UV spectra of the product to co-eluting material.

Dibenzo[*b,ghi*]perylene, dibenzo[*e,ghi*]perylene, naphtho[1,2,3,4-*ghi*]perylene, dibenzo[*cd,lm*]perylene, and phenanthro[2,3-*a*]pyrene, along with five alkylated derivatives of these seven-ring PAH products, have been identified as supercritical *n*-decane pyrolysis products in the ninth fraction. All ten are reported here for the first time as products on *n*-decane pyrolysis or combustion.

3.4.10 Identification of PAH Products in Fractions 10 and 12

The tenth and twelfth fractions of *n*-decane pyrolysis products include the eight- and nine-ring PAH benzo[*a*]coronene, phenanthro[5,4,3,2-*efghi*]perylene, benzo[*pqr*]naphtho-[8,1,2-*bcd*]perylene, and naphtho[8,1,2-*abc*]coronene along with some of their alkylated derivatives. Figures 3.40 and 3.41 present the reversed-phase HPLC chromatograms of these fractions of the products from the highest stressing experimental conditions (570 °C and 100 atm).

The four unsubstituted eight- and nine-ring PAH products in these fractions are identified by matching their UV spectra to those of reference standards for each of these compounds. Comparisons of the UV spectra of these four PAH to the spectra of the corresponding reference standards are shown in Figure 3.42. The spectra of all of these unsubstituted products show good matches with those of the corresponding reference standards, with the exception of the spectrum of benzo[*pqr*]naphtho[8,1,2-*bcd*]perylene (Figure 3.42b). Co-eluting material prevents a good match of the spectrum of this product with that of the appropriate reference standard, particularly below 320 nm and above 420 nm, but the UV spectrum of the product does have absorbance maxima at the same wavelengths as virtually all of the maxima of the reference standard of

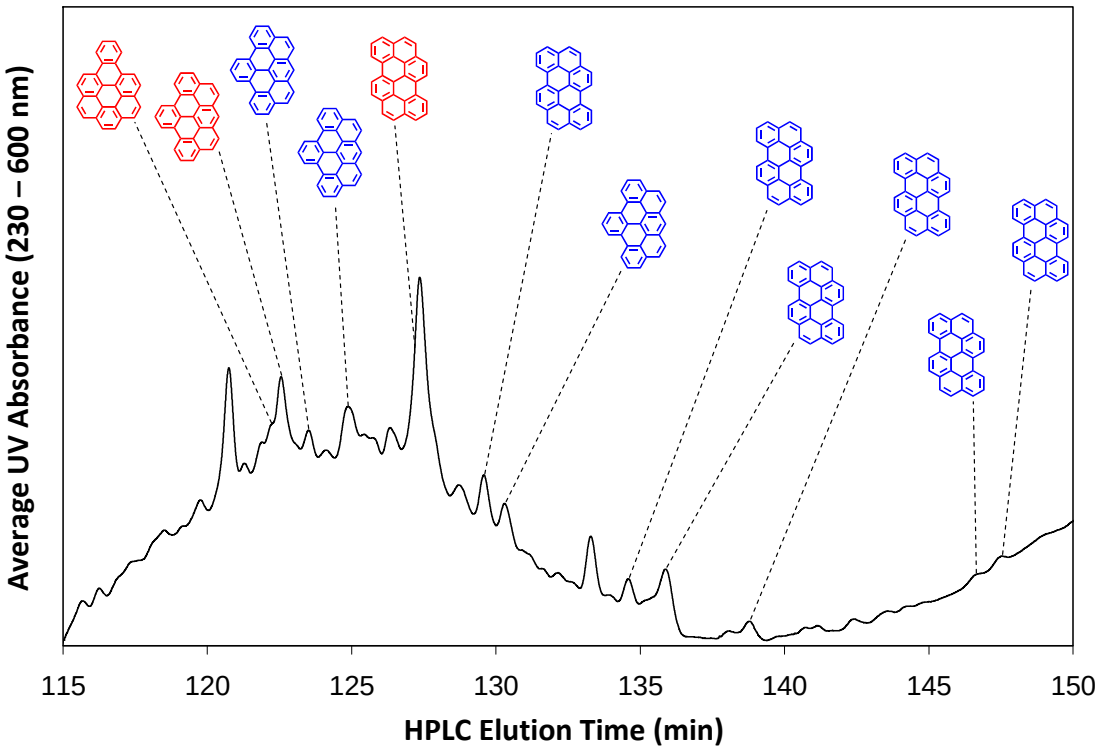

Figure 3.40 A reversed-phase HPLC chromatogram of the tenth fraction of the liquid-phase products of *n*-decane pyrolyzed at 570 °C and 100 atm. This fraction contains the $C_{28}H_{14}$ PAH isomer family and its alkylated derivatives. Red labels represent unsubstituted PAH; blue labels represent alkylated PAH for which the number, positions, and/or identities of the alkyl substituents are not known.

benzo[*pqr*]naphtho[8,1,2-*bcd*]perylene. The chemical formulas, molecular masses, and structures of these compounds are displayed in Table 3.13.

In addition to the four unsubstituted PAH products identified in Figure 3.42, the tenth and twelfth fractions are found to contain six alkylated benzo[*pqr*]naphtho[8,1,2-*bcd*]perylenes, five alkylated naphtho[8,1,2-*abc*]coronenes, and three alkylated phenanthro[5,4,3,2-*efghi*]perylenes for which the number, positions, and/or identities of the alkyl groups are not known with certainty. They are identified by comparing the product UV spectra to the spectra of reference standards of the corresponding unsubstituted parent PAH. Comparisons of the UV spectra of one

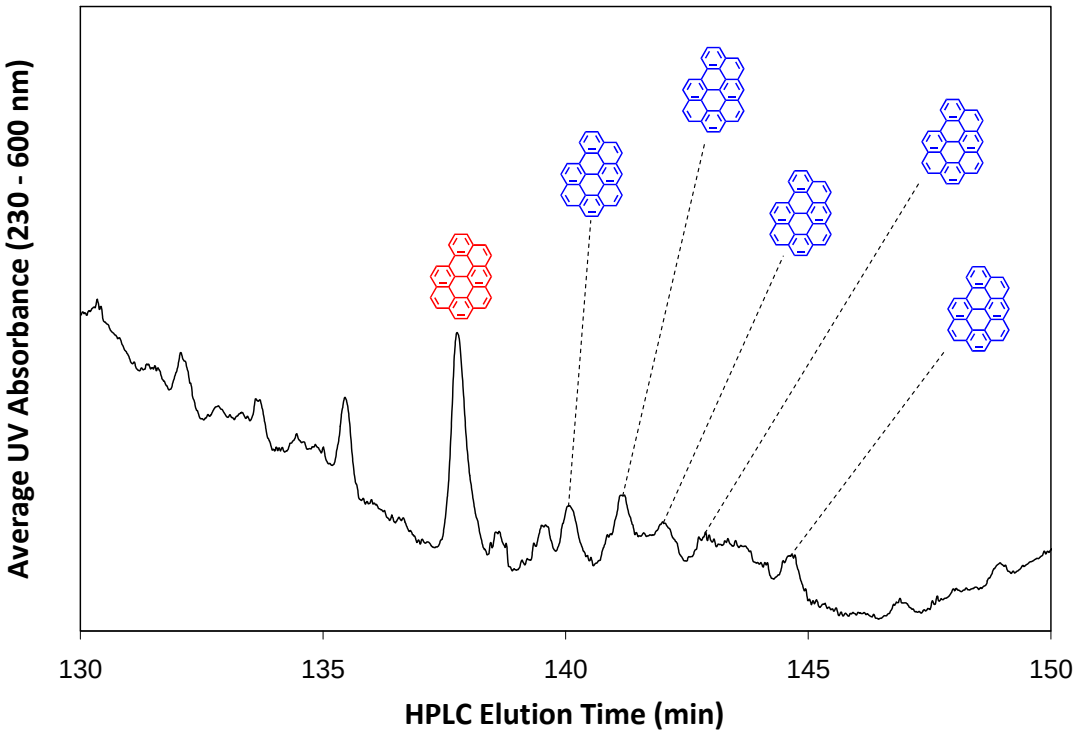

Figure 3.41 A reversed-phase HPLC chromatogram of the twelfth fraction of the liquid-phase products of *n*-decane pyrolyzed at 570 °C and 100 atm. This fraction contains the nine-ring PAH naphtho[8,1,2-*abc*]coronene and some of its alkylated derivatives. Red labels represent unsubstituted PAH; blue labels represent alkylated PAH for which the number, positions, and/or identities of the alkyl substituents are not known.

Table 3.13 PAH identified in the tenth and twelfth fractions of liquid-phase products of *n*-decane pyrolysis.

Product	Chemical Formula	Molecular Mass (Da)	Structure
Phenanthro-[5,4,3,2-*efghi*]perylene	$C_{28}H_{14}$	350	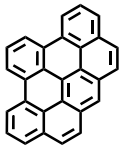
Benzo[*pqr*]naphtho-[8,1,2-*bcd*]perylene	$C_{28}H_{14}$	350	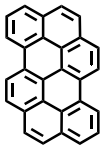
Benzo[*a*]coronene	$C_{28}H_{14}$	350	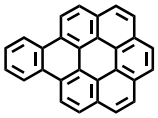
Naphtho[8,1,2-*abc*]-coronene	$C_{30}H_{14}$	374	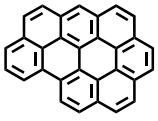

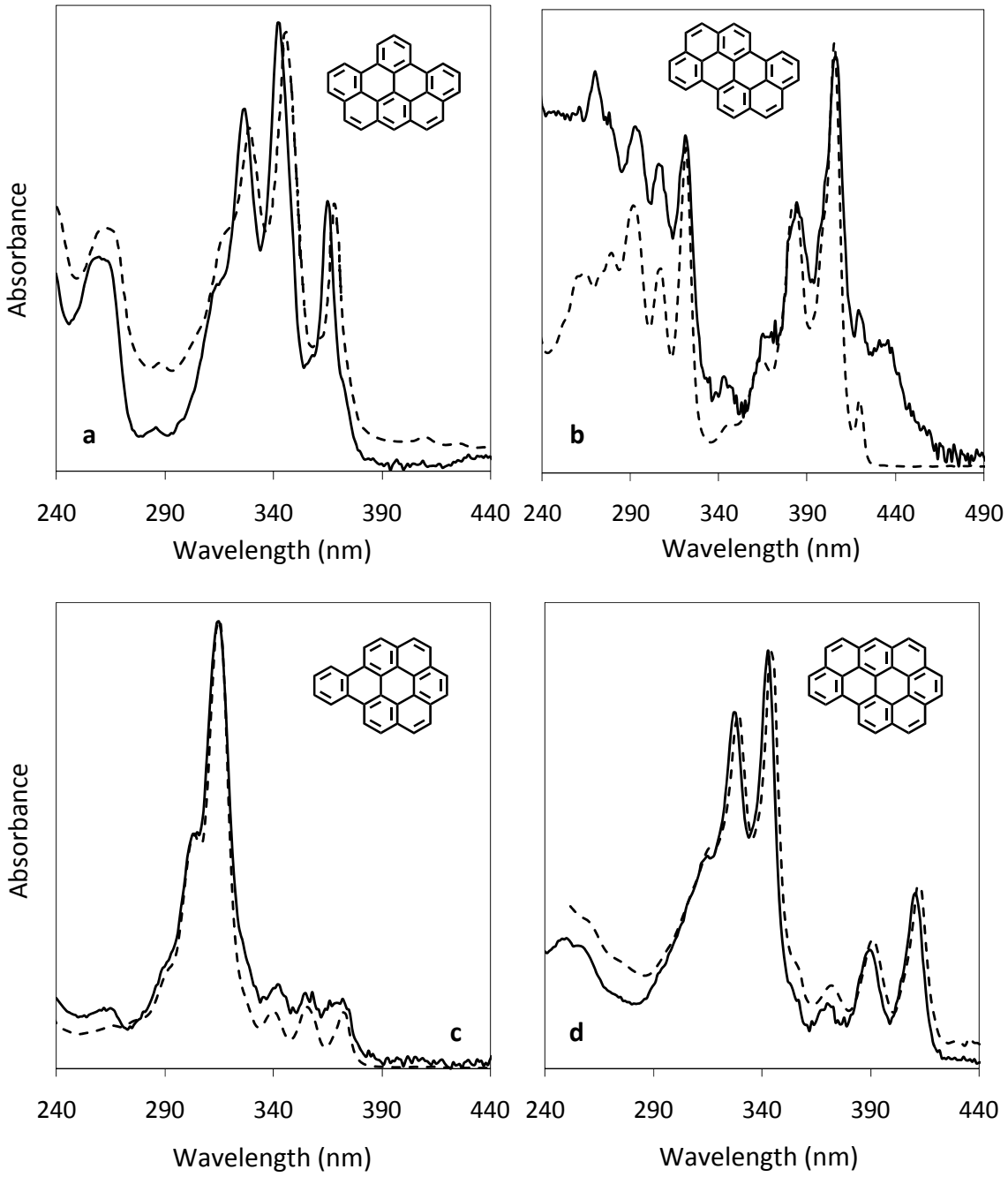

Figure 3.42 Comparisons of the UV spectra of *n*-decane pyrolysis products (solid lines) to the spectra of their corresponding reference standards (dashed lines). Matches are shown for the products identified as (a) phenanthro[5,4,3,2-*efghi*]perylene, eluting at 123 min in the chromatogram in Figure 3.40; (b) benzo[*pqr*]naphtho[8,1,2-*bcd*]perylene, eluting at 127 min in the chromatogram in Figure 3.40; (c) benzo[*a*]coronene, eluting at 122 min in the chromatogram in Figure 3.40; and (d) naphtho[8,1,2-a*bc*]coronene, eluting at 138 min in the chromatogram in Figure 3.41. Structures of these products are shown next to each spectrum. Co-eluting material which absorbs at wavelengths less than 320 nm and greater than 420 nm prevents a match between the UV spectrum of the product benzo[*pqr*]naphtho[8,1,2-*bcd*]perylene (b) and the UV spectrum of the corresponding reference standard in these wavelength ranges.

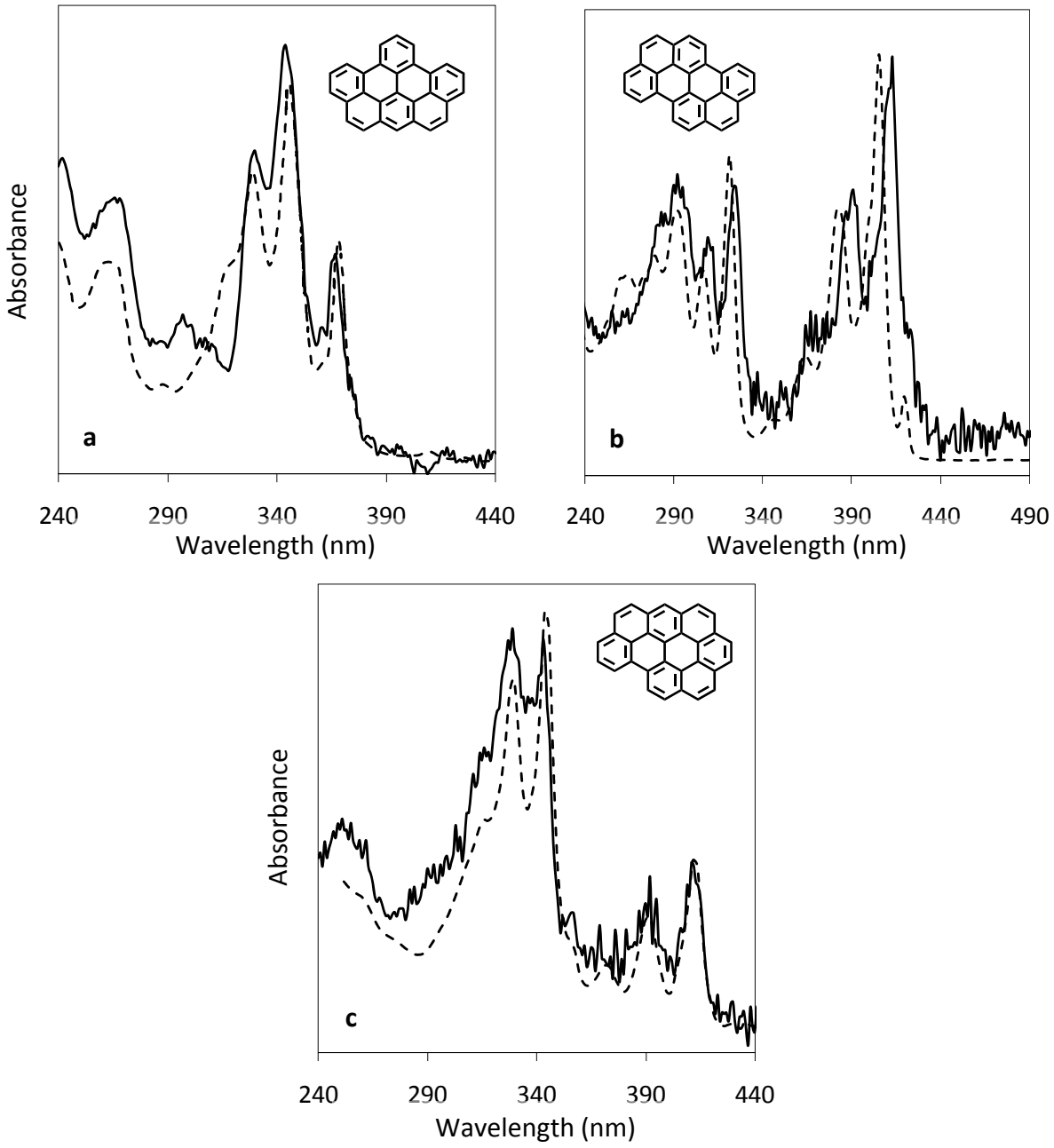

Figure 3.43 Comparisons of the UV spectra of *n*-decane pyrolysis products (solid lines) to the spectra of their corresponding reference standards (dashed lines). Comparisons are shown for the products identified as (a) an alkylated phenanthro[5,4,3,2-*efghi*]perylene, eluting at 125 min in the chromatogram in Figure 3.40; (b) an alkylated benzo[*pqr*]naphtho[8,1,2-*bcd*]perylene, eluting at 127 min in the chromatogram in Figure 3.40; and (c) an alkylated naphtho[8,1,2-a*bc*]coronene, eluting at 140 min in the chromatogram in Figure 3.41. Structures of the unsubstituted parent PAH of these products are shown next to each spectrum. The higher UV absorbance of the product component compared to its reference standard at wavelengths less than 310 nm and greater than 410 nm in Figure (b) is due to co-eluting material.

of each of these three types of alkylated PAH products to the spectra of the corresponding parent PAH standards are shown in Figure 3.43.

Benzo[*a*]coronene, phenanthro[5,4,3,2-*efghi*]perylene, benzo[*pqr*]naphtho[8,1,2-*bcd*]-perylene, and naphtho[8,1,2-*abc*]coronene, along with 14 alkylated derivatives of these PAH products, have been identified in the tenth and twelfth fractions of the liquid-phase products of supercritical *n*-decane pyrolysis. All 19 of these PAH are reported here for the first time as products of *n*-decane pyrolysis.

3.4.11 Identification of PAH Products in Fraction 11

Figure 3.44 presents a reversed-phase HPLC chromatogram of the eleventh fraction of the supercritical *n*-decane pyrolysis products from the highest stressing experimental conditions (570 °C and 100 atm). This fraction includes the seven-ring $C_{28}H_{16}$ isomer family, determined by MS analysis of this fraction as described in Section 2.3.3.3. So far, no products have been identified in this fraction, but many of the compounds in this fraction have distinct UV spectra, indicating that they could be identified if reference standards of these compounds were available. Figures 3.45 and 3.46 present the UV spectra of the eight products in this fraction whose chromatographic peaks are labeled with Roman numerals in Figure 3.44.

3.5 Summary

Forty-five unsubstituted PAH products (not including acenaphthene or cyclopenta[*def*]phenanthrene, which are counted as alkylated PAH) have been identified as products of *n*-decane pyrolysis in this work, compared to 24 previously reported [45-46]. The number of alkylated PAH reported in this work, compared to those previously reported by other researchers, has increased dramatically, from three (including acenaphthene) to 232. Prior to this study, one PAH with more than seven rings, coronene, had been reported as a product of *n*-decane pyrolysis or combustion; 34 are reported here. With the inclusion of single-ring

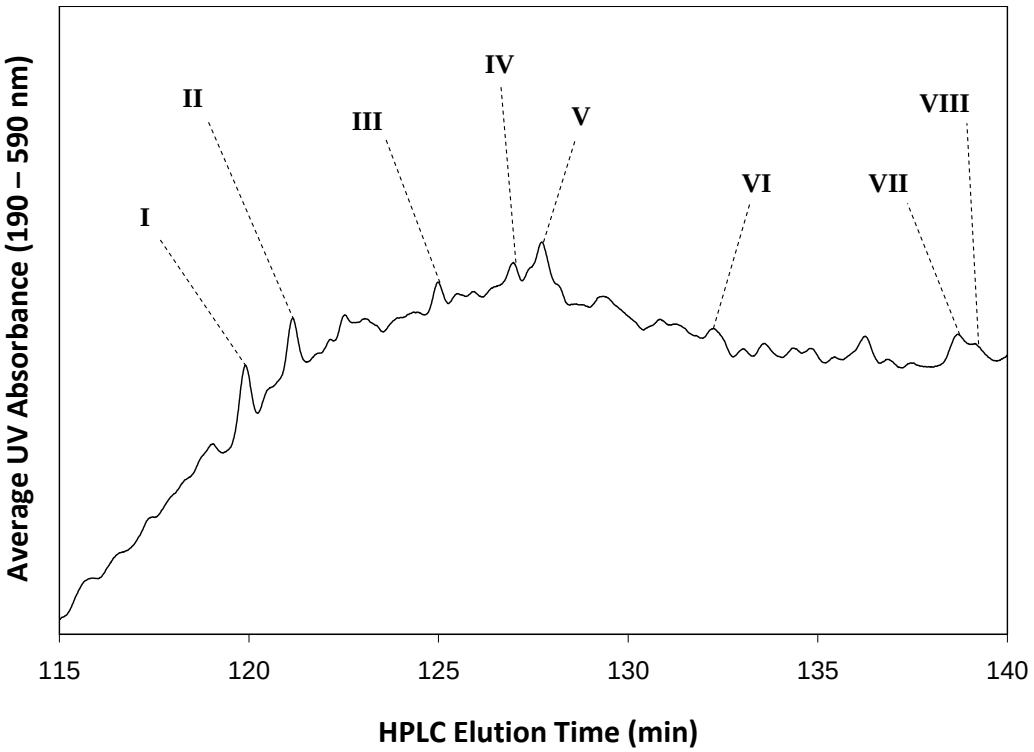

Figure 3.44 A reversed-phase HPLC chromatogram of the eleventh fraction of the liquid- phase products of *n*-decane pyrolyzed at 570 °C and 100 atm. Roman numerals indicate peaks of products whose UV spectra appear in Figures 3.45 and 3.46.

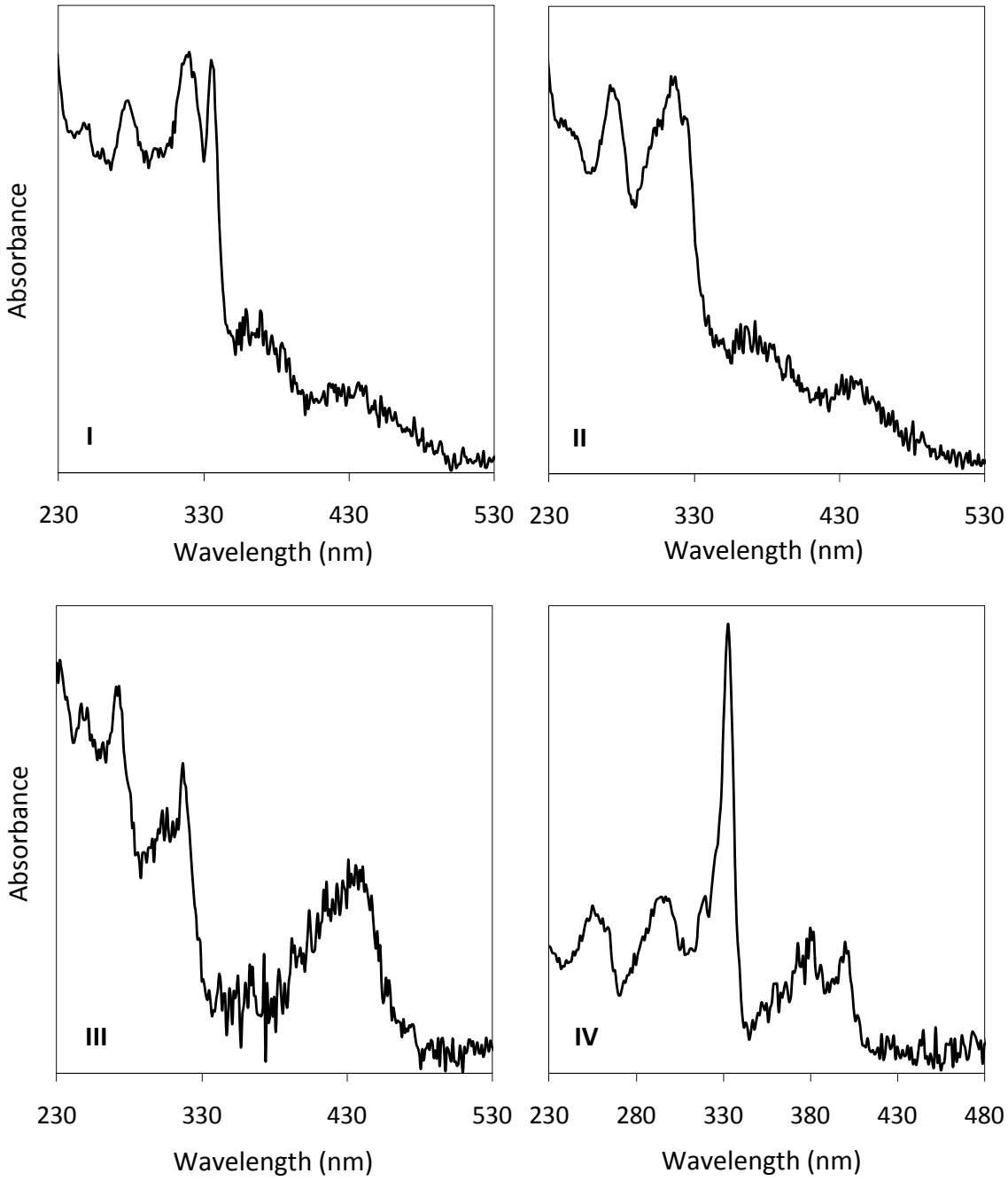

Figure 3.45 UV spectra of unidentified product components of the eleventh fraction of liquid-phase products of *n*-decane pyrolyzed at 570 °C and 100 atm. Roman numerals next to each of the four spectra correspond to product peaks labeled in the chromatogram of Figure 3.44.

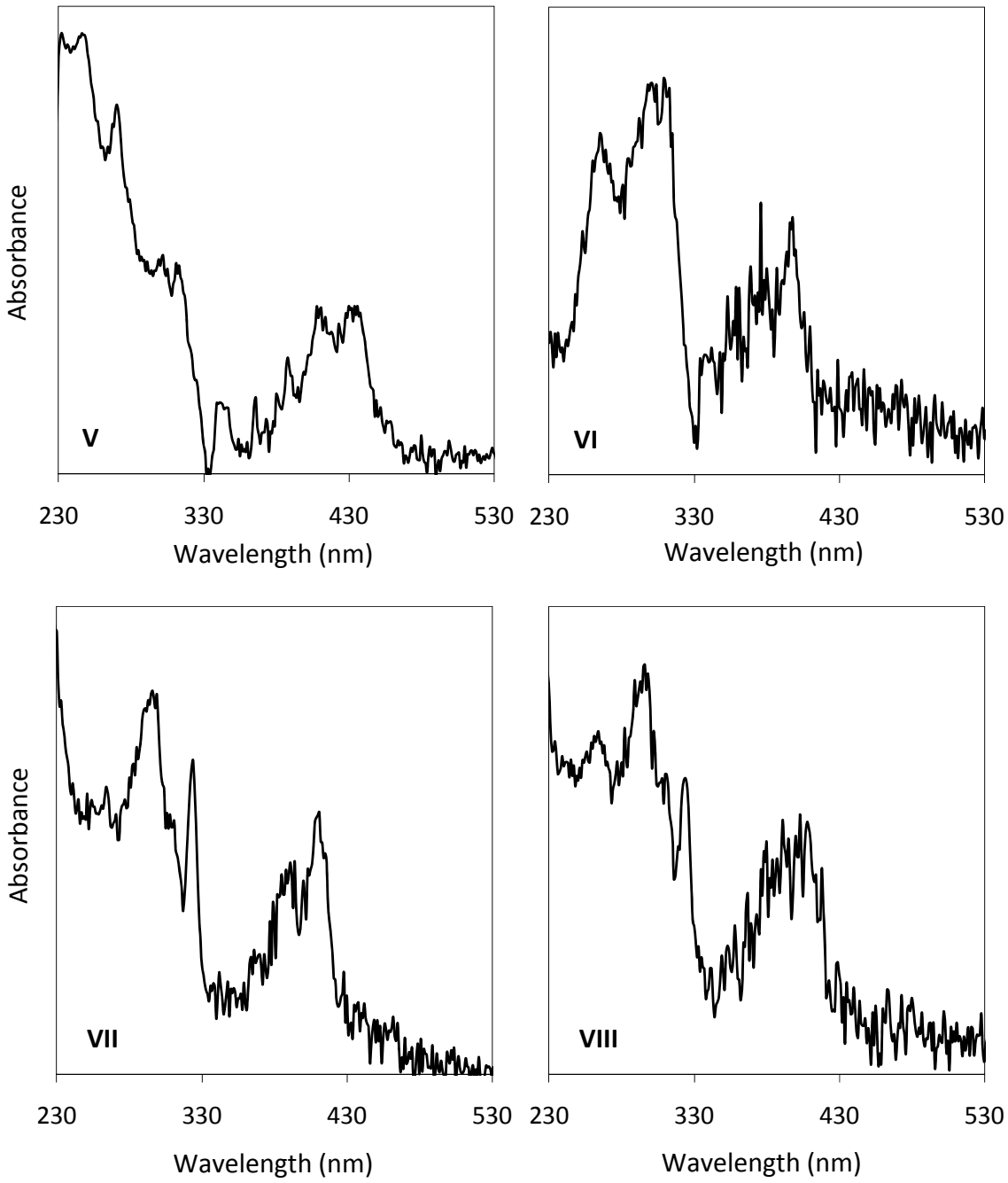

Figure 3.46 UV spectra of unidentified product components of the eleventh fraction of liquid-phase products of *n*-decane pyrolyzed at 570 °C and 100 atm. Roman numerals next to each of the four spectra correspond to product peaks labeled in the chromatogram of Figure 3.44.

products, a total of 73 aromatic products are identified with both the aromatic portion of the structure and the number, position, and identity of any alkyl substituents known.

The power of the two-dimensional HPLC technique for the separation of PAH, described in Section 2.3.3, can be seen in Table 3.14. The table shows the numbers of PAH products identified by applying the two-dimensional HPLC technique to a liquid-phase *n*-decane pyrolysis product mixture compared to the number of products identified when only a single reversed-phase C18 HPLC column is used. Subjecting supercritical *n*-decane pyrolysis products to analysis with a single C18 column only allows the identification of 51 PAH products, of which seven are unsubstituted parent PAH.

Table 3.14 Comparison of the numbers of PAH products identified by the one- and two-dimensional HPLC separation techniques. Note that the two-ring PAH indene, included among the unsubstituted PAH identified in the one-dimensional substitution, is not counted in the two-dimensional separation.

Number of Aromatic Rings	One-dimensional Separation		Two-dimensional Separation	
	Unsubstituted	Alkylated	Unsubstituted	Alkylated
2	2	24	1	49
3	2	6	4	50
4	1	13	7	46
5	0	0	7	24
6	2	1	16	39
7	0	0	6	10
8	0	0	3	9
9	0	0	1	5
Total	7	44	45	232

The improved performance is particularly noticeable when comparing higher-ring-number PAH product identifications of either the one- or two-dimensional techniques. Three six-ring products are identified by the one-dimensional technique, while 89 are identified with the two-dimensional technique. In Chapter 4, yields of products from the *n*-decane pyrolysis

experiments will be presented and reaction mechanisms leading to their formation will be discussed. Due to the large number of aromatic products identified, as well as the quantification of many of these products made possible by the two-dimensional chromatographic technique, the primary reaction pathways leading to the production of several PAH products have been identified. The identification and quantification of large PAH is shown to be extremely valuable in determining the PAH formation mechanisms in supercritical *n*-decane pyrolysis.

Chapter 4. Results and Discussion

4.1 Introduction

This chapter presents the results of the two sets of experiments in which *n*-decane was pyrolyzed in the reactor described in Section 2.2. One set of experiments was performed at a constant pressure of 100 atm, a constant residence time of 140 sec, and at temperatures of 530, 540, 550, 560, 565, and 570 °C. The other set was performed at a constant temperature of 570 °C, a constant residence time of 140 sec, and at pressures of 40, 60, 70, 80, 90, and 100 atm.

In the following sections, product yields as functions of temperature and pressure are presented, product formation mechanisms are shown, and yield trends with respect to temperature and pressure are explained. First discussed are aliphatic and olefinic products, then one-ring aromatic products, and finally polycyclic aromatic hydrocarbons (PAH).

4.2 Alkane and Alkene Products

n-Alkane products with one to nine carbons have been identified by GC/FID/MS as products of supercritical *n*-decane pyrolysis as described in Sections 2.3.1 and 2.3.2. All of these products are quantified except *n*-pentane, which could not be resolved from the injection solvent peak during GC separation. The alkane product *n*-hexane may have been lost by evaporation during preparation of the liquid phase products for GC analysis due to the relatively high volatility of this compound. This loss would result in yields of this product reported as lower than they actually are. Figure 4.1 displays the yields of the quantified C_1 to C_9 alkane products from the set of pyrolysis experiments in which temperature was varied from 530 to 570 °C while pressure and residence time were held constant at 100 atm and 140 sec, respectively. Figure 4.2 displays the yields of these products from the experiments in which pressure was varied from 40 to 100 atm while temperature and residence time were held constant at 570 °C and 140 sec, respectively. Yields are reported as moles of product per moles of *n*-decane fed to the reactor.

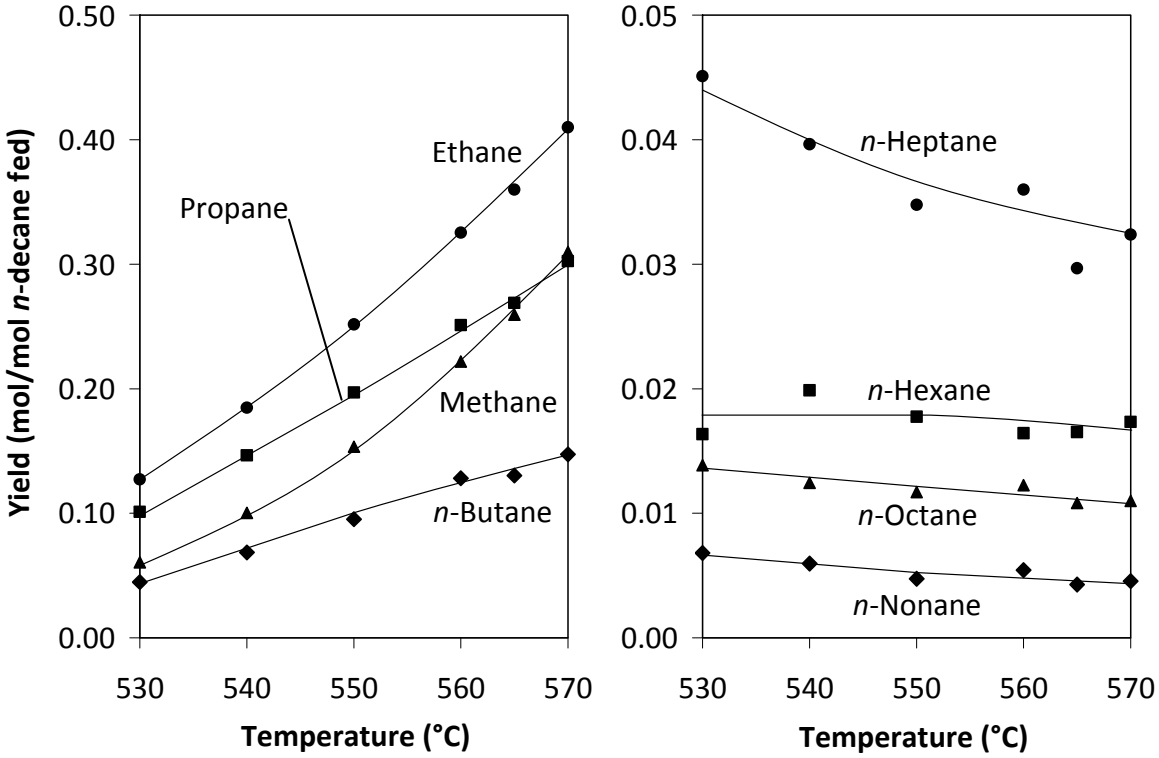

Figure 4.1 Yields of alkane products as functions of temperature, from the supercritical pyrolysis of *n*-decane at 100 atm and 140 sec.

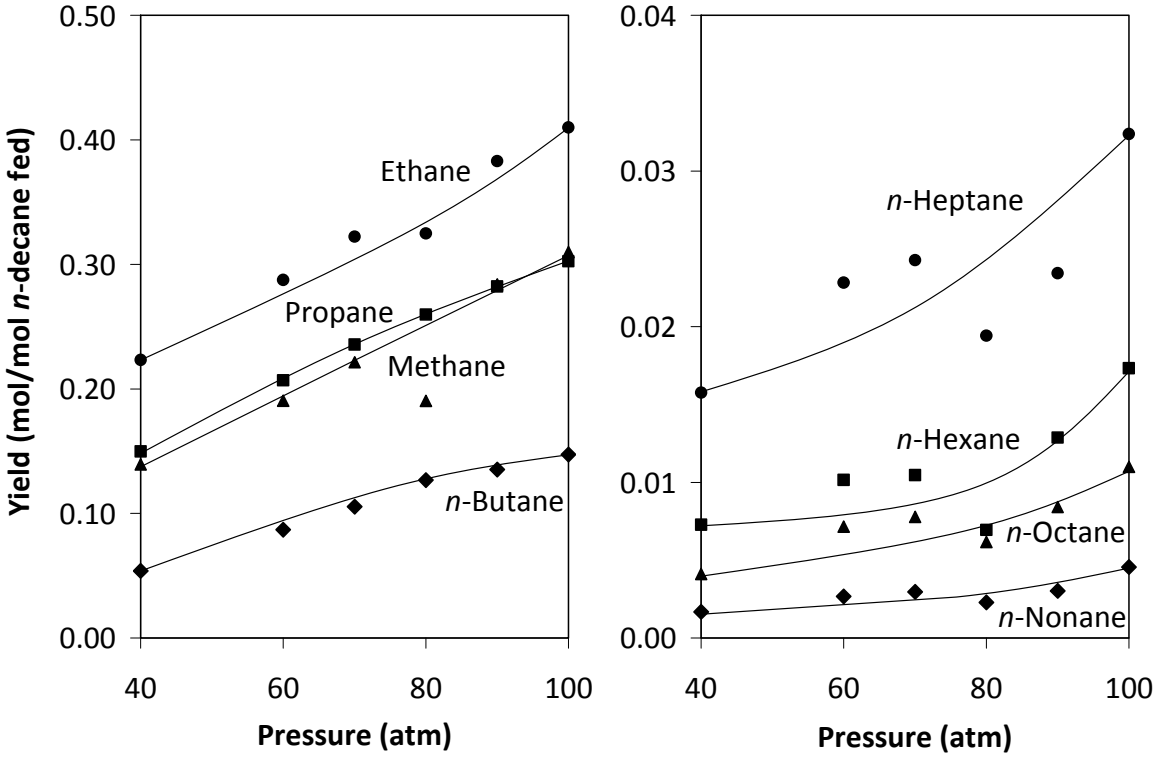

Figure 4.2 Yields of alkane products as functions of pressure, from the supercritical pyrolysis of *n*-decane at 570 °C and 140 sec.

1-Alkene products with two to nine carbons have been identified by GC/FID/MS as products of supercritical *n*-decane pyrolysis in the manner described in Sections 2.3.1 and 2.3.2. All of these are quantified except 1-pentene, which cannot be resolved from the injection solvent peak during GC separation. Yields of 1-hexene are possibly reported as lower than their actual values due to evaporative loss of this volatile product during preparation of the liquid-phase products for GC analysis. The product 1-nonene co-elutes with the aromatic product *o*-xylene, therefore the yield of this alkene product was estimated: first the area of the co-eluting products *m*- and *p*-xylene was halved, then this halved area was subtracted from the area of the co-eluting products 1-nonene and *o*-xylene. The remainder of this subtraction was taken to be the peak area for which 1-nonene was responsible. The assumption that the three isomers of xylene are produced in equal yields is the basis of this estimation.

Figure 4.3 displays the yields of the quantified C_2 to C_9 alkene products from the set of pyrolysis experiments in which temperature was varied from 530 to 570 °C while pressure and residence time were held constant at 100 atm and 140 sec, respectively. Figure 4.4 displays the yields of these products from the set of experiments in which pressure was varied from 40 to 100 atm while temperature and residence time were held constant at 570 °C and 140 sec, respectively. Yields are reported as moles of product per moles of *n*-decane fed to the reactor. One product, notable for its absence, is acetylene, which was not produced at any experimental condition.

4.2.1 Alkane and Alkene Product Formation Mechanisms

The observed alkane and alkene products are the result of a series of reactions starting with the formation of an alkyl radical [50-51]. Formation of this radical is initiated by a carbon-carbon bond of *n*-decane breaking (cracking) to form two primary radicals:

$$R\text{-}R \rightarrow \cdot R + \cdot R \qquad \textit{(initiation)}$$

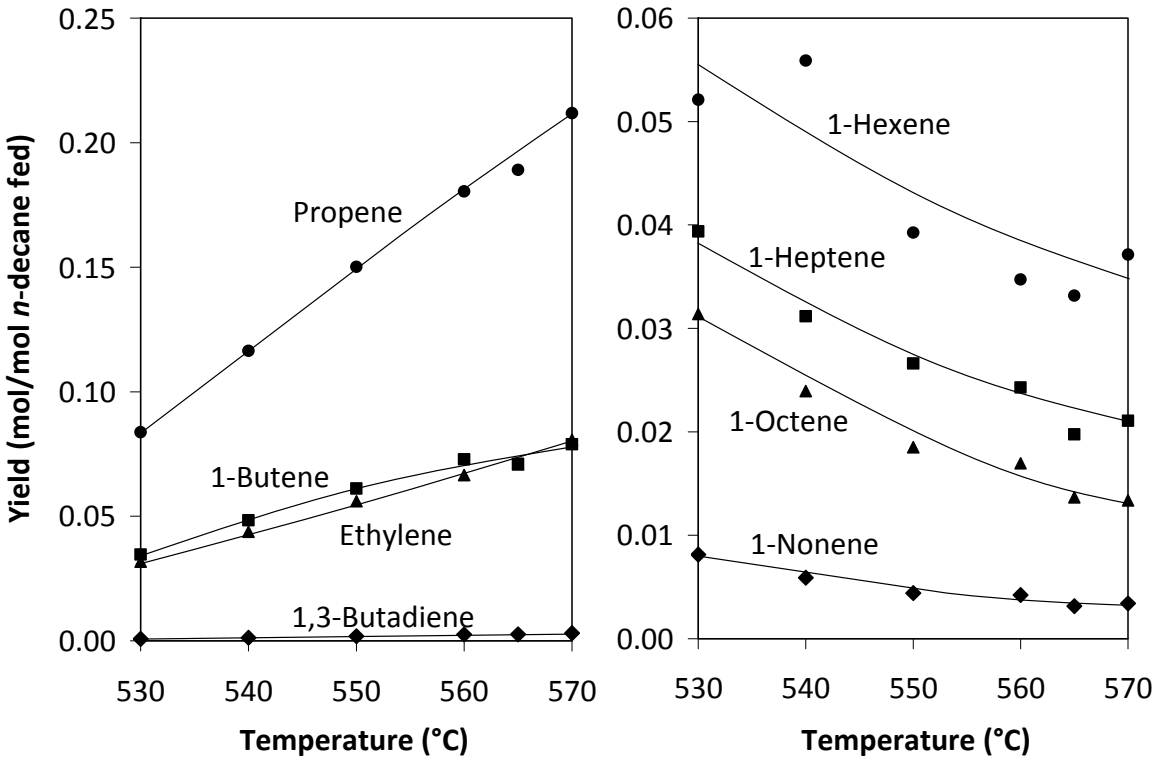

Figure 4.3 Yields of 1-alkene products and 1,3-butadiene as functions of temperature, from the supercritical pyrolysis of *n*-decane at 100 atm and 140 sec..

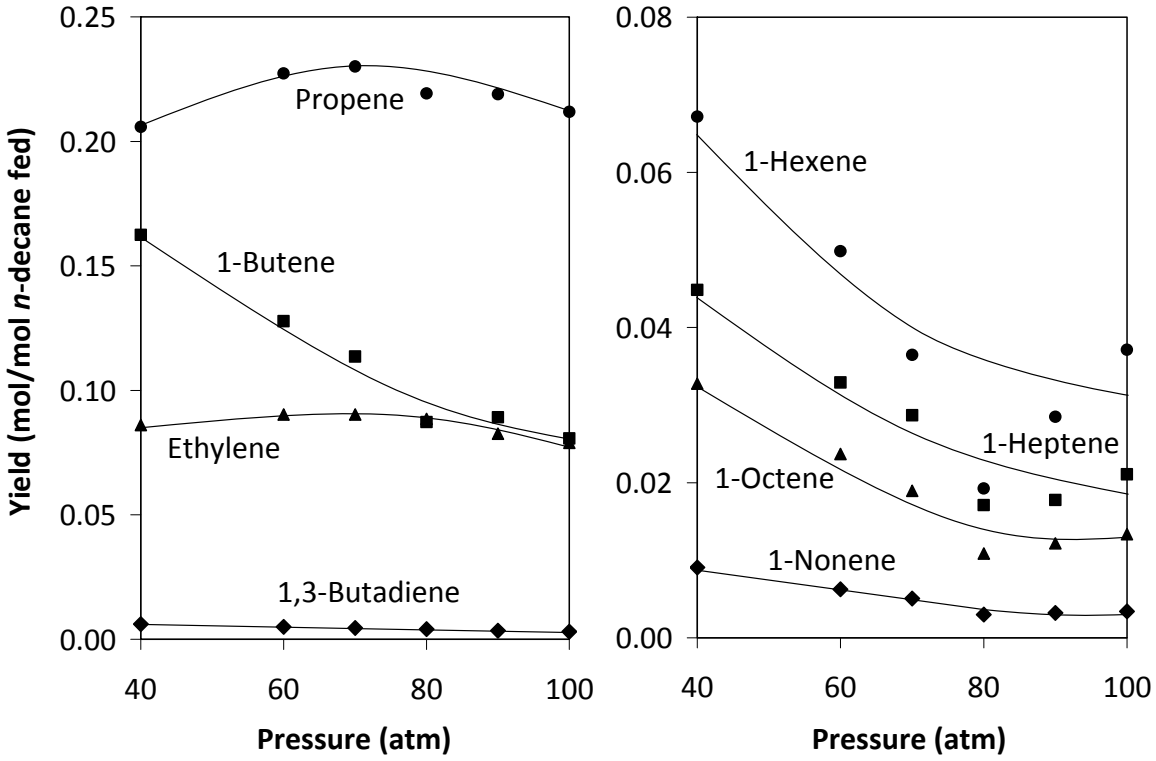

Figure 4.4 Yields of 1-alkene products and 1,3-butadiene as functions of pressure, from the supercritical pyrolysis of *n*-decane at 570 °C and 140 sec.

In this work, “primary” refers to a radical in which the radical site is located at a carbon that is bonded to one other carbon; “secondary” refers to a radical in which the radical site is located at a carbon that is bonded to two other carbons. This difference is illustrated with primary and secondary pentyl radicals as examples:

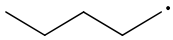

primary radical

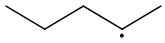

secondary radical

The primary alkyl radical resulting from the initiation reaction shown above can then react further by one of two routes. It may undergo unimolecular decomposition, yielding another primary radical and ethylene, in a process known as beta scission, or abstract a hydrogen from an alkane, yielding an *n*-alkane and another radical:

$\cdot CH_2CH_2R \rightarrow H_2C{=}CH_2 + \cdot R$ *(beta scission)*

$\cdot CH_2CH_2R + HR \rightarrow HCH_2CH_2R + \cdot R$ *(hydrogen abstraction)*

Hydrogen abstraction is the final step in the production of *n*-alkanes. The radical product of hydrogen abstraction can either be a primary or secondary radical, depending on which hydrogen is abstracted from an alkane. Hydrogen abstraction (as opposed to unimolecular decomposition of a carbon-hydrogen bond) is necessary to produce secondary alkyl radicals in the *n*-decane pyrolysis reaction environment ($T < 700$ °C) because the carbon-hydrogen bond dissociation energy (approximately 98 kcal/mol [52]) is too high for such bonds to break without the additional energy carried by a radical. For comparison, the carbon-carbon bond dissociation energy of an *n*-alkane (a bond which *does* break unimolecularly) is approximately 80 to 85 kcal/mol [52-53].

Primary radicals produced by hydrogen abstraction behave the same as those formed from the initiation reaction shown above (carbon-carbon bond cleavage); they participate in the same unimolecular decomposition and hydrogen abstraction reactions. On the other hand,

secondary radicals produced by hydrogen abstraction decompose to yield a primary radical and a 1-alkene by undergoing beta scission—the same reaction that produces ethylene from primary radicals:

$$R\dot{C}HCH_2R \rightarrow RCH{=}CH_2 + \cdot R \qquad \textit{(beta scission)}$$

With a secondary decyl radical as an example, beta scission is illustrated in the following scheme for added clarity:

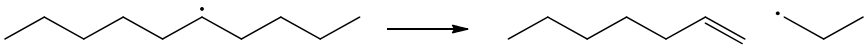

4.1

Beta scission is the final step in 1-alkene production. 1,3-Butadiene, whose yields are shown in Figures 4.3 and 4.4, is the result of hydrogen abstraction followed by beta scission occurring twice on the same molecule.

4.2.2 Alkane and Alkene Product Distributions

Figures 4.1 and 4.2 show that, with the exception of methane, product yields of *n*-alkanes decrease with increasing carbon number. The strength of the carbon-carbon bonds of an *n*-alkane decrease with increasing carbon number, therefore higher-molecular-weight *n*-alkanes are less thermally stable and degrade in the reaction environment, particularly when residence times are sufficiently long for large numbers of secondary reactions to occur [25], as is the case in the experiments conducted in this work. Methane is the result of cleavage of the bond between the first and second carbon atoms of an *n*-alkane, a reaction requiring approximately 2 kcal/mol higher activation energy than the same reaction between the other carbon atoms of an *n*-alkane [51]. The additional energy needed to break this bond reduces the likelihood, hence methane yields fall outside the trend of increasing yields with decreasing molecular weight seen for other alkane products. Yields of *n*-hexane do not follow this trend either, a result most likely due to evaporative loss of this product during analysis.

Yields of 1-alkenes show the same pattern of decreasing yield with increasing molecular weight as do yields of *n*-alkanes. As with *n*-alkanes, decomposition of thermally unstable carbon-carbon single bonds results in the depletion of higher molecular weight products. The exception among them is ethylene, the yields of which are lower than those of both propene and 1-butene. However, unlike other olefinic products, which are produced by both the decomposition of secondary radicals and decomposition of higher-molecular-weight 1-alkenes, ethylene is produced by only one route, decomposition of primary radicals, hence its lower relative yield.

Figures 4.1 and 4.3 demonstrate that increases in temperature favor the formation of lower molecular weight alkane and alkene products over their higher-molecular-weight counterparts. In Figure 4.1, yields of alkanes with one to four carbons show an upward trend with increasing temperature, while those with six or more carbons show a downward trend. This same effect is seen in Figure 4.3; yields of alkenes with two to four carbons increase with temperature, while yields of alkenes with six or more carbons decrease with temperature. The weaker carbon-carbon bonds of higher-molecular-weight products are increasingly broken as temperature increases, converting these products to lower-molecular-weight products.

Increases in pressure increase all *n*-alkane product yields (Figure 4.2). In the gas phase, primary alkyl radicals with more than three carbons are more likely to decompose unimolecularly via beta scission before they have an opportunity to react with other molecules [50]. Such unimolecular decomposition is demonstrated in the diagram below, using the primary hexyl radical as an example. The radical will decompose first to butyl radical and ethylene, and then the butyl radical will decompose to an ethyl radical and another ethylene:

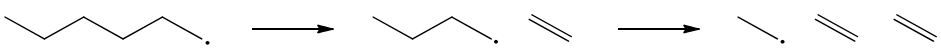

4.2

Pyrolysis of alkanes in the gas phase favors the production of light hydrocarbons such as propylene, ethane, ethylene, methane, and hydrogen, but high pressures stabilize alkyl radicals [54]. Figure 4.2 shows yields of alkanes with more than six carbons increase with pressure. Increasing pressure increases alkyl radical stability; allowing these radicals time to abstract hydrogen from surrounding molecules and produce *n*-alkanes. Increases in pressure have the same effect on secondary radicals, acting to stabilize them and reducing the likelihood of decomposition by beta scission, the reaction which results in 1-alkene products. This effect manifests itself by the overall downward trend of alkene yields with increasing pressure (Figure 4.4). Ethylene and propene do not follow this trend with pressure, but this behavior is likely the result of two competing forces. While the increasing pressure reduces selectivity for alkene products, it also increases the concentration of the reactant in the reaction environment, leading to increased production of all products, including ethylene and propene. Increased concentration likely partially accounts for the increased production of *n*-alkanes with increased pressure as well.

4.3 One-Ring Aromatic Products

Benzene, toluene, ethylbenzene, the three isomers of xylene, isopropylbenzene, *n*-propylbenzene, and *n*-butylbenzene are the single-ring aromatics identified by GC/FID/MS as products of supercritical *n*-decane pyrolysis. More highly alkylated benzenes are also observed: four other alkylbenzenes with three carbons in the alkyl substituents and five others with four carbons in the alkyl substituents, although the positions and lengths of these substituents are not known.

Figure 4.5 displays the yields of the products benzene, toluene, and ethylbenzene and the summed yield of *m*- and *p*-xylene from the two sets of pyrolysis experiments in which (a) temperature was varied from 530 to 570 °C while pressure and residence time were held constant

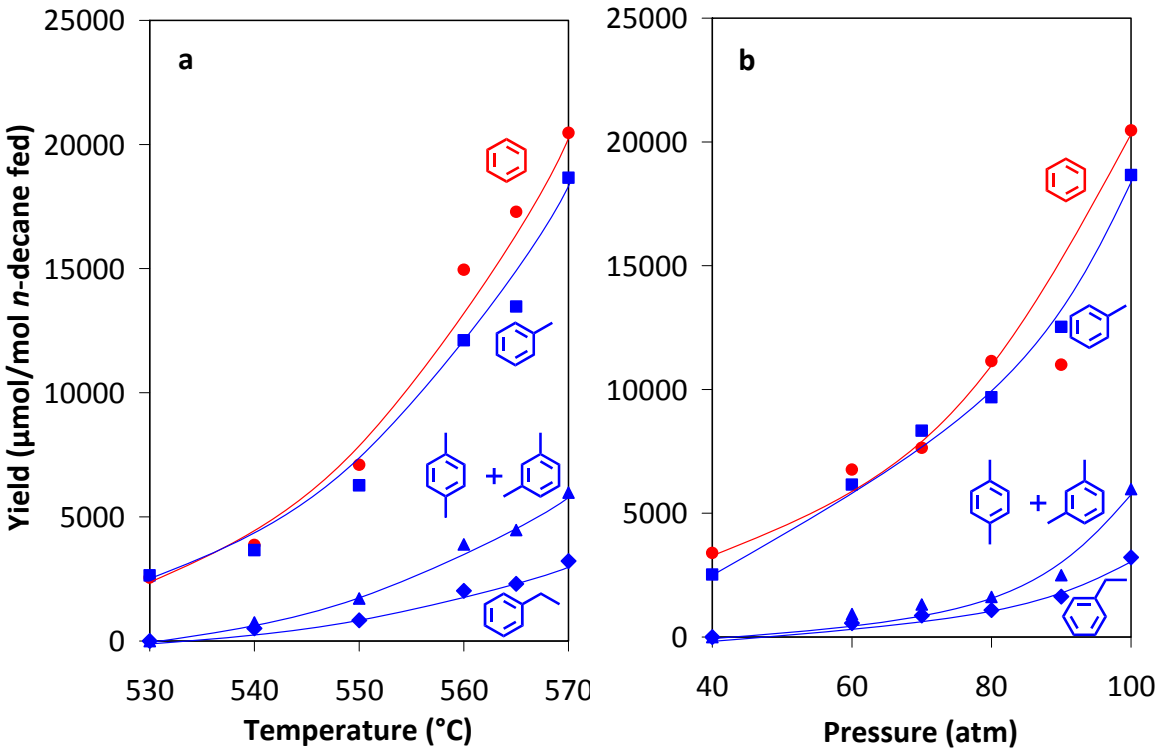

Figure 4.5 Yields of benzene, toluene, and ethylbenzene and the summed yield of *m*- and *p*-xylene from the supercritical pyrolysis of *n*-decane: (a) yields versus temperature, at 100 atm and 140 sec; (b) yields versus pressure, at 570 °C and 140 sec.

at 100 atm and 140 sec, respectively, and (b) pressure was varied from 40 to 100 atm while temperature and residence time were held constant at 570 °C and 140 sec respectively. Yields are reported in terms of µmoles of product per mole of *n*-decane fed to the reactor. Since benzene and toluene are present in both the gas- and liquid-phase products, they are quantified by GC/FID in both phases and the sums of these two yields are reported. The yields of *m*- and *p*-xylene are reported as a sum because these two products co-elute. *o*-Xylene was not quantified because this product co-elutes with 1-nonene, although it was assumed during the estimation of the yield of 1-nonene that all three xylene isomers are produced in equal yields. Higher-molecular-weight alkylbenzenes (those with alkyl substituent(s) composed of more than two carbons) were not quantified due to the presence of undifferentiated material co-eluting with

these products. This material is most likely branched and cyclic alkanes and alkenes, but it could not be identified because the material is found in low quantities and with a large number of products eluting in the same time range as the alkylbenzene products.

As shown in Figure 4.5a, yields of all one-ring aromatic products increase with temperature between 530 and 550 °C, then increase sharply above 550 °C. Products follow a trend of decreasing yields with increasing molecular weight: benzene > toluene > ethylbenzene and xylenes. Alkylbenzenes with more than three carbon atoms in the substituent groups are not quantified due to poor chromatographic separation, but examination of their peak heights indicates that this trend continues to higher-molecular-weight species. Figure 4.5b shows product yields increasing between 40 and 70 atm then increasing sharply above 70 atm. The product yields of Figure 4.5b also follow the trend benzene > toluene > ethylbenzene and xylenes > higher-molecular-weight alkylbenzenes.

The next section will describe the mechanisms leading to the formation of one-ring aromatic products in the *n*-decane pyrolysis environment and show how these mechanisms account for the observation that the yields of single-ring aromatic products decrease with increasing molecular weight. Following that, another section will explain pressure and temperature effects on product yields. While the trends of each single-ring aromatic product yield appear to be the same with respect to either temperature or pressure, these trends are actually the results two distinct effects.

4.3.1 Single-Ring Aromatic Formation Mechanisms

Formation of a single aromatic ring from an *n*-alkane proceeds in two steps. First the alkane must cyclize to either a cycloalkane or cycloalkene, then lose hydrogen to give an aromatic molecule [55]. Dehydrogenation of a cyclic alkane to an aromatic molecule has been shown to occur readily in the supercritical pyrolysis of alkylcyclohexanes, decalin, and tetralin

[35-36,56-57]. Dehydrogenation occurs by the sequential loss of hydrogen from a cyclic alkane [36], first by formation of a cyclic alkyl radical (or alkenyl radical, in the case of cycloalkenes), then further loss to form a cyclic alkene (or diene), and so on, eventually leaving a single aromatic ring.

Formation of cyclic molecules is less straightforward compared to dehydrogenation. A seemingly obvious pathway to a cyclic alkane is cyclization of a primary alkyl radical. The products of primary radicals, *n*-alkanes, are among the highest-yield products of *n*-decane pyrolysis, leading to the conclusion that these radicals are highly concentrated in the reaction environment. Furthermore, it appears plausible that attack by the primary radical on one of its own carbons would yield a cyclic radical, which could then lose a hydrogen to form a cycloalkane. However, experimental data [51] show that this process is unlikely to occur, despite high concentrations of alkyl radicals in the reaction environment. A primary radical cannot cyclize because it cannot attack any of its carbons; these carbons are shielded from attack by hydrogen. Instead of attacking a carbon, the radical will abstract one of its hydrogens, at the same time isomerizing to a secondary radical [51]. This concept is illustrated below with the isomerization of a 1-nonyl radical to a 5-nonyl radical:

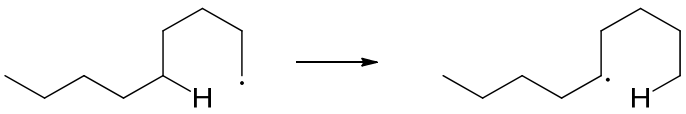

4.3

This process is called a 1,5 shift, indicating a shift in the radical from the "1" to the "5" position. A 1,4 shift is also possible, but due to shielding by hydrogen an alkyl radical cannot attack one of its own carbons. Therefore alkyl radicals are unlikely to play a role in the formation of cyclic alkanes.

Another possibility for the formation of cyclic molecules is the reaction of 1,3-butadiene with the double bond of an alkene through a Diels-Alder type mechanism. Illustrated below, this

reaction has been shown to occur in the gas-phase pyrolysis of 1,3-butadiene at temperatures below 600 °C [58], with styrene as the product:

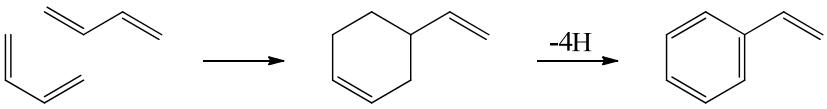

4.4

However, while Figures 4.3 and 4.4 show that alkenes are present in high concentrations in the reaction environment, they also show that yields of 1,3-butadiene are much lower than those of benzene and toluene (Figure 4.5). Presumably a precursor would be found in higher yields than its product, although it is possible that 1,3-butadiene is a short-lived intermediate, being consumed soon after it is formed. Hence its low concentration among the products does not necessarily prove that it does not play an important role in the production of cyclic alkenes. However, in studies using aliphatic fuels where additives were used to inhibit Diels-Alder type reactions, reductions in carbonaceous solid deposit formation were not observed [1]. Cyclic alkanes or alkenes are needed to produce single ring aromatic molecules, single-ring aromatic molecules are necessary to produce multi-ring aromatic molecules, and multi-ring aromatic molecules are required to produce solid deposits [1]. Therefore, if a Diels-Alder type reaction is taking place, it is not a significant contributor of one-ring aromatics in the supercritical *n*-decane pyrolysis system, and the reaction shown in Scheme 4.4 is unlikely to be the primary source of benzene and alkylbenzenes in the supercritical *n*-decane pyrolysis environment.

Alkenyl radicals, unlike alkyl radicals, have unsaturated carbons which are vulnerable to attack [59]. Even though they were not observed directly, alkenyl radicals should be abundant in the supercritical pyrolysis environment: olefins are major products of supercritical *n*-decane pyrolysis (Figures 4.3 and 4.4), and their alkyl carbon-carbon bonds have been shown to break readily under the reaction conditions (Section 4.2.2). As shown in Schemes 4.5 and 4.6, five- and six-membered rings can form by radical attack on one of the carbons in the double bond:

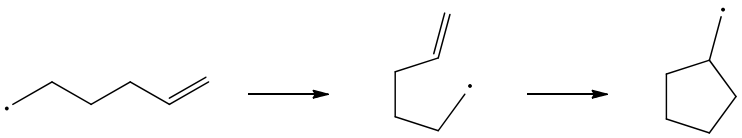

4.5

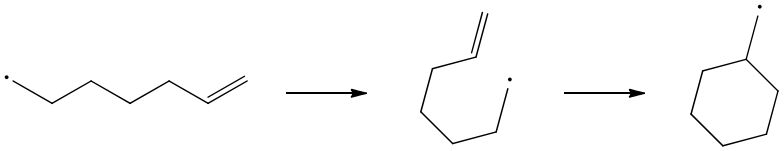

4.6

In the above schemes the radical attacks take place on the carbon in the double bond that is bonded to two carbons; attack on the other carbon in the double bond, the one bonded to a single carbon, is possible but not favored [59].

The product of Scheme 4.5, a cylcopentylmethyl radical, is one possible route to benzene. As shown in Scheme 4.7, loss of hydrogen from this radical results in an isomer of benzene, fulvene, which can then isomerize to form benzene.

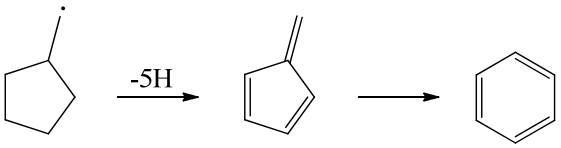

4.7

While fulvene isomerization is believed to occur in combustion systems [60], it is unclear if this isomerization is possible (or if fulvene production even occurs) under the experimental conditions in this work.

On the other hand, the product of Scheme 4.6, a cyclohexylmethyl radical, could form the single-ring aromatic molecule toluene from reactions known to take place under the experimental conditions. Addition of hydrogen to the cyclohexylmethyl radical produces methylcyclohexane, dehydrogenation of which yields toluene [36,61]. Given the availability of olefins in the reaction environment and the susceptibly of their carbon-carbon single bonds to homolytic cleavage, alkenyl radicals should be plentiful. Alkenyl radical cyclization of the types shown in Schemes

4.5 and 4.6, followed by dehydrogenation and possibly isomerization, are the most likely paths to single-ring aromatic molecule formation during the supercritical pyrolysis of *n*-decane.

Highly alkylated aromatic molecules are a distinctive constituent of supercritical alkane pyrolysis products, not observed as either products of supercritical pyrolysis of aromatic fuels [27-32] or products of high-temperature, gas-phase combustion or pyrolysis of hydrocarbons [62]. The formation of highly alkylated aromatics in the supercritical *n*-decane pyrolysis environment can be explained with conclusions drawn from the supercritical pyrolysis of the aromatic fuels toluene and 1-methylnaphthalene. It has been shown that methyl radical attack on aromatic molecules and subsequent hydrogen loss occur readily in these reaction environments [27,32] producing xylene, as shown in Scheme 4.8, and dimethylnaphthalene, as shown in Scheme 4.9.

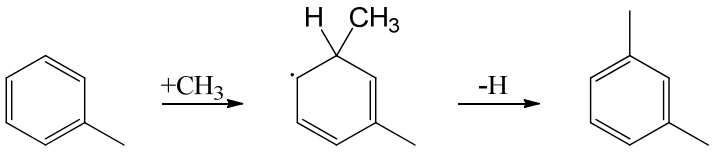

4.8

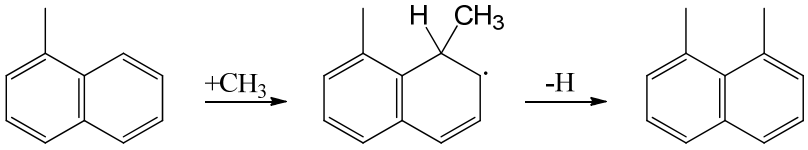

4.9

The only alkyl radicals available in the toluene and 1-methylnaphthalene supercritical pyrolysis environments are methyl radicals, resulting from the cleavage of alkyl-aryl carbon-carbon bonds of the respective reactants [27,32]. The supercritical *n*-decane pyrolysis reaction environment, in contrast, contains high concentrations of alkyl radicals consisting of one to nine carbons. Instead of methyl substituents attacking the aromatic carbons and displacing hydrogen as in Schemes 4.8 and 4.9, alkyl groups consisting of one to nine carbons displace hydrogen from aromatic carbons, forming alkylbenzenes in high yields and with a large variety of alkyl substituents.

This alkyl radical addition mechanism to single-ring aromatic products is consistent with the aforementioned trend of alkylbenzene product yield decreasing with increasing molecular weight. Addition of alkyl groups happens one-at-a-time, so alkylbenzenes with more substituents can only appear after those with fewer substituents have already formed. Furthermore, the carbon-carbon bonds in the alkyl groups are susceptible to the same cracking reactions responsible for the shorter chain *n*-alkane products, a process which favors the production of shorter alkyl substituents. Higher-molecular-weight alkylbenzenes are both less likely to be produced and more likely to be depleted once formed.

Production of benzene and toluene is more complicated, the relative yields of these products being dependent on several factors. First, as described earlier in this section, benzene and toluene are produced by two different mechanisms, so their yields are partially dependent on the rates of their formation. Second, addition of a methyl radical to benzene followed by loss of a hydrogen will form toluene [27,32], while the reverse reaction, addition of a hydrogen radical to toluene followed by loss of a methyl radical, converts toluene to benzene [63]. Therefore the interconversion of the two products also influences their yields.

Finally, the participation of benzene and toluene in secondary reactions, leading to depletion of these two products, must be taken into account. Loss of hydrogen by toluene to form the benzyl radical is much more favorable than loss of hydrogen by benzene to form the phenyl radical, due to the higher bond dissociation energy of the aryl carbon-hydrogen bond of benzene (112.9 kcal/mol [52]) compared to that of the methyl carbon-hydrogen bond of toluene (88.5 kcal/mol [52]). The relatively facile formation of a radical allows toluene to participate in secondary reactions at a higher rate than benzene, reducing the yield of toluene relative to that of benzene. Therefore while the trend of decreasing yield of alkylbenzenes with increasing

molecular weight is well understood, the relative yields of benzene and toluene are the result of several competing factors.

4.3.2 Temperature and Pressure Effects on Single-Ring Aromatic Product Yields

One-ring aromatic product yield trends with respect to temperature (shown in Figure 4.5a) are consistent with radical intermediates being responsible for single-ring aromatic formation. Higher temperatures favor carbon-carbon alkyl bond cleavage, increasing the production of alkenes, and hence the production of alkenyl radicals, secondary products formed by cleavage of carbon-carbon single bonds of the alkenes. These alkenyl radicals then lead to increased production of benzene and toluene by cyclization (Schemes 4.5 and 4.6) followed by dehydrogenation. The alkyl radicals resulting directly from increased carbon-carbon alkyl bond breakage participate in alkyl radical addition reactions to one-ring aromatics (Schemes 4.8 and 4.9), leading to the increased production of ethylbenzene, *m*- and *p*-xylene, and higher-molecular-weight alkylbenzenes.

Product yield trends of benzene and alkylbenzenes with respect to pressure (shown in Figure 4.5b) are the result of three effects, all of which are distinct from the effect of temperature. First, increasing pressure increases the density of the reactant *n*-decane in the reactor. Increasing the density of the reactant increases its concentration, leading to higher production of all products, including one-ring aromatic molecules. Second, as explained in Section 4.2.2, high pressures stabilize alkyl radicals. This effect should also stabilize alkenyl radicals, allowing these radicals time to cyclize before decomposing.

Third, high pressures introduce cage effects, observed previously in the supercritical pyrolysis of methylcyclohexane [36-37]. While the gas phase is characterized by freely moving molecules which collide infrequently with one another, in the liquid-like densities of the supercritical phase each molecule is continuously in contact with neighboring molecules. This

situation creates a cage of solvent molecules around a solute molecule, preventing it from moving freely. Ring opening of a cyclic alkane is prevented inside these cages. This effect is manifested in the production of more single-ring aromatic molecules. Once a cyclic molecule is formed, it is less likely to return to a linear state. The cyclic alkane is stable and survives long enough to lose hydrogens, yielding the aromatic product.

In summary, one-ring aromatic products of supercritical *n*-decane pyrolysis consist of benzene and a large number of alkylbenzenes. Products with at least five carbons in the alkyl substituents have been identified. Yields of these products increase with temperature and pressure and decrease with the degree of alkyl substitution. One-ring aromatic production most likely proceeds through the cyclization of an alkenyl radical to yield a methylated cyclic alkane, followed by dehydrogenation to yield an aromatic molecule. Alkylation of benzene and alkylbenzenes proceeds through alkyl radical attack on the aromatic ring, followed by hydrogen loss.

4.4 Polycyclic Aromatic Hydrocarbon Products

Figures 4.6 through 4.24 present the yields of product PAH from the two sets of experiments in which (a) pressure and residence time were held constant at 100 atm and 140 sec and temperature was varied from 530 to 570 °C and in which (b) temperature and residence time were held constant at 570 °C and 140 sec and pressure was varied from 40 to 100 atm. Yields are reported in terms of μmoles of product PAH per mole of *n*-decane fed to the reactor.

The sections that follow will cover each unsubstituted PAH product and its alkylated derivatives individually. Identified products will be described, and the possible reaction mechanisms leading to the formation of each of these products will be discussed. Dominant reaction pathways will be indicated when possible. PAH products that have common reaction

mechanisms will be grouped together in some sections. Pressure and temperature effects on the yields of PAH products are explained after the sections that cover the identified PAH products.

4.4.1 Naphthalene

Naphthalene, 1-methylnaphthalene, and 2-methylnaphthalene are identified as products of supercritical *n*-decane pyrolysis. Yields of these three two-ring compounds are presented as functions of temperature, at 100 atm and 140 sec, in Figure 4.6a, and as functions of pressure, at 570 °C and 140 sec, in Figure 4.6b. In addition to the products which are quantified, 46 alkylnaphthalenes for which the aromatic structure is known, but not the positions or identities of the alkyl substituents, are also identified but not quantified due to insufficient chromatographic separation.

Alkyl radical addition to naphthalene, followed by hydrogen loss, the same mechanism responsible for alkylbenzene formation (Schemes 4.8 and 4.9), is responsible in part for production of the alkylated derivatives of naphthalene. The large number of higher-ring-number alkylated PAH, an important feature of supercritical *n*-decane pyrolysis, can also be attributed to this mechanism. As with toluene, whose methyl group is not necessarily the result of alkyl radical attack on benzene, many PAH have alkyl substituents which were not added to a less alkylated PAH. These substituents were left as part of the ring-addition process that is responsible for the formation of increasingly large multi-ring aromatic molecules. This concept will be explained below in further detail.

To account for the product naphthalene, Song [26] posited a mechanism, illustrated below in Scheme 4.10, for production of this two-ring compound from the supercritical pyrolysis of jet fuel (of which alkanes are a primary constituent). First, an alkyl radical attacks benzene to yield an alkylbenzene. Then the alkyl substituent of the alkylbenzene breaks unimolecularly between the fourth and fifth carbons, yielding a phenylbutyl radical. This radical attacks one of

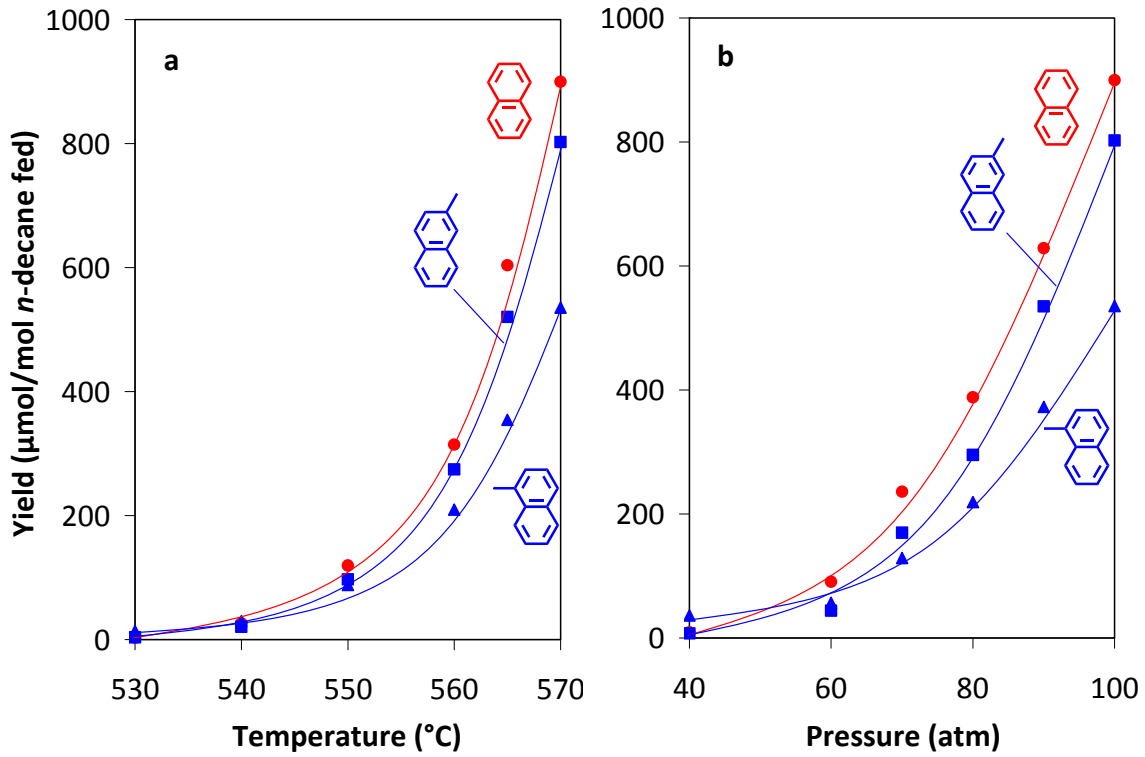

Figure 4.6 Yields of naphthalene, 1-methylnaphthalene, and 2-methylnaphthalene from the supercritical pyrolysis of *n*-decane: (a) yields versus temperature, at 100 atm and 140 sec; (b) yields versus pressure, at 570 °C and 140 sec.

its own aromatic carbons to yield tetralin, which then undergoes dehydrogenation to yield the final two-ring aromatic product.

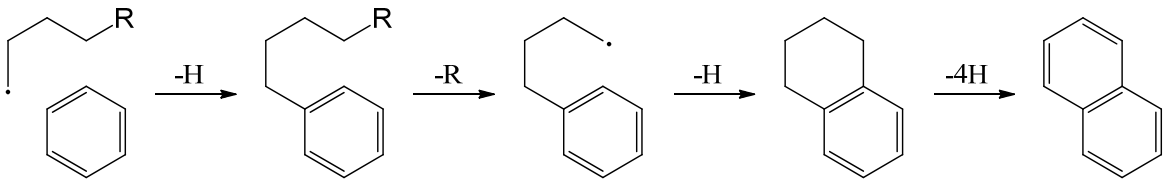

4.10

The intermediate steps—alkyl radical attack, alkyl carbon-carbon bond scission, and dehydrogenation—have all been shown to take place at the same conditions as those in the supercritical *n*-decane pyrolysis experiments [27,32,35-36,56,64]. Furthermore, tetralin (the intermediate species just prior to the final product in Scheme 4.10 between the fourth and final steps) has been reported as a product of supercritical butylbenzene pyrolysis [65].

Another possibility for the formation of naphthalene from benzene involves the pentenyl radical. As shown in Scheme 4.11a, this radical first attacks benzene, and the position of the radical shifts from the alkenyl group to one of the aromatic carbons. Then, this radical attacks a carbon in the double bond of the alkenyl substituent group, closing the ring in a mechanism analogous to Scheme 4.6 for formation of the cyclohexylmethyl radical. Finally, addition of hydrogen to the methyl radical followed by dehydrogenation of the ring yields the fully aromatic product 1-methylnaphthalene.

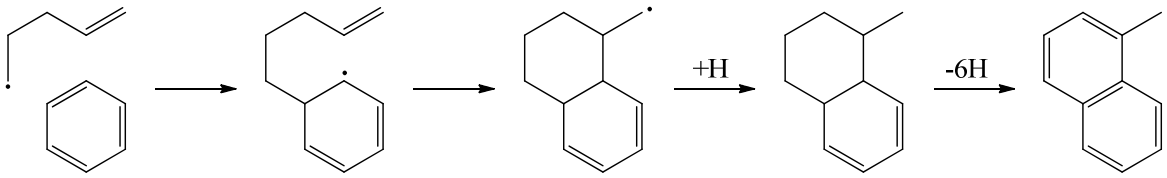

4.11a

Scheme 4.11a shows one pathway for a methylated naphthalene to be produced by a mechanism other than alkyl radical attack on naphthalene. To produce unsubstituted naphthalene, a hydrogen radical attacks 1-methylnaphthalene at the aryl carbon attached to the methyl group, followed by loss of the methyl group (the reverse of the reactions depicted in Schemes 4.8 and 4.9):

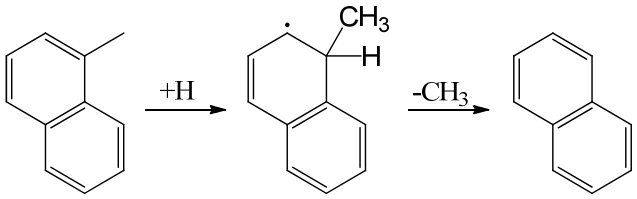

4.11b

Alternatively, butenyl radical addition to benzene would yield a five-membered ring analogous to fulvene (Scheme 4.7), which could then isomerize to a six-membered ring, producing naphthalene; this reaction is shown in Scheme 4.12.

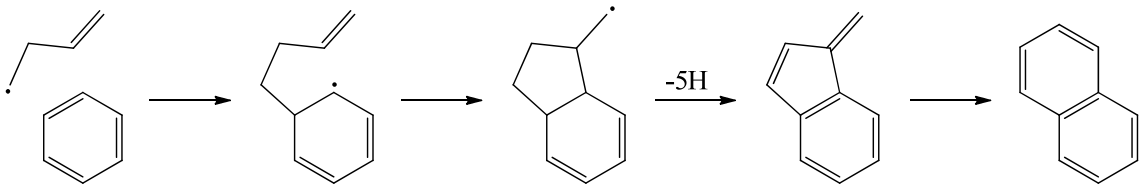

4.12

Experimental evidence does not indicate which of the three schemes described above is responsible for the production of naphthalene during supercritical *n*-decane pyrolysis. But given the lack of alternatives, and based on the reactions currently understood to be possible under the experimental conditions, mechanisms utilizing alkyl or alkenyl radical addition to benzene is most likely responsible for the production of naphthalene (as well as 1-methylnaphthalene, in the case of Scheme 4.11a). The mechanism responsible for addition of a ring to an aromatic molecule to yield a molecule with one additional aromatic ring (which could be Schemes 4.10, 4.11, 4.12, or any combination of these three) will be referred to as "C_4 addition" in this work. Note that this mechanism may result in the addition of a methyl substituent group to the final product as well, as in Scheme 4.11a.

There is no reason to believe that aryl carbons of alkylated aromatic molecules are any less likely than those of unsubstituted aromatic molecules to participate in C_4 addition or any of the other ring-building reactions that will be discussed in the following sections. For the sake of simplicity and clarity, an unsubstituted aromatic is used as the aromatic reactant in Schemes 4.10 through 4.12. For the same reason, unsubstituted PAH will be used in every reaction scheme shown in this work, unless, of course, an alkyl substituent is itself a participant in the reaction. It should be understood that in any reaction involving an aryl carbon, an alkylated PAH could just as easily be a participant, and that its involvement in such a case would represent one more route to the production of alkylated PAH other than alkyl-radical addition to an unalkylated (or less alkylated) PAH.

4.4.2 Fluorene and Benzo[*b*]fluorene

Fluorene and all five isomers of methylfluorene are identified as products of supercritical *n*-decane pyrolysis; yields of these six three-ring PAH are presented in Figure 4.7. The four-ring PAH benzo[*b*]fluorene is also identified among the products; its yields are reported in Figure 4.8.

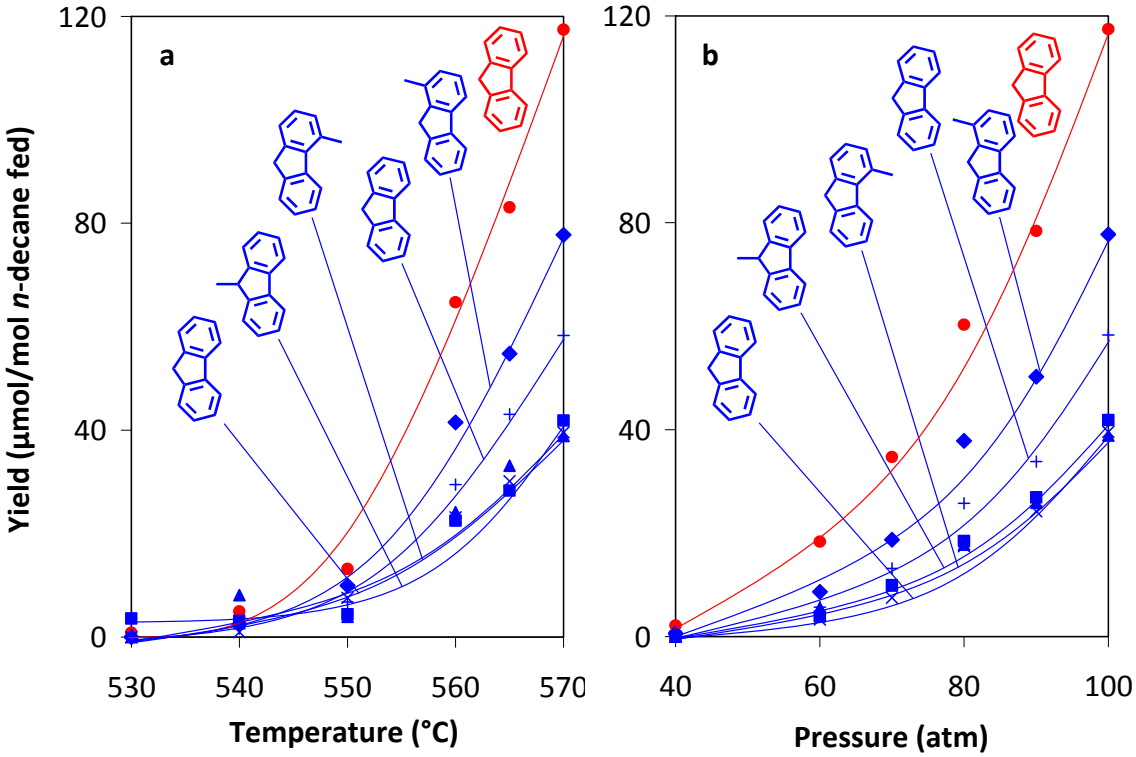

Figure 4.7 Yields of fluorene and the five isomers of methylfluorene from the supercritical pyrolysis of *n*-decane: (a) yields versus temperature, at 100 atm and 140 sec; (b) yields versus pressure, at 570 °C and 140 sec. The position of the methyl group of the methylfluorene is labeled for each product for which it is known; blue labels with no methyl group are used to indicate the methylfluorenes for which the positions of the methyl groups are not known.

In addition to the products which are quantified, 17 alkylfluorenes and one alkylbenzo[*b*]fluorene for which the aromatic structures are known but not the positions or identities of the alkyl substituents, are also identified but not quantified due to insufficient chromatographic separation.

The reaction mechanism responsible for fluorene formation has been determined in experimental work on the gas- and supercritical-phase pyrolysis of toluene [30,66] and is illustrated in Scheme 4.13. The first step (not shown) is the formation of a benzyl radical from an alkylbenzene. This benzyl radical then attacks benzene, and hydrogen loss yields the intermediate molecule diphenylmethane. Next, loss of hydrogen by one of the aromatic rings of

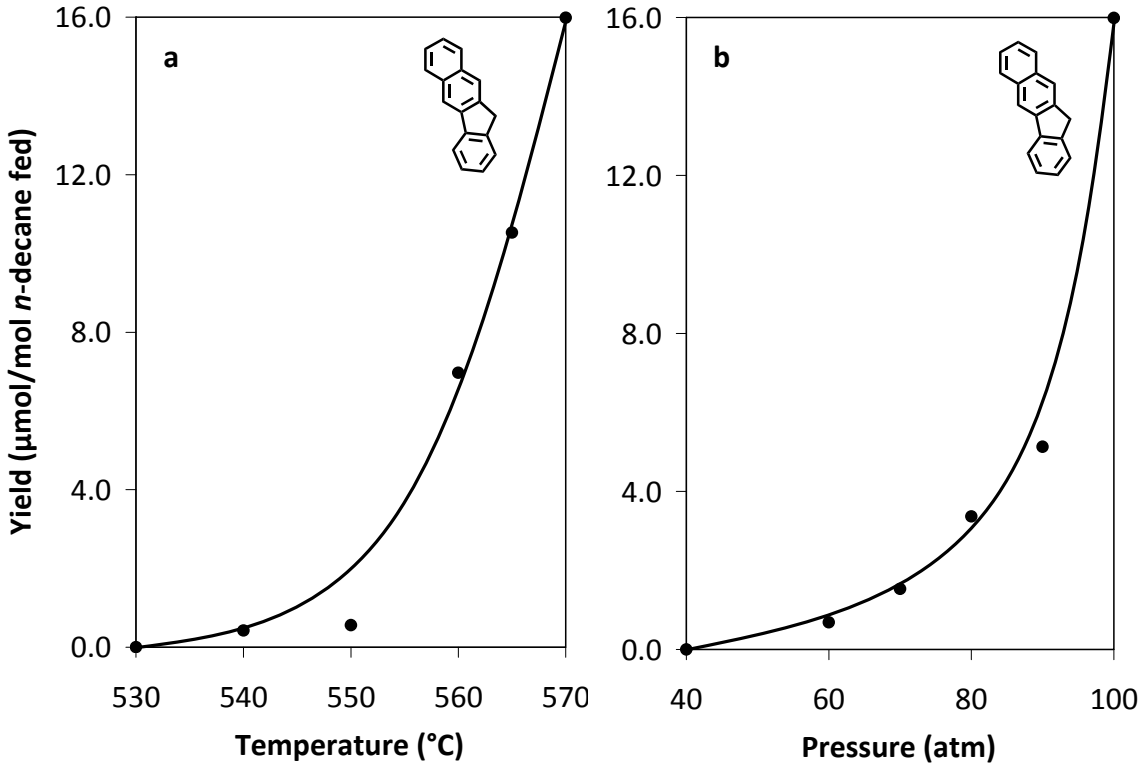

Figure 4.8 Yields of benzo[*b*]fluorene from the supercritical pyrolysis of *n*-decane: (a) yields versus temperature, at 100 atm and 140 sec; (b) yields versus pressure, at 570 °C and 140 sec.

diphenylmethane yields a radical; hydrogen loss must occur specifically at the position ortho to the methylene group of diphenylmethane. A radical in this position can attack the other aromatic ring to form a five-membered ring between the two six-membered rings. Loss of hydrogen yields the final product fluorene.

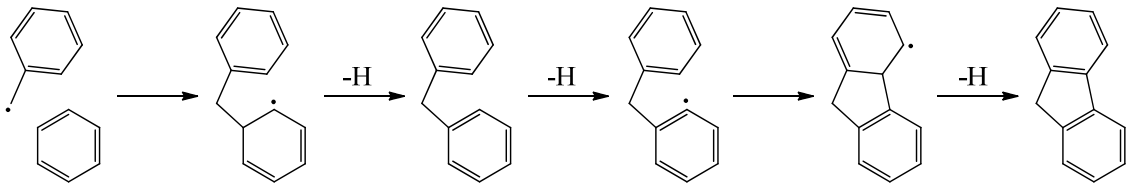

4.13

Based on the bond energy of the aryl carbon-hydrogen bond, hydrogen loss by the phenyl group (the third step of the Scheme 4.13) is probably not a unimolecular reaction. The aryl carbon-hydrogen bond is among the strongest of any bond of the products of supercritical *n*-decane pyrolysis environment; its bond dissociation energy is 112.9 kcal/mole [52]. This is

actually second in strength among bonds of products only to the aromatic carbon-carbon bond, the bond dissociation energy of which is 122.3 kcal/mole [67]. It is therefore very likely that the hydrogen on the phenyl group is actually abstracted by another radical, just as hydrogens are abstracted from alkanes by alkyl radicals. In both situations, the molecule does not have sufficient energy for the carbon-hydrogen bond to break on its own; the radical provides the extra energy necessary for the bond to be broken. "Loss" of hydrogen by an aromatic molecule will often be referred to in this work and shown as a simple unimolecular reaction, as it is in Scheme 4.13. Omission of the alkyl radical abstraction of hydrogen in reactions schemes is done for simplicity, and it should be understood that when an aromatic molecule loses a hydrogen it is most likely abstracted by a radical.

Interestingly, biphenyl is not observed as a product, even though Scheme 4.13 implies that it should be. Specifically, the fourth step in Scheme 4.13, attack by the phenyl radical substituent on the phenyl substituent on the opposite side of the methylene group, is analogous to attack by a free phenyl radical on benzene, which, after loss of hydrogen, would yield biphenyl. The key difference between these two reactions, one yielding fluorene and the other biphenyl, is that the two aromatic rings in the intermediate to fluorene are joined together by a methylene group. It is possible that while the loss of hydrogen is a rare occurrence for both benzene (to yield a free phenyl radical) and the phenyl group of diphenylmethane (to yield a phenyl radical substituent), the methylene group of diphenylmethane ensures that once such a radical does form it is already in close proximity to the other phenyl group, allowing attack by the radical on this phenyl group. In contrast, a simple phenyl radical is very likely to encounter an alkane or an alkene from which it would abstract hydrogen, converting back to benzene long before it has an opportunity to attack benzene and produce biphenyl.

It is also possible that hydrogen loss by a phenyl group is not a necessary step in the formation of fluorene. In this alternative mechanism, benzyl radical attack on benzene (the first step in Scheme 4.13) is the same. However, as shown in Scheme 4.14, instead of forming the intermediate diphenylmethane, the radical, which has shifted position from the benzyl radical to one of the phenyl groups, immediately attacks the opposite phenyl group. Dehydrogenation would yield the final product.

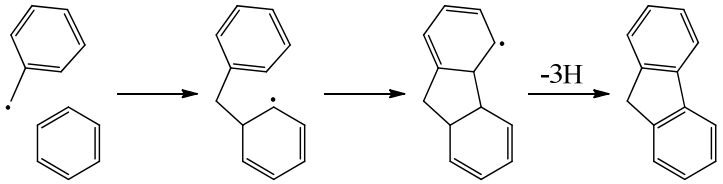

4.14

The high yields of methyl-substituted fluorenes identified from supercritical *n*-decane pyrolysis are consistent with either mechanism. Although the reactants are presented as a benzyl radical and benzene, it is equally likely that they are toluene and a benzyl radical or benzene and a methylated benzyl radical—a radical easily produced by loss of hydrogen by xylene. Either of these alternatives would result in one of the methylated fluorene products.

Benzo[*b*]fluorene is produced by the same mechanism as that which is responsible for formation of fluorene (Scheme 4.13 or 4.14), with the only difference being that the initial step is either a naphthylmethyl radical attack on benzene or a benzyl radical attack on naphthalene. It is also possible that the mechanism responsible for conversion of benzene into naphthalene, the C_4 addition mechanism discussed in Section 4.4.1, is also responsible for production of benzo[*b*]fluorene from fluorene. However, if the assumption is made that C_4 addition occurs at the same rate to benzene (to yield naphthalene) as it does to fluorene (to yield benzo[*b*]fluorene), then yields of fluorene (Figure 4.7) are too low to account for yields of benzo[*b*]fluorene (Figure 4.8). For example, at the highest stressing experimental condition (570 °C, 100 atm), the yield of the supposed precursor fluorene is approximately seven times higher than the yield of the

product benzo[*b*]fluorene. On the other hand, the yield of benzene is more than twenty times higher than that of naphthalene at these same conditions. If it is assumed that C_4 addition happens at the same rate to a benzene molecule as it does to a fluorene molecule, then the yield of benzo[*b*]fluorene is too high to result primarily from C_4 addition to fluorene.

Comparison of the yields of benzene and naphthalene to those of fluorene and benzo[*b*]fluorene at all other experimental conditions leads to the same conclusion, that there is insufficient fluorene to account for benzo[*b*]fluorene by the C_4 addition mechanism, and that the benzyl radical addition mechanism elucidated in Schemes 4.13 and 4.14 (or naphthylmethyl radical addition to benzene) must be the dominant mechanism responsible for production of this four-ring PAH.

4.4.3 Phenanthrene and Anthracene

Phenanthrene, cyclopenta[*def*]phenanthrene, and all five isomers of methylphenanthrene are identified as products of supercritical *n*-decane pyrolysis; yields of these products are presented in Figure 4.9. In addition to the products which are quantified, 13 alkylphenanthrenes for which the aromatic structures are known, but not the positions or identities of the alkyl substituents, are also identified. Anthracene and all three isomers of methylanthracene are identified as products of supercritical *n*-decane pyrolysis. Figure 4.10 presents the yields of anthracene and 1- and 9-methylanthracene. In addition to the products which are quantified, four alkylanthracenes for which the aromatic structures are known, but not the positions or identities of the alkyl substituents, are also identified. 2-Methylanthracene as well as the more highly alkylated three-ring PAH products were not quantified due to insufficient chromatographic separation. Unless otherwise stated, throughout this work poor HPLC separation is the reason any identified product is not quantified.

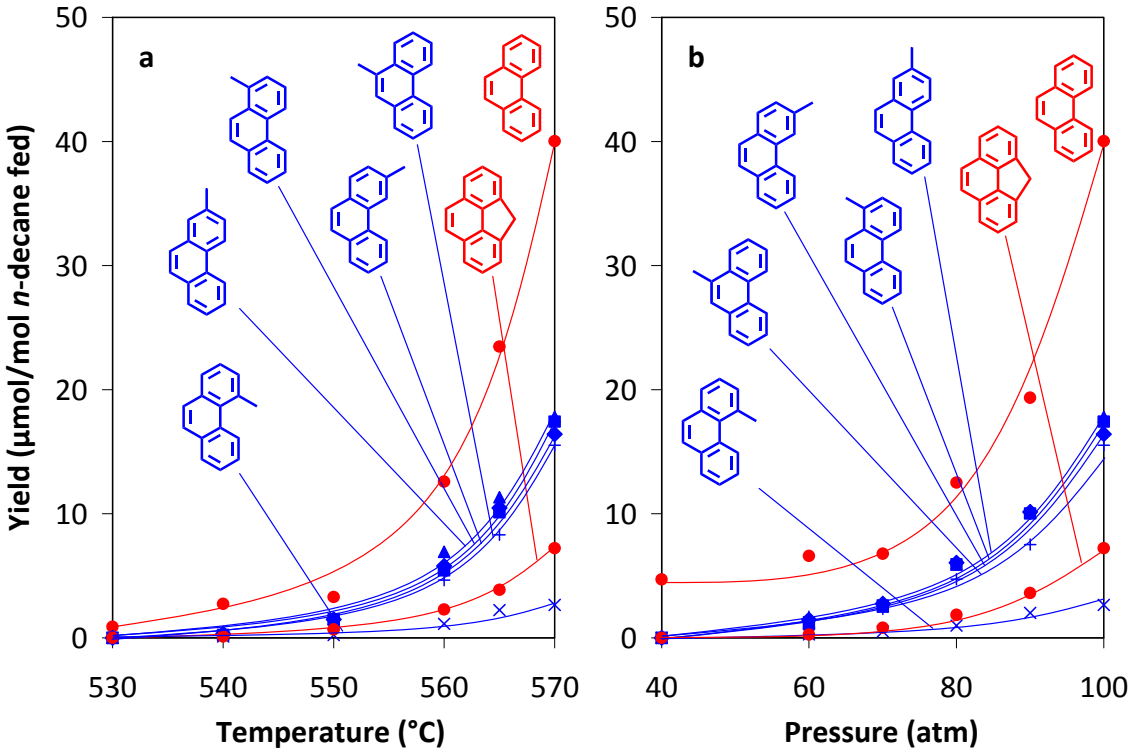

Figure 4.9 Yields of phenanthrene, cyclopenta[*def*]phenanthrene, and the five isomers of methylphenanthrene from the supercritical pyrolysis of *n*-decane: (a) yields versus temperature, at 100 atm and 140 sec; (b) yields versus pressure, at 570 °C and 140 sec.

Like fluorene, the reaction mechanism responsible for phenanthrene formation has already been elucidated in experimental work on the gas-phase pyrolysis of toluene [66] and the supercritical pyrolysis of toluene [30]. First, as shown below in Scheme 4.15, two benzyl radicals (which are the result of hydrogen loss from the product toluene) combine to form the stable intermediate diphenylethane. Hydrogen loss by one of the phenyl groups, at a position ortho to the alkyl group, forms a radical which then attacks the other phenyl group, forming a new six-membered ring. Dehydrogenation gives the final three-ring PAH product phenanthrene.

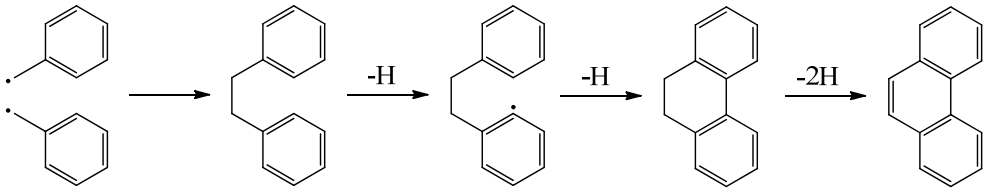

4.15

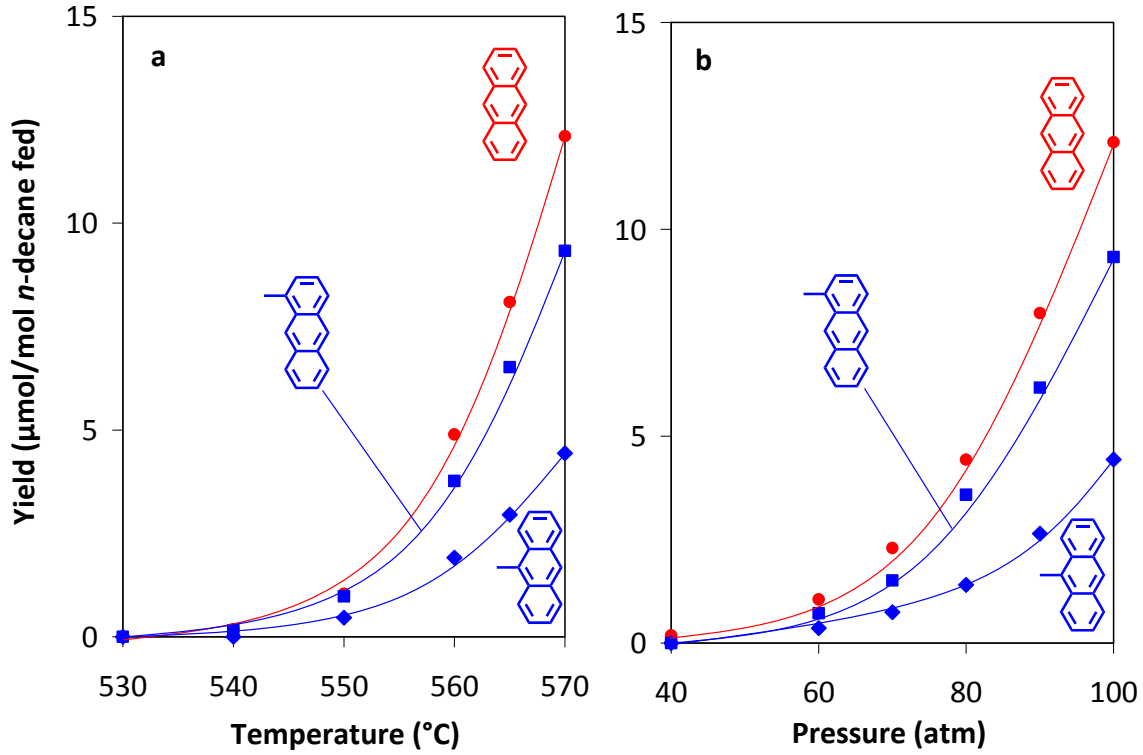

Figure 4.10 Yields of anthracene, 1-methylanthracene, and 9-methylanthracene from the supercritical pyrolysis of *n*-decane: (a) yields versus temperature, at 100 atm and 140 sec; (b) yields versus pressure, at 570 °C and 140 sec.

Scheme 4.16 depicts another possible route to the first intermediate in Scheme 4.15, diphenylethane: radical attack on benzene by a phenylethyl radical. This attack is very similar to alkyl radical addition shown in Schemes 4.8 and 4.9. Once the intermediate diphenylethane is formed, phenanthrene formation would proceed as shown in Scheme 4.15.

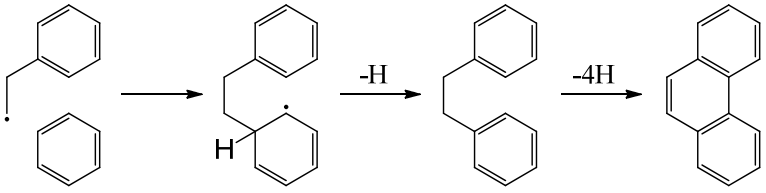

4.16

The phenylethyl radical should exist in the reaction environment; it would be formed by breaking the carbon-carbon bond of alkylbenzenes, products known to result from supercritical *n*-decane pyrolysis. This mechanism was not identified as part of toluene pyrolysis [30] because toluene is

much less likely than an alkane fuel to form benzenes with alkyl substituents composed of two or more carbons, necessary precursors to the phenylethyl radical.

As with the formation process of naphthalene from benzene (C_4 addition), there are more than one possible routes starting with a single-ring precursor (either benzene or toluene), adding two aromatic rings, and ending with the product phenanthrene. Both of these phenanthrene production pathways, Schemes 4.15 and 4.16, share similar features and will be grouped together as a single type of mechanism. This mechanism will be referred to as "naphtho *a* addition" in this work, denoting the addition of two more aromatic rings (a naphtho substituent) to an aromatic molecule, which, in the case of phenanthrene production, is benzene or toluene. The infix "*a*" refers to the orientation of these two added rings with respect to the aromatic molecule to which they are added. Such an addition can be generalized to account for a number of the observed products of supercritical *n*-decane pyrolysis, and it will be demonstrated in the following sections that naphtho *a* addition occurs to a number of aromatic molecules to yield higher-ring-number PAH.

Formation of anthracene has also been determined previously in the supercritical pyrolysis of toluene [27]. The initial step, benzyl radical attack on an aromatic ring, is the same as the initial step in fluorene production in Schemes 4.13 and 4.14. Illustrated in Scheme 4.17, if this attack takes place on toluene or some other alkylated benzene, at a position ortho to the alkyl group, that alkyl group will be in position to form a six-membered ring instead of the five-membered ring of fluorene. The intermediate formed from the radical attack is an alkylated diphenylmethane. The alkyl group of this intermediate then loses hydrogen or an alkyl group, forming a benzyl-like radical. This radical attacks the other aromatic ring, forming a new six-membered ring. Dehydrogenation yields the final three-ring PAH product anthracene.

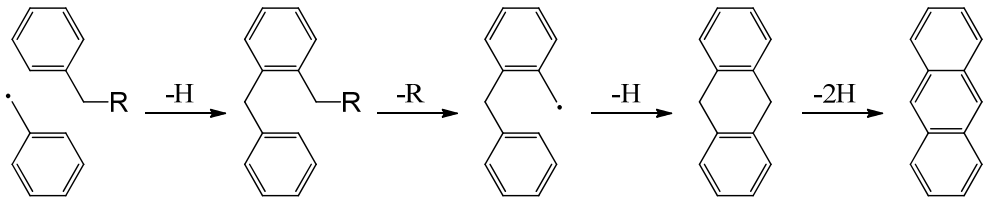

4.17

Alternatively, the alkyl substituent group could be at an aryl position of the attacking benzyl radical that is ortho to the methyl radical. Once this alkylated benzyl radical attacks benzene, the reaction is exactly the same as the one detailed in Scheme 4.17:

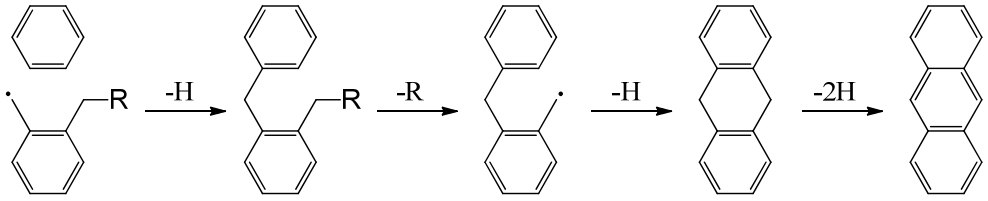

4.18

Yields of anthracene are approximately one order of magnitude lower than those of fluorene, despite the first step in their formation, benzyl radical attack on a benzene ring, being the same for both compounds. This difference in yields is almost certainly due to the necessity of an alkyl group to be located at a very specific position for formation of anthracene to occur. Additions of two rings to an aromatic molecule, forming three-ring anthracene-like structures by the mechanisms described above also occur to higher-ring-number PAH and will be referred to as "naphtho *b* addition" in this work. For example, anthracene is the result of naphtho *b* addition to benzene. The adduct benzene may or may not have alkyl substituents which participate in the reaction. How this mechanism is related to the formation of larger PAH will be explained in greater detail in later sections.

C_4 addition to naphthalene is also a possible reaction mechanism leading to the formation of both anthracene and phenanthrene. Experimental evidence does not indicate which mechanism, C_4 addition or the combination of two single-ring aromatic molecules, is the dominant one.

Figure 4.9 reveals that, with the exception of 4-methylphenanthrene, at a given pyrolysis condition all isomers of methylphenanthrene are produced at approximately the same yield. As shown in Scheme 4.19, loss of hydrogen from the methyl group of 4-methylphenanthrene would produce a phenanthrylmethyl radical. This methyl radical is in position to attack the carbon on the opposite side of the bay region (in the 5 position of phenanthrene) to form a five-membered ring. Hydrogen loss completes the conversion to the final product cyclopenta[*def*]phenanthrene.

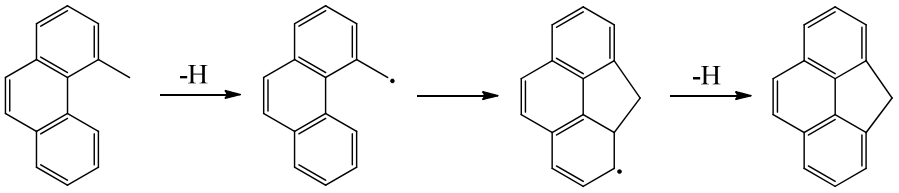

4.19

By analogy to toluene and 1-methylnaphthalene, the methyl carbon-hydrogen bond of methylphenanthrene is the weakest [52], so hydrogen loss from the methyl group should occur readily. 4-Methylphenanthrene is likely depleted from the final *n*-decane pyrolysis products by the formation of cyclopenta[*def*]phenanthrene, explaining the lower yield of this product, compared to those of the other isomers of methylphenanthrene, in Figure 4.9.

4.4.4 Pyrene

Pyrene and the three isomers of methylpyrene are identified as products of supercritical *n*-decane pyrolysis; yields of these 4-ring PAH products are presented in Figure 4.11. In addition to the products which are quantified, 22 alkylpyrenes for which the aromatic structures are known, but not the positions or identities of the alkyl substituents, are also identified.

In Scheme 4.20, shown below, alkyl radical addition to the bay region of phenanthrene produces pyrene. This scheme was proposed by Song [26] to account for pyrene production from the supercritical pyrolysis of a predominately aliphatic jet fuel. First, an alkyl radical attacks a carbon in the bay region. Then the alkyl group breaks at the second and third carbons to yield a

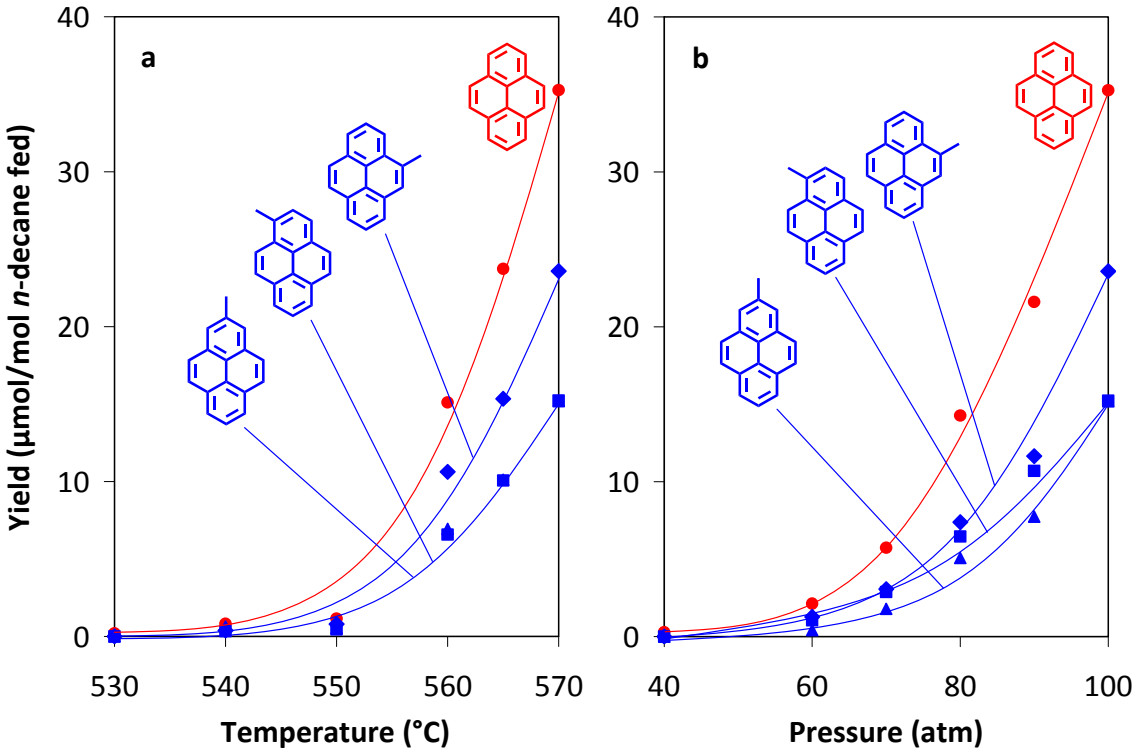

Figure 4.11 Yields of pyrene, 1-methylpyrene, 2-methylpyrene, and 4-methylpyrene from the supercritical pyrolysis of *n*-decane: (a) yields versus temperature, at 100 atm and 140 sec; (b) yields versus pressure, at 570 °C and 140 sec.

phenanthrylethyl radical. This radical attacks the carbon on the opposite side of the bay region to lose the six-membered ring. Dehydrogenation yields the final product pyrene.

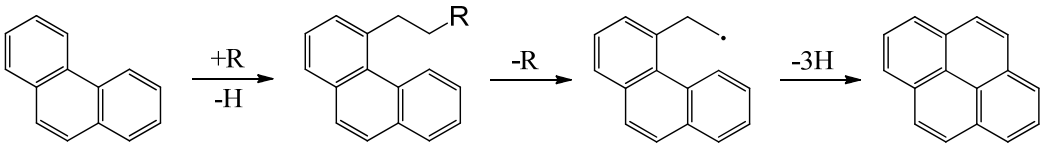

4.20

However, if we assume bond dissociation energies similar to an alkylbenzene, the weakest and therefore most likely bond to break is the bond between the first and second carbons in the alkyl substituent [52,68-70] and not the bond between the second and third carbons, as depicted in the second step in Scheme 4.20. It is certainly possible to break the bond between the second and third carbons; for example ethylbenzene is a product of supercritical *n*-butylbenzene pyrolysis [65]. However, yields of ethylbenzene from *n*-butylbenzene pyrolysis are an order of magnitude

lower than yields of toluene, indicating that carbon-carbon bond cleavage between the second and third carbons is much less favored, compared to cleavage between the first and second.

There is another route to pyrene, shown in Scheme 4.21, which does not require the formation of the phenanthrylethyl radical (the second step in Scheme 4.20); it involves a phenanthryl radical attack on the double bond of an alkene. First, phenanthrene loses hydrogen from one of the carbons in the bay region (not shown). The resulting radical attacks an alkene at one of the carbons in the double bond, shifting the radical to the alkene. Because of this shift, the alkene becomes an alkyl radical. This radical is in position to attack the carbon on the opposite side of the bay region, forming a new six-membered ring. Dehydrogenation yields the final product pyrene.

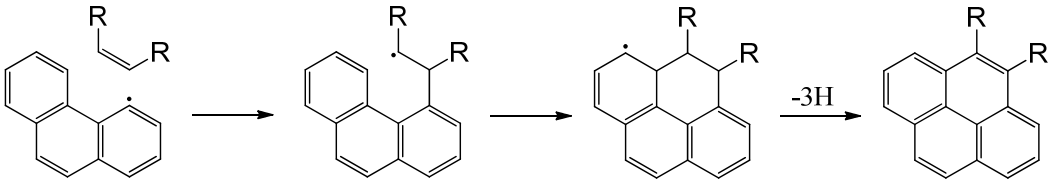

4.21

In the above example, "R" represents either hydrogen or an alkyl group (a convention which will be followed throughout the rest of this chapter). Therefore the final product of this reaction could be an alkylated pyrene or an unsubstituted pyrene, and another pathway is revealed for the formation of alkylated PAH through processes other than alkyl-radical attack followed by hydrogen loss (Schemes 4.8 and 4.9). Also, the mechanism of Scheme 4.21 is deliberately vague as to which carbon of a 1-alkene is involved in the initial radical attack, as no information exists to suggest which of the two carbons would be most susceptible to such an attack.

The mechanism by which a new aromatic ring forms in the bay region of a PAH, as in the conversion of phenanthrene to pyrene, will be referred to as "C_2 bay region addition" in this work. It is unclear if the reaction proceeds through an alkyl radical attack on phenanthrene (Scheme 4.20) or a phenanthryl radical attack on an alkene (Scheme 4.21), but it is clear that

some kind of addition to the bay region of phenanthrene is responsible for the product pyrene. As will be shown in following sections, C_2 bay region addition is an important reaction accounting for a large number of PAH products from supercritical *n*-decane pyrolysis.

In addition to mechanisms requiring the three-ring PAH phenanthrene as an intermediate (Schemes 4.20 and 4.21), reactions involving single-ring compounds are attractive alternatives as mechanisms for the formation of the four-ring PAH pyrene. The yields of alkylbenzenes (Figure 4.5) are very high relative to those of phenanthrene (Figure 4.9), and, as demonstrated in Scheme 4.22, several alkylbenzenes have carbons in positions that would appear to readily form the product pyrene:

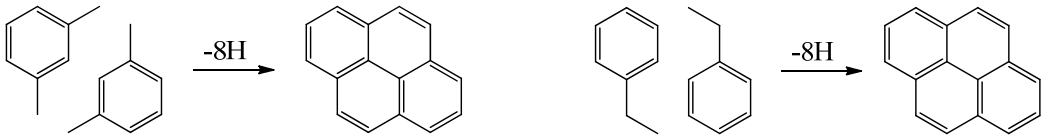

4.22

However, this scheme shows three new carbon-carbon bonds forming between the two precursors and implies that the bonds form simultaneously, with the carbons of both reactants lying in the same plane. In fact the bonds must form sequentially, and the three dimensional orientation of the intermediates must be taken into account. To determine the feasibility of pyrene formation from alkylbenzenes it is necessary to first examine the possible ways in which an initial carbon-carbon bond can form between two single-ring aromatic molecules, then establish how additional bonds could subsequently form.

Formation of an initial bond between two of the aryl carbons can be ruled out simply on the basis that biphenyl is not found as a product of supercritical *n*-decane pyrolysis. There is no reason to believe alkylbenzenes would be any more likely to participate in a reaction of this type than benzene. On the other hand, formation of an ethyl group joining two phenyl groups has been shown to be possible as part of phenanthrene production, either by combination of two benzyl

radicals or by attack of a phenylethyl radical on a single-ring aromatic molecule. These reactions are depicted in Scheme 4.22 for reactants which also have additional alkyl substituents:

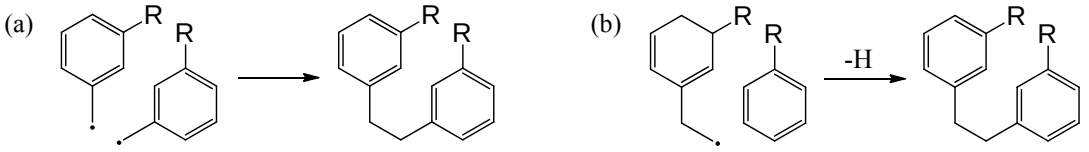

4.22

In order to produce pyrene from these alkylated diphenylethanes, the next carbon-carbon bond would have to form at one of two positions, between either the two phenyl groups or at the alkyl group(s). While formation of another ethyl group between the two phenyl groups would simply be a repetition of the reactions described in Scheme 4.22, steric hindrance by the aryl hydrogens of the phenyl groups would most likely prevent this reaction from occurring:

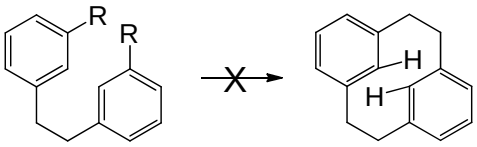

4.23

However, a carbon-carbon bond could be formed between two of the aryl carbons. Shown in Scheme 4.24, loss of hydrogen by one of the aromatic groups to form an aryl radical, followed by attack by this aryl radical on the opposite aromatic group, leads to a bond between the two phenyl groups. Loss of hydrogen yields a fully aromatic molecule.

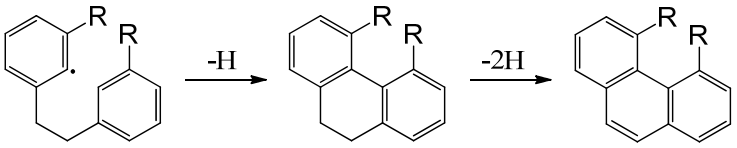

4.24

If both alkyl groups in the bay region are methyl radicals, it is unclear if formation of a ring in the bay region is possible. Loss of hydrogen by one of these methyl groups to form a radical would not lead to ring closure, since the carbon in the adjacent methyl group is shielded from attack by its hydrogens. Hydrogen loss by both methyl groups could lead to carbon-carbon bond formation between these two groups, but two radical sites on a single molecule are unlikely. On

the other hand, if one of the groups is an alkyl substituent with two or more carbons, the reaction could proceed to form pyrene by formation of an ethyl radical, attack by this ethyl radical on the aryl carbon on the opposite side of the bay region, and finally by dehydrogenation and possibly loss of an alkyl substituent:

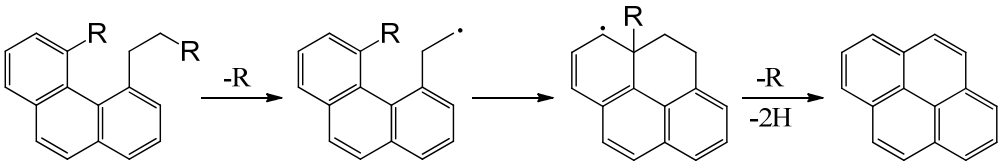

4.25

Essentially what is shown above in Schemes 4.22 (production of alkylated diphenylethane), 4.24 (production of alkylated phenanthrene), and 4.25 (production of pyrene) is the same as phenanthrene formation followed by C_2 bay region addition, with the individual reaction steps ordered differently. Instead of an alkyl group displacing hydrogen in the bay region after phenanthrene is formed, an alkyl group displaces the hydrogen on a single-ring aromatic molecule which then goes on to form phenanthrene. The alkyl group must be in a very specific position for pyrene to be formed by the mechanism outlined in Schemes 4.22, 4.24, and 4.25, and the alkyl group of an alkylated phenanthrene is much more likely to break between the first and second carbons to form a benzyl-like radical than between the second and third carbons to give a phenanthrylethyl radical [52,68-70]. Therefore the mechanism (if it can be considered a distinct mechanism) described in Schemes 4.22, 4.23, and 4.25 likely plays only a small role in the production of pyrene, compared to phenanthrene formation followed by C_2 bay region addition, as illustrated in Schemes 4.20 and 4.21.

By the same reasoning applied to C_4 addition in Section 4.4.2, some idea of the facility with which C_2 bay region addition takes place can be determined. At the highest stressing experimental conditions, 570 °C and 100 atm, the summed molar yield of pyrene and the three methylpyrenes of Figure 4.11 is 89 μmoles per mole *n*-decane fed, and that of phenanthrene and

the five methylphenanthrenes of Figure 4.9 is 109 μmoles per mole *n*-decane fed. Over the range of experimental conditions, the ratio of phenanthrene to pyrene varies between approximately one and two. Put another way, approximately one half to one third of the phenanthrene molecules produced are converted into pyrene. By comparison, the ratio of the summed yield of benzene and toluene of Figure 4.5 to that of naphthalene and the two methylnaphthalenes of Figure 4.6 varies approximately from 15 to as high as 250. Therefore C_2 bay region addition is much more likely than C_4 addition to play a significant role in PAH product formation.

4.4.5 Cyclopenta-Fused PAH

Three cyclopenta-fused PAH are identified as products of *n*-decane pyrolysis: acenaphthylene, acephenanthrylene, and cyclopenta[*cd*]pyrene, along with a methylacenaphthylene (the position of the methyl group is not known). Figure 4.12 presents the yields of acenaphthylene and methylacenaphthylene; Figure 4.13 presents the yields of acephenanthrylene and cyclopenta[*cd*]pyrene.

A reaction scheme for the formation of the three cyclopenta-fused PAH, similar to the one for C_2 bay region addition in Section 4.4.5, is supported by the abundance of the products naphthalene, phenanthrene, and pyrene, which are the likely precursor molecules to the three cyclopenta-fused products. Shown in Scheme 4.26, using the example of naphthalene conversion to acenaphthylene, formation of the cyclopenta ring could proceed through alkyl radical addition to naphthalene. Once the alkylnaphthalene forms, cleavage of the carbon-carbon bond in the alkyl group between the second and third carbons yields an ethyl radical which attacks a nearby aryl carbon, forming a five-membered ring and the product acenaphthene (observed but not quantified in the supercritical *n*-decane pyrolysis products). Dehydrogenation of acenaphthene yields the final product acenaphthylene. R represents either hydrogen or an alkyl group in the scheme.

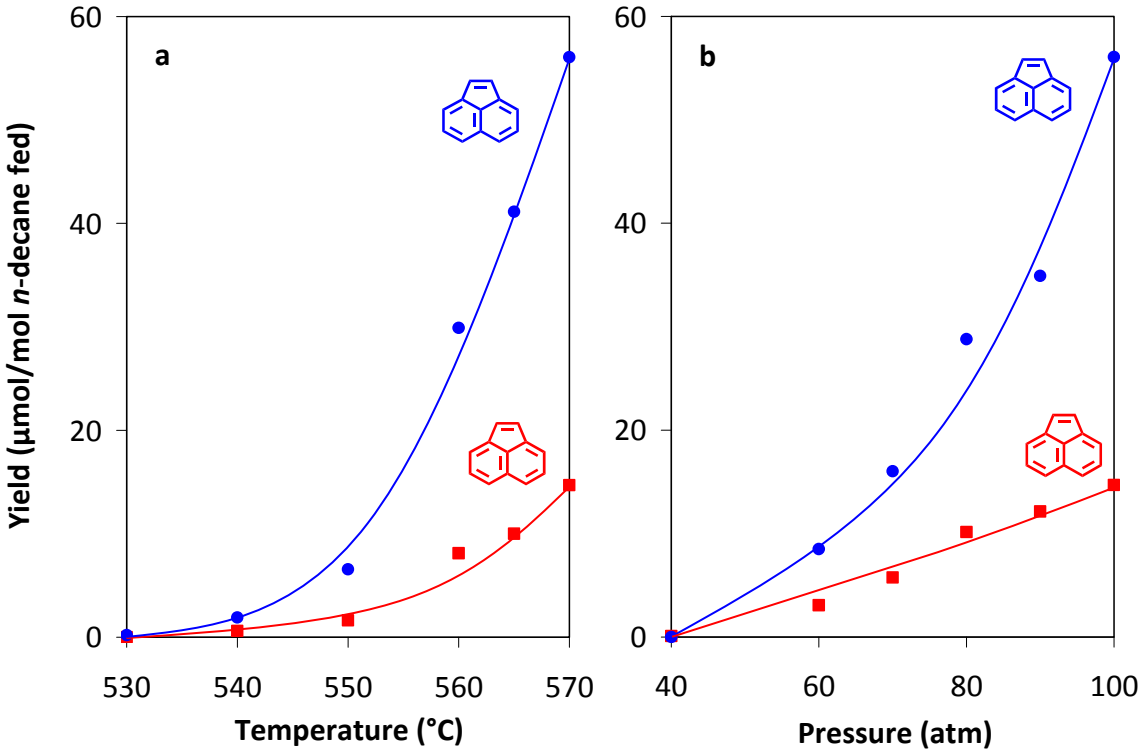

Figure 4.12 Yields of acenaphthylene (red) and methylacenaphthylene (blue) from the supercritical pyrolysis of *n*-decane: (a) yields versus temperature, at 100 atm and 140 sec; (b) yields versus pressure, at 570 °C and 140 sec.

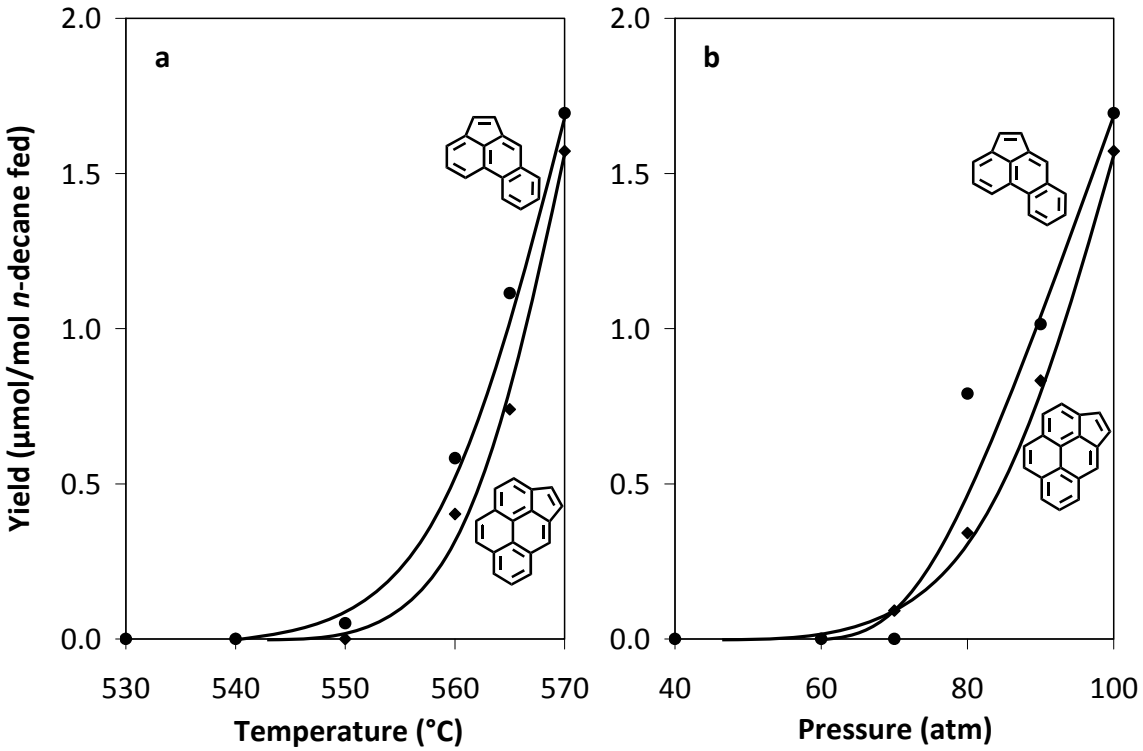

Figure 4.13 Yields of the four-ring PAH acephenanthrylene and the five-ring PAH cyclopenta[*cd*]pyrene from the supercritical pyrolysis of *n*-decane: (a) yields versus temperature, at 100 atm and 140 sec; (b) yields versus pressure, at 570 °C and 140 sec.

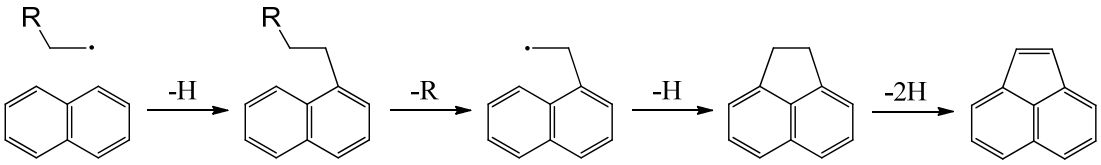

4.26

Formation of the other two cyclopenta-fused PAH products, the four-ring PAH acephenanthrylene and five-ring PAH cyclopenta[*cd*]pyrene, would proceed by the same sequence as in Scheme 4.26, except the initial radical addition would occur to phenanthrene and pyrene, respectively.

Alternatively, addition of a cyclopenta ring could proceed through an aryl radical attack on an alkene, illustrated in Scheme 4.27 with the example of naphthalene conversion to acenaphthylene. Once the aryl radical attacks the alkene, the radical shifts to a position allowing it to attack the aromatic molecule, forming a five-membered ring. Dehydrogenation (and possibly loss of an alkyl group) yields the final product, acenaphthylene.

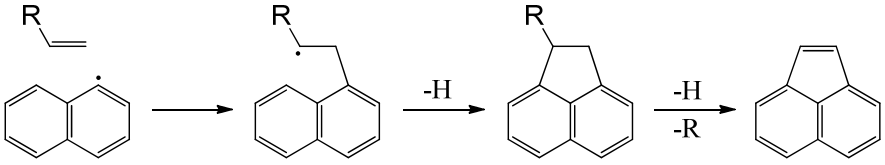

4.27

Again, R represents either hydrogen or an alkyl group in the scheme, and attack by the aryl radical could take place on either carbon of the double bond of the alkene. The presence of acenaphthene in the *n*-decane pyrolysis products is a sign of the intermediate step after ring closure but before dehydrogenation in both reaction schemes.

A comparison of the yields of the precursors to those of their products—for both the cyclopenta ring addition schemes, 4.26 and 4.27, and the C_2 bay region addition schemes, 4.20 and 4.21—indicates that cyclopenta ring formation is significantly less favorable than C_2 bay region addition, even though there are similarities between the two sets of mechanisms. Yield ratios of precursors of cyclopenta-fused PAH to the cyclopenta-fused products are much higher

than the ratio of phenanthrene (the precursor of a product of C_2 bay region addition) to pyrene (the product). For example, at the highest stressing experimental condition (570 °C, 100 atm), the ratio of yields of naphthalene to acenaphthylene is approximately 60 (Figures 4.6 and 4.12), phenanthrene to acephenanthrylene is approximately 24 (Figures 4.9 and 4.13), and pyrene to cyclopenta[*cd*]pyrene is approximately 23 (Figures 4.11 and 4.13). At these experimental conditions, the ratio of the yield of phenanthrene to the yield of pyrene, formed by C_2 bay region addition, is approximately one. Comparisons of ratios at all experimental conditions show similar disparity and lead to the conclusion than addition of two carbons to a bay region is much more likely than addition of two carbons to form a cyclopenta fused ring.

The lower likelihood of cyclopenta ring addition relative to C_2 bay region addition is not surprising given some important differences between the two mechanisms. First, a five-membered ring introduces ring strain into a molecule by including bond angles that deviate from 120°, while a six-membered ring resulting from C_2 bay region addition has no ring strain. Also, during the ring closure step to form a five-membered ring (either Scheme 4.26 or 4.27), when the alkyl radical attacks one of the aromatic carbons, the radical is separated from the aromatic carbon by a greater distance than during ring closure in a bay region to form a six-membered ring. This difference is illustrated in Scheme 4.28 with a comparison of the distance separating a radical from an aromatic carbon during the ring closure step in cyclopenta ring formation and C_2 bay region addition. The structures of (a) a 9-phenanthrylethyl radical, an intermediate in the formation of acephenanthrylene from phenanthrene, and (b) a 4-phenanthryethly radical, an intermediate in the formation of pyrene from phenanthrene, are shown.

(a) 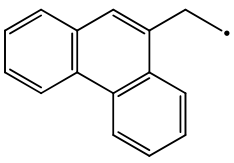 (b) 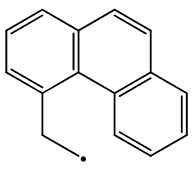

4.28

4.4.6 Fluoranthene

Fluoranthene, four methylfluoranthenes, and one alkylfluoranthene are identified as products of supercritical *n*-decane pyrolysis. The position of the methyl substituent on each of the four identified methylfluoranthenes is not known, and neither the position(s) nor identity(s) of the alkyl substituent(s) of the alkylfluoranthene are known. Figure 4.14a presents yields of fluoranthene and three of the isomers of methylfluoranthene from the set of pyrolysis experiments in which temperature was varied from 530 to 570 °C while pressure and residence time were held constant at 100 atm and 140 sec. Figure 4.14b presents yields of fluoranthene and four of the isomers of methylfluoranthene from the set of pyrolysis experiments in which pressure was varied from 40 to 100 atm while temperature and residence time were held constant at 570 °C and 140 sec. For an explanation of why four methylfluoranthenes are reported in one set of experiments and three are reported in another, see Appendix A.

The reaction mechanism leading to fluoranthene formation is analogous to the mechanism that has been shown by Somers to be responsible for benzo[*k*]fluoranthene and benzo[*j*]fluoranthene production in supercritical 1-methylnaphthalene pyrolysis [22]. The reaction mechanism producing those two benzofluoranthenes is readily adapted to explain fluoranthene production; the adapted version is shown in Schemes 4.29 and 4.30. First naphthalene loses hydrogen to form a naphthyl radical. Then the naphthyl radical attacks benzene, and loss of hydrogen yields the intermediate product 1-phenylnaphthalene. (Phenyl radical attack on naphthalene is an alternative pathway which would yield the same intermediate.)

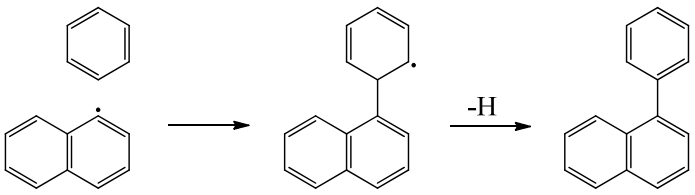

4.29

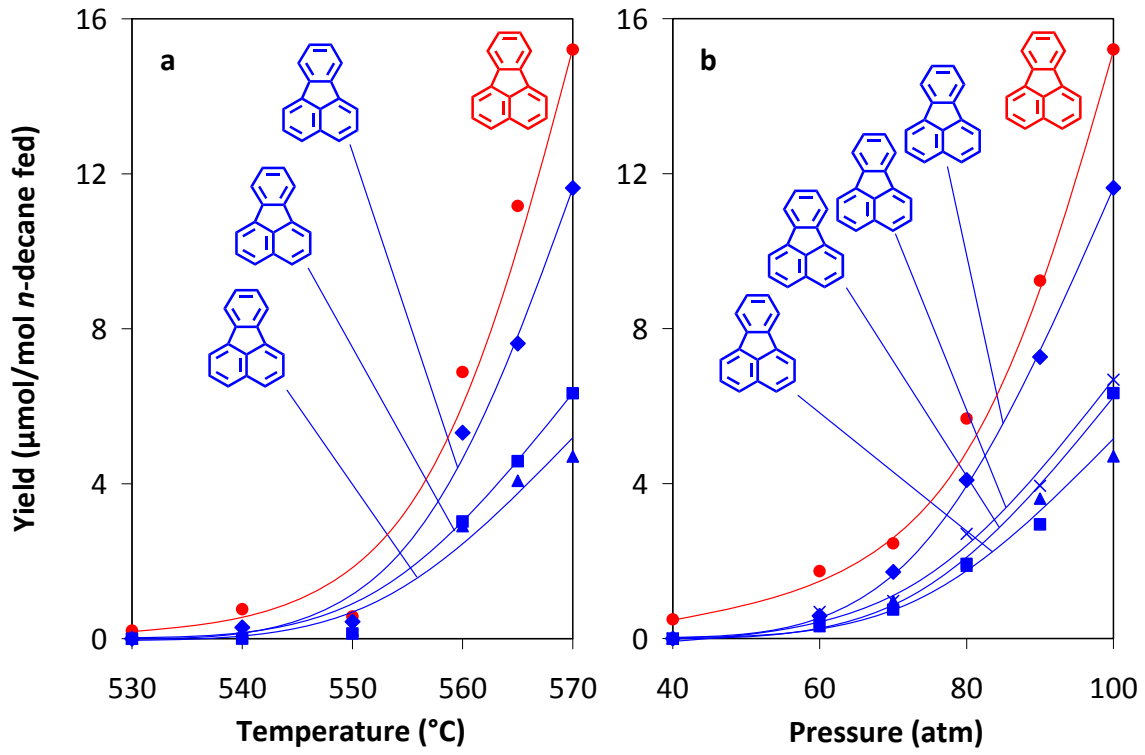

Figure 4.14 (a) Yields of fluoranthene (red) and three methylfluoranthenes (blue) from the supercritical pyrolysis of *n*-decane versus temperature, at 100 atm and 140 sec; and (b) yields of fluoranthene and four methylfluoranthenes from the supercritical pyrolysis of *n*-decane versus pressure, at 570 °C and 140 sec.

Phenyl-substituted naphthalenes have been identified as products of supercritical pyrolysis of jet fuels [26,61], and binaphthyls, the result of naphthyl radical attack on naphthalene, have been identified as products of supercritical 1-methylnaphthalene pyrolysis [31]. Neither phenyl- nor naphthyl-substituted PAH have been identified among the products of *n*-decane pyrolysis in this work, but failure to identify these products may be due to limitations in the analytical methods. Phenyl- and naphthyl-substituted PAH have not been specifically ruled out as products either. Biphenyl has been specifically ruled out as a product, however, so it follows that the phenyl radical intermediate is much less likely than the naphthyl radical to participate in the initial step of Scheme 4.29.

Illustrated in Scheme 4.30, following formation of the intermediate 1-phenylnaphthalene, loss of hydrogen by either the phenyl or naphthyl group yields a radical which attacks the other aromatic group. Hydrogen loss must occur in one of two specific positions in order to attack the other aromatic group: the 8 position of the naphthyl group or the 2 position of the phenyl group (this example uses loss of hydrogen by the naphthyl group). Following ring closure, dehydrogenation leads to the final product fluoranthene.

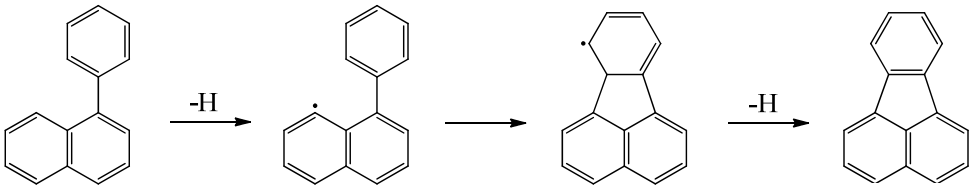

fluoranthene

4.30

This reaction mechanism (Schemes 4.29 and 4.30), in which an aryl radical attacks an aromatic molecule, followed by ring closure to yield a fully aromatic molecule as the final product, will be referred to as "aromatic-aromatic addition" in this work. For simplicity, the reactants that participate in any aromatic-aromatic addition will not be referred to as radicals, but instead the aromatic molecules which are the precursors to these radicals. For example, the reactants which produce fluoranthene by aromatic-aromatic addition will be referred to as benzene and naphthalene rather than naphthyl radical and benzene or phenyl radical and naphthalene. It should be implicitly understood that either of the reactants can lose hydrogen and attack the other.

4.4.7 Triphenylene, Chrysene, and Benz[*a*]anthracene

Triphenylene, chrysene, and benz[*a*]anthracene are identified as four-ring $C_{18}H_{12}$ PAH products of supercritical *n*-decane pyrolysis. Ten alkylated derivatives of chrysene, four of benz[*a*]anthracene, and one of triphenylene for which the aromatic structures are known, but not the positions or identities of the alkyl substituents, are also identified. Figure 4.15 presents the

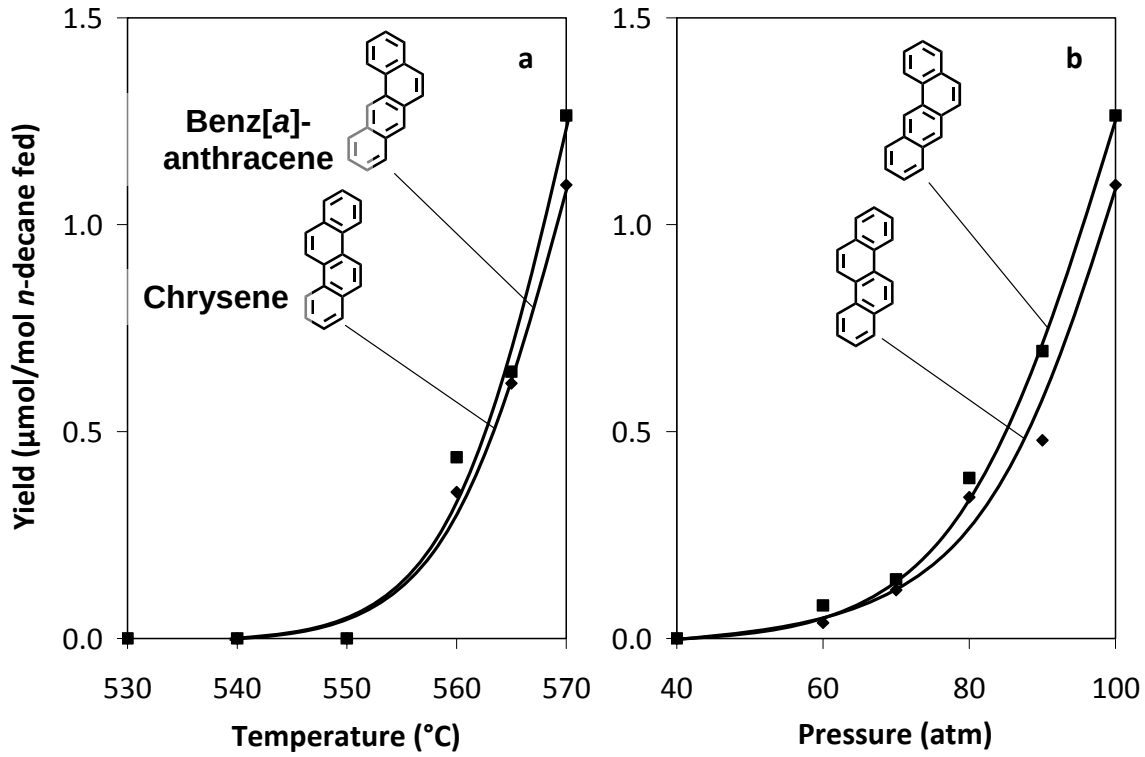

Figure 4.15 Yields of chrysene and benz[*a*]anthracene from the supercritical pyrolysis of *n*-decane: (a) yields versus temperature, at 100 atm and 140 sec; (b) yields versus pressure, at 570 °C and 140 sec.

yields of two of the $C_{18}H_{12}$ products, chrysene and benz[*a*]anthracene, from the supercritical pyrolysis experiments.

All three of the $C_{18}H_{12}$ products could be the result of C_4 addition to the $C_{14}H_{10}$ PAH phenanthrene and, in the case of benz[*a*]anthracene, C_4 addition to the $C_{14}H_{10}$ anthracene. However, if the assumption is made that C_4 addition happens at the same rate to every available position of phenanthrene and anthracene, the relative yields of these products and precursors indicate that C_4 addition is not the primary mechanism for production of chrysene or benz[*a*]anthracene. With this assumption, chrysene should be produced in yields twice as high as triphenylene, because phenanthrene has two positions to which C_4 addition would add an additional ring (the *a* and *i* positions) to yield chrysene and only one (the *l* position) for which C_4

addition would yield triphenylene. Triphenylene could not be quantified due to poor chromatographic resolution, but an estimation of its yield, determined by comparison of its peak height to that of chrysene from a chromatogram of the products of the highest stressing experimental condition (570 °C, 100 atm, Figure 3.21), reveals that its yield is approximately ten times lower than the yield of chrysene. So while the expectation is that chrysene yields should be higher than triphenylene yields, the chrysene yields are too high to be entirely the result of C_4 addition and must be accounted for by some other mechanism.

To explain the higher yields of chrysene relative to triphenylene, naphtho *a* addition to naphthalene (which may or may not be alkylated) is proposed. Illustrated in Scheme 4.31, the intermediate phenylnaphthylethane is formed first by one of several possibilities: combination of a benzyl radical and a naphthylmethyl radical, attack by a phenylethyl radical on naphthalene, or attack by a naphthylethyl radical on benzene. A combination of all three reactions is likely, but Scheme 4.31 is shown with a methyl group on each aromatic for simplicity, a convention which will be followed throughout this work. In this example, in the first step the two methyl groups each lose hydrogen to form a benzyl and a naphthylmethyl radical, then combine to produce phenylnaphthylethane. Formation of phenylnaphthylethane is followed by radical formation, radical attack, ring closure, and dehydrogenation to yield the final product chrysene.

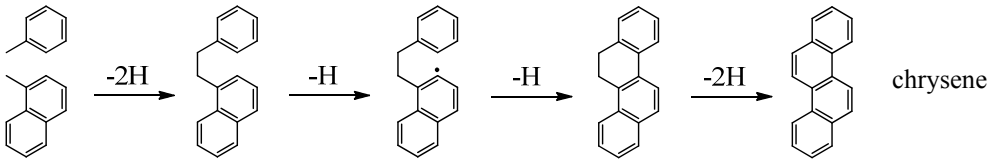

4.31

The same mechanism with the same aromatic units and alkyl substituents in different positions would be responsible for benz[*a*]anthracene formation (Scheme 4.32). This is naphtho *a* addition to a different position of naphthalene.

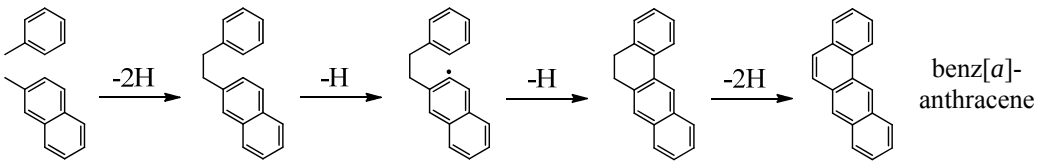

4.32

In addition, naphtho *b* addition, (Scheme 4.33) is also likely responsible in part for benz[*a*]anthracene formation. Note that, just as with anthracene production, the alkyl groups could be on either or both of the aromatic precursors; their positions in the scheme below are only one example of several.

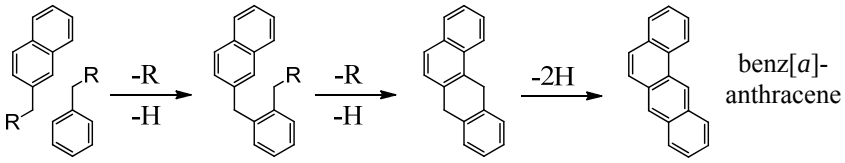

4.33

Triphenylene can only be arrived at by C_4 addition to phenanthrene, hence its low yield relative to those of chrysene and benz[*a*]anthracene.

4.4.8 Benzofluoranthenes and Perylene

Benzo[*b*]fluoranthene, benzo[*j*]fluoranthene, and benzo[*k*]fluoranthene are identified as five-ring $C_{20}H_{12}$ PAH products of supercritical *n*-decane pyrolysis; yields of these products from the supercritical pyrolysis experiments are presented in Figure 4.16. In addition to the $C_{20}H_{12}$ products that are quantified, perylene and two alkylated benzo[*k*]fluoranthenes for which the aromatic structures are known, but not the positions or identities of the alkyl substituents, are also identified. The unsubstituted PAH perylene is not quantified because of its low yield relative to the other products in its fraction and co-elution with benzo[*b*]fluoranthene.

All of these five-ring products are most likely the result of aromatic-aromatic addition of two naphthalene molecules or, in the case of benzo[*b*]fluoranthene, aromatic-aromatic addition of a benzene and a phenanthrene molecule. Illustrated in Scheme 4.34 is the addition of two naphthalene molecules to yield one of these five-ring PAH products, benzo[*j*]fluoranthene:

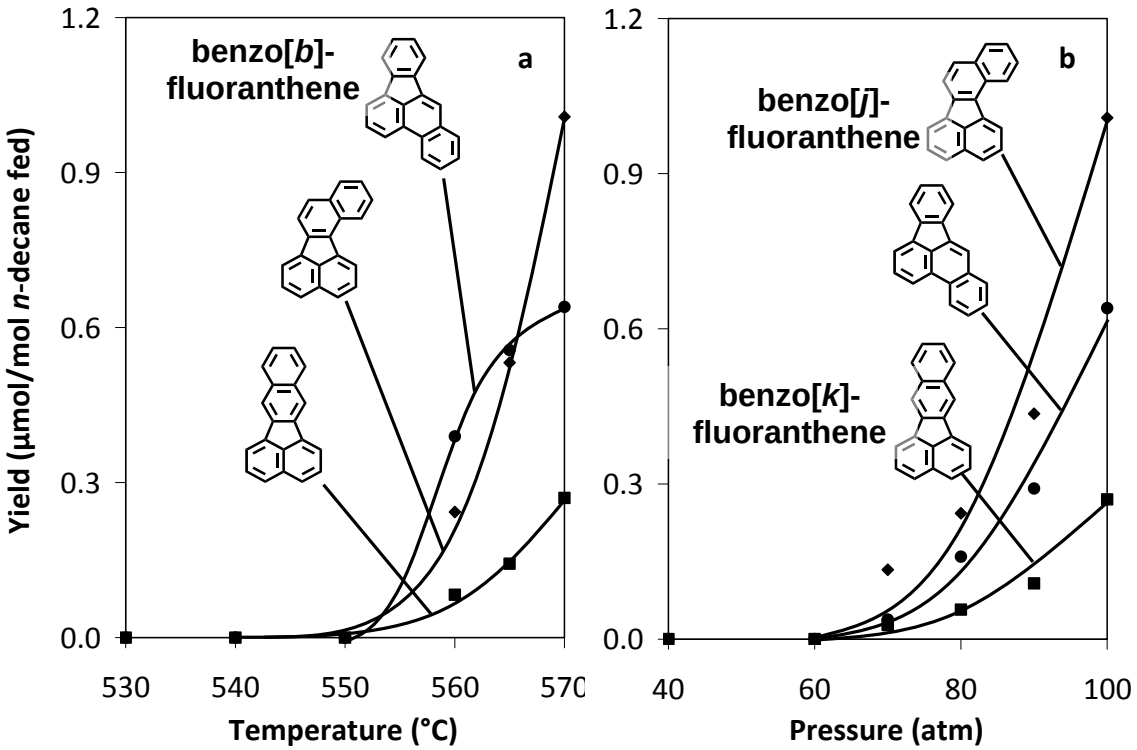

Figure 4.16 Yields of benzo[*b*]fluoranthene, benzo[*j*]fluoranthene and benzo[*k*]fluoranthene from the supercritical pyrolysis of *n*-decane: (a) yields versus temperature, at 100 atm and 140 sec; (b) yields versus pressure, at 570 °C and 140 sec.

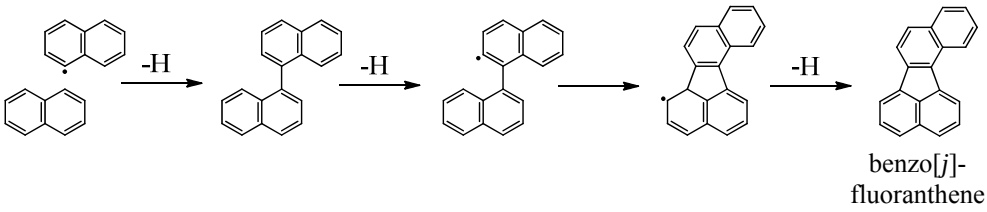

4.34

While the benzofluoranthenes have a five-membered ring incorporated into their aromatic structures, the presence of perylene among the $C_{20}H_{12}$ PAH products shows that aromatic-aromatic additions also result in PAH composed entirely of six-membered rings. The formation of perylene, starting with the intermediate 1,1'-binaphthyl (for which the formation mechanism from two naphthalene units is obvious), is shown in Scheme 4.35. The reaction proceeds exactly like Scheme 4.34 for the formation of benzo[*j*]fluoranthene, only with hydrogen loss and the subsequent radical attack occurring from a different position during ring closure.

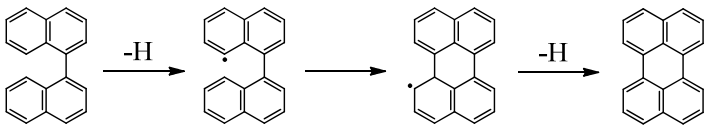

perylene

4.35

In addition to the aromatic-aromatic addition mechanisms, C_4 addition to the $C_{16}H_{10}$ PAH fluoranthene is another route to the $C_{20}H_{12}$ benzofluoranthenes. Evidence from the *n*-decane pyrolysis experiments does not indicate the relative importance of C_4 addition or aromatic-aromatic addition to benzofluoranthene production.

4.4.9 Benzo[*a*]pyrene and Benzo[e]pyrene

Benzo[*a*]pyrene and benzo[*e*]pyrene are identified as five-ring $C_{20}H_{12}$ products of supercritical *n*-decane pyrolysis; yields of these two $C_{20}H_{12}$ PAH are presented in Figure 4.17. In addition to the products which are quantified, 14 alkylated benzo[*a*]pyrenes and eight alkylated benzo[*e*]pyrenes for which the aromatic structures are known, but not the positions or identities of the alkyl substituents, are also identified.

Aromatic-aromatic addition of benzene and phenanthrene is the most likely mechanism responsible for the formation of benzo[*e*]pyrene. As shown in Scheme 4.36, this reaction is very similar to the formation of fluoranthene (Schemes 4.29 and 4.30), the three benzofluoranthenes (Scheme 4.34), and perylene (Scheme 4.35), but with the addition of the aromatic molecule occurring at a bay region.

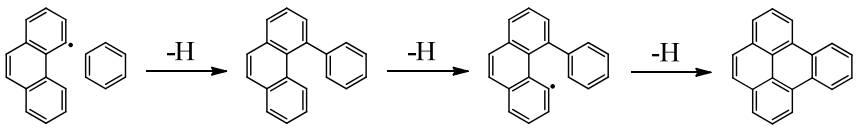

benzo[*e*]pyrene

4.36

The precursors, benzene, phenanthrene, or their alkylated derivatives, are abundant compared to the product, as shown in Figures 4.5, 4.9, and 4.17.

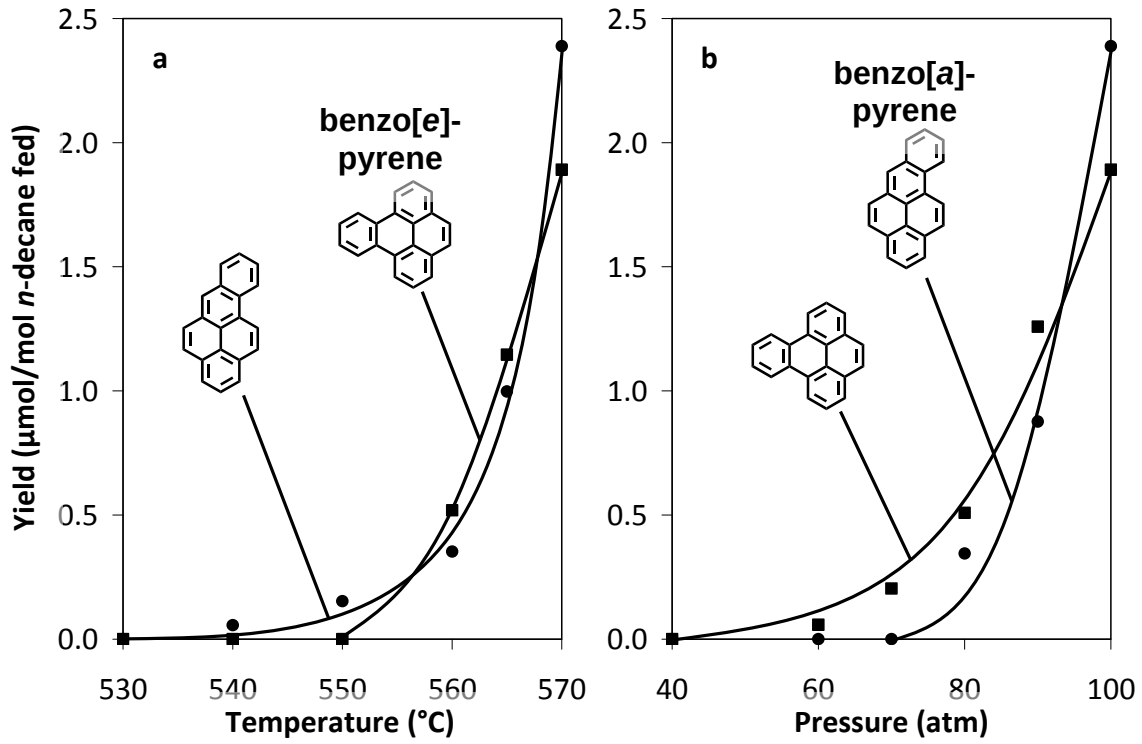

Figure 4.17 Yields of benzo[*a*]pyrene and benzo[*e*]pyrene from the supercritical pyrolysis of *n*-decane: (a) yields versus temperature, at 100 atm and 140 sec; (b) yields versus pressure, at 570 °C and 140 sec.

As with the formation mechanisms posited for pyrene in Section 4.4.5, it is also possible that formation mechanisms incorporating aromatic molecules with alkyl substituent groups composed of two or more carbons are additional routes to the formation of benzo[*e*]pyrene. Shown in Scheme 4.37, the possible reaction scheme starts with the joining of two alkylated aromatic molecules to form a phenyl- and naphthyl-substituted butane. There are a large number of reactions, either combination of two alkylated aryl radicals or attack on an aromatic molecule by an alkyl radical with an aryl substituent group, which lead to the intermediate phenylnaphthylbutane. After this intermediate is formed by one of many reactions pathways, the mechanism would proceed first by cyclization of the alkyl group, followed by dehydrogenation to produce a phenyl-substituted phenanthrene. Then loss of hydrogen by the phenyl group and

attack by that phenyl group on the newly formed phenanthryl group yields the final product, benzo[*e*]pyrene.

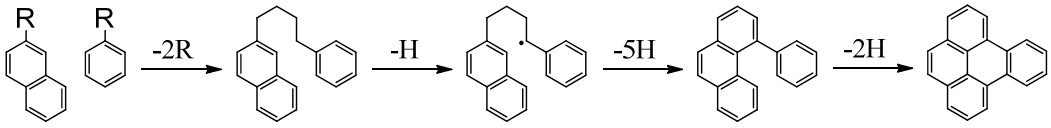

benzo[*e*]pyrene

4.37

The intermediate steps leading to benzo[*e*]pyrene of both aromatic-aromatic addition (Scheme 4.36) and the mechanism involving alkylated benzene and naphthalene (Scheme 4.37) are actually the same; they simply happen in a different order. The difference is a matter of when the phenyl group is added to the intermediate molecules. In aromatic-aromatic addition (Scheme 4.36) the phenyl addition takes place after phenanthrene is formed. In the combination of benzene and naphthalene (Scheme 4.37, in which one or both precursors have alkyl substituents), a phenyl group is added to an alkyl radical at some prior time, and is then brought along as phenanthrene is formed by C_4 addition.

C_2 bay region addition to the four-ring PAH triphenylene is another route to the formation of benzo[*e*]pyrene, but triphenylene is estimated to have yields very small in comparison to those of benzo[*e*]pyrene, and therefore insufficient for C_4 addition to triphenylene to be an important pathway to benzo[*e*]pyrene. Consumption by C_2 bay region addition could however be a significant factor in the final yield of the four-ring product triphenylene. C_4 addition to the four-ring PAH pyrene could also be responsible for benzo[*e*]pyrene, but for reasons explained below is probably not a significant contributor to the yield either.

Depicted in Scheme 4.38, C_2 bay region addition to (a) chrysene and (b) benz[*a*]anthracene is the most likely route to the formation of benzo[*a*]pyrene. The determination of C_2 bay region addition as the dominant one for production of benzo[*a*]pyrene will be explained below, along with discussion of the alternative mechanisms.

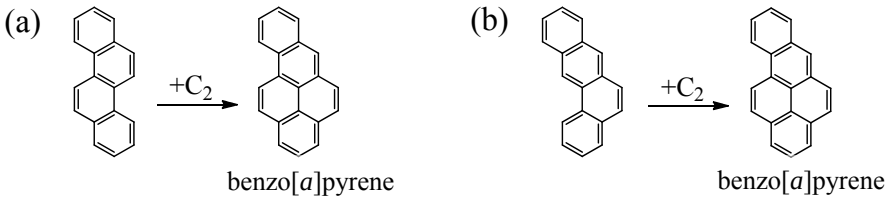

4.38

A mechanism for the formation of the six-ring PAH naphtho[2,1-*a*]pyrene from the supercritical pyrolysis of 1-methylnaphthalene has been proposed by Walker [22] and can be adapted to the formation of the product of supercritical *n*-decane pyrolysis, benzo[*a*]pyrene. The adapted mechanism for the formation of this $C_{20}H_{12}$ product is shown in Figure 4.39. The reactive intermediates are the benzyl radical and a propenylnaphthalene. While no propenyl-substituted naphthalenes have been identified as products of *n*-decane pyrolysis, they would be readily formed by an alkenyl radical attack on naphthalene. Naphthalene has been identified as a product, and there is strong evidence for the presence of alkenyl radicals in the *n*-decane pyrolysis reaction environment that could readily add themselves to naphthalene by displacing hydrogen. The reaction is initiated with an attack by the benzyl radical on the double bond of the propenyl group, and a series of dehydrogenation reactions leads to the final product benzo[*a*]pyrene:

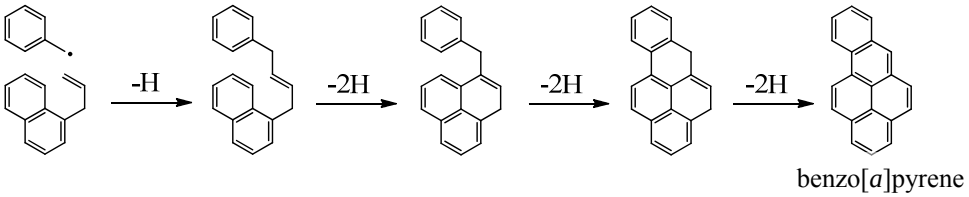

4.39

The first step, in which benzyl radical attacks the double bond of the propenyl group, could be substituted with any number of combinations of substituted or unsubstituted benzenes and naphthalenes to yield a phenylnaphthyl*butane* molecule as the intermediate (analogous to the first step of Scheme 4.37), instead of the phenylnaphthyl*butene* intermediate in Scheme 4.39.

Dehydrogenation of this intermediate (with the dehydrogenation reactions taking place in a different order) would also result in the product benzo[*a*]pyrene.

Finally, C_4 addition to pyrene could also be responsible for benzo[*a*]pyrene. However, yield data indicate that C_2 bay region addition to the four-ring PAH chrysene and benz[*a*]anthracene is the dominant mechanism in the production of benzo[*a*]pyrene. In Section 4.4.5 it was shown that approximately one half to one third of all phenanthrene molecules are converted to pyrene by C_2 bay region addition. Examination of the yields of chrysene and benz[*a*]anthracene—the precursors to benzo[*a*]pyrene by C_2 bay region addition—reveals that the sum of the yields of these two products (Figure 4.15) is approximately equal to the yield of benzo[*a*]pyrene (Figure 4.17) at the highest stressing experimental condition, 570 °C and 100 atm. Examination of product yields at other experimental conditions leads to the conclusion that yields of chrysene and benz[*a*]anthracene are also sufficient to account for all benzo[*a*]pyrene production, if the assumption is made that C_2 bay region addition occurs at the same rate to chrysene and benz[*a*]anthracene to produce benzo[*a*]pyrene as it does to phenanthrene to produce pyrene. If C_2 bay region addition already accounts for the entire yield of benzo[*a*]pyrene, then other mechanisms cannot be contributing significantly to the yield of this PAH product.

If the additional assumption is made that C_4 addition occurs at the same rate to any position of pyrene (very slowly, if at all), then C_4 addition to pyrene cannot be a primary contributor to the formation of benzo[*e*]pyrene either. Furthermore, if reactions between alkylated aromatic molecules such as Scheme 4.39 have been ruled out as part of benzo[*a*]pyrene production for reasons related to yield data, it is reasonable to assume they are also not a part of benzo[*e*]pyrene production either. The instability of phenylnaphthylbutane (an intermediate to the production of benzo[*e*]pyrene in Scheme 4.37) is probably the primary reason that the

pathway shown in Scheme 4.37 does not take place. Phenylnaphthylbutane would be more likely to break between two of the alkyl carbon-carbon bonds than survive long enough to have a hydrogen atom abstracted, particularly when abstraction must occur at a very specific position. Once this abstraction occurs, it is further necessary for the radical formed by hydrogen abstraction to attack the aromatic naphthyl group, instead of decomposing by beta scission. Therefore aromatic-aromatic addition of benzene and phenanthrene (Scheme 4.36) is most likely the primary mechanism for the formation of benzo[*e*]pyrene.

4.4.10 Benzo[*ghi*]perylene, Anthanthrene, and Coronene

Benzo[*ghi*]perylene and coronene are identified as products of supercritical *n*-decane pyrolysis; yields of these six- and seven-ring PAH products are presented in Figure 4.18. Anthanthrene, an isomer of benzo[*ghi*]perylene, is also identified but not quantified due to co-elution of this PAH with other products during HPLC separation.

The most obvious mechanism for formation of benzo[*ghi*]perylene and anthanthrene is C_2 bay region addition to benzo[*e*]pyrene and benzo[*a*]pyrene, respectively. In Scheme 4.40, bay region addition is illustrated for (a) benzo[*ghi*]perylene and (b) anthanthrene:

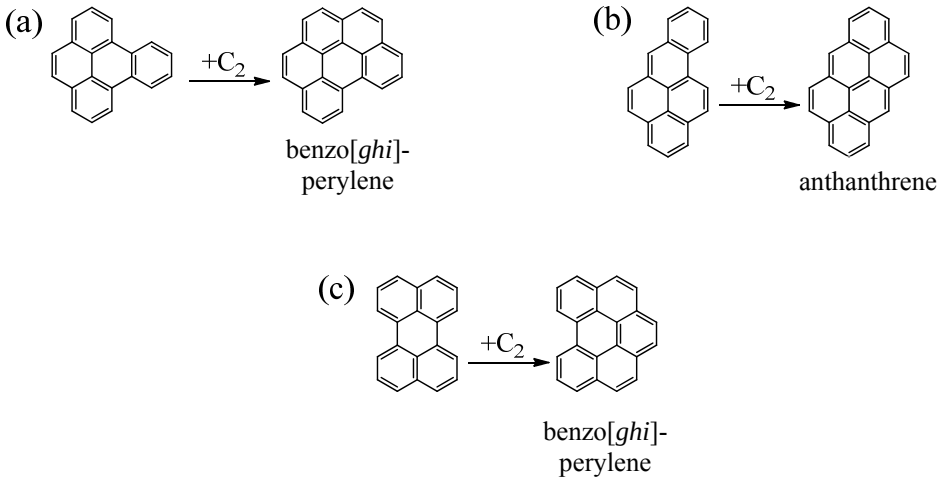

4.40

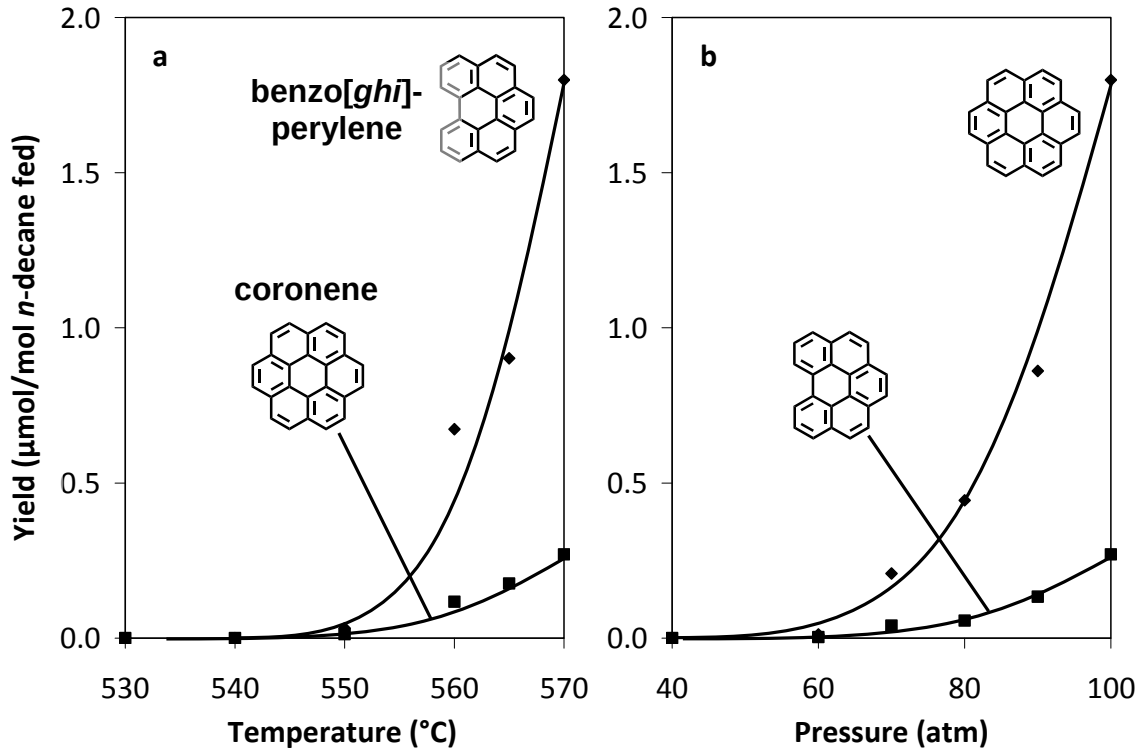

Figure 4.18 Yields of the six-ring PAH benzo[*ghi*]perylene and the seven-ring PAH coronene from the supercritical pyrolysis of *n*-decane: (a) yields versus temperature, at 100 atm and 140 sec; (b) yields versus pressure, at 570 °C and 140 sec.

Yields of benzo[*e*]pyrene (Figure 4.17) and benzo[*ghi*]perylene (Figure 4.18) are approximately equal at all experimental conditions, consistent with comparisons of the yields of other C_2 bay region addition products to yields of their precursors.

C_2 bay region addition to perylene, (c) in Scheme 4.40, might also be a source of benzo[*ghi*]perylene. While perylene is not quantified due to poor chromatographic separation, comparison of its peak heights to those of benzo[*e*]pyrene indicates that perylene is produced at a much lower yield than benzo[*e*]pyrene. Due to its low yield, C_2 addition to perylene is unlikely to be a significant contributor to the formation of benzo[*ghi*]perylene, although production of benzo[*ghi*]perylene may be a significant consumer of perylene.

Combinations of methylnaphthalenes yielding benzo[*ghi*]perylene or anthanthrene (Scheme 4.41) are plausible for the same reason combinations of alkylbenzenes and alkylnaphthalenes were plausible as the precursors to pyrene and benzopyrenes (Schemes 4.22, 4.37, and 4.39): the precursors are abundant in the reaction environment and the methyl substituents are already in the necessary positions to form the additional aromatic rings. Furthermore, combinations of methylnaphthalenes would not require intermediates with long, thermally unstable alkyl chains.

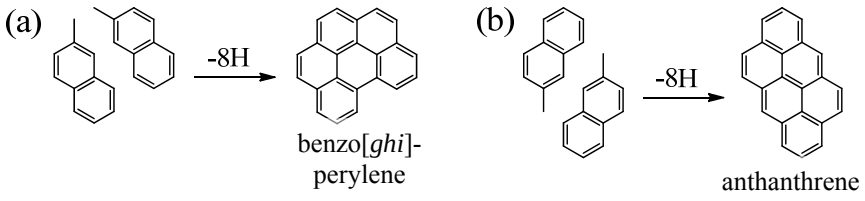

4.41

But neither benzo[*ghi*]perylene nor anthanthrene is formed during the supercritical pyrolysis of 1-methylnaphthalene despite high concentrations of both 1- and 2-methylnaphthalene within that reaction environment [22] relative to their concentrations in the supercritical *n*-decane pyrolysis environment. Furthermore, yields of benzo[*e*]pyrene are already sufficient to fully account for the yields of benzo[*ghi*]perylene by C_2 bay region addition, negating the need for additional reaction pathways to that product. Most likely steric hindrance by aryl hydrogens or methyl groups would keep carbons separated once an initial carbon-carbon bond is formed between two methylnaphthalenes, preventing more carbon-carbon bonds from forming between the two pairs of molecules shown in Scheme 4.41 [71].

Mechanisms for the formation of coronene that involve alkylated naphthalenes, for example the combination of two molecules of dimethylnaphthalene, can also be considered unlikely for the same reasons. Therefore C_2 bay region addition to benzo[*ghi*]perylene, shown in Scheme 4.42, is the most likely reaction pathway to coronene.

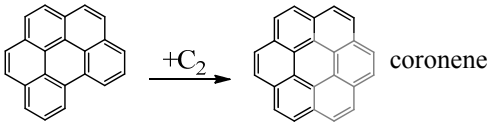

4.42

Yields of benzo[*ghi*]perylene are high relative to the those of coronene, and C_2 bay region addition is known to occur readily in the reaction environment.

4.4.11 Fluoranthene Benzologues and Benzo[*b*]perylene

Indeno[1,2,3-*cd*]pyrene and naphtho[1,2-*b*]fluoranthene are identified as six-ring PAH products of supercritical *n*-decane pyrolysis; yields of these products from the pyrolysis experiments are presented in Figure 4.19 and Figure 4.20, respectively. Dibenzo[*j,l*]fluoranthene, dibenzo[*a,k*]fluoranthene, and benzo[*b*]perylene are produced in detectable quantities at only one condition, the highest stressing experimental condition (570 °C and 100 atm); yields of these three six-ring products can be found in Appendix B. Naphtho[2,3-*b*]fluoranthene, naphtho[2,3-*j*]fluoranthene, and an alkylated naphtho[1,2-*k*]fluoranthene (for which the position(s) and identity(s) of any alkyl substituent(s) are not known) are identified as products but not quantified.

Based on examination of the structures of these six-ring products, the obvious conclusion is that each of these products is at least in part the result of aromatic-aromatic addition. Shown in Scheme 4.43 (p. 154) are each of these products and their precursors. They are: (a) indeno[1,2,3-*cd*]pyrene (benzene and pyrene), (b) naphtho[1,2-*b*]fluoranthene (benzene and chrysene), (c) dibenzo[*j,l*]fluoranthene (naphthalene and phenanthrene), (d) dibenzo[*a,k*]fluoranthene (naphthalene and anthracene), (e) benzo[*b*]perylene (naphthalene and phenanthrene), (f) naphtho[2,3-*b*]fluoranthene (benzene and benz[*a*]anthracene), (g) naphtho[2,3-*j*]fluoranthene (naphthalene and anthracene), and (h) the alkylated naphtho[1,2-*k*]fluoranthene, shown without any alkyl substituent(s) (naphthalene and phenanthrene).

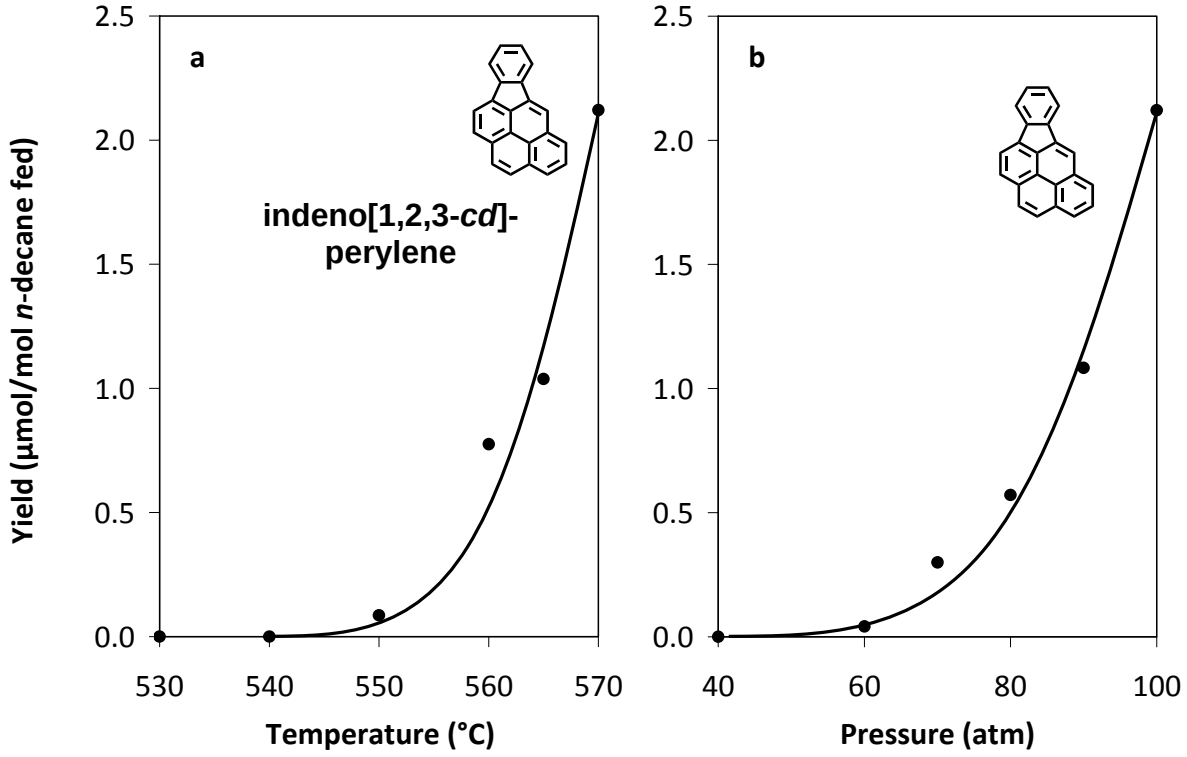

Figure 4.19 Yields of indeno[1,2,3-*cd*]pyrene from the supercritical pyrolysis of *n*-decane: (a) yields vs. temperature, at 100 atm and 140 sec; (b) yields vs. pressure, at 570 °C and 140 sec.

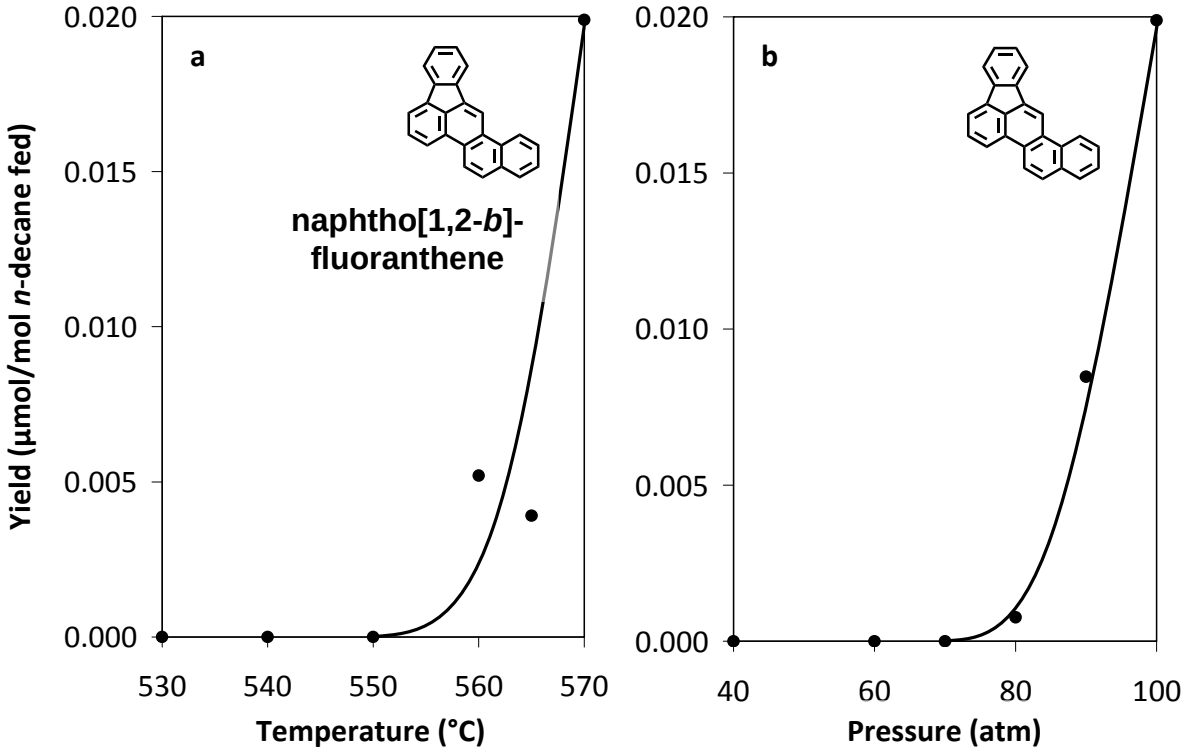

Figure 4.20 Yields of naphtho[1,2-*b*]fluoranthene from the supercritical pyrolysis of *n*-decane: (a) yields vs. temperature, at 100 atm and 140 sec; (b) yields vs. pressure, at 570 °C and 140 sec.

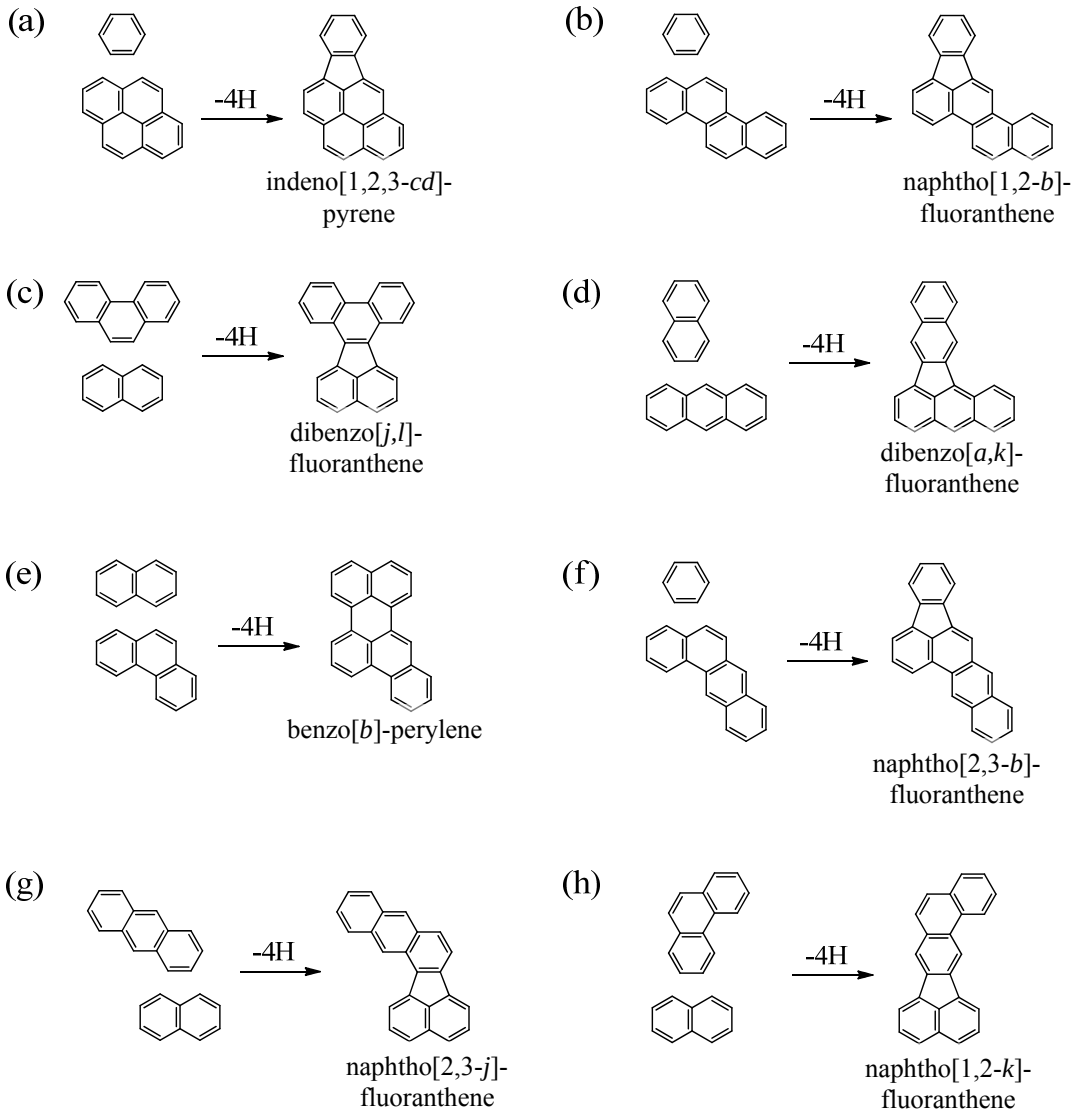

4.43

Additionally, C_4 addition to perylene (to yield benzo[*b*]perylene) or to a benzofluoranthene (to yield the dibenzo- or naphthofluoranthenes) would be another route to these products. The four-ring PAH fluoranthene would yield by naphtho *b* addition the six-ring products naphtho[2,3-*b*]fluoranthene and naphtho[2,3-*j*]fluoranthene and by naphtho *a* addition the products naphtho[1,2-*b*]fluoranthene and naphtho[1,2-*k*]fluoranthene. C_2 bay region addition to benzo[*b*]fluoranthene would give the product indeno[1,2,3-*cd*]pyrene. All these reactions are

likely taking place parallel to each other in the supercritical *n*-decane pyrolysis environment, but the relative rates of each are impossible to know from the available data.

One other reaction, which has not been observed in the supercritical pyrolysis of any other model fuel and hence remains somewhat speculative, is the addition of a naphthylmethyl radical to fluorene. While such an addition has not been observed, the intermediate steps are consistent with the intermediate steps understood to be parts of other reactions. Shown in Figure 4.44 are the precursors to the products (a) naphtho[1,2-*b*]fluoranthene and (b) naphtho[2,3-*b*]fluoranthene:

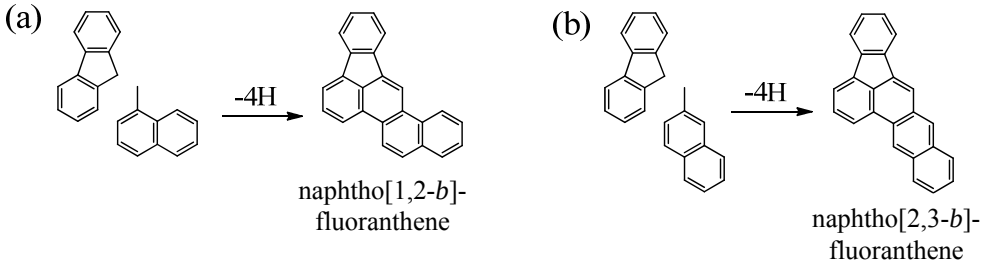

4.44

Scheme 4.45 shows how such a reaction would take place for the product naphtho[1,2-*b*]fluoranthene. The first step is the combination of the fluorenyl and naphthylmethyl radicals. Ring closure is the result of loss of hydrogen by either the naphthyl or fluorenyl aromatic group and shown in this example as loss by the naphthyl group. Once ring closure is accomplished, hydrogen loss gives the fully aromatic six-ring PAH final product.

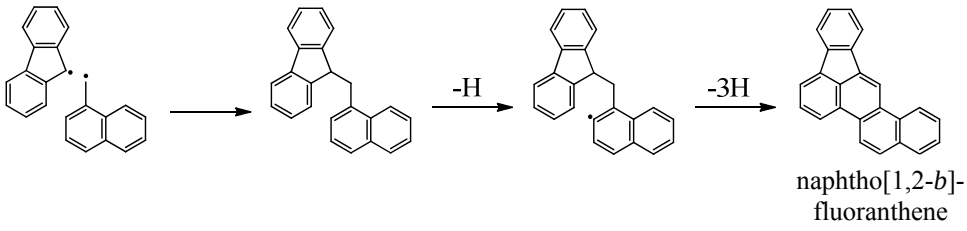

4.45

The intermediate resulting from the first step of the above mechanism could also result from fluorenylmethyl radical attack on naphthalene:

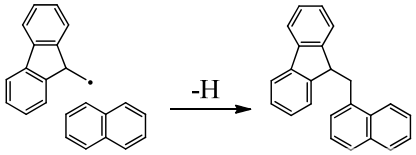

naphtho[1,2-*b*]-
fluoranthene

4.46

Similarly, combinations of a methylated benzo[*b*]fluorene and benzene or benzo[*b*]fluorene and toluene could yield the product dibenzo[*a,k*]fluoranthene. Such a mechanism is depicted in Scheme 4.47 using the example of toluene and benzo[*b*]fluorene.

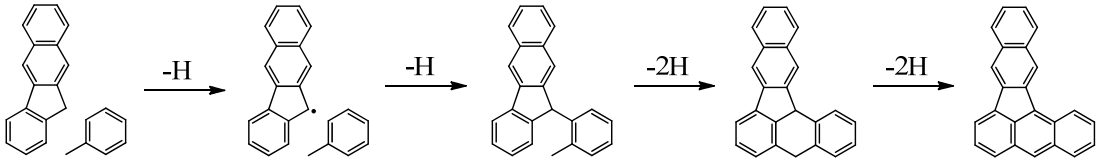

dibenzo[*a,k*]-
fluoranthene

4.47

4.4.12 Dibenzo- and Naphthopyrenes and Dibenzo[*cd,lm*]perylene

Naphtho[2,3-*e*]pyrene, naphtho[2,1-*a*]pyrene, dibenzo[*a,i*]pyrene, and dibenzo[*a,e*]pyrene are identified as six-ring $C_{24}H_{14}$ products of supercritical *n*-decane pyrolysis; yields of these products from the pyrolysis experiments are presented in Figure 4.21. Dibenzo[*cd,lm*]perylene and phenanthro[2,3-*a*]pyrene are also identified; yields of these seven-ring PAH are presented in Figure 4.22. In addition to these products, naphtho[2,3-*a*]pyrene, dibenzo[*a,h*]pyrene, and dibenzo[*e,l*]pyrene are produced in detectable quantities at only one condition, the highest stressing experimental condition (570 °C and 100 atm); yields of these three $C_{24}H_{14}$ products can be found in Appendix B. Four alkylated derivatives of dibenzo[*a,i*]pyrene, four of naphtho[2,1-*a*]pyrene, four of naphtho[2,3-*e*]pyrene, two of dibenzo[*a,e*]pyrene, two of dibenzo[*a,h*]pyrene, two of dibenzo[*cd,lm*]perylene and one of dibenzo[*e,l*]pyrene, for which the aromatic structures are known, but not the positions or identities of the alkyl substituents, are also identified.

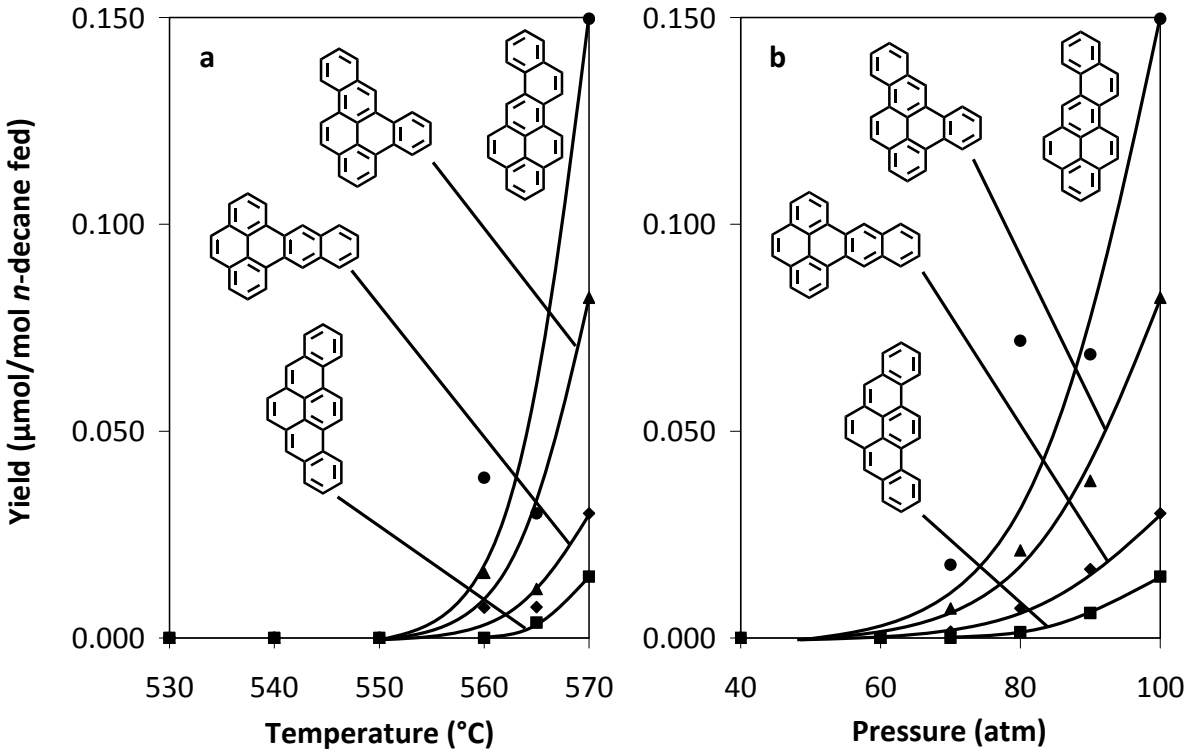

Figure 4.21 Yields of six-ring PAH products from the supercritical pyrolysis of *n*-decane: (a) yields versus temperature, at 100 atm and 140 sec; (b) yields versus pressure, at 570 °C and 140 sec. Labeled clockwise from the bottom left of each chart, yields are shown for dibenzo[*a*,*i*]pyrene, naphtho[2,3-*e*]pyrene, dibenzo[*a*,*e*]pyrene, and naphtho[2,1-*a*]pyrene.

Each of the dibenzo- and naphthopyrenes could be the result of C_4 addition to either benzo[*a*]pyrene or benzo[*e*]pyrene, and C_4 addition to naphtho[2,3-*a*]pyrene would yield phenanthro[2,3-*a*]pyrene. Many of these products can also be arrived at by several alternative mechanisms, each of which will be detailed below.

Dibenzo[*e*,*l*]pyrene and naphtho[2,3-*e*]pyrene could be produced by aromatic-aromatic addition. (a) Benzene adding to the bay region of triphenylene yields dibenzo[*e*,*l*]pyrene, and (b) naphthalene adding to the bay region of phenanthrene yields naphtho[2,3-*e*]pyrene:

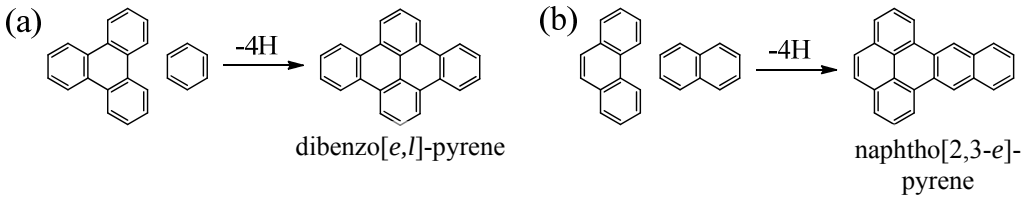

4.48

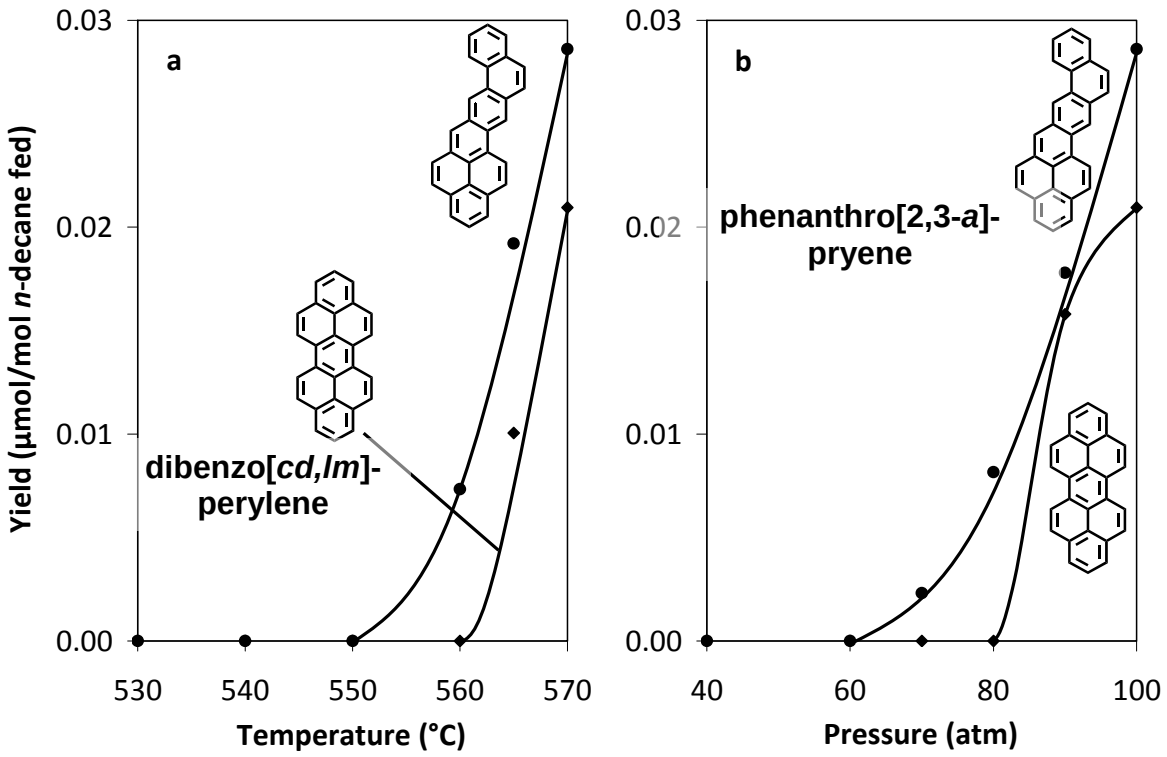

Figure 4.22 Yields of dibenzo[*cd*,*lm*]perylene and phenanthro[2,3-*a*]pyrene from the supercritical pyrolysis of *n*-decane: (a) yields versus temperature, at 100 atm and 140 sec; (b) yields versus pressure, at 570 °C and 140 sec.

Naphtho[2,1-*a*]pyrene and naphtho[2,3-*a*]pyrene, shown below, could be produced by naphtho *a* addition and naphtho *b* addition, respectively, to pyrene:

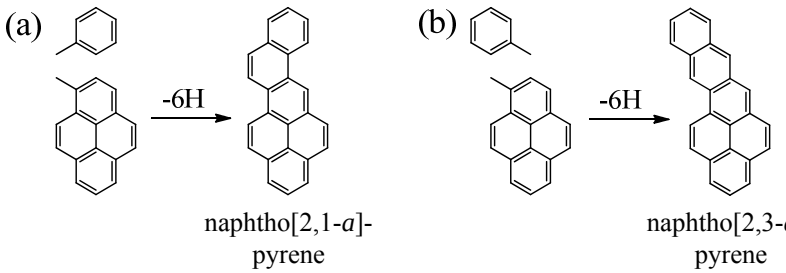

4.49

Phenanthro[2,3-*a*]pyrene is also possibly the result of (a) naphtho *a* addition to benzo[*a*]pyrene or (b) a mechanism very similar to naphtho *b* addition involving the addition of three rings to pyrene:

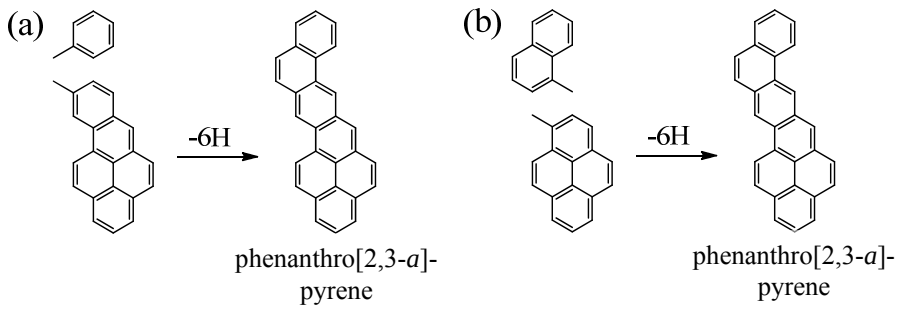

4.50

While Schemes 4.49 and 4.50 are shown with both reactants having a single methyl group each, any number of combinations of alkyl groups would still allow naphtho addition to take place as explained in Section 4.4.3.

Several of the $C_{24}H_{14}$ naphtho- and dibenzopyrene products of supercritical *n*-decane pyrolysis could be the result of C_2 bay region addition to the $C_{22}H_{14}$ five-ring PAH dibenz[*a,h*]anthracene, benzo[*b*]chrysene, picene, and dibenz[*a,c*]anthracene. None of these five-ring precursors has been identified as products of supercritical *n*-decane pyrolysis, but there is evidence that they are nonetheless among the products. Compounds with molecular weight 278 do elute with the sixth fraction in the first dimension of chromatographic separation, although they could not be fully resolved during the second dimension of separation. Furthermore, all four of these five-ring products can be formed from reactions known to take place in the supercritical *n*-decane pyrolysis reaction environment from precursors that have been identified as products. Shown below are examples of possible production routes for (a) picene, (b) dibenz[*a,h*]anthracene, (c) benzo[*b*]chrysene, and (d) dibenz[*a,c*]anthracene by mechanisms analogous to phenanthrene and anthracene production (Section 4.4.3) from products known to be present in the supercritical *n*-decane pyrolysis environment.

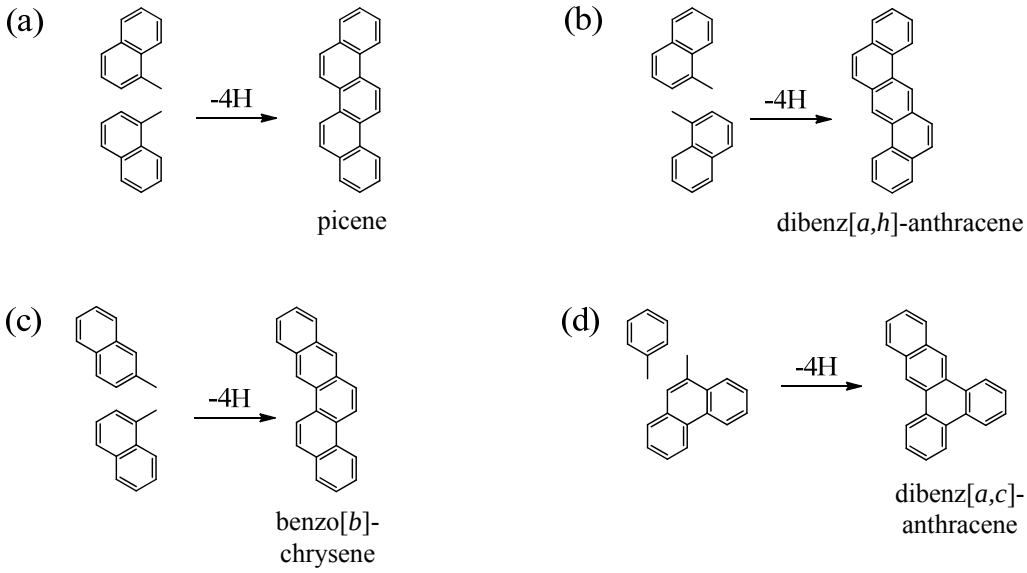

4.51

Scheme 4.52 illustrates the five six-ring products of C_2 bay region addition and their five-ring precursors; they are (a) picene and dibenzo[*a*,*i*]pyrene, (b) dibenz[*a*,*h*]anthracene and naphtho[2,1-*a*]pyrene, (c) benzo[*b*]chrysene and naphtho[2,3-*a*]pyrene, (d) benzo[*b*]chrysene and dibenzo[*a*,*h*]pyrene, and (e) dibenz[*a*,*c*]anthracene and dibenzo[*a*,*e*]pyrene. Note that some of these products can be arrived at by C_2 bay region addition to more than one of these precursors.

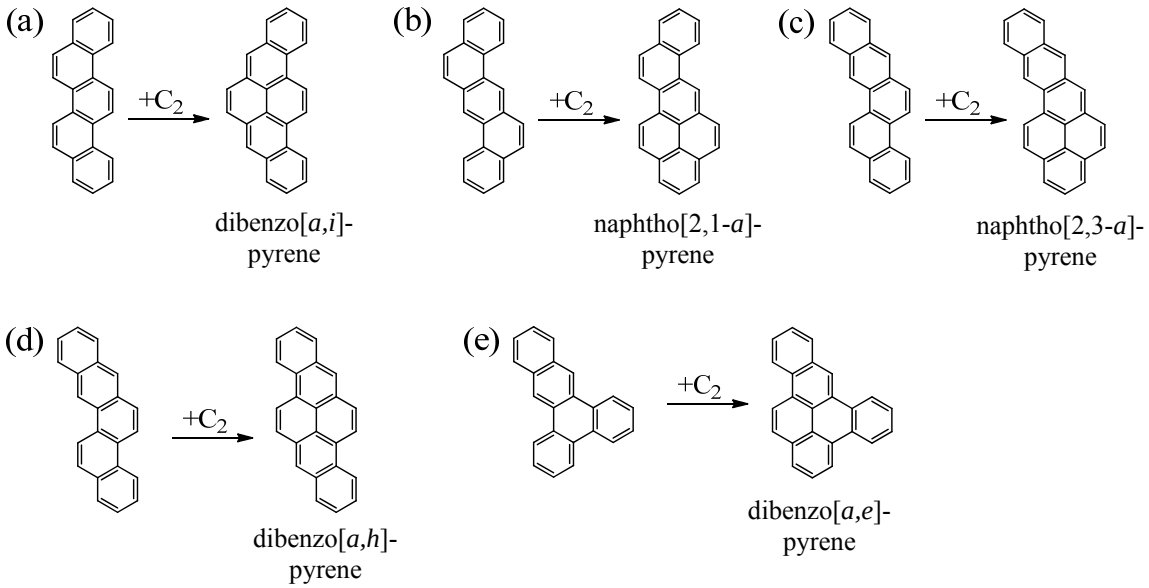

4.52

Similarly, the 7-ring dibenzo[*cd,lm*]perylene is most likely the result of C_2 bay region addition to naphtho[2,1-*a*]pyrene:

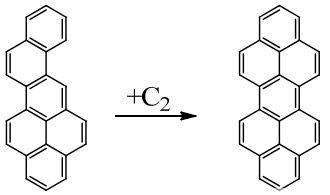

dibenzo[*cd,lm*]-perylene

4.53

The relative contributions of each of the mechanisms discussed in this section are not known. Reaction pathways involving intermediates composed of aryl groups connected by long alkyl chains, analogous to those that were ruled out for the production of the five-ring benzopyrenes in Section 4.4.10, can also be ruled out for the production of the six-ring dibenzo- and naphthopyrenes. Such reactions require intermediates which could not survive in the reaction environment, and since they have been shown to be unimportant to the formation of the benzopyrenes, it is very unlikely that the same mechanisms would be important for the structurally similar, higher-ring-number species.

4.4.13 Dibenzo- and Naphthoperylenes

Dibenzo[*b,ghi*]perylene, dibenzo[*e,ghi*]perylene, and naphtho[1,2,3,4-*ghi*]perylene are seven-ring $C_{26}H_{14}$ PAH identified as products of supercritical *n*-decane pyrolysis; yields of these products are presented in Figure 4.23. Two alkylated derivatives of dibenzo[*e,ghi*]perylene and one of dibenzo[*b,ghi*]perylene, for which the aromatic structures are known, but not the positions or identities of the alkyl substituents, are also identified.

C_4 addition to benzo[*ghi*]perylene could be responsible for all three of these products. Shown in Scheme 4.54, another possible mechanism responsible for this group of seven-ring compounds is C_2 bay region addition to (a) benzo[*b*]perylene, yielding dibenzo[*b,ghi*]perylene;

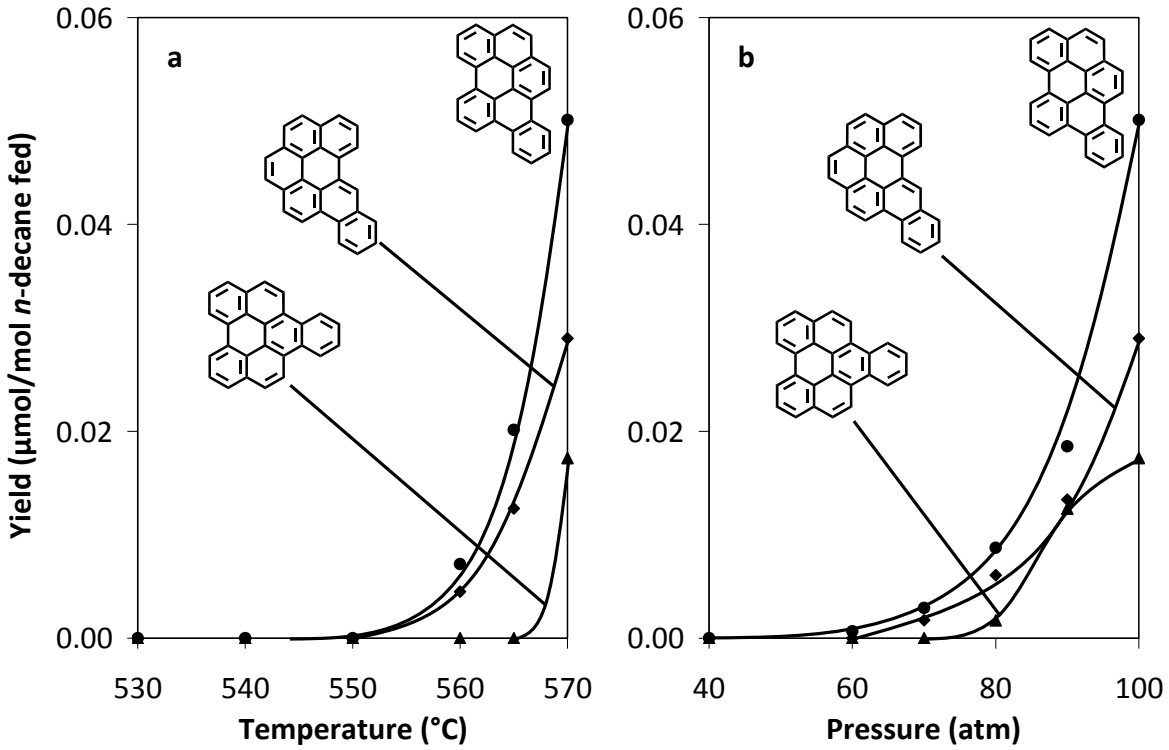

Figure 4.23 Yields of seven-ring PAH products from the supercritical pyrolysis of *n*-decane: (a) yields versus temperature, at 100 atm and 140 sec; (b) yields versus pressure, at 570 °C and 140 sec. Labeled clockwise from the bottom left of each chart, yields are shown for naphtho[1,2,3,4-*ghi*]perylene, dibenzo[*b*,*ghi*]perylene, and dibenzo[*e*,*ghi*]perylene.

(b) dibenzo[*e*,*l*]pyrene, yielding dibenzo[*e*,*ghi*]perylene; and (c) dibenzo[*a*,*e*]pyrene, yielding naphtho[1,2,3,4-*ghi*]perylene:

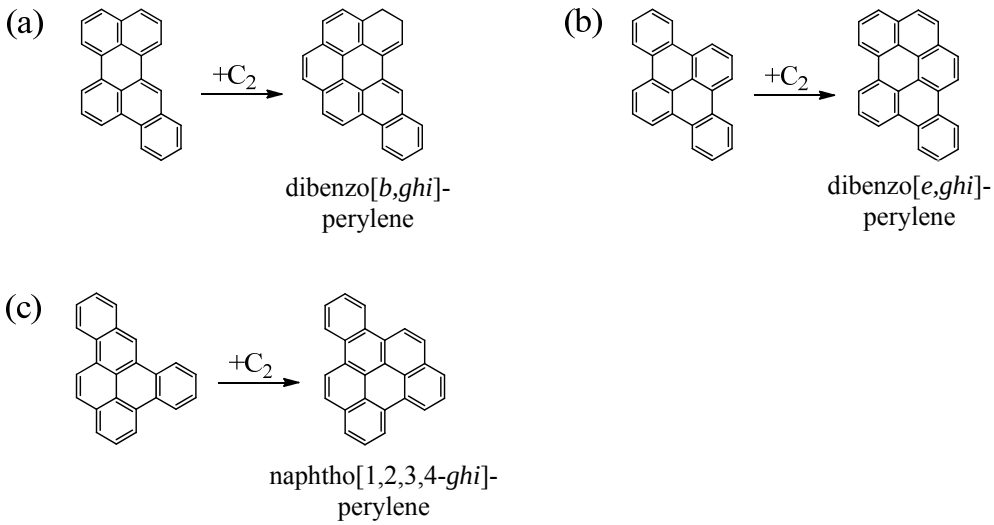

4.54

Shown in Scheme 4.55, another alternative mechanism, aromatic-aromatic addition of benzene to the bay region of (a) benzo[*e*]pyrene yields dibenzo[*e,ghi*]perylene and (b) perylene yields naphtho[1,2,3,4-*ghi*]perylene.

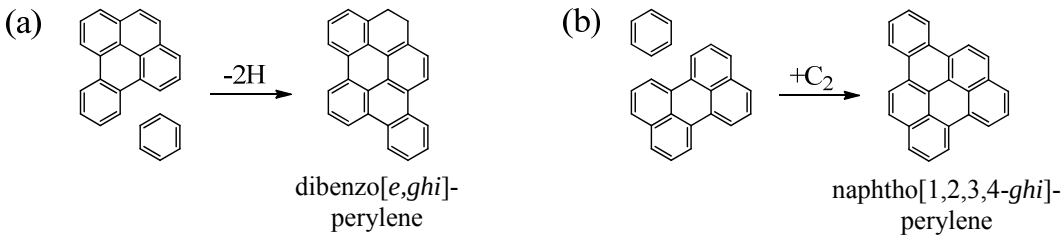

4.55

As with other higher-molecular-weight species, the relative contributions of these mechanisms are not known.

4.4.14 Eight- and Nine-Ring PAH

Benzo[*a*]coronene, phenanthro[5,4,3,2-*efghi*]perylene, and naphtho[8,1,2-*abc*]coronene are identified as eight- and nine-ring PAH products of supercritical *n*-decane pyrolysis; yields of these products are presented in Figure 4.24. Benzo[*pqr*]naphtho[8,1,2-*bcd*]perylene is another unsubstituted eight-ring PAH product identified; this product was not quantified due to insufficient chromatographic separation. Six alkylated derivatives of benzo[*pqr*]naphtho[8,1,2-*bcd*]perylene, five of naphtho[8,1,2-*abc*]coronene, and three of phenanthro[5,4,3,2-*efghi*]perylene, for which the aromatic structures are known, but not the positions or identities of the alkyl substituents, are also identified.

Illustrated in Scheme 4.56, C_2 bay region addition (a) to dibenzo[*b,ghi*]perylene, dibenzo[*e,ghi*]perylene, or naphtho[1,2,3,4-*ghi*]perylene results in benzo[*a*]coronene; (b) to dibenzo[*e,ghi*]perylene results in phenanthro[5,4,3,2-*efghi*]perylene; and (c) to dibenzo[*e,ghi*]perylene results in benzo[*pqr*]naphtho[8,1,2-*bcd*]perylene.

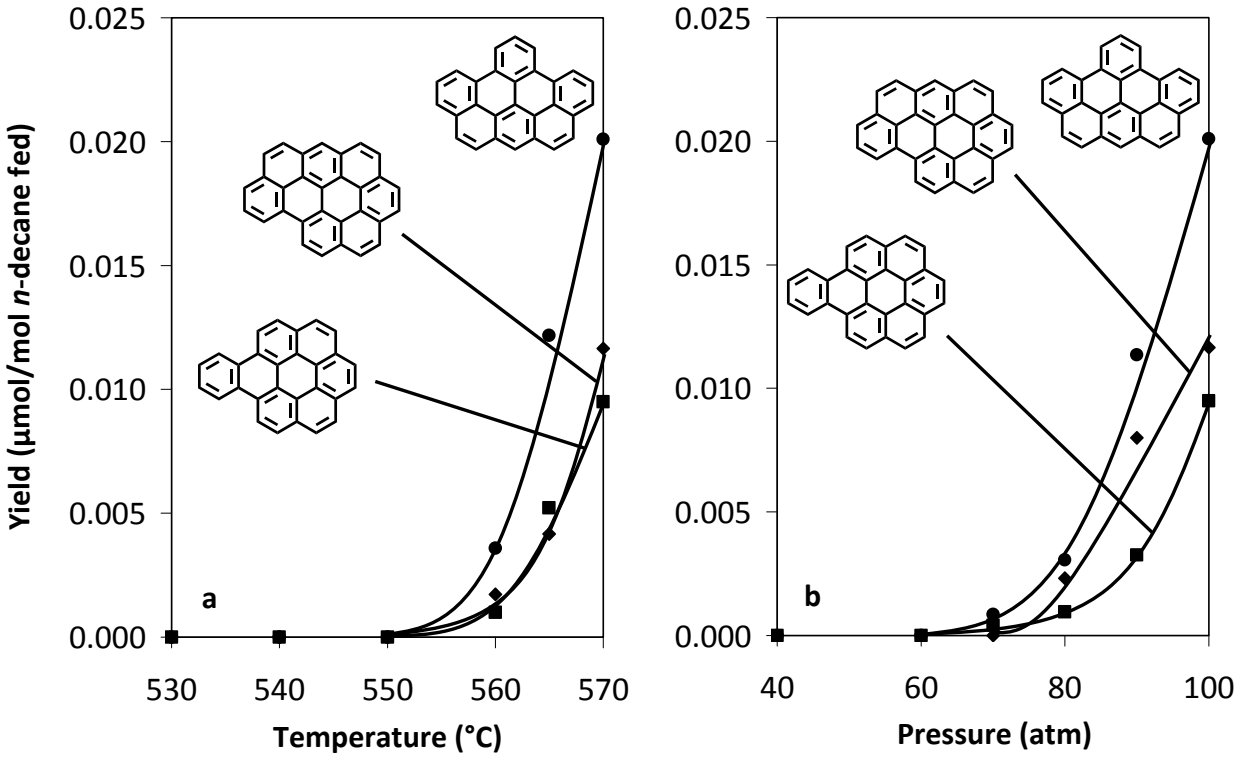

Figure 4.24 Yields of eight- and nine-ring PAH products from the supercritical pyrolysis of *n*-decane: (a) yields versus temperature, at 100 atm and 140 sec; (b) yields versus pressure, at 570 °C and 140 sec. Labeled clockwise from the bottom left of each chart, yields are shown for benzo[a]coronene, naphtho[8,1,2-*abc*]coronene, and phenanthro[5,4,3,2-*efghi*]perylene.

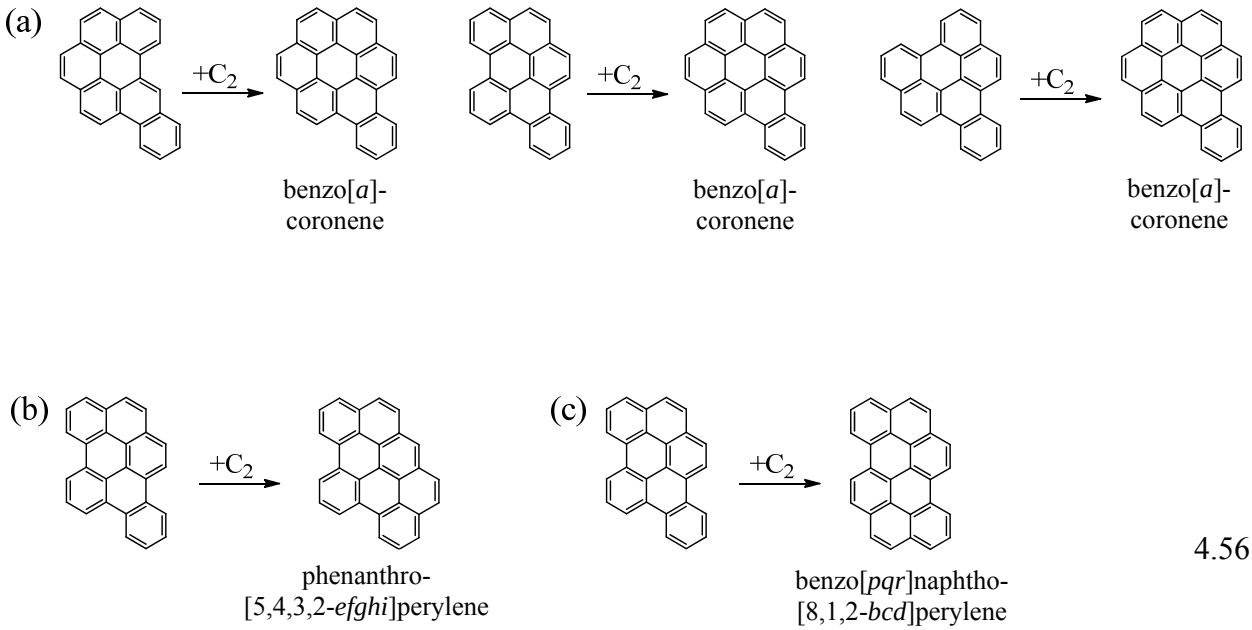

4.56

Two alternative routes to benzo[*a*]coronene are (a) aromatic-aromatic addition of benzene and benzo[*ghi*]perylene and (b) C_4 addition to coronene:

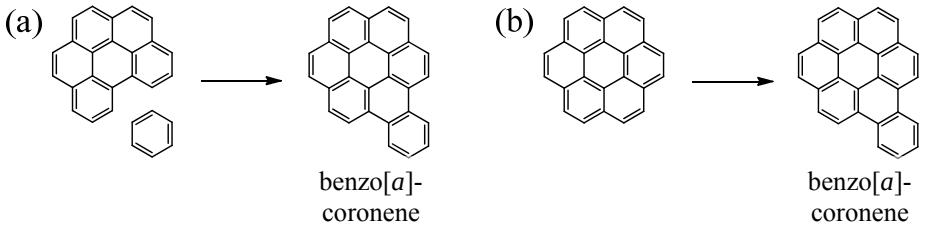

4.58

As with other high-ring-number products of supercritical *n*-decane pyrolysis, the large number of possible reaction pathways for the formation of benzo[*a*]coronene precludes definitive statements regarding the relative importance of each.

C_2 bay region addition to any of the eight-ring $C_{28}H_{14}$ products would result in the nine-ring PAH product naphtho[8,1,2-*abc*]coronene:

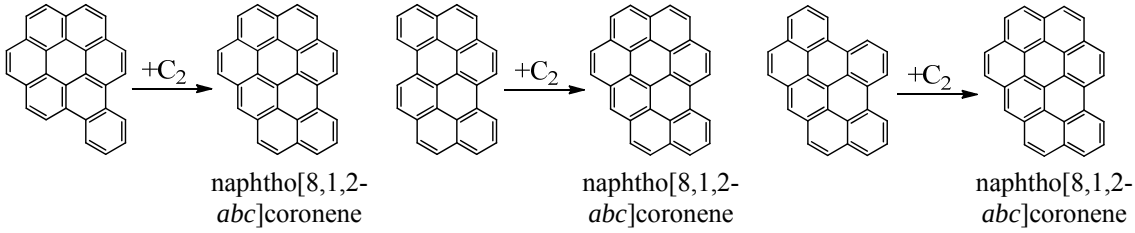

4.57

Relatively high levels of the nine-ring PAH product naphtho[8,1,2-*abc*]coronene (no other nine-ring PAH are found as products of *n*-decane pyrolysis) are likely due the fact that it can be formed from every observed eight-ring product by C_2 bay region addition.

4.4.15 Summary of Results and Conclusions Related to PAH

Altogether, 48 unsubstituted PAH products have been identified as products of supercritical *n*-decane pyrolysis, along with 227 alkylated derivatives of those PAH. These products include compounds with as many as nine aromatic rings. Formation of these products has been shown to be a result of five major pathways: C_4 addition, C_2 bay region addition, aromatic-aromatic addition, and naphtho *a* and *b* addition. Previous research with the

supercritical pyrolysis of the aromatic reactants toluene and 1-methylnaphthalene [27,30-32] has shown that the aromatic carbon-carbon bond never breaks at the temperature conditions at which the supercritical *n*-decane pyrolysis of this work was conducted. Therefore all reaction mechanisms lead from lower- to higher-ring-number PAH, and never the reverse.

As shown in Figures 4.6 to 4.24, yields of all PAH products increase with temperature between 530 and 550 °C, then increase sharply above 550 °C. PAH product yield trends with respect to temperature are consistent with temperature-induced increases in the production of the radical intermediates responsible for PAH formation. Higher temperatures favor carbon-carbon single bond cleavage in the alkane-rich *n*-decane pyrolysis environment, increasing the production of alkyl radicals and olefins, the secondary products of which are alkenyl radicals. These alkyl and alkenyl radicals are the intermediates in the C_4 addition and C_2 bay region addition reactions leading to PAH. Furthermore, increasing the temperature increases the production of aryl and arylmethyl radicals from aromatic and methylated aromatic molecules. Increasing production of these radical intermediates increases the likelihood of the PAH formation reactions that require them as intermediates.

Figures 4.6 to 4.24 also show PAH product yields increasing between 40 and 70 atm, then increasing sharply above 70 atm. Product yield trends of PAH with respect to pressure are the result of three effects, the same effects which lead to increased production of one-ring aromatics with increasing temperature. First, increasing pressure increases the density of the supercritical fluid *n*-decane in the reactor. Increasing the density of the reactant increases its concentration, leading to higher formation rates of all products, including PAH. Second, high pressures stabilize long-chain alkyl and alkenyl radicals, which are the intermediates in C_4 addition and C_2 bay region addition. Third, high pressures introduce cage effects, stabilizing

cyclic intermediate molecules which are not fully aromatic, allowing sufficient time for these molecules to lose hydrogens and become fully aromatic products.

Chapter 5. Conclusions and Recommendations

The model compound *n*-decane (critical temperature, 345ºC; critical pressure, 20.8 atm), chosen to represent the aliphatic components of hydrocarbon aircraft fuels, has been pyrolyzed to improve understanding of the reaction pathways that lead to the formation of polycyclic aromatic hydrocarbons (PAH) and, by extension, solid deposits in the pre-combustion environment of future-generation high-speed jet aircraft. Pyrolysis of *n*-decane was conducted at temperatures, pressures, and residence times similar to those expected to be encountered by fuels used in these aircraft. Specifically, experiments have been performed in a flow reactor (1) at temperatures ranging from 530 to 570 °C at a pressure of 100 atm and a residence time of 140 sec and (2) at pressures ranging from 40 to 100 atm at a temperature of 570 °C and a residence time of 140 sec. These conditions are beyond the critical point of aviation fuels as well as *n*-decane.

GC/FID/MS and HPLC/UV/MS analyses have been used to identify the pyrolysis products and to determine their yields. The major products of supercritical *n*-decane pyrolysis, identified and quantified as functions of temperature and pressure by GC/FID/MS, are *n*-alkanes consisting of one to nine carbons, 1-alkenes consisting of two to nine carbons, and benzene and alkylbenzenes. In addition to these aliphatic, olefinic, and single-ring aromatic products, 72 PAH products were quantified, and their yields have been reported as functions of pyrolysis temperature and pressure.

In order to analyze the highly complex mixture of PAH produced from supercritical *n*-decane pyrolysis, a two-dimensional HPLC separation technique was developed specifically for this work. *n*-Decane pyrolysis produces large amounts of alkylated PAH in addition to their unsubstituted parent compounds, and only by application of this technique can the necessary component resolution be achieved in order to identify and quantify PAH consisting of more than

four aromatic rings. This is the first time this technique has been applied to the problem of solid deposition in the pre-combustion environment of high-speed jet aircraft.

By using this two-dimensional chromatographic technique, the PAH products resulting from the supercritical *n*-decane pyrolysis experiments have been well enough resolved that 45 two- to nine-ring unsubstituted PAH products have been identified in this work, 23 of which are reported here for the first time as products of *n*-decane pyrolysis. The number of alkylated PAH reported has increased dramatically to 232, compared to three in previous studies. Only a single aromatic compound with more than six rings, coronene, had ever before been reported as a product of *n*-decane pyrolysis or combustion; while ten unsubstituted PAH consisting of seven or more rings are reported here, along with another 24 of their alkylated derivatives.

Solid deposits in the pre-combustion environment are believed to be PAH of such high molecular weight that they are insoluble in and thus precipitate out of a supercritical-phase jet fuel (or a model compound such as *n*-decane, used to represent jet fuel in this work). Identification of PAH of up to nine aromatic rings, which are soluble in the *n*-decane reactant, is necessary to understand solid deposition because these compounds are the precursors to even higher-ring-number PAH which are not soluble in the reactant.

One set of experiments was conducted at a constant temperature of 570 °C, a constant residence time of 140 sec, and individual runs at constant pressures of 40, 60, 70, 80, 90, and 100 atm. These parameters were chosen to determine the effect of varying pressure on *n*-decane pyrolysis product yields at conditions relevant to the problem of solid formation in the pre-combustion environment, without being so severe as to form solids in quantities that clog the reactor system. Yields of aromatic products were found to increase with pressure, increasing at rates which themselves increase with pressure. Increases in product yields with respect to pressure are the result of three effects: First, increasing pressure increases the density of the

supercritical fluid *n*-decane in the reactor. Increasing the density of the reactant increases its concentration, leading to higher formation of all products. Second, high pressures stabilize long-chain alkyl and alkenyl radicals, key intermediates in aromatic ring-building mechanisms. Third, high pressures introduce cage effects, stabilizing cyclic intermediate molecules which are not fully aromatic, allowing sufficient time for these molecules to lose hydrogen and become fully aromatic products.

A second set of experiments was conducted at a constant pressure of 100 atm, a constant residence time of 140 sec, and individual runs at constant temperatures of 530, 540, 550, 560, 565, and 570 °C. These parameters were chosen to study the effect of varying temperature on *n*-decane pyrolysis product yields at conditions relevant to solid formation, but not so severe as to actually form solids in amounts which would clog the reactor system. Yields of aromatic products were found to increase with temperature, increasing at rates which themselves increase with temperature. This trend is consistent with radical intermediates being responsible for the formation of aromatic products. Higher temperatures favor carbon-carbon alkyl bond cleavage, increasing the production of alkyl and alkenyl radicals, two key species in ring-addition mechanisms. Furthermore, increasing the temperature increases the production of aryl and arylmethyl radicals by promoting loss of hydrogen from aromatic and methylated aromatic molecules, thereby increasing the rates of reactions in which these radicals participate.

In each experiment yields of one- and two-ring aromatic products are several orders of magnitude higher than those of eight- and nine-ring PAH, and only at the most severe conditions in both sets of experiments are the largest PAH (consisting of seven or more aromatic rings) produced. These larger PAH have much greater sensitivity to temperature and pressure conditions than lower-molecular-weight PAH, and the highest temperature and pressure condition (570 °C, 100 atm) coincides with the onset of solid formation. The observation that

large PAH appear at conditions just prior to solid formation and then increase rapidly at the condition at which solids are produced provides further evidence that carbonaceous solids are in fact PAH of such high molecular weight—higher than the highest-molecular-weight product identified in this work—that they precipitate out of the supercritical phase and condense as a distinct solid phase. This behavior, which mirrors the PAH and solid formation tendencies of real-world jet fuels, demonstrates the applicability of supercritical *n*-decane pyrolysis to the broader problem of solid deposition during the high-pressure thermal stressing of these fuels.

Due to the large number of aromatic products identified, and drawing on previous work with both aliphatic reactants as well as model compounds, the primary reaction pathways leading to PAH formation and growth from supercritical *n*-decane pyrolysis have been identified. After the production of single-ring aromatic molecules by cyclization and then dehydrogenation of the *n*-decane reactant, PAH growth occurs through five key reaction mechanisms which are referred to in this work as: C_4 addition, C_2 bay-region addition, aromatic-aromatic addition, and naphtho *a* and *b* addition. Examples of each of these are shown in Table 5.1.

Table 5.1 The five primary mechanisms for the formation of PAH from the supercritical pyrolysis of *n*-decane with examples of each.

C_4 Addition	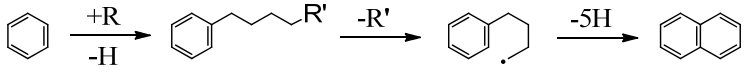
C_2 Bay-Region Addition	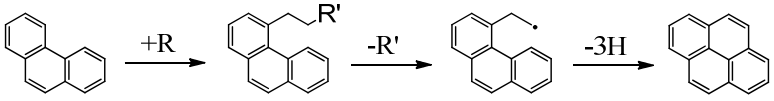
Aromatic-Aromatic Addition	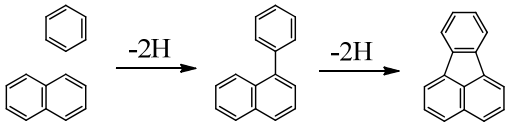
Naphtho *a* Addition	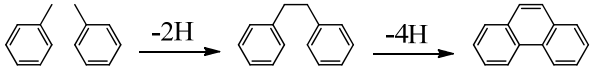
Naphtho *b* Addition	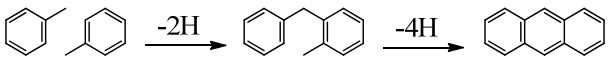

The production of the two-ring PAH naphthalene from the one-ring benzene is an example of C_4 addition. The addition occurs first by attack on an aromatic molecule by an alkyl or alkenyl radical, followed by formation of a cyclic six-carbon structure, and finally the loss of hydrogen to yield one additional ring to the original aromatic molecule. C_2 bay-region addition is a similar ring-addition mechanism in that it involves a radical attack followed by cyclization and dehydrogenation, but differs in that a ring is added in the bay region of a PAH, as in the formation of the four-ring $C_{16}H_{10}$ pyrene from the three-ring $C_{14}H_{10}$ phenanthrene.

Two aromatic molecules can combine to form a higher-ring-number PAH by joining at two pairs of aryl carbons. In this reaction, referred to as aromatic-aromatic addition, first loss of hydrogen by one aromatic compound yields an aryl radical, then attack by this aryl radical on another aromatic molecule (followed by loss of hydrogen) produces a new carbon-carbon bond between the two aromatics. Repetition of each of these steps gives a second carbon-carbon bond and creates an additional ring in between the two initial aromatic compounds. For example, this process is responsible for the two-ring naphthalene and the one-ring benzene yielding the four-ring PAH fluoranthene or the three-ring phenanthrene and the one-ring benzene yielding the five-ring benzo[*e*]pyrene.

Combinations of alkylated aromatic molecules are possible in which the alkyl carbons participate in the reactions. In these types of reactions, the naphtho *a* and *b* addition mechanisms, two alkyl carbons will become part of a new ring, formed between two aromatic molecules. For example, two single-ring toluene molecules, each with one carbon in a methyl group, produce the three-ring product phenanthrene.

Each of these five reaction mechanisms leads to the creation of products of a higher ring number than their precursors. Previous work with the supercritical pyrolysis of the aromatic fuels toluene and 1-methylnaphthalene showed that at the experimental conditions used in this work,

aromatic carbon-carbon bonds will not break. Therefore, in the supercritical *n*-decane reaction environment, pyrolysis reactions only lead to the formation of increasingly large PAH, and never to decomposition of aromatic compounds to lower-ring-number products.

While these key ring-building mechanisms have been identified, the dominant mechanisms responsible for a given product are known in only a small number of cases. Much work is still needed to determine the relative importance of each mechanism in the reaction environment. To this end, future work in supercritical fuel pyrolysis should focus on use of pure alkane reactants other than *n*-decane as well as adding to *n*-decane small amounts of certain compounds that have been identified as reaction intermediates to the formation of larger aromatic products.

Use of other alkane fuels would provide a greater understanding of the role of alkyl and alkenyl radicals in the reaction environment. For example, unlike *n*-decane, *n*-heptane would not readily decompose to the heptenyl radical, the radical intermediate believed to be responsible for the production of toluene from *n*-decane, under supercritical pyrolysis conditions. If the heptenyl radical truly does play an important role in the formation of toluene, a significant difference in the production of this molecule, and by extension PAH products, should be observed in comparison to other, higher-molecular-weight *n*-alkanes.

Several PAH, particularly large PAH, have many possible reaction pathways leading to their formation. The addition to *n*-decane of particular PAH intermediates that are “between” the alkane fuel and the larger PAH, would allow one to distinguish the viability of different candidate pathways. For instance, the five-ring $C_{20}H_{12}$ product benzo[*a*]pyrene may either result from C_4 addition to the four-ring $C_{16}H_{10}$ pyrene or from C_2 bay-region addition to the four-ring $C_{18}H_{12}$ compounds chrysene and benz[*a*]anthracene. While the experimental data indicate that it is the C_2 addition mechanism that is responsible for the final product, a definitive answer would

be provided by separate pyrolysis experiments in which each of these four-ring aromatic intermediates were added to the reactant *n*-decane and the effects on the final yield of the five-ring benzo[*a*]pyrene were compared. Experiments of this type could be extremely useful in determining which mechanisms play important roles in the overall formation of aromatic products, as well as determining which of the multiple possible pathways lead to the formation of individual products.

References

1. T. Edwards, Combustion Science and Technology 178 (2006) 307-334.

2. J. Yu, S. Eser, Industrial and Engineering Chemistry Research 34 (1995) 404-409.

3. H. Huang, L.J. Spadaccini, D.R. Sobel, Journal of Engineering for Gas Turbines and Power 126 (2004) 284-293.

4. H. Lander, A.C. Nixon, Journal of Aircraft 8 (1971) 200-207.

5. D.R. Sobel, L.J. Spadaccini, Journal of Engineering for Gas Turbines and Power 119 (1997) 344-351.

6. A.C. Nixon, H.T. Henderson, Industrial and Engineering Chemistry Product Research and Development 5 (1966) 87-92.

7. W.F. Taylor, Industrial and Engineering Chemistry Product Research and Development 13 (1974) 133-138.

8. R.N. Hazlett, Thermal Oxidation Stability of Aviation Turbine Fuels, American Society for Testing and Materials, Philadelphia, 1991.

9. S.P. Heneghan, S. Zabarnick, D.R. Ballal, W.E. Harrison III, Journal of Energy Resources Technology 118 (1996) 170-179.

10. F.R. Mayo, B.Y. Lan, Industrial and Engineering Chemistry Product Research and Development 25 (1986) 333-348.

11. P.J. Marteney, L.J. Spadaccini, Journal of Engineering for Gas Turbines and Power 108 (1986) 648-653.

12. E.G. Jones, W.J. Balster, J.M. Pickard, Journal of Engineering for Gas Turbines and Power 118 (1996) 286-291.

13. W.J. Balster, E.G. Jones, Journal of Engineering for Gas Turbines 120 (1998) 289-293.

14. O. Altin, S. Eser, Industrial and Engineering Chemistry Research 40 (2001) 596-603.

15. O. Altin, S. Eser, Industrial and Engineering Chemistry Research 40 (2001) 589-595.

16. A.J. Giovanetti, E.J. Szetela, Journal of Propulsion and Power 2 (1986) 450-456.

17. P.H. Taylor, W.A. Rubey, Energy and Fuels 2 (1988) 723-728.

18. J.W. Frankenfeld, W.F. Taylor, Industrial and Engineering Chemistry Product Research and Development 19 (1980) 65-70.

19. S. Eser, Carbon 34 (1996) 539-547.

20. T. Sasaki, R.G. Jenkins, S. Eser, H.H. Schobert, Energy and Fuels 7 (1993) 1039-1046.

21. T. Sasaki, R.G. Jenkins, S. Eser, H.H. Schobert, Energy and Fuels 7 (1993) 1047-1053.

22. M. Walker, Ph.D. Thesis, Department of Chemical Engineering, Louisiana State University, 2009.

23. J.M. Andrésen, Energy and Fuels 15 (2001) 714-723.

24. M. DeWitt, E. Corporan, J. Graham, D. Minus, Energy and Fuels 22 (2008) 2411-2418.

25. C. Song, W. Lai, H.H. Schobert, Industrial and Engineering Chemistry Research 33 (1994) 534-547.

26. C. Song, Y. Peng, H. Jiang, H.H. Schobert, Preprints - American Chemical Society Division of Petroleum Chemistry 37 (1992) 484-492.

27. E.B. Ledesma, M.J. Wornat, P.G. Felton, J.A. Sivo, Proceedings of the Combustion Institute 30 (2005) 1371-1379.

28. J.W. McClaine, J.O. Oña, M.J. Wornat, Journal of Chromatography A 1138 (2007) 175-183.

29. J.W. McClaine, X. Zhang, M.J. Wornat, Journal of Chromatography A 1127 (2006) 137-146.

30. J.W. McClaine, M.J. Wornat, Journal of Physical Chemistry C 111 (2007) 86-95.

31. M.L. Somers, M.J. Wornat, Polycyclic Aromatic Compounds 27 (2007) 261–280.

32. M.L. Somers, J.W. McClaine, M.J. Wornat, Proceedings of the Combustion Institute 31 (2007) 501–509.

33. P.E. Savage, S. Gopalan, T.I. Mizan, C.J. Martino, E.E. Brock, AIChE Journal 41 (1995) 1723-1778.

34. K.P. Johnston, C. Haynes, AIChE Journal 33 (1987) 2017-2026.

35. J.F. Stewart, K. Brezinsky, I. Glassman, Combustion Science and Technology 136 (1998) 373-390.

36. J.F. Stewart, Ph.D. Thesis, Department of Mechanical and Aerospace Engineering, Princeton University, 1999.

37. G.D. Davis, M.S.E. Thesis, Department of Mechanical and Aerospace Engineering, Princeton University, 1994.

38. S. Darrah, Jet Fuel Deoxygenation, AFWAL-TR-88-2081 (1988).

39. H.Y. Tong, F.W Karasek, Analytical Chemistry 56 (1984) 2124-2128.

40. S.A. Wise, S.N. Chesler, H.S. Hertz, L.R. Hilpert, W.E. May, Analytical Chemistry 49 (1977) 2306-2310.

41. R. N. Jones, Journal of the American Chemical Society 67 (1945) 2127-2150.

42. J.C. Fetzer, Large (C>=24) Polycyclic Aromatic Hydrocarbons: Chemistry and Analysis, Wiley-Interscience, New York, 2000.

43. E.V. Dose, G. Guiochon, Analytical Chemistry 61 (1989) 2571-2579.

44. A.L. Lafleur, P.A. Monchamp, E.F. Plummer, M.J. Wornat, Analytical Letters 20 (1987) 1171-1192.

45. G.M. Badger, J. Novotny, Australian Journal of Chemistry 16 (1963) 613-622.

46. O.S.L. Bruinsma, J.A. Moulijn, Fuel Processing Technology 18 (1988) 213-236.

47. S.A. Wise, L.C. Sander, Journal of High Resolution Chromatography 8 (1985) 248-255.

48. M.J. Wornat, E.B. Ledesma, N.D. Marsh, Fuel 80 (2001) 1711-1726.

49. S. Thomas, M.J. Wornat, International Journal of Environmental Analytical Chemistry 88 (2008) 825-840.

50. F.O. Rice, Journal of the American Chemical Society 55 (1933) 3035-3040.

51. F.O. Rice, A. Kossiakoff, Journal of the American Chemical Society 65 (1943) 590-595.

52. R. Luo, Handbook of Bond Dissociation Energies in Organic Compounds, CRC Press, Boca Raton, 2003.

53. I. Safarik, O.P. Strausz, Research on Chemical Intermediates 22 (1996) 275-314.

54. B.M. Fabuss, J.O. Smith, R.I. Lait, A.S. Borsanyi, C.N. Satterfield, Industrial and Engineering Chemistry Product Research and Development 4 (1962) 293-299.

55. C. Song, W. Lai, H.H. Schobert, Industrial and Engineering Chemistry Research 33 (1994) 548-557.

56. J. Yu, S. Eser, Industrial and Engineering Chemistry Research 37 (1998) 4601-4608.

57. W. Lai, C. Song, Fuel Processing Technology 48 (1996) 1-27.

58. D. Nohara, T. Sakai, Industrial and Engineering Chemistry Research 31 (1992) 14-19.

59. J.E. Baldwin, Journal of the Chemical Society, Chemical Communications (1976) 734-736.

60. H. Richter, J.B. Howard, Progress in Energy and Combustion Science 26 (2000) 565-608.

61. J. Oña, Ph.D. Thesis, Department of Chemical Engineering, Louisiana State University, 2008.

62. P.E. Savage, Journal of Analytical and Applied Pyrolysis 54 (2000) 109-126.

63. H. Freund, W.N. Olmstead, International Journal of Chemical Kinetics 21 (1989) 561-574.

64. F.O. Rice, W.R. Johnston, B.L. Evering, Journal of the American Chemical Society 54 (1932) 3529-3543.

65. J. Yu, S. Eser, Industrial and Engineering Chemistry Research 37 (1998) 4591-4600.

66. M.B. Colket, D.J. Seery, Proceedings of the Combustion Institute 25 (1994) 883-891.

67. R.T. Sanderson, Chemical Bonds in Organic Compounds, Sea and Sand, Scottsdale, AZ, 1976.

68. G.L. Esteban, J.A. Kerr, A.F. Trotman-Dickenson, Journal of the Chemical Society (1963) 3873-3879.

69. C.H. Leigh, M. Szwarc, Journal of Chemical Physics 20 (1952) 403-406.

70. C.H. Leigh, M. Szwarc, Journal of Chemical Physics 20 (1952) 407-411.

71. M.J. Wornat, A.F. Sarofim, A.L. Lafleur, Proceedings of the Combustion Institute 24 (1992) 955-963.

Appendix A. HPLC Chromatograms for the Quantification of Two- to Five-Ring PAH

This appendix presents the HPLC chromatograms of Fractions 2-6, generated by separation methods designed to achieve maximum separation of unsubstituted products and methylated PAH. The methods are described in Section 2.3.3.2. Figures A.1 through A.3 display reversed-phase HPLC chromatograms of Fractions 2 through 6.

Figure A.2b, in which the HPLC chromatogram of Fraction 4 is displayed, shows the separation of four methylfluoranthene products. The *n*-decane pyrolysis products from the series of experiments in which temperature was varied were analyzed with a different C18 column than the one used to separated products of the series of experiments in which pressure was varied (both of which were of the same type and dimensions). Separation with the former column was such that only three methylfluoranthene isomers could be fully resolved and quantified.

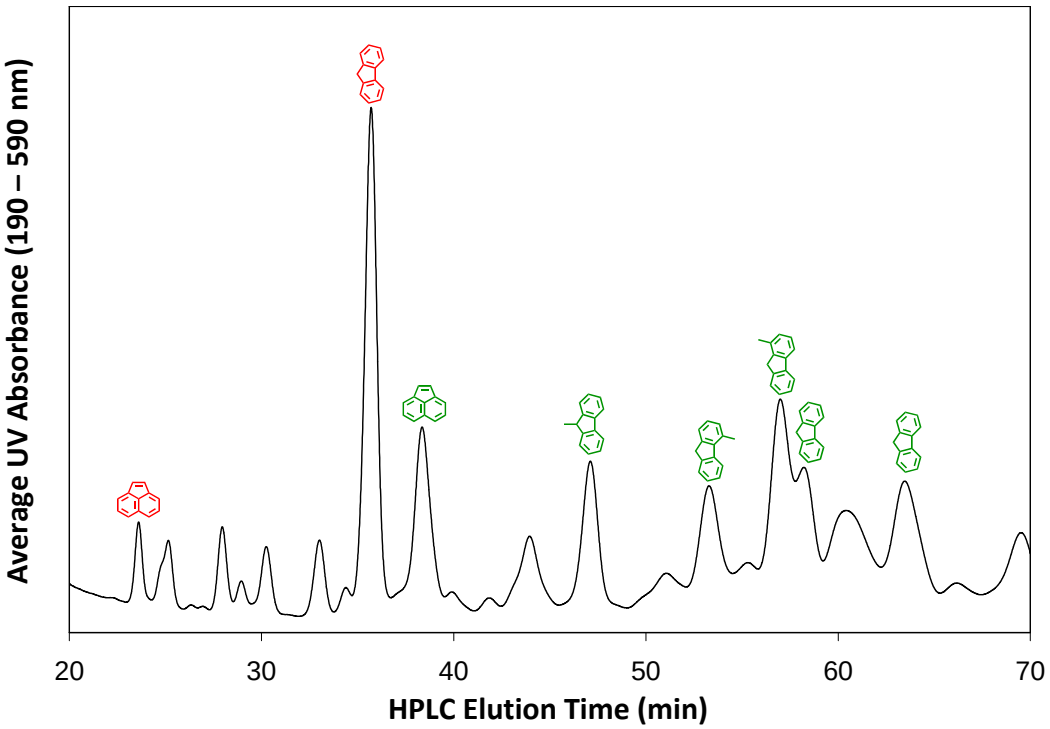

Figure A.1 A reversed-phase HPLC chromatogram of the second fraction of the liquid phase pyrolysis products of *n*-decane stressed at 570 °C and 100 atm. This fraction contains the three-ring PAH acenaphthylene and fluorene and their singly methylated derivatives. Red labels represent unsubstituted PAH; green labels represent singly methylated PAH with the position of the methyl group labeled when known.

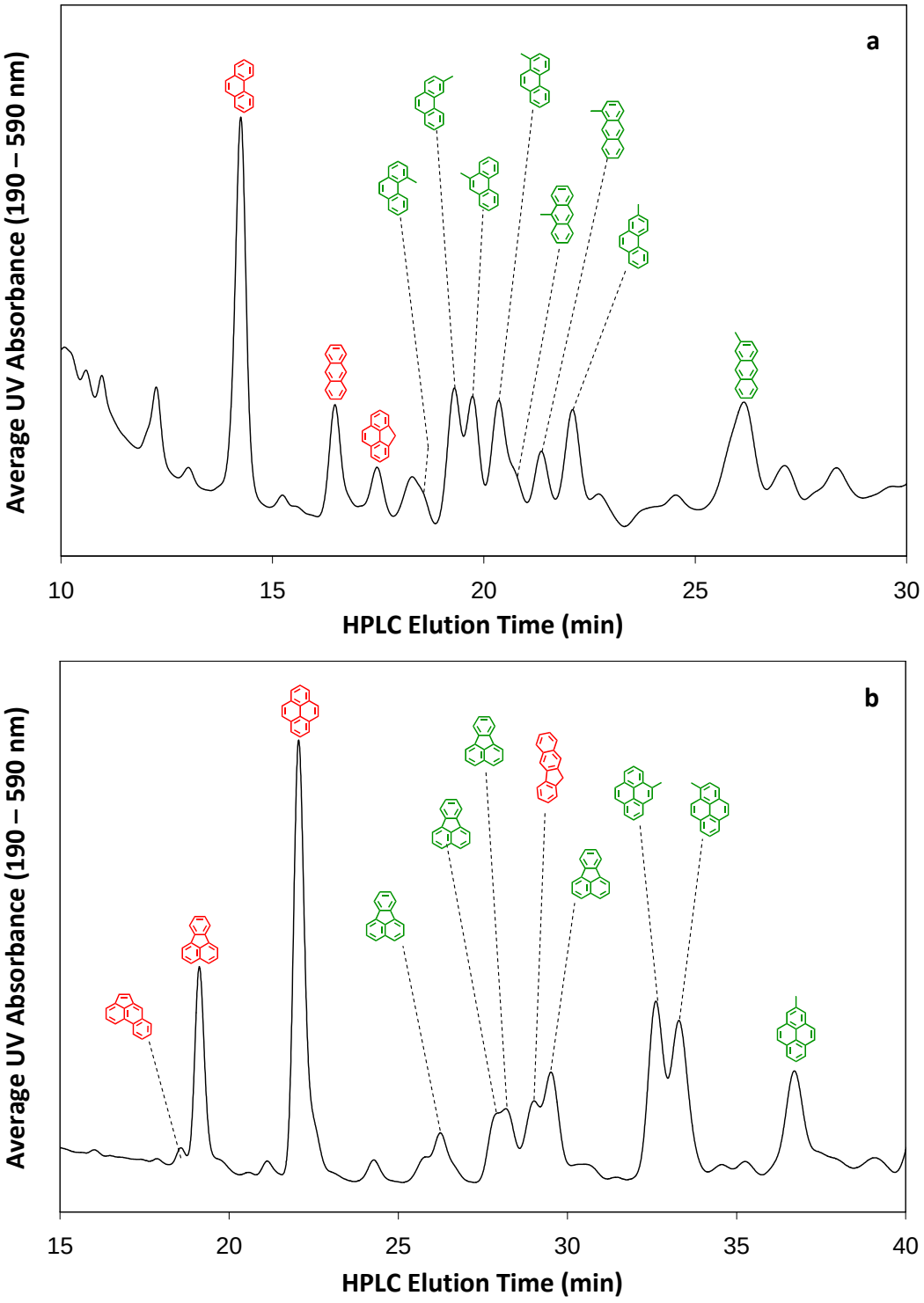

Figure A.2 Reversed-phase HPLC chromatograms of the (a) third and (b) fourth fractions of the liquid- phase pyrolysis products of *n*-decane stressed at 570 °C and 100 atm. These chromatograms resolve three- and four-ring PAH products and their singly methylated derivatives. Red labels represent unsubstituted PAH; green labels represent singly methylated PAH with the position of the methyl group labeled when known.

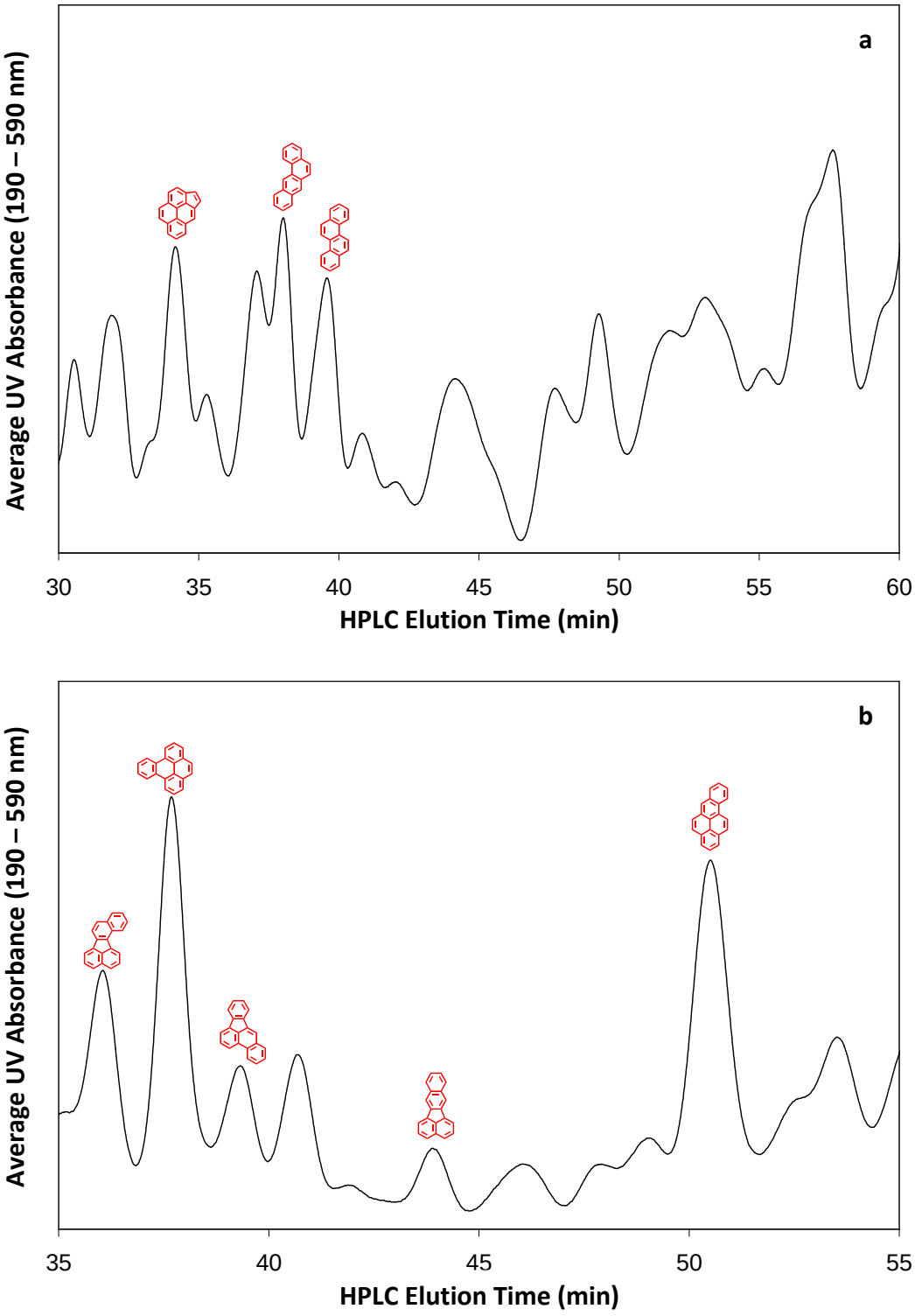

Figure A.3 Reversed-phase HPLC chromatograms of the (a) fifth and (b) sixth fractions of the liquid- phase pyrolysis products of *n*-decane stressed at 570 °C and 100 atm. These chromatograms resolve unsubstituted four- and five-ring PAH.

Appendix B. Numerical Values of Product Yields

B.1 Alkane Product Yields

Alkane product yields are reported in mol product per mol *n*-decane fed to the reactor.

Temperature (°C); (Pressure, 100 atm; Residence Time, 140 sec)

	530	540	550	560	565	570
Methane	0.061	0.100	0.153	0.222	0.260	0.310
Ethane	0.127	0.185	0.252	0.325	0.360	0.410
n-Propane	0.101	0.146	0.197	0.251	0.269	0.302
n-Butane	0.045	0.069	0.095	0.128	0.130	0.147
n-Hexane	0.016	0.020	0.018	0.016	0.017	0.017
n-Heptane	0.045	0.040	0.035	0.036	0.030	0.032
n-Octane	0.014	0.012	0.012	0.012	0.011	0.011
n-Nonane	0.007	0.006	0.005	0.005	0.004	0.005

Pressure (atm); (Temperature, 570 °C; Residence Time, 140 sec)

	40	60	70	80	90	100
Methane	0.139	0.191	0.221	0.190	0.284	0.310
Ethane	0.223	0.287	0.322	0.325	0.383	0.410
n-Propane	0.150	0.207	0.236	0.260	0.282	0.302
n-Butane	0.054	0.087	0.106	0.127	0.135	0.147
n-Hexane	0.007	0.010	0.010	0.007	0.013	0.017
n-Heptane	0.016	0.023	0.024	0.019	0.023	0.032
n-Octane	0.004	0.007	0.008	0.006	0.008	0.011
n-Nonane	0.002	0.003	0.003	0.002	0.003	0.005

B.2 Alkene Product Yields

Alkene product yields are reported in mol product per mol *n*-decane fed to the reactor. Note that the yield of 1-nonene is estimated; see Section 4.2 for an explanation of how its yield was determined.

Temperature (°C); (Pressure, 100 atm; Residence Time, 140 sec)

	530	540	550	560	565	570
Ethylene	0.032	0.044	0.056	0.067	0.071	0.081
Propene	0.084	0.116	0.150	0.180	0.189	0.212
1-Butene	0.035	0.048	0.061	0.073	0.071	0.079
1,3-Butadiene	0.001	0.001	0.002	0.003	0.003	0.003
1-Hexene	0.052	0.056	0.039	0.035	0.033	0.037
1-Heptene	0.039	0.031	0.027	0.024	0.020	0.021
1-Octene	0.031	0.024	0.019	0.017	0.014	0.013
1-Nonene	0.008	0.006	0.004	0.004	0.003	0.003

Pressure (atm); (Temperature, 570 °C; Residence Time, 140 sec)

	40	60	70	80	90	100
Ethylene	0.162	0.128	0.114	0.087	0.089	0.081
Propene	0.206	0.227	0.230	0.219	0.219	0.212
1-Butene	0.086	0.090	0.090	0.089	0.083	0.079
1,3-Butadiene	0.006	0.005	0.005	0.004	0.003	0.003
1-Hexene	0.067	0.050	0.036	0.019	0.028	0.037
1-Heptene	0.045	0.033	0.029	0.017	0.018	0.021
1-Octene	0.033	0.024	0.019	0.011	0.012	0.013
1-Nonene	0.009	0.006	0.005	0.003	0.003	0.003

B.3 Benzene and Naphthalene Product Yields

Benzene and naphthalene product yields and the yields of their alkylated derivatives are reported in μmol product per mol *n*-decane fed to the reactor. Co-eluting products *m*- and *p*-xylene are reported as a summed yield.

	Temperature (°C); (Pressure, 100 atm; Residence Time, 140 sec)					
	530	540	550	560	565	570
Benzene	2552	3869	7095	14956	17283	20466
Toluene	2637	3663	6272	12117	13470	18657
Ethylbenzene	0	512	833	2021	2300	3221
m- and *p*-Xylene	0	749	1717	3889	4467	5978
Naphthalene	3	26	120	314	604	900
2-Methylnaphthalene	4	21	97	275	520	802
1-Methylnaphthalene	14	30	88	210	354	536

	Pressure (atm); (Temperature, 570 °C; Residence Time, 140 sec)					
	40	60	70	80	90	100
Benzene	3394	6764	7647	11147	10998	20466
Toluene	2528	6162	8342	9690	12528	18657
Ethylbenzene	0	566	874	1085	1634	3221
m + *p*-Xylene	0	925	1321	1618	2498	5978
Naphthalene	9	91	236	388	629	900
2-Methylnaphthalene	7	44	170	295	535	802
1-Methylnaphthalene	37	57	129	219	373	536

B.4 Fluorene and Methylfluorene Product Yields

Fluorene and methylfluorene product yields are reported in μmol product per mol *n*-decane fed to the reactor.

Temperature (°C); (Pressure, 100 atm; Residence Time, 140 sec)

	530	540	550	560	565	570
Fluorene	0.85	4.95	13.17	64.71	83.10	117.43
1-Methylfluorene	0	2.49	9.98	41.51	54.79	77.75
4-Methylfluorene	0	8.11	3.93	24.16	33.15	38.87
9-Methylfluorene	3.58	3.14	4.42	22.51	28.32	41.88
Methylfluorene	0	0.95	7.60	23.15	30.13	39.57
Methylfluorene	0	1.63	6.79	29.48	43.08	58.33

Pressure (atm); (Temperature, 570 °C; Residence Time, 140 sec)

	40	60	70	80	90	100
Fluorene	2.16	18.37	34.72	60.30	78.42	117.43
1-Methylfluorene	0.58	8.67	18.74	37.83	50.24	77.75
4-Methylfluorene	0	5.61	9.90	17.78	25.86	38.87
9-Methylfluorene	0	3.87	9.96	18.47	26.91	41.88
Methylfluorene	0	3.28	7.51	17.48	24.20	39.57
Methylfluorene	0	5.69	13.18	25.77	33.86	58.33

B.5 Acenaphthylene and Methylacenaphthylene Product Yields

Acenaphthylene and methylacenaphthylene product yields are reported in μmol product per mol *n*-decane fed to the reactor.

	Temperature (°C); (Pressure, 100 atm; Residence Time, 140 sec)					
	530	540	550	560	565	570
Acenaphthylene	0	0.61	1.63	8.11	10.01	14.70
Methylacenaphthylene	0.20	1.92	6.56	29.90	41.14	56.08

	Pressure (atm); (Temperature, 570 °C; Residence Time, 140 sec)					
	40	60	70	80	90	100
Acenaphthylene	0.09	3.07	5.77	10.15	12.15	14.70
Methylacenaphthylene	0	8.50	16.03	28.79	34.90	56.08

B.6 Anthracene and Methylanthracene Product Yields

Anthracene and methylanthracene product yields are reported in μmol product per mol *n*-decane fed to the reactor.

	Temperature (°C); (Pressure, 100 atm; Residence Time, 140 sec)					
	530	540	550	560	565	570
Anthracene	0	0.18	1.04	4.89	8.09	12.11
1-Methylanthracene	0	0.16	0.98	3.77	6.52	9.33
9-Methylanthracene	0	0	0.46	1.91	2.95	4.44

	Pressure (atm); (Temperature, 570 °C; Residence Time, 140 sec)					
	40	60	70	80	90	100
Anthracene	0.19	1.05	2.30	4.43	7.97	12.11
1-Methylanthracene	0	0.72	1.52	3.58	6.17	9.33
9-Methylanthracene	0	0.36	0.75	1.41	2.64	4.44

B.7 Phenanthrene and Methylphenanthrene Product Yields

Phenanthrene, methylphenanthrene, and cyclopenta[*def*]phenanthrene product yields are reported in μmol product per mol *n*-decane fed to the reactor.

	Temperature (°C); (Pressure, 100 atm; Residence Time, 140 sec)					
	530	540	550	560	565	570
Phenanthrene	0.90	2.73	3.29	12.59	23.47	40.02
Cyclopenta[*def*]phenanthrene	0	0.11	0.68	2.29	3.87	7.23
1-Methylphenanthrene	0	0.23	1.49	5.43	10.11	17.41
2-Methylphenanthrene	0	0.30	1.51	6.93	11.34	17.80
3-Methylphenanthrene	0	0.32	1.48	5.79	10.48	16.41
4-Methylphenanthrene	0	0.11	0.24	1.13	2.24	2.66
9-Methylphenanthrene	0	0.46	1.03	4.65	8.30	15.51

	Pressure (atm); (Temperature, 570 °C; Residence Time, 140 sec)					
	40	60	70	80	90	100
Phenanthrene	4.70	6.61	6.77	12.51	19.35	40.02
Cyclopenta[*def*]phenanthrene	0	0.25	0.82	1.85	3.62	7.23
1-Methylphenanthrene	0	1.10	2.61	5.91	10.02	17.41
2-Methylphenanthrene	0	1.26	2.52	5.91	10.08	17.80
3-Methylphenanthrene	0	1.47	2.75	6.05	10.15	16.41
4-Methylphenanthrene	0	0.28	0.50	0.99	2.01	2.66
9-Methylphenanthrene	0	1.70	2.35	4.72	7.52	15.51

B.8 Four- and Five-Ring Product Yields

Acephenantrhylene, benzo[*b*]fluorene, cyclopenta[*cd*]pyrene, benz[*a*]anthracene, and chrysene product yields are reported in μmol product per mol *n*-decane fed to the reactor.

	Temperature (°C); (Pressure, 100 atm; Residence Time, 140 sec)					
	530	540	550	560	565	570
Acephenanthrylene	0	0	0.05	0.58	1.11	1.69
Benzo[*b*]fluorene	0	0.42	0.56	6.97	10.53	15.99
Cyclopenta[*cd*]pyrene	0	0	0	0.40	0.74	1.57
Benz[*a*]anthracene	0	0	0	0.44	0.64	1.26
Chrysene	0	0	0	0.35	0.62	1.10

	Pressure (atm); (Temperature, 570 °C; Residence Time, 140 sec)					
	40	60	70	80	90	100
Acephenanthrylene	0	0	0	0.79	1.01	1.69
Benzo[*b*]fluorene	0	0.68	1.53	3.37	5.13	15.99
Cyclopenta[*cd*]pyrene	0	0	0.09	0.34	0.83	1.57
Benz[*a*]anthracene	0	0.08	0.14	0.39	0.69	1.26
Chrysene	0	0.04	0.12	0.34	0.48	1.10

B.9 Pyrene Product Yields

Pyrene and methylpyrene yields are reported in μmol product per mol *n*-decane fed to the reactor.

	Temperature (°C); (Pressure, 100 atm; Residence Time, 140 sec)					
	530	540	550	560	565	570
Pyrene	0.20	0.82	1.14	15.11	23.73	35.26
1-Methylpyrene	0	0.34	0.44	6.58	10.07	15.23
2-Methylpyrene	0	0.63	0.53	6.94	10.11	15.19
4-Methylpyrene	0	0.38	0.79	10.63	15.35	23.58

	Pressure (atm); (Temperature, 570 °C; Residence Time, 140 sec)					
	40	60	70	80	90	100
Pyrene	0.28	2.13	5.74	14.27	21.60	35.26
1-Methylpyrene	0	1.05	2.88	6.46	10.70	15.23
2-Methylpyrene	0	0.42	1.79	5.08	7.74	15.19
4-Methylpyrene	0	1.27	3.06	7.38	11.65	23.58

B.10 Fluoranthene Product Yields

Fluoranthene and methylfluoranthene product yields are reported in μmol product per mol *n*-decane fed to the reactor. Three methylfluoranthenes are identified in the set of experiments in which temperature is varied; four are identified in the series in which pressure was varied (the difference between the quantifications from the two sets of experiments is explained in Appendix A).

	Temperature (°C); (Pressure, 100 atm; Residence Time, 140 sec)					
	530	540	550	560	565	570
Fluoranthene	0.21	0.76	0.58	6.89	11.17	15.20
Methylfluoranthene	0	0	0.14	3.03	4.58	6.33
Methylfluoranthene	0	0.18	0.22	2.91	4.08	4.70
Methylfluoranthene	0	0.29	0.44	5.32	7.62	11.63

	Pressure (atm); (Temperature, 570 °C; Residence Time, 140 sec)					
	40	60	70	80	90	100
Fluoranthene	0.49	1.74	2.46	5.68	9.24	15.20
Methylfluoranthene	0	0.36	0.75	1.93	2.95	6.33
Methylfluoranthene	0	0.32	0.97	1.89	3.61	4.70
Methylfluoranthene	0	0.68	0.97	2.70	3.94	6.68
Methylfluoranthene	0	0.59	1.72	4.09	7.27	11.63

B.11 Five, Six, and Seven-Ring PAH Product Yields

Benzo[*a*]pyrene, benzo[*e*]pyrene, benzo[*b*]fluoranthene, benzo[*j*]fluoranthene, benzo[*k*]fluoranthene, benzo[*ghi*]perylene, indeno[1,2,3-*cd*]pyrene, and coronene yields are reported in µmol product per mol *n*-decane fed to the reactor.

	Temperature (°C); (Pressure, 100 atm; Residence Time, 140 sec)					
	530	540	550	560	565	570
Benzo[*a*]pyrene	0	0	0	0.345	0.876	2.389
Benzo[*e*]pyrene	0	0	0	0.519	1.146	1.891
Benzo[*b*]fluoranthene	0	0	0	0.390	0.556	0.640
Bbenzo[*j*]fluoranthene	0	0	0	0.243	0.532	1.008
Benzo[*k*]fluoranthene	0	0	0	0.083	0.143	0.270
Benzo[*ghi*]perylene	0	0	0.032	0.673	0.902	1.799
Indeno[1,2,3-*cd*]pyrene	0	0	0.086	0.775	1.038	2.121
Coronene	0	0	0.012	0.117	0.176	0.270

	Pressure (atm); (Temperature, 570 °C; Residence Time, 140 sec)					
	40	60	70	80	90	100
Benzo[*a*]pyrene	0	0.056	0.153	0.353	0.997	2.389
Benzo[*e*]pyrene	0	0.058	0.204	0.509	1.258	1.891
Benzo[*b*]fluoranthene	0	0	0.038	0.159	0.291	0.640
Bbenzo[*j*]fluoranthene	0	0	0.134	0.244	0.436	1.008
Benzo[*k*]fluoranthene	0	0	0.028	0.057	0.108	0.270
Benzo[*ghi*]perylene	0	0.012	0.208	0.444	0.861	1.799
Indeno[1,2,3-*cd*]pyrene	0	0.041	0.299	0.571	1.083	2.121
Coronene	0	0.003	0.040	0.056	0.133	0.270

B.12 Six-Ring PAH Product Yields

Dibenzo[*j*,*l*]fluoranthene, dibenzo[*a*,*k*]fluoranthene, naphtho[1,2-*b*]fluoranthene, dibenzo[*a*,*e*]pyrene, dibenzo[*a*,*h*]pyrene, dibenzo[*a*,*i*]pyrene, dibenzo[*e*,*l*]pyrene, naphtho[2,1-*a*]pyrene, naphtho[2,3-*a*]pyrene, naphtho[2,3-*e*]pyrene, and benzo[*b*]perylene yields are reported in µmol product per mol *n*-decane fed to the reactor.

Temperature (°C); (Pressure, 100 atm; Residence Time, 140 sec)

	530	540	550	560	565	570
Dibenzo[*j*,*l*]fluoranthene	0	0	0	0	0	0.0109
Dibenzo[*a*,*k*]fluoranthene	0	0	0	0	0	0.0110
Naphtho[1,2-*b*]fluoranthene	0	0	0	0.0052	0.0039	0.0199
Dibenzo[*a*,*e*]pyrene	0	0	0	0.0158	0.0118	0.0823
Dibenzo[*a*,*h*]pyrene	0	0	0	0	0	0.0136
Dibenzo[*a*,*i*]pyrene	0	0	0	0	0.0037	0.0148
Dibenzo[*e*,*l*]pyrene	0	0	0	0	0	0.0333
Naphtho[2,1-*a*]pyrene	0	0	0	0.0387	0.0301	0.1497
Naphtho[2,3-*a*]pyrene	0	0	0	0	0	0.0129
Naphtho[2,3-*e*]pyrene	0	0	0	0.0073	0.0074	0.0301
Benzo[*b*]perylene	0	0	0	0	0	0.0477

Pressure (atm); (Temperature, 570 °C; Residence Time 140 sec)

	40	60	70	80	90	100
Dibenzo[*j*,*l*]fluoranthene	0	0	0	0	0	0.0109
Dibenzo[*a*,*k*]fluoranthene	0	0	0	0	0	0.0110
Naphtho[1,2-*b*]fluoranthene	0	0	0	0.0008	0.0085	0.0199
Dibenzo[*a*,*e*]pyrene	0	0	0.0071	0.0212	0.0380	0.0823
Dibenzo[*a*,*h*]pyrene	0	0	0	0	0	0.0136
Dibenzo[*a*,*i*]pyrene	0	0	0	0.0014	0.0060	0.0148
Dibenzo[*e*,*l*]pyrene	0	0	0	0	0	0.0333
Naphtho[2,1-*a*]pyrene	0	0	0.0177	0.0718	0.0685	0.1497
Naphtho[2,3-*a*]pyrene	0	0	0	0	0	0.0129
Naphtho[2,3-*e*]pyrene	0	0	0.0015	0.0072	0.0166	0.0301
Benzo[*b*]perylene	0	0	0	0	0	0.0477

B.13 Seven-, Eight, and Nine-Ring PAH Product Yields

Phenanthro[2,3-*a*]pyrene, dibenzo[*b,ghi*]perylene, dibenzo[*e,ghi*]perylene, dibenzo-[*cd,lm*]perylene, naphtho[1,2,3,4-*ghi*]perylene, benzo[*a*]coronene, phenanthro[5,4,3,2-*efghi*]-perylene, and naphtho[8,1,2-*abc*]coronene yields are reported in µmol product per mol *n*-decane fed to the reactor.

	Temperature (°C); (Pressure, 100 atm; Residence Time, 140 sec)					
	530	540	550	560	565	570
Phenanthro[2,3-*a*]pyrene	0	0	0	0.00734	0.01921	0.02861
Dibenzo[*b,ghi*]perylene	0	0	0	0.00450	0.01255	0.02899
Dibenzo[*e,ghi*]perylene	0	0	0	0.00716	0.02015	0.05011
Dibenzo[*cd,lm*]perylene	0	0	0	0	0.01005	0.02095
Naphtho[1,2,3,4-*ghi*]perylene	0	0	0	0	0.00000	0.01743
Benzo[*a*]coronene	0	0	0	0.00100	0.00522	0.00950
Phenanthro[5,4,3,2-*efghi*]-perylene	0	0	0	0.00359	0.01218	0.02009
Naphtho[8,1,2-*abc*]coronene	0	0	0	0.00173	0.00416	0.01165

	Pressure (atm); (Temperature, 570 °C; Residence Time 140 sec)					
	40	60	70	80	90	100
Phenanthro[2,3-*a*]pyrene	0	0	0.00231	0.00816	0.01780	0.02861
Dibenzo[*b,ghi*]perylene	0	0	0.00175	0.00611	0.01339	0.02899
Dibenzo[*e,ghi*]perylene	0	0.00068	0.00294	0.00875	0.01856	0.05011
Dibenzo[*cd,lm*]perylene	0	0	0	0	0.01580	0.02095
Naphtho[1,2,3,4-*ghi*]perylene	0	0	0	0.00173	0.01252	0.01743
Benzo[*a*]coronene	0	0	0.00041	0.00096	0.00326	0.00950
Phenanthro[5,4,3,2-*efghi*]-perylene	0	0	0.00085	0.00306	0.01136	0.02009
Naphtho[8,1,2-*abc*]coronene	0	0	0	0.00233	0.00800	0.01165

Vita

Sean Patrick Bagley was born in Port Arthur, Texas, and grew up in Slidell, Louisiana. After graduating high school, he attended the University of New Orleans for one year, before moving to Baton Rouge, Louisiana, to study chemical engineering at Louisiana State University. He received his bachelor's degree in 2003 and began graduate school at LSU that same year. As a graduate student, he has attended conferences and presented his work in Germany, Norway, Canada, and China. He expects to graduate in the fall of 2010.